ALTERTATIONS IN EXCITATORY / INHIBITORY CIRCUITRY IN THE ADULT RAT BRAIN FOLLOWING POSTNATAL GLUTAMATERGIC SYSTEM ACTIVATION

BY

DAPHNE A. GILL

A Thesis
Submitted to the Graduate Faculty
in Partial Fulfillment of the Requirements
for the Degree of

DOCTOR OF PHILOSOPHY

Department of Biomedical Sciences
Faculty of Veterinary Medicine
University of Prince Edward Island

Your file Votre référence
ISBN: 978-0-494-64479-9
Our file Notre référence
ISBN: 978-0-494-64479-9

CONDITIONS FOR THE USE OF THE THESIS

SIGNATURE PAGE

(iii) & (iv)

REMOVED

ABSTRACT

A critical period for maturation and final organization of excitatory and inhibitory function in the brain occurs during perinatal development when network connections are being formed and refined. In the rat hippocampus, many of these connections reach adult levels by the end of the second postnatal week. Subsequently, insult or injury to the brain at this time may have far-reaching consequences that manifest as changes in behaviour resulting from modifications in underlying neuronal structure and function. It has been previously demonstrated that low daily doses of the glutamate agonist domoic acid (DOM), administered to rat pups throughout the second postnatal week of life, can result in seizure-like behaviours in adulthood similar to temporal lobe epilepsy (TLE) in humans, as well as produce cellular changes in the dentate gyrus and area CA3 of the hippocampus. Now known as the novelty-induced, seizure-like (NIS-L) rat, these animals represent a new developmental model for TLE.

The objective of this dissertation was to further characterize the NIS-L model, thus providing additional information regarding potential alterations in neurologic function and underlying mechanistic properties that may result from early-life glutamate system activation. Subsequently, *in vivo* studies were performed to provide an electrophysiological assessment of electroencephalogram (EEG) in NIS-L rats. This investigation revealed a distinct EEG waveform pattern during NIS-L manifestation as well as subtle alterations in wave band expression, along with decreased seizure threshold levels and increased mossy fibre sprouting, but no difference in seizure propagation to the rest of the brain. In addition, altered sleep patterns were also reported, similar to what is seen in other animal models of TLE. To assess possible underlying mechanisms responsible for these changes, an immunohistochemical study of inhibitory cells in the hippocampus and amygdala showed region and sex-dependent changes in specific interneuronal subpopulations in the model, as well as decreases in a population of susceptible excitatory neurons, while an *in vitro* evaluation of field post-synaptic potentials in the dentate gyrus and area CA3 of the hippocampus revealed no differences in baseline activity, but did show a concentration-dependent alteration in response to acute DOM perfusion. A final study investigating possible glutamatergic pathways for DOM-mediated effects indicated no involvement for the *N*-methyl-D-aspartate (NMDA) receptor, but appeared to implicate α-amino-3-hydroxy-5-methyl-4-isoazolepropionic acid (AMPA)-sensitive mechanisms. Additionally, a dramatic and unexpected response to early-life glutamate antagonism was discovered.

These data provide a demonstration of some of the possible changes that may occur in excitatory and inhibitory circuitry in the brain as a result of interference with early developmental processes, and have revealed several underlying mechanisms that may be responsible for these changes. Future studies assessing spontaneity of behavioural seizure expression and evaluating sex-dependent differences in the model, as well as an investigation of the role of GABAergic mechanisms may help further elucidate the possible consequences of interference in the intricate interplay between glutamate and GABA systems during critical developmental stages.

ACKNOWLEDGEMENTS

One of the most important facets of research is an unswerving dedication to the search for knowledge and the subsequent sharing of that knowledge with others. During the course of my studies, I have been blessed with the support and guidance of many talented and enthusiastic individuals committed to research excellence. Without their assistance, this thesis and the work contained within would not have been possible.

First and foremost, I would like to thank my supervisor, Dr. Andrew Tasker, whose advice and constant encouragement has been invaluable.

I would also like to thank the members of my supervisory committee (past and present) for their assistance during this work, as well as express my sincere thanks and appreciation to Dr. William Watson, Dr. David Reynolds, Dr. Tine Stensbøl, Dr. Jesper Bastlund, Dr. Neil Anderson and Kasper Larsen for support and supervision during my studies at H. Lundbeck A/S in Copenhagen, Denmark. In addition, a special thank you goes to my earliest mentor, Dr. Catherine Ryan, for inspiring me to continue in the research field.

Financial support from the Atlantic Innovation Fund (AIF), the Atlantic Centre for Comparative Biomedical Research (ACCBR), the Natural Sciences and Engineering Research Council (NSERC), and H. Lundbeck A/S is also acknowledged and greatly appreciated.

Due to space constraints, it is impossible for me to list all of the individuals who have contributed to the completion of this work, but please know that your help and encouragement has not gone unnoticed.

And last, but not least, I would like to thank my family for enduring all the long hours and missed weekends without complaint, and for always being there when I needed you.

DEDICATION

I would like to dedicate this thesis to my parents,

Don and Hazel Sears

whose passion for learning and knowledge has been my inspiration

and to my husband

Ron Gill

for giving me the courage to pursue my dreams

TABLE OF CONTENTS

LIST OF TABLES

LIST OF FIGURES

ABBREVIATIONS

Abbreviation	Term
ABC	avidin-biotin complex
aCSF	artificial cerebral spinal fluid
ACTH	adrenocorticotropic hormone
AD	after discharge
ADD	after discharge duration
ADT	after discharge threshold
AED	antiepileptic drug
AMPA	α-amino-3-hydroxy-5-methyl-4-isoazolepropionic acid
AMPAR	α-amino-3-hydroxy-5-methyl-4-isoazolepropionic acid receptor
ANOVA	analysis of variance
ATP	adenosine triphosphate
BDNF	brain derived neurotrophic factor
BNF	buffered neutral formalin
BSA	bovine serum albumin
BZP	benzodiazapine
Ca^{++}	calcium ion
cAMP	cyclic adenosine monoposphate
CA	cornu ammonis
$CaCl_2$	calcium chloride
CGRP	calcitonin gene-related peptide

Cl^-	chloride ion
$[Cl^-]_i$	intracellular chloride
CNS	central nervous system
CO_2	carbon dioxide
CORT	corticosterone
CPP	(RS)-3-((+/–)-2-carboxypiperazin-4-yl)-propyl-1-phosphonic acid
C-terminus	carboxy-terminal domain
DAB	diaminobenzidine
DAG	diacylglycerol
DCPP	DOM + CPP
DG	dentate gyrus
DK	DOM + kindle
DNBQX	DOM + NBQX
DOM	domoic acid
DSK	DOM stress + kindle
EC	entorhinal cortex
EEG	electroencephalogram
EMG	electromyogram
fEPSP	field excitatory post-synaptic potential
fIPSP	field inhibitory post-synaptic potential
FFT	fast Fourier transform
FST	forced swim test
G	glycine

G_i	inhibitory guanosine triphosphate-binding protein
G-protein	guanosine triphosphate-binding protein
GABA	γ-aminobutyric acid
GABAR	γ-aminobutyric acid receptor
GABA-T	γ-aminobutyric acid transaminase
GAD	glutamic acid decarboxylase
GBR	GABA-B receptor
GC	granule cell
GDP	giant depolarizing potential
GIRK	G-protein gated inward-rectifying K^+ channel
Glu	glutamate (glutamic acid)
Gluδ	glutamate delta
GluK	glutamate kainic acid
GluR	glutamate receptor
GPCR	guanosine triphosphate-binding protein coupled receptor
HC	hippocampus
HIER	heat-induced epitope retrieval
HIPP	hippocampal to perforant path
IgG	immunoglobulin G
IML	inner molecular layer
iGluR	ionotropic glutamate receptor
I/O	input/output
i.p.	intraperitoneal
IP_3	inositol-1,4,5-triphosphate

IPSP	inhibitory post-synaptic potential
ir	immunoreactivity
I/V	isoleucine/valine
K^+	potassium ion
KA	kainate (kainic acid); 2-carboxy-3-carboxymethyl-4-isopropenylpyrrolidine
KAR	kainate receptor
KCC2	potassium-chloride co-transporter
KCl	potassium chloride
K_D	dissociation constant (for receptors, refers to the affinity of ligand to the receptor; higher affinity = lower K_D value)
LTP	long-term potentiation
M	membrane spanning domain
MBS	maximal behavioural seizure
MCJ	myoclonic jerk
MF	mossy fibre
MFS	mossy fibre sprouting
Mg^{++}	magnesium ion
$MgSO_4$	magnesium sulfate
mGluR	metabotropic glutamate receptor
mRNA	messenger riboneucleic acid
MWM	Morris water maze
Na^+	sodium ion
NaCl	sodium chloride

$NaHCO_3$	sodium bicarbonate
NaH_2PO_4	monosodium phosphate
NBQX	2,3-Dioxo-6-nitro-1,2,3,4-tetrahyrobenzo[f]quinoxaline-7-sulfonamide disodium salt
NIS-L	novelty induced, seizure-like
NKCC	sodium-potassium-chloride co-transporter
NMDA	*N*-methyl-D-aspartate
NMDAR	*N*-methyl-D-aspartate receptor
NR	*N*-methyl-D-aspartate receptor subunit
NREM	non-rapid eye movement
N-terminus	amino terminal domain
O_2	oxygen
PBS	phosphate buffered saline
PBST	phosphate buffered saline with Tween 20
PCL	principal cell layer
PDT	postnatal DOM-treated
PKA	protein kinase A
PKC	protein kinase C
PLC	phospholipase C
PLP	pyridoxal phosphate (vitamin B_6)
PND	postnatal day
PP	perforant path
PPN	pedunculopontine
PS	paradoxical sleep

PSp	population spike
PTZ|	pentylenetetrazol
PV	parvalbumin
Q	glutamine
R	arginine
REM	rapid eye movement
RIA	radio immunoassay
RNA	riboneucleic acid
ROI	region of interest
RT	room temperature
S	ligand binding site
SAL	saline
SC	Schaffer collaterals
s.c.	subcutaneous
SCPP	saline + CPP
SE	status epilepticus
SEM	standard error of the mean
SER	spontaneous epileptic rats
SK	saline + kindle
SL	stratum lucidum
SL-M	stratum lacunosum-moleculare
SNBQX	saline + NBQX
SO	stratum oriens
SSK	saline stress + kindle

SST	somatostatin
SR	stratum radiatum
SWS	slow wave sleep
TBS	tris buffered saline
TLE	temporal lobe epilepsy
TM	transmembrane
TrkB	tyrosine kinase receptor B
TTX	tetrodotoxin
VOCC	voltage-operated calcium channel
Y/C	tyrosine/cysteine
$[Zn^{++}]_i$	intracellular zinc

Chapter 1: GENERAL INTRODUCTION

1.0 Introduction

Excitatory and inhibitory function in the brain relies on a variety of different structures and systems, and may vary depending upon the age of the organism. Achieving appropriate balance between excitation and inhibition is a complex and crucial stage in early development and disruptions to this process may have far-reaching consequences. The current chapter will outline some of the many aspects surrounding this fascinating topic.

1.1 Glutamate

Glutamate (Glu), the conjugate base of the non-essential amino acid glutamic acid, serves a multi-functional role in mammalian physiology, involved in such widespread bodily processes as cellular metabolism, excess nitrogen removal, and neurotransmission. It is this latter role that will be the focus for the current dissertation.

1.1.1 Glutamate receptors

As the most abundant excitatory transmitter in the mammalian central nervous system (CNS), Glu is required for basic information processing, as well as for the facilitation of learning, memory and other functions relating to synaptic efficacy (for review, see Dingledine *et al.*, 1988; Mayer and Westbrook, 1987; Monaghan *et al.*, 1989). Glutamate release activates Glu receptors that can be broadly divided into ionotropic (ligand gated) and metabotropic (G-protein coupled) receptors. In light of the universal prevalence of Glu in the brain, it is unsurprising that dysfunction in glutamatergic transmission has been implicated in a wide variety of neuropathological disorders,

including schizophrenia, autism, stroke, Alzheimer's disease, Huntington's disease, Parkinson's disease, and epilepsy (Choi, 1988; Choi and Rothman, 1990; Meldrum and Garthwaite, 1990; Rothman and Olney, 1986).

1.1.2 Ionotropic glutamate receptors

There are three major classes of ionotropic Glu receptors (iGluRs) that can be differentiated pharmacologically, electrophysiologically and through sequence homology, and are named according to the agonists that were originally found to selectively activate each: *N*-methyl-D-aspartate (NMDA), α-amino-3-hydroxy-5-methyl-4-isoazolepropionic acid (AMPA), and 2-carboxy-3-carboxymethyl-4-isopropenylpyrrolidine (kainate – KA) (Monaghan *et al.*, 1989). All iGluRs are believed to be tetrameric, with each subunit comprising three transmembrane spanning domains (M1, M3 and M4) plus a re-entrant loop (M2) that forms the channel pore and determines ion permeability and selectivity (Wollmuth and Sobolevsky, 2004). A basic schematic of iGlu structure is presented in Figure 1.1 (pg.3). Ligand binding occurs at a hinged 'clamshell-like' site formed from a region of the amino terminal (N-terminus) portion of M1 (referred to as S1) and the extracellular portion of M3 and M4 (called S2) (e.g. Gouaux, 2004; Mayer and Armstrong, 2004; see Mayer, 2005 for review). The N-terminus also houses binding sites for various modulatory molecules (Herin and Aizenman, 2004), while an intracellular carboxy-terminal domain (C-terminus) allows interactions with signal transduction and scaffolding proteins (Kim and Sheng, 2004) and provides receptor localization and trafficking within the membrane (Perez-Otano and Ehlers, 2005; Song and Huganir, 2002; Wenthold *et al.*, 2003). For a more comprehensive review of these receptors, readers are referred to Dingledine *et al* (1999).

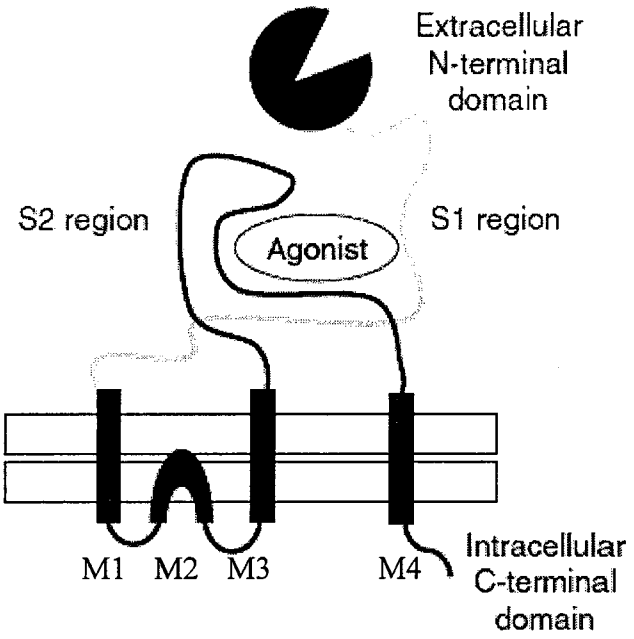

Figure 1.1. Schematic representation of basic iGluR structure.

(Kew and Kemp, 2005. Reproduced with permission)

1.1.2.1 NMDA receptors

The NMDA Glu receptor (NMDAR) subfamily consists of seven subunits which are all derived from separate genes: NR1, NR2A-D and NR3A and B (Figure 1.2, pg 5). In addition, there are eight functional splice variants of NR1 (McBain and Mayer, 1994), which confer a variety of different properties to the channel, including altering channel sensitivity to modulators such as zinc (Durand *et al.*, 1993; Hollmann *et al.*, 1993; Traynelis *et al.*, 1998). Widely distributed throughout the mammalian CNS, particularly in cerebral cortex and hippocampus (HC), functional NMDARs consist of 'dimers of dimers' with NR1 paired with various NR2 subunits (Benveniste and Mayer, 1991; Clements and Westbrook, 1991; Furukawa *et al.*, 2005), although an NR3 subunit may sometimes be substituted for one of the NR2 family, an insertion that changes channel conductance due to slight differences in the M2 (pore) region. However, it should be noted that NR3 subunits have considerably restricted spatio-temporal distributions, with NR3A expressed predominantly (but not exclusively) during development, and NR3B found in motoneurones of the brainstem and spinal cord (Nishi *et al.*, 2001; Paoletti and Neyton, 2007).

Activation of NMDARs requires binding of both Glu and the essential coagonist glycine (Dingledine *et al.*, 1990; Johnson and Ascher, 1987; Kleckner and Dingledine, 1988). Glutamate binding sites are located on NR2, while glycine binds to NR1 and NR3 subunits (Furukawa *et al.*, 2005). Additionally, many other molecules (including the selective agonist NMDA) can act as ligands, serving in either facilitative or antagonist roles, or performing modulatory functions (e.g. Davies *et al.*, 1988; Monnet

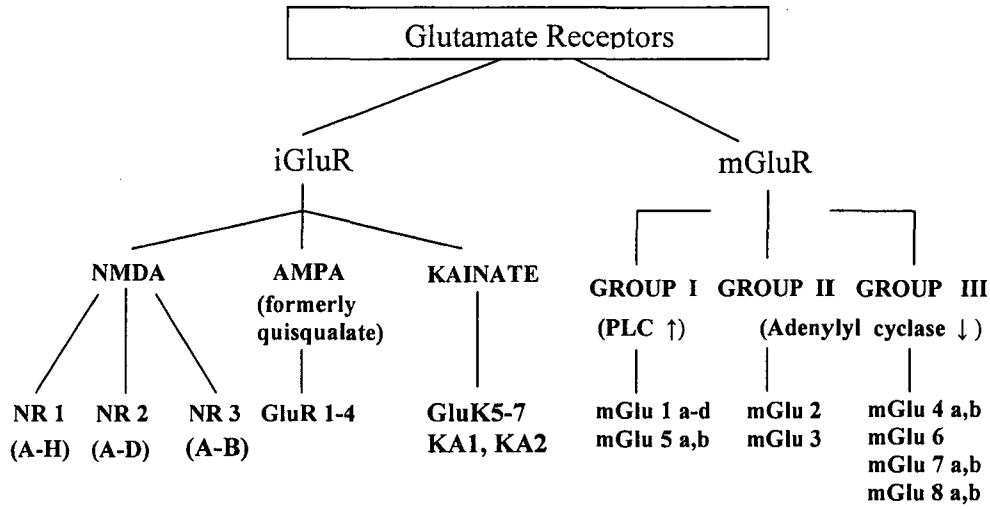

Figure 1.2. Classification of glutamate receptors.

(Adapted from Watkins and Jane, 2006.)

et al., 1992; Ransom and Deschenes, 1988; Wong *et al.*, 1986; Paoletti and Neyton, 2007). However, for the NMDA channel, ligand binding alone is not sufficient to allow ion conductance, since passage is further inhibited by a voltage-dependent Mg^{2+} block that does not release unless sufficient membrane depolarization occurs (Johnson and Ascher, 1990; Mayer *et al.*, 1984). For this reason, even though NMDARs are much more sensitive to Glu than other iGluRs (McBain and Mayer, 1994), they will not respond if they are the only receptors expressed at a synapse (a phenomenon known as the 'silent synapse'). Also, when the pore does open, NMDAR channels perform more slowly than the other members of the iGluR family, with longer activation and deactivation times, as well as a comparably lengthy and complex desensitization process (Lester *et al.*, 1990). The actual rates of these processes are subunit-dependent, governed primarily by the particular NR1/NR2 subtypes contained in the structure of each receptor (Chang and Kuo, 2008; Furukawa *et al.*, 2005).

Another notable difference between NMDAR and the other iGluR channels is ion permeability. While all iGluR channels will flux Na^{+} and K^{+}, NMDA channels are also highly permeable to Ca^{++} (MacDermott *et al.*, 1986), a cation that is only very selectively allowed access to the cell through non-NMDA iGluR routes. Overall, the NMDAR requirement for both voltage- and ligand-gated access, plus the slow-gating kinetics and high permeability to Ca^{++} when it is activated, uniquely positions this channel as a key player in synaptic plasticity, as well as making it a prime target for therapeutic interventions during neuropathological conditions involving excess excitability.

1.1.2.2 AMPA receptors

Fast excitatory neurotransmission is the domain of AMPA receptors (AMPARs), and like NMDARs, channel kinetics depend on subunit composition (Mosbacher *et al.*, 1994). Although there are only four AMPAR subunits (GluR1-4; see Figure 1.2, pg 5), each exists in two different forms, "flip" and "flop", created by alternative splicing of a 115-base pair region immediately preceding M4 (Sommer *et al.*, 1990). Functionally, channels with the "flip" form have a slow desensitization rate, while "flop" channels can desensitize up to 4x faster (Mosbacher *et al.*, 1994). In addition, RNA editing provides further diversity by making posttranscriptional changes to the nucleotide sequence of the mRNA, and may occur at one or both of two sites; the Q/R (Q, glutamine – unedited; R, arginine – edited) on the GluR2 subunit (Sommer *et al.*, 1991), and/or the R/G (R, arginine – unedited; G, glycine – edited) site on GluR2, GluR3 and GluR4 (Lomeli *et al.*, 1994). The presence of a GluR2 subunit edited at the Q/R site makes the channel impermeable to Ca^{++} (Hume *et al.*, 1991), while R/G editing alters the sensitization properties of the receptor (Lomeli *et al.*, 1994). Additionally, subunit composition also determines the trafficking of the receptor into and out of the membrane, a function that depends on the sequence, length, and phosphorylation sites on the cytosolic C-terminus (Greger and Esteban, 2007). This property is of particular importance during synaptic plasticity (Kim and Sheng, 2004).

Distributed ubiquitously throughout the CNS, AMPARs are able to express as either homomeric or heteromeric oligomers, and in adulthood, primarily flux Na^+ and K^+, since nearly 100% of adult receptors include an edited GluR2 protein. However, if the GluR2

subunit is not present, or if it is present in its unedited form (glutamine instead of arginine), Ca^{++} will also be allowed access to the cell, a possibility that has led to much interest in the relationship between GluR2 status and neuropathological disorders such as epilepsy (Pellegrini-Giampietro *et al.*, 1997; Sprengel *et al.*, 1999). AMPAR binding regions include the primary Glu site, a desensitization site, and channel blocker sites, all of which have been, and continue to be, investigated as targets for pharmacological therapies, particularly for antiepileptic compounds (Rogawski and Donevan, 1999; Rogawski, 2006). In addition, inappropriate AMPAR trafficking has been implicated as a key player in excitotoxic disorders, both on its own, and in conjunction with increased NMDAR activation (Kortenbruck *et al.*, 2001; Vollmar *et al.*, 2004).

1.1.2.3 Kainate receptors

Although kainic acid has been known to be a potent Glu analogue for many years (Olney *et al.*, 1974),with the discover y of distinct kainate receptors (KARs) first reported in 1982 (Evans *et al.*, 1982), actual KAR function has remained elusive, primarily due to a lack of specific antagonists to allow study of KAR synaptic physiology. In the last decade, however, better pharmacological tools and the development of KAR subunit-deficient mice have considerably enhanced understanding of this intriguing iGluR subfamily. There are five KAR subunits (Figure 1.2, pg 5), two with high-affinity binding for kainic acid (KA1 and KA2; K_D = ~5nM), and three with low-affinity binding (GluK5-7; K_D = ~50nM) (London and Coyle, 1979; Unnerstall and Wamsley, 1983). Of these, studies to date suggest that KA1 requires a partnering with low-affinity subunits to form functional channels, while KA2 and GluK5-7 can combine in either heteromeric or homomeric configurations (Hayes *et al.*, 2003; Ren *et al.*, 2003), although the actual

functionality of the homomeric KA2 channel *in vivo* is still under investigation (for review, see Huettner, 2003). While KARs are widespread throughout the CNS, they are particularly well expressed in amygdalar and hippocampal regions (Wisden and Seeburg, 1993; Braga *et al.*, 2003; Lerma, 2006).

Similarly to AMPA receptors, KARs can undergo alternative splicing to increase the number of subunit isoforms available. While the exact role of the different KAR splice variants is as yet unknown, it is believed that these alterations influence both ligand binding (N-terminus region) and intracellular interactions (N- and C-terminus regions) (Fleck *et al.*, 2003; Mah *et al.*, 2005; Valluru *et al.*, 2005; Priel *et al.*, 2006 ; for review, see Coussen, 2009). Additionally, GluK5 and GluK6 are also subject to RNA editing at the Q/R site, and unlike GluR2, a significant portion (up to 40%) remains unedited in the adult (Bernard *et al.*, 1999), providing Ca^{++} permeability. GluK6 can also undergo further editing at two more sites in the M1 domain. At the I/V site, isoleucine may be changed to valine, while at the Y/C site, tyrosine may switch to cysteine. While all eight variants of GluK6 are present in the CNS, the fully edited version (R/V/C) is the one most prevalent in the adult brain (Kohler *et al.*, 1993).

Although many of the pharmacological agonists and antagonists that activate KARs also interact with AMPARs (for review, see Lerma *et al.*, 2001), KA-mediated receptors have a distinct role in the iGluR family, with their function dependent upon their subcellular location. Postsynaptically, KAR channels generally produce a low amplitude, slowly decaying current that allows for prolonged and repetitive firing

(Castillo *et al.*, 1997; Frerking *et al.*, 1998). Presynaptically, they modulate the release of both Glu (Chittajallu *et al.*, 1996; Jiang *et al.*, 2001) and γ-aminobutyric acid (GABA) (Cunha *et al.*, 1997; Jiang *et al.*, 2001) in a bidirectional manner that is dependent upon specific subunit composition (Lerma, 2006). In general, low concentrations of agonist increase neurotransmission, while high concentrations result in a decreased release rate (Braga *et al.*, 2003). Interestingly, while KAR stimulation enhances GABA release somato- and/or axo-dendritically between interneurons (Cossart *et al.*, 2001), it appears to inhibit GABA release in presynaptic locations at interneuron-to-pyramidal cell synapses (Cossart *et al.*, 2001; Frerking *et al.*, 1999). This inhibitory function is believed to be conducted through a G protein-coupled (phospholipase C: PLC) signaling pathway (see Figure 3, pg 11 for proposed mechanism) triggered in some yet-unknown manner by ion channel activation, and appears to involve the participation of either the GluK5 or the GluK6 subunit (Lerma, 2006). To date, while much has yet to be discovered regarding KAR function, it is abundantly clear that this iGluR subfamily plays an integral part in the control of network excitability.

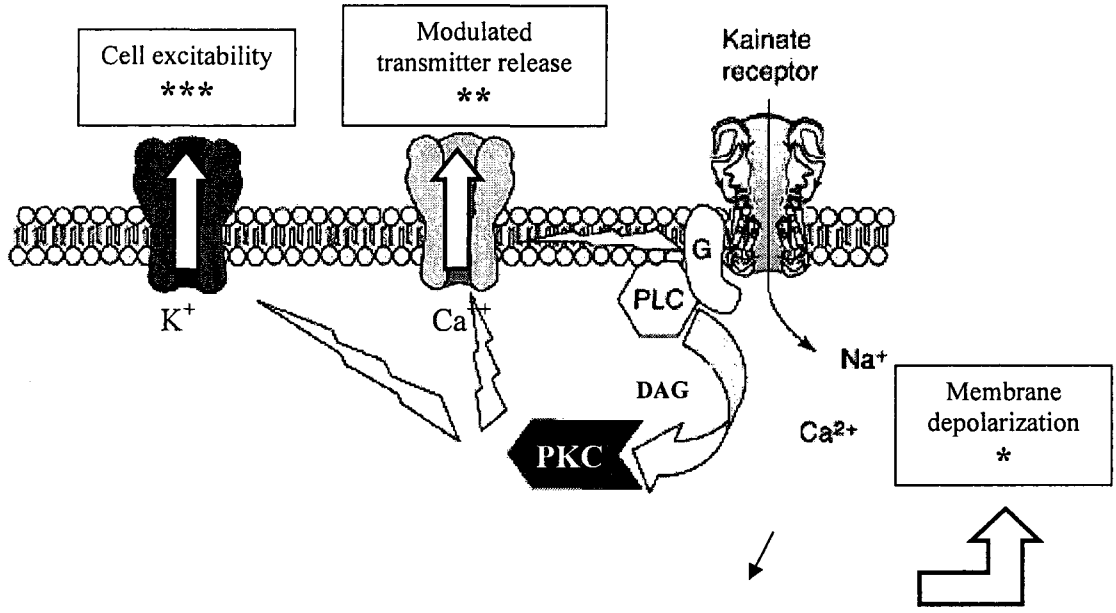

(Adapted from Lerma, 2006)

Figure 1.3. Proposed dual signaling pathways initiated by presynaptic kainate receptors. When the KA channel opens, ionic activity depolarizes the membrane (*), while simultaneous activation of a G protein (G) is achieved, triggering phospholipase C (PLC) and subsequent protein kinase C (PKC) activation through increased diacylglycerol (DAG). This second messenger system might inhibit Ca^{++} channels, leading to the modulation of transmitter release (**), or produce inhibition of the Ca^{++}-dependent K^+ afterhyperpolarization current, which would increase membrane excitability (***).

1.1.3 Metabotropic receptors

The metabotropic Glu receptors (mGluRs) comprise a heterogeneous receptor family linked to a variety of signal transduction pathways through guanine nucleotide or guanosine triphosphate-binding proteins (i.e. G-proteins). Binding of Glu to these receptors does not directly result in channel opening; instead, they regulate synaptic transmission and neuronal excitability through stimulatory or inhibitory G protein-coupled effector systems, thus providing a slower onset of activity that extends over a relatively long period of time (Conn and Pin, 1997). Like other G-protein coupled receptors (GPCRs), the mGluRs have a 7 transmembrane domain with an extracellular N-terminus and an intracellular C-terminus. However, mGluRs are much larger than most other GPCRs, and their ligand binding domain is located in the N-terminus rather than in the transmembrane region which links them most closely with the metabotropic GABA receptor family ($GABA_B$) (Brauner-Osborne *et al.*, 2007).

Metabotropic GluRs have been divided into three main groups (Figure 1.2) based on pharmacology, sequence similarities, and signal transduction systems. Signaling pathways linked to mGluR activation are summarized in Figure 4 (pg 13). Group I receptors are usually located postsynaptically, and include mGlu1 and mGlu5 along with their various splice variants. These receptors are coupled to a stimulatory G-protein, activating the PLC → inositol-1,4,5-triphosphate (IP_3) / diacylglycerol (DAG) → protein kinase C (PKC) pathway, ultimately leading to a variety of changes including altered membrane trafficking and intracellular Ca^{++} levels, activation of voltage-operated

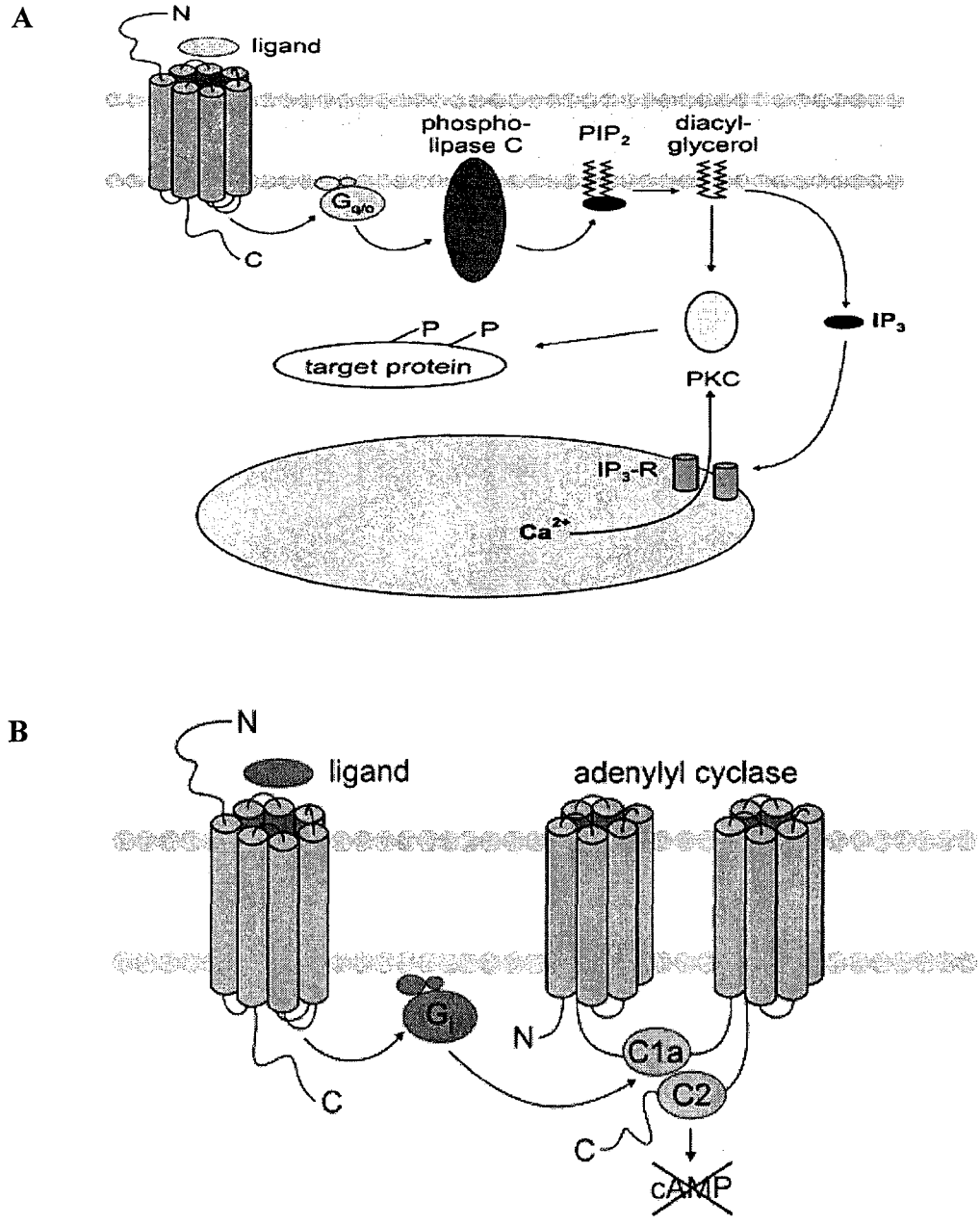

Figure 1.4. Signaling pathways activated by mGlu receptors. A) Group I mGlu receptors couple preferentially to Gq-proteins, leading to activation of phospholipase C and mobilization of intracellular Ca^{++} and activation of protein kinase C (PKC), via IP_3 and diacylglycerol (DAG) respectively. B) Group II & III mGluRs act through an inhibitory G-protein (G_i) to inhibit adenylate cyclase activity, decreasing cyclic adenosine monophosphate (cAMP) formation, and resulting in the inhibition of voltage-operated calcium channels (VOCCs).

(images downloaded from http://www.fz-juelich.de/isb/isb-1/GPCR)

Ca^{++} channels (VOCCs), and K^+ efflux through Ca^{++} sensitive K^+ channels (Hermans and Challiss, 2001). Group II receptors (mGlu2 and mGlu3) have no known splice variants, and are mostly presynaptic on axons rather than near synapses. They have a high affinity for Glu and appear to respond to synaptic "spillover". They act via an inhibitory G-protein (G_i) that inhibits adenylate cyclase activity, thereby decreasing cyclic adenosine monophosphate (cAMP) formation, and ultimately resulting in the inhibition of VOCCs (Moldrich *et al.*, 2003). And finally, Group III mGluRs (mGlu4, 6, 7, and 8) and their variants are also located presynaptically and act through the G_i coupled pathway, but their location and their affinity for Glu is dependent upon the particular isoform expressed (Schoepp, 2001; see Figure 4, pg 13). Like their iGluR cousins, the mGluR family has been implicated in a variety of neurological pathologies, including absence epilepsy and various mood disorders (for review, see Moldrich *et al.*, 2003; Pilc *et al.*, 2008).

1.1.4 Delta glutamate receptors

Technically considered members of the iGluR family (Lomeli *et al.*, 1993), the 'orphan' δ Glu receptors are believed to play a role in cerebellar long-term depression (LTD) (Kashiwabuchi *et al.*, 1995). As well, the Lurcher mutant mouse is attributed to a gain-of-function mutation in Gluδ2 (Zuo *et al.*, 1997). However, recent studies have shown that the Gluδ2 receptor does not appear to serve as an ion channel, and may actually function as a non-ionotropic receptor, mediating signals by interaction with intracellular molecules (Kakegawa *et al.*, 2007). Although not enough is known about Gluδ function to speculate too deeply as yet, it has been suggested that these receptors may represent a

class of iGluRs that have both ionotropic and non-ionotropic functions (Kakegawa *et al.*, 2007), and along with the putative "metabotropic-ionotropic" KAR, really highlights the incredible anatomical and functional diversity that exists within the Glu receptor family as a whole.

1.1.5 Development of the glutamate system

Development of an organism is a complex series of exquisitely timed events involving the precise coordination of multiple processes that rely on appropriate cellular signaling and growth. In the CNS, once neurons have formed and migrated to their final destinations they must develop dendritic and axonal projections and form synapses with suitable postsynaptic targets to create functional neuronal networks. In addition, superfluous connections must be pruned to allow maximal efficiency in information transmission (Luthi *et al.*, 2001). Understandably, then, even subtle disruptions to these developmental processes during critical periods have the potential to cause long-lasting alterations that may ultimately manifest as pathological disorders. As well, it is easy to see why, during a time of such constant and rapid change, an immature organism cannot be considered as merely a small adult, and how compounds that have a reliably predicable consequence in the mature system can elicit a completely different response during development, dependent upon the specific developmental phase in which they are administered (Dobbing and Smart, 1974; Dobbing and Sands, 1979).

In the mature system, Glu serves as the primary mechanism through which excitatory impulses are conducted. However, during early (embryonic) development, only a few

GluRs are functional, with NMDA receptors providing the majority of Glu signaling (Durand *et al.*, 1996; Liao and Malinow, 1996). One of the key alterations in the developing Glu system occurs during network development as the system comes 'on-line', gradually taking over the excitatory role it will serve in adulthood. During this phase (~postnatal day (PND) 4-21 in the rat) there is a transient overshoot of Glu receptors with AMPA and NMDA binding sites increasing to as much as 160% of adult values before leveling off, while KARs rise rapidly within the same time period (for review, see Lujan *et al.*, 2005; McDonald and Johnston, 1990).

Additionally, subunit composition of GluRs during early postnatal development has been shown to vary considerably from that seen in adulthood (Seeburg, 1993). In AMPA receptors, this means a greater predominance of both the flip isoform and unedited GluR2 subunits, providing a slower desensitization rate and more Ca^{++} permeability to the cell (Simeone *et al.*, 2004). NMDARs have a higher prevalence of the NR2B subunit, conveying slower channel kinetics and an easing of the Mg^{++} block, resulting in enhanced excitatory responses (Seeburg, 1993). Less is known about KAR involvement during CNS ontogeny, but current research suggests that the GluK5 subunit may play a distinct role in network development, as postnatal network activity is altered in GluK5 knock-out mice, and mice having both GluK5 and GluK6 knockouts have impaired synaptic transmission (Breustedt and Schmitz, 2004; Fisahn *et al.*, 2004).

1.2 GABA

In the normal adult brain, GABA acts in an inhibitory role, responsible for reducing overall neuronal excitability to maintain the correct balance between excitation and inhibition, as well as for generating the waveforms and oscillations required to ensure appropriate CNS function (Engel *et al.*, 2001; Klausberger *et al.*, 2004; O'Keefe and Recce, 1993; Paulsen and Moser, 1998; Skaggs *et al.*, 1996). Decreases in GABA activity readily produce seizure due to reduced inhibitory control, and as a result, this system has often been the target for therapies designed to treat epilepsy and other seizure producing disorders. However, under certain circumstances, including during development and following severe seizure activity, GABA binding may actually produce an excitatory response (e.g. Ben-Ari, 2002; Ben-Ari, 2006b; Khalilov *et al.*, 2005), making a basic understanding of this dual-purpose neurotransmitter intrinsic to any study involving neuronal excitability.

Biosynthesis of GABA begins with L-glutamate as a precursor, and the reaction is catalyzed by glutamic acid decarboxylase (GAD), an enzyme that exists in two distinct isoforms (GAD_{65} and GAD_{67}) encoded by two separate genes (Martin and Rimvall, 1993; see Figure 1.5, pg 18). Located in the presynaptic terminals, GAD_{65} is believed to synthesize GABA under normal physiological conditions, while cytoplasmic GAD_{67} appears to be most active during pathological circumstances (Wu *et al.*, 2007). Completion of GABA biosynthesis also requires pyridoxal phosphate (PLP—vitamin B_6) as a cofactor (Martin and Rimvall, 1993). Termination of GABA transmission is through reuptake into presynaptic boutons or by glial cells, and it may then be

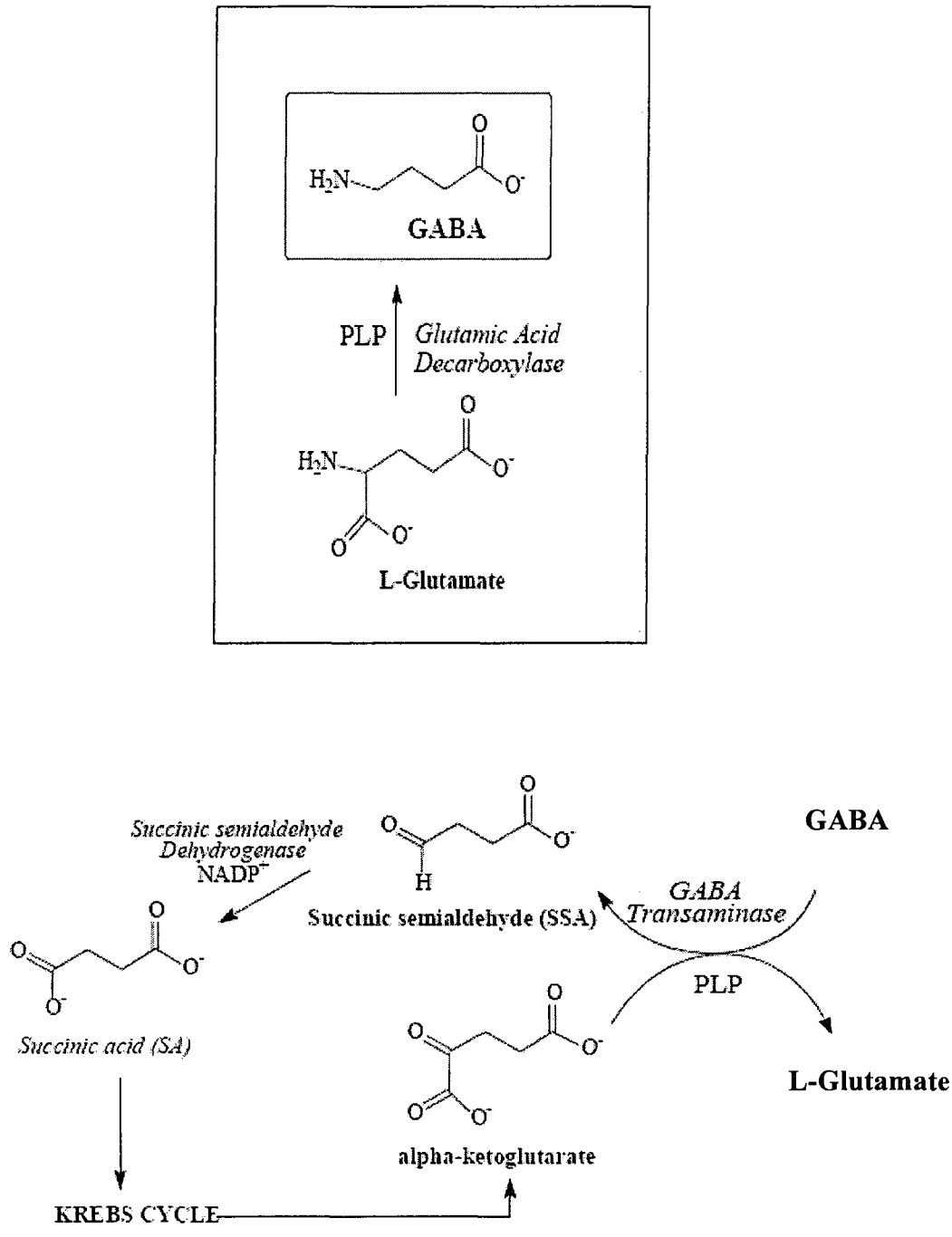

Figure 1.5. GABA biosynthesis and metabolism. GABA is biosynthesized directly from L-glutamate through the action of glutamic acid decarboxylase and pyridoxal phosphate (PLP –see box inset). Following reuptake, GABA is catabolized by GABA transaminase and through a series of steps, converted back to L-glutamate (lower panel).
(Image adapted from J. DeRuiter, http://www.auburn.edu/~deruija/GABA_Intro2002.pdf)

catabolized by GABA-transaminase (GABA-T) and PLP through a series of steps back to Glu (Martin and Rimvall, 1993).

1.2.1 GABA receptors

There are two main classes of GABA receptors (GABARs): $GABA_A$, and $GABA_B$. (A third class, $GABA_C$, found primarily in retina, is now considered to be encompassed by the $GABA_A$ family, and is currently designated as $GABA_A$-ρ) (Zhang *et al.*, 2001). $GABA_A$ receptors are ligand-gated ion channels, consisting of a pentameric subunit assembly around a central pore permeable mainly to chloride (Cl^-) (Macdonald and Olsen, 1994), and to a lesser extent, bicarbonate (Kaila, 1994), while $GABA_B$ receptors exert a wide range of neuronal effects through slower, metabotropic mechanisms. In chloride-fluxing $GABA_A$ channels, the actual net result of receptor activation on the cell is dependent upon the electrochemical gradient of the anion. During adulthood, the usual physiological consequence of channel opening is a hyperpolarizing event that reduces the probability of action potential generation. However, under certain physiological or pathological conditions, GABA can also depolarize the cell (Tretter and Moss, 2008). For example, in the suprachiasmatic nucleus, the GABA response is hyperpolarizing at night, but produces an excitatory response during the day (Wagner *et al.*, 1997). Activity can also trigger this sort of switchover, with aspects of synaptic development and plasticity dependent upon GABA's depolarizing abilities (for reviews, see Ben-Ari *et al.*, 2007; Payne *et al.*, 2003; Tretter and Moss, 2008). In addition, pathological events such as concussion (van den Pol *et al.*, 1996), hypoxia-ischemia (Yan *et al.*, 2001), and seizure activity (Rivera *et al.*, 2002) can also cause GABA to become more excitatory.

1.2.2 Ionotropic GABA receptors

The $GABA_A$ receptor is a member of the nicotinic superfamily of heteropentameric ligand-gated ion channels, and is composed of five subunits (Mohler, 2006; Tretter *et al.*, 1997), each consisting of a large N-terminal extracellular domain, four transmembrane (TM1-4) domains with a large intracellular regulatory loop between TM3 and TM4, a pore region at TM2, and a very short, extracellular C-terminus (Macdonald and Olsen, 1994) (Figure 1.6A, pg 21). Currently, 19 $GABA_A$ subunits have been cloned (α1-6, β1-3, γ1-3, δ, ε, θ, π, ρ1-3) a diversity which becomes even more complex following alternative splicing (Macdonald and Olsen, 1994; Sieghart *et al.*, 1999). While the potential for a huge array of subunit combinations exists, it is believed that the most common stoichiometry consists of 2α:2β:1γ (Farrar *et al.*, 1999; Miller *et al.*, 1994; Sieghart *et al.*, 1999). Diversity is most often achieved through combinations of different α or β subunits, or by replacing the γ subunit with something else (i.e. δ, ε, θ, π, or ρ), although a recent *in vitro* study has also reported on a small population of extrasynaptic receptors with a high sensitivity to Zn^{++} that appears to consist solely of $\alpha1\beta3$ subunits (Mortensen and Smart, 2006). As with the GluRs, subunit composition influences fundamental features of the receptor, including sensitivity to GABA, channel kinetics and desensitization, neuronal location and pharmacological properties (Hanchar *et al.*, 2005; Hevers and Luddens, 2002; Sieghart and Sperk, 2002).

There are a wide range of agonists, antagonists, and modulators that can affect $GABA_A$ activity. In particular, α subunits are instrumental in determining $GABA_AR$ affinity and sensitivity to modulatory agents such as zinc, steroids, ethanol, and pharmacological

A

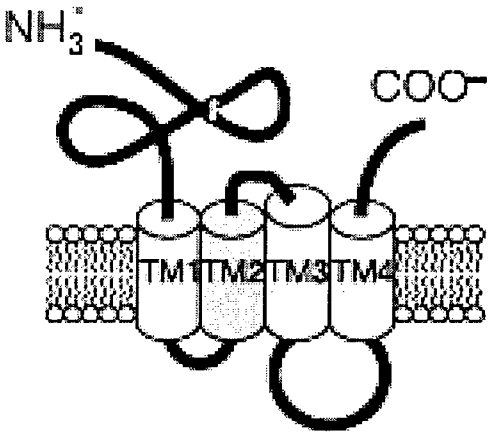

B

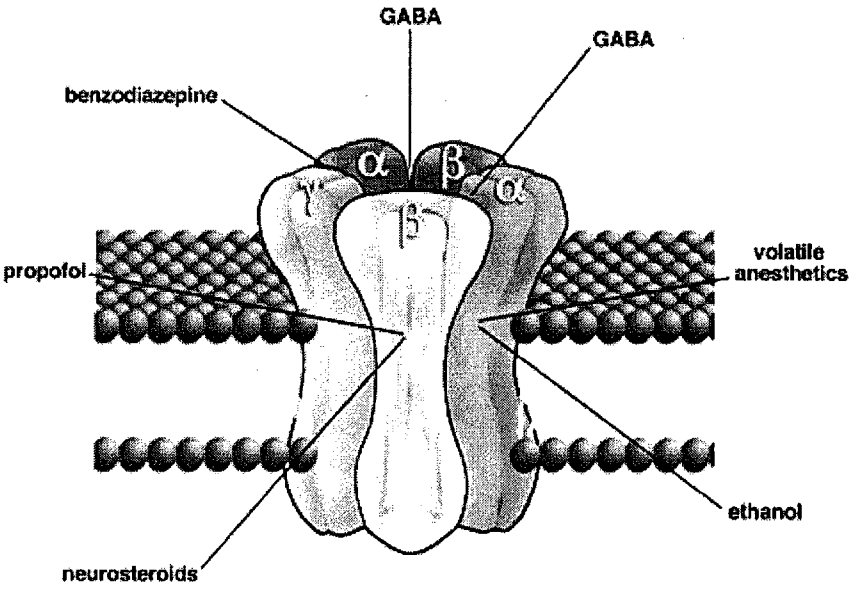

Figure 1.6. The $GABA_A$ receptor. A) Schematic representation of $GABA_A$ subunit structure (Adapted from Khakh and North, 2006). B) Binding sites for various GABA agonists, antagonists, and modulators (National Institutes of Health (NIH) website, 2009).

agents such as benzodiazapines (BZPs), barbiturates, and general anesthetics (Barnard *et al.*, 1998). Similarly, γ subunits also affect some of these parameters, as well as mediate $GABA_AR$ anchoring to synapses via interaction with gephyrin, a scaffolding protein important in forming and stabilizing synapses for both Glu and GABA (Essrich *et al.*, 1998).

The δ containing receptors ($GABA_AR\delta$) are generally found extra- and perisynaptically, an ideal location for sensing GABA spillover from synapses (Wei *et al.*, 2003) to allow for lengthening of inhibitory potentials (Isaacson *et al.*, 1993; Rossi and Hamann, 1998), and/or to respond to ambient GABA levels for the mediation of tonic (continuously underlying) inhibition, an integral component in the creation of network oscillations (Hausser and Clark, 1997). The importance of GABA-mediated tonic activity to neuronal networks has become increasingly evident in the last decade, sparking much interest in the role of δ subunits in both physiological and pathological conditions. Interestingly, $GABA_AR\delta$s have a high affinity for GABA and low desensitization rates in the continuous presence of agonist (Bianchi *et al.*, 2001; Haas and Macdonald, 1999; Wohlfarth *et al.*, 2002), but are inefficient at GABA binding (Glykys and Mody, 2007), an intriguing property that has been postulated to allow for a sensitive network-directed enhancement of receptor conductance through the modulatory effects of endogenous molecules such as neuropeptides (e.g. somatostain, neuropeptide Y, cholecystokinin), and calcium-binding proteins (e.g. calbinden, parvalbumin) found co-localized within certain interneuronal populations (Bacci *et al.*, 2005). While the functional role of the $GABA_AR\delta$-mediated tonic current is still under investigation, it has been established that the net effect of tonic current increases input conductance (Chadderton *et al.*, 2004). In

fact, the total charge carried by the tonic current in hippocampal granule cells and interneurons is actually 2-3x larger than the averaged charge carried by spontaneous phasic (activity-directed) current (Hamann *et al.*, 2002; Nusser and Mody, 2002), highlighting its pivotal role in regulating network excitability.

1.2.3 Metabotropic GABA receptors

Metabotropic $GABA_B$ receptors are heterodimers formed from $GABA_B$ receptor subunits 1 (GBR_1) and 2 (GBR_2) (Bettler *et al.*, 2004; Kaupmann *et al.*, 1998) (Figure 1.7, pg 24) or their splice variants (Kuner *et al.*, 1999). Neither GBR_1 or GBR_2 are functional when expressed separately (Kuner *et al.*, 1999). In the rat brain, both GBR_1 and GBR_2 are found in high levels in most regions (Bischoff *et al.*, 1999; Durkin *et al.*, 1999). Presynaptically, they are negatively coupled to N- and P/Q- type Ca^{++} channels through a G-protein cascade to decrease transmitter release (Anwyl, 1991), while postsynaptically, they open G-protein gated inward-rectifying K^+ channels (GIRK) (Lüscher et al., 1997), causing a slow inhibitory postsynaptic potential (IPSP) (Andrade *et al.*, 1986; Misgeld *et al.*, 1995) .

Activation of $GABA_B$ receptors can also modulate cAMP production (Simonds, 1999), producing a wide range of actions on ion channels and target proteins for cAMP-dependent kinase (protein kinase A or PKA), allowing modulation of neuronal and synaptic functions (Gerber and Gahwiler, 1994). For a recent review of $GABA_B$ receptor structure and physiology, see (Bettler *et al.*, 2004).

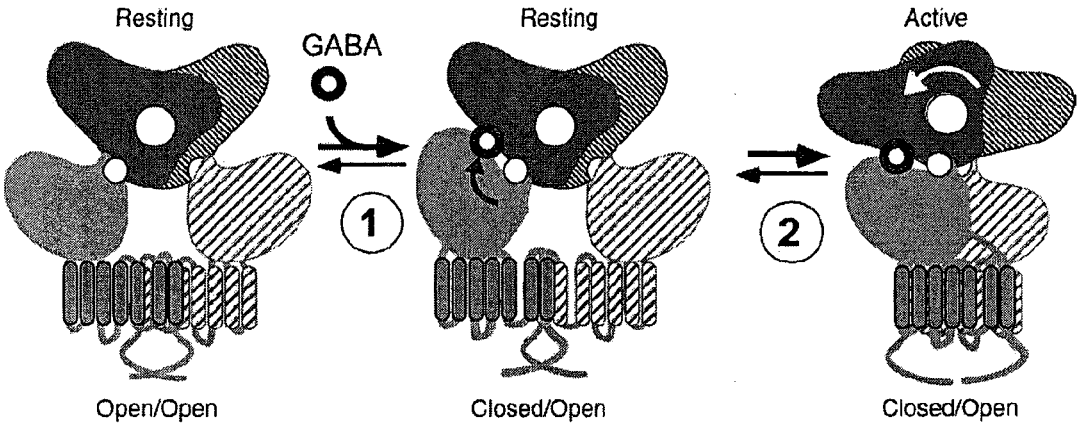

Figure 1.7. Putative activation mechanism of the $GABA_B$ heterodimer. Left: schematic representation of the inactive receptor with both receptor binding sites in the open state and in the resting position. Step 1: Binding of GABA closes the binding site and induces a change in the orientation of the two binding site modules to that of the active orientation (Step 2). The small white circles represent the axis allowing the opening and closing of each binding site. The large white circle represents the axis for the change in the orientation of the two binding site modules.

(Bettler *et al.*, 2004)

1.2.4 GABA in Development

In 1978, Obata and colleagues reported that GABA, a neurotransmitter believed at that time to be solely inhibitory, could actually depolarize chick spinal neurons in early development. Today, it is well-known that GABA serves an excitatory role in development (for a comprehensive review, see Ben-Ari *et al.*, 2007), and subsequently switches to its predominantly inhibitory role in conjunction with the maturation of the Glu system, which in the rat, occurs within the first three postnatal weeks (Ben-Ari, 2006a; Tyzio *et al.*, 2007). Much of our current knowledge has been determined from a plethora of studies sparked by a 1989 investigation looking at developmental changes in GABAergic signaling in neonatal hippocampal slices (Ben-Ari *et al.*, 1989). While many refinements and more specific knowledge has since been garnered, the four basic findings this investigation provided remain intact: 1) acting through $GABA_A$ receptors, GABA excites immature neurons due to an elevated concentration of $[Cl^-]_i$ that gradually decreases as development progresses 2) network activity in early development is driven by giant depolarizing potentials (GDPs) that occur in a synchronized fashion through $GABA_A$Rs. 3) GABAergic networks are expressed first, preceding glutamatergic (AMPAR-mediated) synaptic transmissions 4) early glutamatergic events primarily occur through postsynaptic NMDARs (Ben-Ari *et al.*, 1989).

Developmental changes in GABA signaling are dependent upon $[Cl^-]_i$ concentrations, which are primarily controlled by two chloride co-transporters (for review, see Delpire, 2000). Accumulation of $[Cl^-]_i$ is achieved through the NKCC1 membrane transport protein, which transports one Na^+, one K^+ and two Cl^- into the cell through an electroneutral, ATP-independent mechanism (Payne *et al.*, 2003), while the KCC2 co-

transporter is responsible for Cl^- extrusion, removing one K^+ and two Cl^- molecules using the large outward K^+ gradient to drive the process (Delpire, 2000; Jarolimek *et al.*, 1999). In early development, NKCC1 is present at high levels while KCC2 is only weakly expressed, resulting in $[Cl^-]_i$ concentrations that, upon $GABA_AR$ activation, can cause depolarization through an efflux of Cl^- upon channel opening if the gradient is large enough, or an inhibitory shunting action if the resting membrane and the Cl^- reversal potentials are similar (Banke and McBain, 2006; Ben-Ari, 2002). As the system matures, however, this situation reverses, lowering $[Cl^-]_i$ levels and promoting Cl^- influx in response to channel activation, thus hyperpolarizing the cell and making the occurrence of action potentials less likely (Ben-Ari *et al.*, 2007; Chudotvorova *et al.*, 2005) (Figure 1.7, pg 24).

While the timing of this GABA-excitatory/GABA-inhibitory switch is generally agreed to occur within the first three postnatal weeks in the rat, it is now evident that neuronal type, brain structure, strain and sex also play pivotal roles (Galanopoulou, 2008b; McCutcheon and Marinelli, 2009). In Sprague-Dawley rat HC, the mean age for this switch appears to be around PND13 (Khazipov *et al.*, 2004). However, the time course also depends on sex, with females maturing at a faster rate than males (Galanopoulou, 2008a; Kyrozis *et al.*, 2006), a difference that may have substantial repercussions on studies involving manipulations during this critical developmental stage.

1.3 Domoic Acid

Domoic acid (DOM), an amino acid structurally similar to KA, is a naturally-occurring, hydrophilic excitotoxin produced by several marine organisms (e.g. *Chondria armata* and various strains of *Pseudo-nitzschia*) under specific environmental conditions (for review, see Jeffery *et al.*, 2004; Pulido, 2008). Capable of accumulating to various degrees in a wide variety of shellfish species, DOM became infamous in 1987, when 107 people fell ill from eating cultivated blue mussels (*mytilus edulis*) grown in Prince Edward Island, Canada. Of these original 107 individuals, most experienced gastrointestinal symptoms, more than 40% reported severe headaches, 19 were hospitalized, with 12 requiring intensive care due to coma, seizure, and/or other serious complications, and 4 died within four months (Perl *et al.*, 1990; Teitelbaum *et al.*, 1990). An investigation of the neuropathology of those who had died revealed hippocampal and amygdalar cell loss and astrocytosis similar to that found in animals treated with KA (Teitelbaum *et al.*, 1990). Neuropsychological testing of 14 of the most severely affected survivors ~5 months after the incident showed that 12 had major anterograde memory deficits, but no other cognitive disturbances, although electroencephalogram (EEG) tracings revealed a mild-to-moderate slowing of background activity in 11 of the 14 tested (Teitelbaum *et al.*, 1990). In addition, one man developed complex partial epilepsy 12 months after DOM ingestion, with subsequent pathological evaluation at time of death revealing severe bilateral hippocampal sclerosis (Cendes *et al.*, 1995). It should be noted that, while the symptoms of DOM poisoning tended to become worse in a dose-dependent fashion, both age and sex also appeared to be major risk factors, with older males most susceptible (Perl *et al.*, 1990).

Since this incident, a number of studies examining DOM toxicity in adult mice, rats, and non-human primates have found similar dose-dependent neurobehavioural responses to DOM exposure that progress through a series of sequelae including hypoactivity, scratching, tremors, seizures, and death (Grimmelt *et al.*, 1990; Iverson *et al.*, 1989; Scallet *et al.*, 2004; Tasker *et al.*, 1991; Tryphonas *et al.*, 1990a; Tryphonas *et al.*, 1990b). In addition, tests of learning and memory have shown impairments following acute DOM administration (Nakajima and Potvin, 1992), as well as dose-dependent hippocampal alterations and other neuropathologies (for review, see Pulido, 2008) equivalent to that seen in the human condition described above, and in animal models using kainic acid. Changes in behaviour along with altered EEG activity and increased *c-fos* immunoreactivity in the HC has also been reported in adult rats following acute DOM (Robertson *et al.*, 1992; Scallet *et al.*, 2004).

Investigations into the effects of age on DOM exposure have revealed a 40-80x increase in sensitivity in neonatal rats as measured by seizure activity and behavioural alterations (Xi *et al.*, 1997). It has been postulated that this heightened response is due to incomplete blood-brain barrier protection during early development (Mayer, 2000), and indeed, a study using PND0 to PND22 rat pups has shown a decrease in DOM potency with increasing maturity (Doucette *et al.*, 2000). A recent investigation looking at the transfer of DOM *in utero* has found concentrations as high as 5% of the maternally circulating DOM in both foetal brain and amniotic fluid (Maucher and Ramsdell, 2007). Effects of foetal exposure to DOM indicate an increased risk of abortion, death, and/or reabsorption by the dam (Khera *et al.*, 1994). Foetuses that survive show a lower seizure threshold to subsequent DOM exposure at a variety of postnatal time points

(Dakshinamurti *et al.*, 1993). A similar reduction in seizure threshold to the chemical convulsant pentylenetetrazole (PTZ) has been reported in larval zebrafish following embryonic DOM administration (Tiedeken and Ramsdell, 2007).

1.3.1 Mechanism of action

Since the histopathology of DOM exposure in human and animal brains resembles that following KA-induced excitotoxicity, and its structure is similar to that of both KA and Glu, it is not surprising that studies have shown DOM-induced activation of Glu receptors (Lomeli *et al.*, 1992; Sommer *et al.*, 1992), and in particular, ionotropic KA subunits GluK5 and GluK6 (Debonnel *et al.*, 1990; Lomeli *et al.*, 1992), for which it demonstrates an affinity considerably greater than either KA or Glu (for review, see Bleakman *et al.*, 2002; Lerma *et al.*, 2001). However, the exact mechanism responsible for DOM's excitotoxic effects is still largely unknown, although it appears tied to the ability of DOM to block desensitization in KARs at both pre- and postsynaptic sites (for review, see Jeffery *et al.*, 2004; Pulido, 2008), with subsequent increases in intracellular Ca^{++} levels (Dakshinamurti *et al.*, 1993; Xi and Ramsdell, 1996).

1.4 The Limbic System

Some of the most readily excitable regions in the brain are contained within a group of structures often referred to as the 'limbic system' (MacLean, 1952). Functions mediated by the limbic system include emotion and motivation, as well as the ability to learn and remember. While there is no real agreement over the exact structures that comprise this system, it is generally considered to consist of both cortical and subcortical regions

including the HC, amygdala, hypothalamus, nucleus accumbens, thalamus, cingulate cortex, and regions of the prefrontal cortex (for review, see Morgane *et al.*, 2005). The two areas most central to the limbic system are the amygdala and the HC. Both are involved in learning and memory processes and are highly excitable, allowing for fast, flexible transmission of information (Kim *et al.*, 2006; Morgane *et al.*, 2005). They are also the regions most susceptible to seizuregenesis (Bertram *et al.*, 1998), and as such, will be the focus for the remainder of this dissertation.

The amygdala, known to be a key player in mediating fear (Davis and Whalen, 2001; Walker and Davis, 2002) is also critical for mediating the effects of stress on hippocampal long-term potentiation (LTP) and HC-dependent memory processes (McGaugh, 2002). The effects of stress on learning and memory and the processes that underlie it can be many and varied (Sapolsky, 2003). Interestingly, stress has been shown to alter dendrite morphology, neurotoxicity and neurogensis in the HC (McEwen, 2002), and is also a known trigger for seizure activity in individuals with epilepsy (Frucht *et al.*, 2000; Temkin and Davis, 1984). During most forms of stress, high levels of corticosterone (CORT) produce a distinct inhibitory effect on hippocampal plasticity (e.g. LTP) with chronic stress altering the balance between excitation and inhibition, thus leading to dendritic remodeling and changes in hippocampal function (Sapolsky *et al.*, 1985; Sapolsky, 1990). In addition, CORT has been shown to modify the actions of GABA neurotransmission (Freund and Buzsaki, 1996) and alter the pharmacological properties of $GABA_A$ receptors (Orchinik *et al.*, 2001). For a review of the role of stress on limbic system function and plasticity, the reader is referred to Sapolsky (2003).

1.4.1 Hippocampus

With its highly organized laminar structure and its ability to adapt quickly and readily in response to external stimuli, the HC is perhaps the most studied region of the mammalian brain. In the rat, the HC is an approximately C-shaped structure located in both hemispheres that sits in an anteriorally-facing dorsal/ventral alignment. It can be divided into two main sections; namely the dentate gyrus (DG) and the HC proper. However, there are other areas that, while not necessarily considered part of the HC, are closely associated, including the presubiculum, the parasubiculm, and the entorhinal cortex (EC). Since they are part of the overall hippocampal network, they will also be described. In addition, there are several notable pathways that are associated with the HC (Figure 1.8, pg 32). Contained entirely within the HC network is the mossy fibre pathway, running from the DG to area CA3 in the HC proper, which may then project further into the HC via the Schaffer collaterals. The perforant path consists of efferent EC projections that perforate the subicular region on their way to the DG and the HC proper. Entorhinal projections may also reach the HC via the alvear pathway (also known as the temporoammonic pathway), particularly in dorsal regions (Deller *et al.*, 1996). And finally, the fimbria-fornix system is the main route for subcortical afferent and efferent connections (for review, see Amaral *et al.*, 2007).

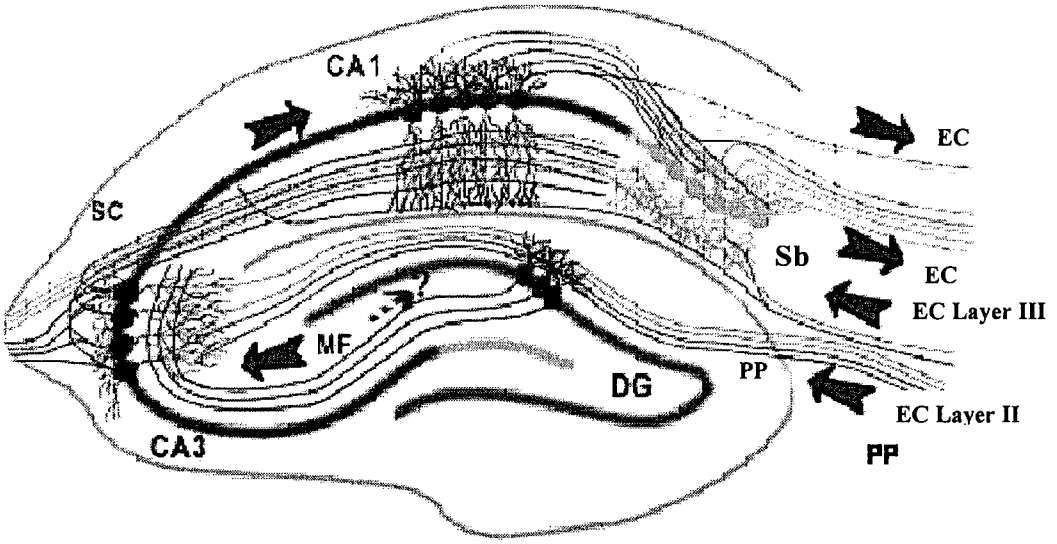

Figure 1.8. Pathways of the hippocampus. In the traditional view, input from layers II and III of the entorhinal cortex (EC), via the perforant path (PP), form connections with the dentate gyrus (DG) as well as with hippocampal area CA3 and CA1 pyramidal cells. CA3 neurons also receive input from the DG through the mossy fibres (MF), which subsequently innervate CA1 via the Schaffer collaterals (SC). CA1 neurons then send axons to the subiculum (Sb) which forwards the processed information back to the EC, forming a loop. However, it has recently been proposed that there may be a 'backprojection' as well, from CA3 through the MF pathway back to the DG (broken arrow).

(Adapted from: www.bristol.ac.uk/.../pathway/hippocampal.htm)

1.4.1.1 Dentate gyrus

The DG consists of three layers (Figure 1.9, pg 34). The layer closest to the hippocampal fissure (the region separating the DG from the HC proper) is relatively cell-free, and is called the molecular layer. In the rat, it is ~250μm thick, and is often further divided into the 'outer' molecular layer (the outer two-thirds) and the 'inner' molecular layer (the region closest to the principal cell layer). The principal, or granule cell (GC) layer is densely packed and approximately 4-8 granule cells thick, with each excitatory GC having an elliptical cell body (~10μm wide by 18μm high) and spiny dendrites that extend into the molecular layer (Spruston and McBain, 2007). The GC and molecular layer (together known as the fascia dentata) form a V-shape in the dorsal (septal) portion of the rat brain, and a U-shape in the more ventral (temporal) regions. The third layer of the DG is the polymorphic layer, or hilus, situated within the fascia dentata. The hilus contains a huge variety of cell types, most of which are GABAergic interneurons (Freund and Buzsaki, 1996). Often, these inhibitory cells are classified based on neurochemical markers as well as morphology, since neurons expressing distinct neurochemistry have been found to have different dendritic structure (Gulyas *et al.*, 1999). In addition, one notable excitatory cell, the large (25-35μm) triangular mossy cell is also located in this region. These cells have been shown to project to hilar interneurons, as well as to innervate dendrites of granule cells in both the ipsilateral and contralateral DG (for review, see Amaral *et al.*, 2007).

1.4.1.2 Hippocampus proper

As shown in Figure 1.9 (pg 34), the HC proper, like the DG, can also be divided into layers. The most superficial is the alveus, which contains axons from

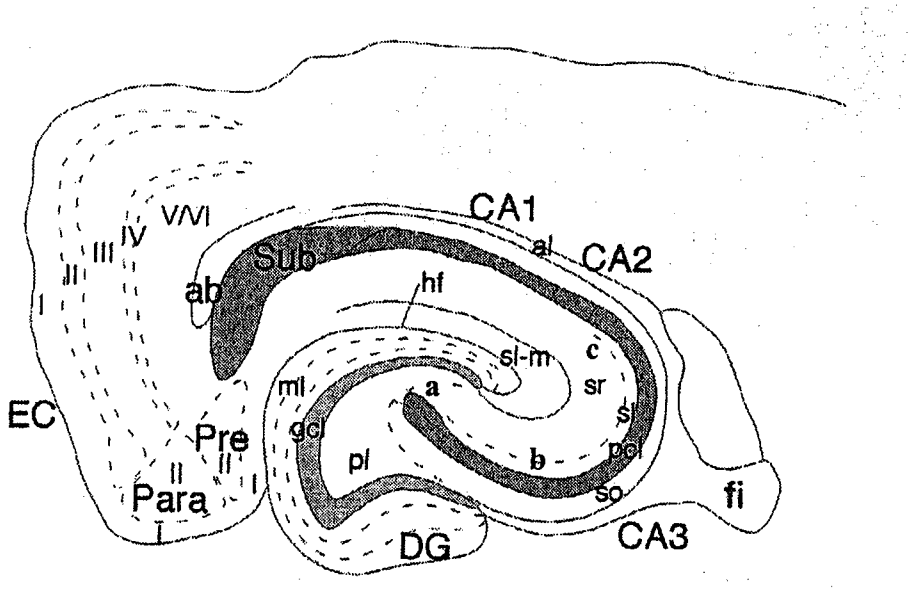

Figure 1.9. Regions and layers of the hippocampus. EC- entorhinal cortex; Sub- subiculum; Para- parasubiculm; Pre- presubiculum; DG- dentate gyrus; CA1- CA1 field of the hippocampus; CA2- CA2 field of the hippocampus; CA3- CA3 field of the hippocampus; ab- angular bundle; al- alveus; hf- hippocampal fissure; fi- fimbria; ml- molecular layer; gcl- granule cell layer; pl- polymorphic layer (hilus); sl-m- stratum lacunosum-molecular; sr- stratum radiatum; sl- stratum lucidum; pcl- pyramidal cell layer; so- stratum oriens; a- region CA3a; b- region CA3b; c- region CA3c; Roman numerals- cortical layers.

(Amaral *et al.*, 2007. Reproduced with permission)

pyramidal neurons that run to the fimbria. The next layer is stratum oriens (SO), where basal dendrites of pyramidal neurons are located. Stratum pyramidale consists of three sub-fields: CA3, CA2, and CA1 (CA: cornu ammonis), terminology originally implemented by Lorente de Nó (circa 1934). It is the principal (excitatory) cell layer in the HC proper, commonly called the pyramidal cell layer (PCL). In region CA3, this is also the area where mossy fibers from the granule cells of the DG synapse on pyramidal cell bodies. Also in CA3, but not CA2 or CA1, is a thin region called the stratum lucidum (SL), where GC mossy fibers run before forming synapses on their targets in the PCL. The stratum radiatum (SR), located inside the SL in CA3 and directly above the PCL in CA2 and CA1, houses CA3 to CA3 associational connections and the CA3 to CA1 Schaffer collateral axons. And finally, in stratum lacunosum-moleculare (SL-M) are the Schaffer collaterals and layer III perforant path fibres from the entorhinal cortex where they terminate on the distal, apical dendrites of CA1 pyramidal cells (for review, see Amaral *et al.*, 2007).

1.4.1.3 Subiculum, presubiculum, parasubiculum and entorhinal cortex

The subicular region in the rat is evident as a sudden widening at the end of the CA1 PCL (O'Mara *et al.*, 2001). It is a major source of efferent projections from the hippocampal formation (Ishizuka, 2001; for review, see Amaral *et al.*, 2007). At the tip of the subiculum, adjacent to the molecular layer of the DG, is the presubiculum, which subsequently neighbours the parasubiculum. Both these regions have a number of associational and commissural connections, including reciprocal connections with the EC, as well as projections to structures such as the thalamus (Amaral *et al.*, 2007).

The entorhinal cortex consists of six layers and is the main entry point for information to enter the HC, as well as the primary relay for processed information to travel back to neocortical regions. As such, this area is both the beginning and the end of a complex loop of information processing mediated through hippocampal activity. Of the six EC layers, layer II, which projects to the DG and CA3 via the perforant pathway and layer III, which gives rise to perforant and alvear path connections with CA1 and the subiculum contribute directly to hippocampal input (see Figure 1.8, pg 32), as the other layers form mostly associational connections within the EC itself, and/or receive return projections (i.e. layer V, VI, and I).

1.4.1.4 Hippocampal information flow

The traditional view of HC information flow has been that of a trisynaptic circuit, composed of three sequential glutamatergic synapses. In this model, perforant path axons from layer II neurons in the EC project to the outer two-thirds of the DG molecular layer to synapse on distal granule cell dendrites. Subsequently, mossy fibre axons of GCs project to proximal dendrites of area CA3 pyramidal cells (through the SL layer), which then forward the information on through Schaffer collateral axons to the apical dendrites of CA1 neurons (located in SR) (Amaral and Witter, 1989). However, many studies have shown that this projection may not be the only one responsible for hippocampal activity. In fact, there is now considerable evidence that a 'backprojection' from CA3 to the DG may exist (Figure 1.8, pg 32) (for review, see Scharfman, 2007).

Interestingly, evidence for a backprojection appears to be most predominant in the ventral HC (Li *et al.*, 1994), and rather than resulting in a direct excitatory influence on

GCs, seems to inhibit these cells indirectly through activation of GABAergic neurons in the hilus (Acsady *et al.*, 1998). The implications of this projection are quite intriguing, especially under pathological conditions such as epilepsy, where loss of hilar interneurons is often a defining feature.

1.4.2 Amygdala

Deep within the temporal lobe, the almond-shaped amygdala is situated just anterior to the ventral portion of the HC. It is composed of ~13 nuclei which may then be further subdivided, and that have extensive connections both within and between each other. For the purposes of this dissertation, these nuclei will be divided into three groups based on divisions described by Sah and colleagues (2003) (Figure 1.10, pg 38): 1) the deep or basolateral group, including the lateral nucleus, the basal nucleus, and the accessory basal nucleus 2) the superficial or cortical-like group, which includes the cortical nuclei and nucleus of the lateral olfactory tract, and 3) the centromedial group, including the medial and central nuclei.

The basolateral or deep nuclei are often collectively referred to as the basolateral complex (as opposed to the basolateral nucleus which is made up of the lateral and the basal nuclei), and contain two main types of cells. The first is a randomly organized pyramidal-like, excitatory cell that comprises ~70% of the cell population in this region (Faber *et al.*, 2001), and receives inputs from both cortical and thalamic regions (Farb *et al.*, 1995). The second type has a smaller soma (~10-15μm) and a stellate appearance, and provides an inhibitory function (for review, see Sah *et al.*, 2003). About half of these cells contain parvalbumin, while the other half express calbindin and/or calretinin

Basolateral Group	**Corticomedial Group**	**Centromedial Group**
Lateral nucleus -dorsolateral division -ventrolateral division -medial division	*Nucleus of the lateral olfactory tract* *Bed nucleus of the accessory olfactory tract*	*Central nucleus* -capsular division -lateral division -intermediate division
Basal nucleus -magnocellular division -intermediate division -parvicellular division	*Anterior cortical nucleus* *Periamygdaloid cortex* -medial division -sulcal division	*Medial nucleus* -rostral division -central division dorsal portion ventral portion -caudal division
Accessory basal nucleus -magnocellular division -parvicellular division		

Figure 1.10. Divisions of the amygdala nuclei.

(Adapted from Sah et al., 2003)

(Kemppainen and Pitkanen, 2000; McDonald and Mascagni, 2001). In addition, a minor population of several other types of cells (believed to be inhibitory) have been described (Sah *et al.*, 2003).

The cortical-like group have, as the name suggests, many cortical characteristics including a layered structure, and are located near the surface of the brain. These nuclei are most specifically involved with functions related to olfaction, and contain a variety of intra-amygdalar connections. The centromedial nuclei (historically often grouped with the cortical region), is found in the dorsomedial portion of the amygdalar complex and processes many autonomic inputs (Sah *et al.*, 2003).

1.4.2.1 Amygdala Information Flow

Inputs to the amygdala can be divided into those from cortical and thalamic structures (sensory and memory systems), and those from the hypothalamus or brain stem (behaviour and autonomic response). In the most basic sense, information input is primarily through the lateral region, while response output occurs through centromedial areas (Sah *et al.*, 2003). Sensory information is transmitted from all modalities (olfactory, somatosensory, auditory, visual, gustatory and visceral) (Sah *et al.*, 2003), and there are also particularly strong (and reciprocal) connections between many amygdalar nuclei and the HC (McDonald, 1998). Efferent connections to cortical, hypothalamic, and brain stem regions are widespread, with olfactory projections being especially substantial. However, as mentioned above, the most extensive connections are those with the HC, although other major targets include the prefrontal cortex,

nucleus accumbens, and thalamus. Figure 1.11 (pg 41) provides a schematic view of inputs to and outputs from the amygdala.

1.5 Seizures and Epilepsy

An epileptic seizure, according to The International League against Epilepsy (ILAE) is "*a transient occurrence of signs and/or symptoms due to abnormal excessive or synchronous neuronal activity in the brain*", while epilepsy is defined as "*a chronic disorder of the brain characterized by an enduring predisposition to generate epileptic seizures, and by the neurobiological, cognitive, psychological, and social consequences of this condition. The definition of epilepsy requires the occurrence of at least one epileptic seizure*" (Commission on Classification and Terminology of the International League Against Epilepsy, 1981). It is important to note that epilepsy is a variable disorder (hereafter referred to as 'the epilepsies'), able to manifest in different ways depending on the brain region(s) affected (Ure and Perassolo, 2000), and exhibits many diverse etiologies, including genetic alterations, childhood fever, or head trauma (Meldrum and Chapman, 1999; Wong, 2005). As well, the epilepsies have also been associated with conditions such as depression (Jobe, 2003) and other psychiatric disorders including schizophrenia (for review, see Gaitatzis *et al.*, 2004).

1.5.1 *Epidemiology and treatment*

Approximately 50 million people worldwide are estimated to suffer from some form of epilepsy, with over 300,000 diagnosed yearly (Porter, 1988). In 60-70% of these cases, there is no apparent cause identified. In addition, males are slightly more likely to

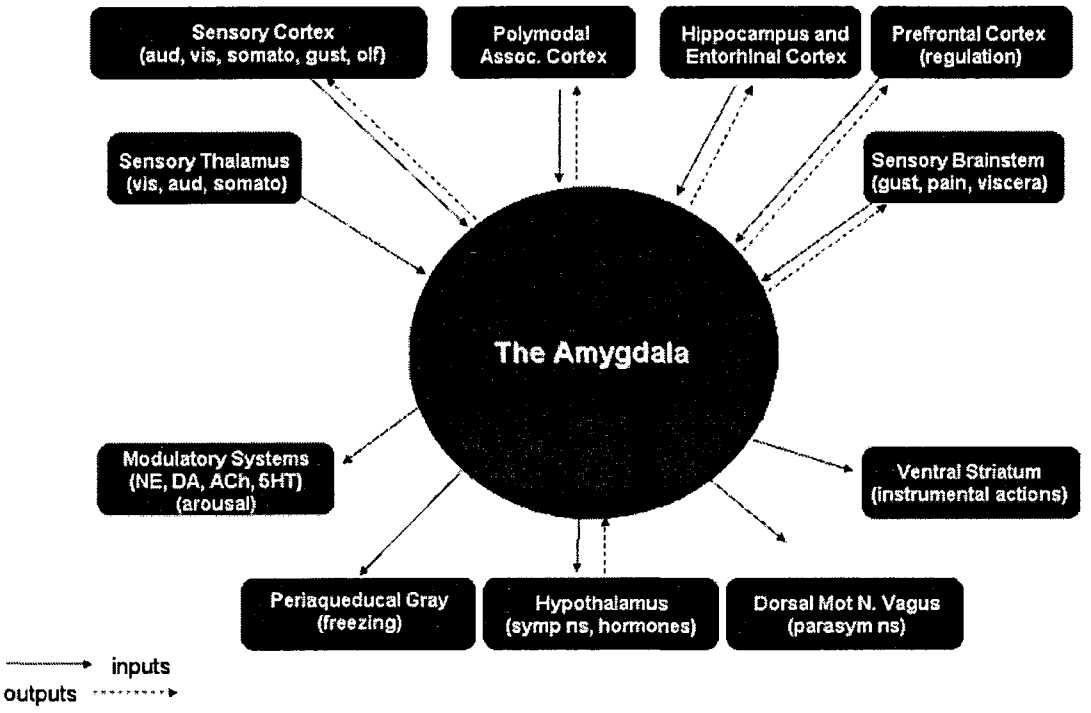

Figure 1.11. Schematic view of various amygdalar inputs and outputs.

(Dr. Joseph E. LeDoux, Center for Neural Science, NYU, New York
http://www.scholarpedia.org/article/Amygdala)

develop this disorder than are females (World Health Organization, 2009). Although epilepsy can occur at any age, there is a strong link between precipitating events during childhood (e.g. head trauma) and the development of epilepsy later on in life, particularly for temporal lobe epilepsy (TLE), one of the most common forms (Blume, 2006; Meldrum and Chapman, 1999). It is currently believed that developmental processes that guide neuronal growth and maturation may contribute to this increased adulthood risk for epileptogenesis following CNS insult or injury during the early years (Figure 1.12, pg 43 presents a visual conceptualization of possible contributing factors; for review, see Wong, 2005). To date, the most common treatment for the epilepsies is symptomatic, usually through the use of antiepileptic drugs (AEDs), but for those who do not respond to medication (~30%, for review see Blume, 2006), surgery is often the only alternative (Epilepsy Foundation of America, 2009).

1.5.2 *Classification of epileptic seizures*

Classification of an epileptic seizure is initially determined by the site of seizure initiation. If the seizure involves the entire cortex it is considered to be generalized. If it is confined to one area (e.g. the limbic (or temporal) region), it is referred to as a partial seizure. Further classification is based on seizure characteristics, such as whether loss of consciousness occurs during partial seizure, or whether a partial seizure spreads to involve the rest of the cortex (i.e. becomes generalized). Additionally, behaviours such as automatisms (purposeless movements such as repetitive lip-smacking) also help define seizure type (Parton and Cockerell, 2003). Normally, seizures are self-limiting, and stop on their own. Very occasionally, however, seizure activity will continue for extreme periods of time. This phenomenon is called status epilepticus (SE), and it can

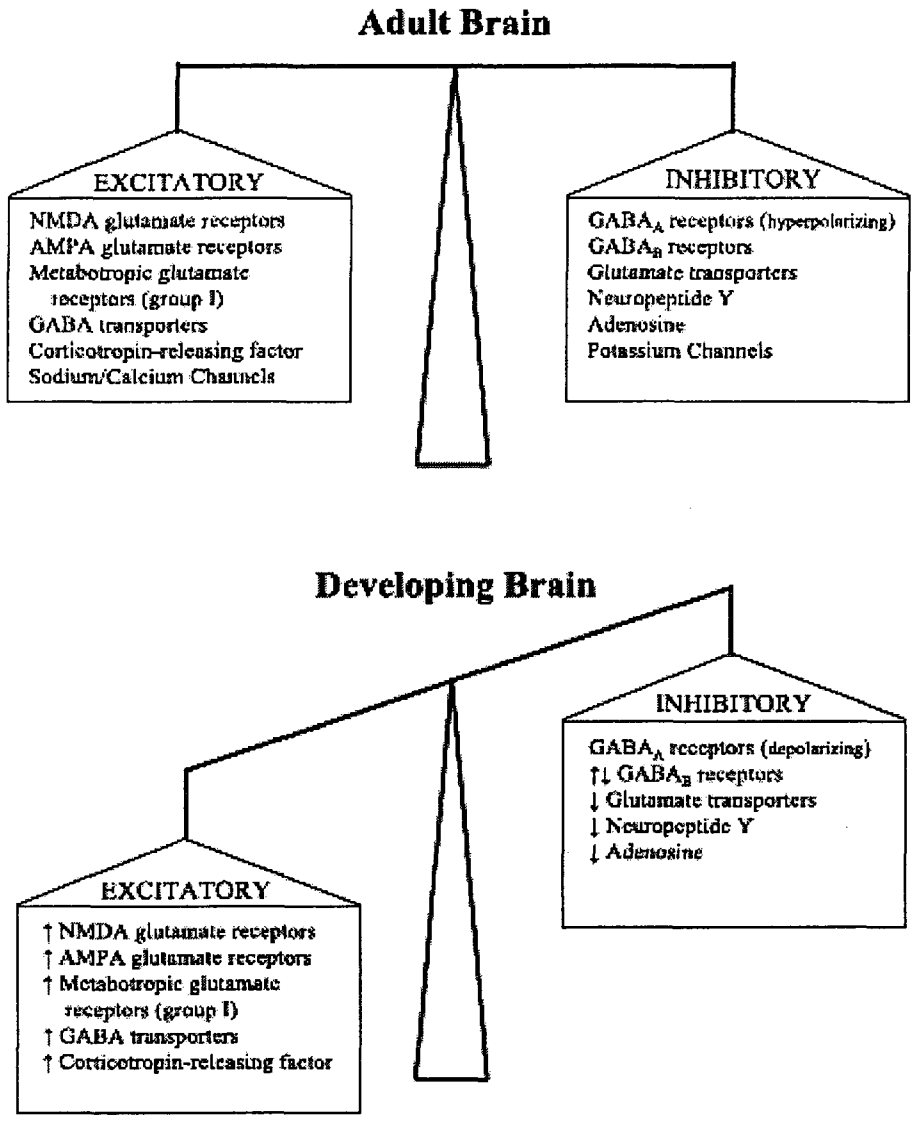

Figure 1.12. Factors that may contribute to seizure susceptibility in the developing brain. Under normal conditions in adulthood, there is a carefully maintained balance between excitation and inhibition, but during development, many systems exhibit an increased tendency toward excitation to aid in neuronal growth, differentiation, and network formation. Central nervous system insult or injury experienced at this time may therefore result in permanent alterations that ultimately lead to epileptogenesis.

(Wong, 2005. Used with permission)

become life-threatening. The ILAE classification chart for epileptic seizures, as well as a brief description of accompanying clinical features, can be found in Figure 1.13, pg 45. The ability to classify seizures is considered to be an important part of diagnosis, and plays an important role in subsequent AED selection (Stern, 2009).

1.5.3 *Seizure threshold*

The concept of seizure threshold is that everyone has a preset balance (probably genetically determined) between excitatory and inhibitory forces in the brain (see Figure 1.12, pg 43). If this threshold is low, then the individual will be more predisposed to seizure activity and the possibility of developing epilepsy, whereas someone with a high seizure threshold will be far less susceptible (Epilepsy Foundation of America, 2009). As with many other physiological functions, the threshold level can vary depending on external and internal conditions, or may even be permanently altered through environmental experiences, including head trauma, high fever during infancy, exposure to prenatal and postnatal toxins, as well as previous seizure incidents (Wong, 2005). However, little is known as yet about how seizure threshold mechanisms work, or what underlying system(s) regulate its balance.

1.5.4 *Underlying functional and structural changes in epileptogenesis*

During a seizure, many neurons fire simultaneously as a result of synchronous excitatory inputs, leading to alterations in ionic flow (e.g. Na^+, K^+, Ca^{++}) (for review, see Avanzini and Franceschetti, 2003). Locally, this activity may spread through the progressive recruitment of cells within one discrete brain region (e.g. amygdala and/or hippocampus

I. Partial Seizures (originating from a discrete brain region)

A. Simple partial seizures (no loss of consciousness)

1. Motor, sensory or somatosensory symptoms (e.g. movements, tingling, hearing buzzing noises or visualizing flashing lights)
2. Autonomic symptoms (e.g. flushing, sweating, piloerection)
3. Psychic symptoms (e.g. déjà vu, hearing music)

B. Complex partial seizures (with impaired consciousness)

1. Delayed impairment of consciousness (with or without automatisms)
2. Immediate impairment of consciousness (with or without automatisms)

C. Partial seizures (simple or complex) evolving into generalized seizures

II. Generalized Seizures (convulsive and non-convulsive)

A. Absence seizures (also known as 'petit mal' seizure; consists of staring/lapses of awareness lasting only a few seconds)
B. Myoclonic seizures (rapid, brief muscular contractions, usually occurring on both sides of the body simultaneously)
C. Clonic seizures (rhythmic jerking of the limbs)
D. Tonic seizures (sudden extreme stiffening of muscles)
E. Atonic seizures (abrupt loss of muscle tone –also known as 'drop attacks')
F. Tonic-clonic seizures (also known as 'grand mal' seizure; begins with limb stiffening and progresses to alternating contraction and relaxation of muscles)

III. Unclassified Epileptic Seizures

Seizures that cannot be classified due to incomplete data.

Figure 1.13. Classification of epileptic seizures.
(Adapted from the Commission on Classification and Terminology of the International League Against Epilepsy, 1981)

in TLE), or through the broader recruitment of neurons located in more distally located structures (seizure generalization). Epileptic activity, then, does not result just from abnormalities in specific individual cells, but is rather a consequence of the synchronous activation of large populations of hyperexcitable neurons through both normal and pathological fibre connections (for reviews, see Avanzini and Franceschetti, 2003; Meldrum and Chapman, 1999). How and why these neurons collectively become hyperexcitable in the first place is still largely unknown, but through careful use of relevant animal models, the pieces of this complex and important puzzle are gradually falling into place.

As stated previously, epilepsy encompasses a broad range of seizure types and related pathologies, and a massive amount of research has been dedicated to determining possible causes and mechanisms for each in the hopes of aiding development of better therapeutic interventions, or ultimately, a cure. It is well beyond the scope of the current document to discuss all of these different epileptiform manifestations at every organizational level. Instead, an overview of the major changes that have been noted in both the human condition, and in animal models for TLE will be presented, as this is the form of epilepsy that is most relevant to the work described herein.

The most commonly identified region for the initiation of TLE is the amygdala and HC (for review, see Bertram, 2009). With a complex network of highly interconnected excitatory cells (e.g. pyramidal) regulated by a vast array of inhibitory interneurons (Aroniadou-Anderjaska *et al.*, 2007; Ehrlich *et al.*, 2009; Freund and Buzsaki, 1996) that, among other things, control neuronal oscillations, the amygdalar/hippocampal

region is a prime location for generating synchronous bursting activity (for review, see McCormick and Contreras, 2001). For instance, in hippocampal area CA3 there are subsets of pyramidal cells that intrinsically generate bursts of 2 to 5 action potentials just from one brief depolarization (Franceschetti *et al.*, 1995). Functionally, the consequence of burst activity is increased input to postsynaptic regions, and can result in the recruitment of many different neurons simultaneously (Miles and Wong, 1983). In addition, the burst discharges that occur can back-propagate into pyramidal dendrites, triggering further dendritic spikes (Larkum *et al.*, 1999). Normally, this extraordinarily powerful excitatory activity is tightly contained through both tonic and phasic GABAergic inhibition (Eugene *et al.*, 2007; Farrant and Nusser, 2005) as well as through highly regulated extra- and intracellular ion distribution (mediated neuronally and through locally situated glial cells) (Kofuji and Newman, 2004; Nadler, 2003). However, there are several alterations that occur during TLE development that appear to promote increased excitation in these structures. The most characteristic of these is mossy fibre sprouting (MFS) in the DG, with a pathological extension of granule cell axons into the inner molecular layer (e.g. Babb, 1991; Houser, 1990; Sutula *et al.*, 1989), and sometimes also into the SO of area CA3 as well (Ben-Ari and Cossart, 2000). This sprouting may be visualized histologically using Timm staining, a method that labels all heavy metals present in the tissue. Since mossy fibres normally contain high levels of unbound zinc (Nadler, 2003; Paoletti *et al.*, 2009), this method can provide a good representation of MF location and allow for subsequent quantification and statistical evaluation (Slomianka, 1992). However, the functional purpose of MFS is still under investigation, since the synaptic connections from these fibres have been shown to target both excitatory and inhibitory neurons (Kotti *et al.*, 1997; Okazaki *et al.*, 1995; Wenzel

et al., 2000; Zhang and Houser, 1999). It has subsequently been suggested that the likelihood of seizures occurring in a system altered in this manner may depend in large part upon fluctuations in physiological conditions, thus helping to explain why seizure activity is so variable among individuals (Scharfman, 2002).

Another alteration commonly seen in TLE is hippocampal cell loss, particularly in the hilar region of the DG. Some of the first hilar cells to die are interneurons (Buckmaster and Dudek, 1997b; Kobayashi and Buckmaster, 2003), implicating loss of inhibition as an important driving factor in seizure progression. Interestingly, interneuronal susceptibility appears to be quite selective, with cells that contain somatostatin (HIPP—hippocampal to perforant path) among those hardest hit (Binaschi *et al.*, 2003; Buckmaster and Dudek, 1997b; de Lanerolle *et al.*, 1989; Kobayashi and Buckmaster, 2003; Sperk *et al.*, 1992), as well as interneuronal populations containing the calcium-binding protein parvalbumin (primarily basket cells; Sloviter, 1989). Loss of somatostatin-containing neurons has also been reported in the basolateral amygdala (Pitkanen *et al.*, 1998; Tuunanen *et al.*, 1997). In addition, a substantial loss of excitatory hilar mossy cells has also been noted (Buckmaster and Schwartzkroin, 1994), a phenomenon that has sparked several theories regarding network connectivity, particularly since it appears that surviving mossy cells experience dramatic increases in excitability (Scharfman, 2002).

There are many other alterations that may occur as a consequence of seizure, including increases in gliosis (Bordey and Sontheimer, 1998; D'Ambrosio *et al.*, 1999; Hinterkeuser *et al.*, 2000), brain derived neurotrophic factor (BDNF) and its receptor,

tropomyosin-related kinase B (TrkB) (for review, see McNamara *et al.*, 2006), and *c-fos* gene expression (Dragunow and Robertson, 1988; Morgan *et al.*, 1987), as well as increased granule cell neurogenesis (Bengzon *et al.*, 1997; Parent *et al.*, 1997; Parent *et al.*, 1998; Scott *et al.*, 2000), often to ectopic sites in the hilus (Scharfman *et al.*, 2000). In addition, a reduction in KCC2 co-transporter expression has been reported (Kahle *et al.*, 2008; Li *et al.*, 2008).

1.5.5 The use of EEG in epilepsy diagnosis

As stated previously, seizures result from the synchronous discharge of many cortical neurons, and in humans, this electrical activity is often recorded through electrodes placed on the scalp to provide a printout of activity patterns. Normal EEG tracings can be seen as continuously varying waveforms that are classified depending on frequency (number of waveforms per second: Hz), amplitude (magnitude of change: μV), and shape (see Figure 1.14, pg 50). There are 5 commonly acknowledged waveforms in human EEGs: 1) delta—0.5-4Hz 2) theta—4-8Hz 3) alpha—8-13Hz 4) beta—13-30Hz and 5) gamma >30Hz. In alert adult humans, only beta and alpha waves are normally present, although a few theta may be seen, particularly in hippocampal regions (Buzsaki, 2002). Recent studies have shown that fast gamma waveforms play an important role in sensory processing (Deco and Thiele, 2009; Jensen *et al.*, 2007), are associated with attention and learning and memory processes (for reviews, see Deco and Thiele, 2009; Jensen *et al.*, 2007), and appear to be crucial for network formation during development (Yang *et al.*, 2009). During slow-wave sleep (SWS), waveforms such as theta and delta are prevalent, along with complexes known as sleep spindles (intermittent short bursts of 12-14Hz activity), while rapid-eye movement (REM) sleep (also called paradoxical

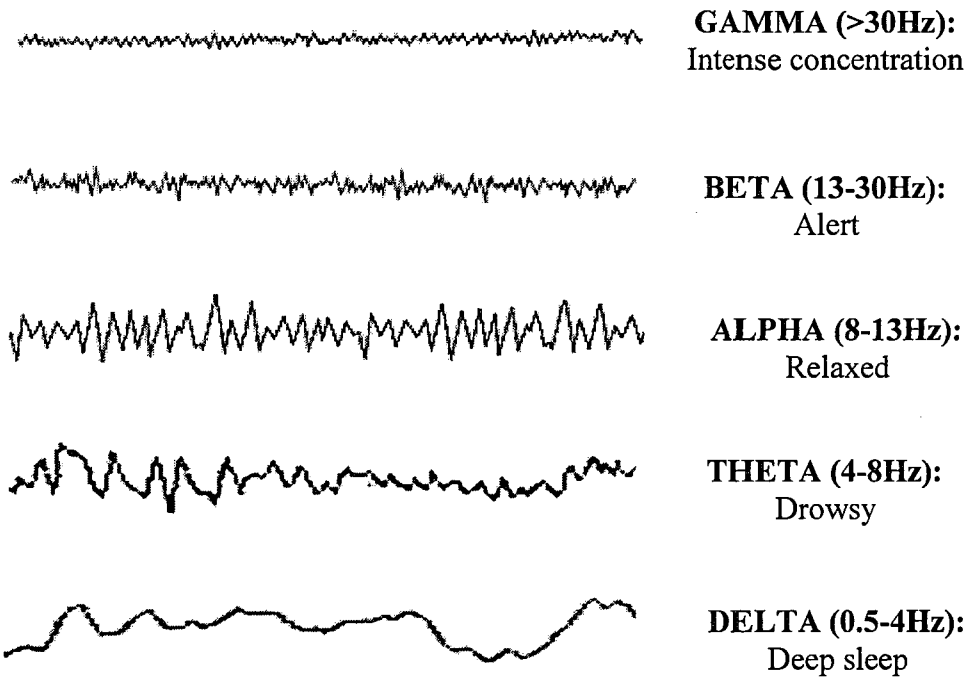

Figure 1.14. Normal EEG waveforms. Each tracing represents ~3 seconds of recording time.

(www.webpub.allegheny.edu/.../Peeking%20Inside.htm)

sleep) that occurs during periods of dreaming consists of low-amplitude, high frequency beta-like waveforms (Shouse *et al.*, 2000).

During seizure, alterations in EEG (Figure 1.15, pg 52) are most commonly seen as sudden spikes that feature high amplitude activity, or repetitive spike and wave patterns that may manifest as rhythmic bursts or in association with intervening slow waves (Meldrum and Chapman, 1999). EEG abnormalities may be present between seizures (interictal) as well, or there may be interictal focal or generalized slowing of normal EEG rhythms. However, interictal activity may also be perfectly normal between seizure episodes, so for diagnosis, efforts are often made to induce seizure during EEG recordings through the use of mild stressors such as flashing lights (photosensitivity), hyperventilation (a common trigger for absence seizure), or sleep deprivation (Bazil, 2007). While interictal abnormalities may be suggestive of epilepsy, a definite diagnosis can only be made based on EEG activity during behavioural seizure (Epilepsy Foundation of America). If standard 'in-lab' methods fail to produce evidence of seizures, 24-hour EEGs, or portable home EEG monitoring devices may be used to allow for longer assessments. When the type and cause of the seizures are unclear, video-EEG can provide a visual reference during the EEG recording session to help with diagnosis. Monitoring of this type also helps distinguish between true epileptic seizures caused by electrical discharge and non-epileptic seizures caused by psychological factors (Alsaadi *et al.*, 2004). Alternatively, grid or depth electrodes may be implanted in the brain to provide more precise information prior to surgical resection.

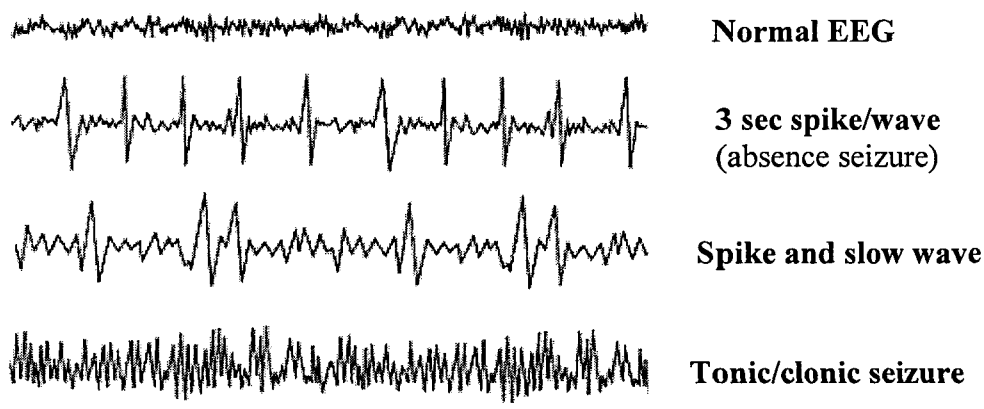

Figure 1.15. EEG during seizure activity. Each tracing represents ~3 seconds of recording time.

(www.cs.tut.fi/sgn/SSSAG/EpilAna.htm)

Often, EEG monitoring during sleep will reveal underlying activity that is not readily apparent during periods of wakefulness (for review, see Rodriguez and Kuzniecky, 2008). This is particularly likely during slow-wave sleep, since the synchronous waveforms generated during this time are conducive to seizure precipitation (Sammaritano *et al.*, 1991). Conversely, the faster, desynchronous EEG waveforms generated during REM sleep appear to afford protection against seizure activity (Jaseja, 2004; Kumar and Raju, 2001). In animal models, decreased REM sleep is one of the defining hallmarks of epilepsy (Kumar and Raju, 2001; Raol and Meti, 1998; Schilling *et al.*, 2006; Stone and Gold, 1988).

1.5.6 Seizure triggers

Triggers that appear to increase seizure susceptibility have been known for many years, but only lately has their identification been considered of clinical value (Koutsogiannopoulos *et al.*, 2009). A recent study looking at seizure precipitants has reported that, from a sample of 309 people with epilepsy, ~66% were convinced their seizures were precipitated by specific triggers, while ~90% reported experiencing at least one of the 42 recognized triggers prior to a seizure event (Pinikahana and Dono, 2009). As noted in previous studies (Frucht *et al.*, 2000; Temkin and Davis, 1984) stress is the most common trigger (56%), followed by lack of sleep and fatigue (~38% each). Other triggers identified included specific foods, too much noise, feeling cold, flashing light, and strenuous physical activity. There was also a high corroboration regarding these triggers between reports of people with epilepsy and reports from their caregivers/family (Pinikahana and Dono, 2009), further substantiating their validity.

1.6 Animal Models of Epilepsy

Animal models are one of the most important tools available to investigate basic mechanisms of the epilepsies and epileptogenesis, as well as to develop and validate new diagnostic techniques and therapeutic treatments (Engel and Schwartzkroin, 2006; Loscher, 2002; Sarkisian, 2001). To date, over 100 animal models for epilepsy have been reported (Buckmaster, 2004), highlighting both the heterogeneity of this disorder, as well as difficulties inherent in developing models that accurately represent the human condition in all its diversity. Accurate representation is important, since the more precisely a model reflects the pathophysiology of a disorder, the more progress can be made toward understanding the underlying mechanisms inherent in its development, and ultimately, finding a cure (Sloviter, 2005).

In this dissertation, only those animal (i.e. rat) models deemed most relevant to the current paper will be presented here. However, for a broader view of seizure and epilepsy models in general, a number of excellent resources are available (Fisher, 1989; Jefferys, 2003; Morimoto *et al.*, 2004; Pitkänen *et al.*, 2006; Sarkisian, 2001).

1.6.1 Pentylenetetrazol (PTZ) absence seizure model

One of the most commonly used classes of drugs for seizure induction are those affecting the GABA system, including $GABA_A$ antagonists (e.g. PTZ, bicuculline) chloride channel blockers (e.g. picrotoxin), and GABA synthesis inhibitors (i.e. GAD inhibitors—e.g. allylglycine) (Velíšek, 2006). Behaviourally, all these drugs produce a dose-dependent sequence of phenomena: 1) behavioural arrest 2) myoclonic twitches

3) clonic seizures, and 4) tonic-clonic seizures. High enough doses will usually cause death (Velíšek, 2006).

Although all $GABA_A$ antagonists will cause similar effects, PTZ is the compound most often used to produce generalized absence-like seizures in otherwise normal rats at intraperitoneal (i.p.) doses ranging from 20-30mg/kg (Andre *et al.*, 1998; Cortez and Snead, 2006). While the only visible behaviour during these seizures is a 'motionless stare', the EEG pattern is quite distinct, consisting of spindle-shaped discharges, so seizure assessment must include EEG recordings (Ono *et al.*, 1990; Willoughby and Mackenzie, 1992). The seizure normally ends very abruptly, with the animal immediately resuming its preictal activity (Cortez and Snead, 2006). With increasingly larger doses of PTZ, clonic seizures will appear, followed by tonic-clonic manifestations (Ono *et al.*, 1990).

1.6.2 Electrical kindling model

Kindling is the progressive development of seizures in response to a previously subconvulsant stimulus (Goddard *et al.*, 1969). The stimulus may be either chemical or electrical. In electrical kindling, an electrode is stereotaxically implanted into a discrete region of the brain (most commonly either amygdala or HC) to allow stimulus administration, as well as to provide a recording of the resultant neuronal activity. Baseline sensitivity (afterdischarge threshold: ADT) can be assessed through electrographically-recorded responses (afterdischarge: AD) to increasingly intense stimulation levels (Racine, 1972b; for review, see McIntyre, 2006). Subsequent stimulations are then applied (usually once per day) at a level equal to or slightly exceeding the ADT. Measures include the duration of ADs and maximum behavioural

seizure stage (Racine, 1972a) exhibited following each stimulation. As kindling progresses, behavioural manifestations increase as well, with initial stimulations eliciting no response, while fully kindled animals are defined by generalized tonic-clonic seizure activity (Racine, 1972a; see Table 1.1, pg 57).

One of the most important aspects of kindling is its progressive nature, and in this respect, kindling is considered a good model for frequently experienced seizures that begin in discrete, focal regions of the brain (partial seizures) and gradually progress to more generalized forms (McIntyre, 2006). Interestingly, a recent study of amygdala-kindled seizure propagation has provided a fascinating look at the sequential recruitment of hippocampal regions involved in this process (Hewapathirane and Burnham, 2005). Results show that, in normal rats, several stimulations are required before ADs propagate from the amygdala to the HC, and during this time, no overt behavioural manifestations are seen. Stage 1 seizures appear with ventral hippocampal involvement on the side ipsilateral to stimulation, while Stage 2 occurs with dorsal recruitment. Stage 3-5 seizures only occur after propagation to the contralateral HC (running dorsally to ventrally), in agreement with the concept of 'generalized' activity. The authors note that transition to contralateral HC occurs significantly slower than does progression within ipsilateral sites, and suggest that, while generalized seizure do involve both hippocampal hemispheres, this is probably not the main pathway mediating seizure propagation to the rest of the brain (Hewapathirane and Burnham, 2005). Instead, it seems that the recruitment of other structures external to the HC (e.g. thalamus) that have widespread, bilateral connections are necessary for the induction of generalized seizures (Bertram *et al.*, 1998; Bertram *et al.*, 2001). Exactly how and why

Table 1.1. The typical progression of motor seizure stages in amygdala kindling. Stage 1 and 2 are considered to be equivalent to partial seizures, while stages 3-5 represent more generalized seizure activity. (Racine, 1972)

Seizure Stage	Behavioural Manifestation
1	Oralimentary movements
2	Head bobbing
3	Forelimb clonus
4	Rearing
5	Rearing and falling

generalization occurs, however, is not currently understood.

1.6.3 Hippocampal Slices

The use of *in vitro* electrophysiological techniques have greatly enhanced understanding of neurobiological processes, providing options for studying mechanisms of seizure generation, spread, and termination that would be difficult or impossible *in vivo*. Acute slice preparations, particularly from the HC, allow investigation of specific circuitries and network properties without the complexities associated with the intact brain (Heinemann *et al.*, 2006). Extracellular recordings provide a means to study discrete cell populations (e.g. synaptic responses and neuronal firing) under baseline conditions, as well as during and after experimental manipulations such as electrical stimulation or pharmacologic treatment. Intracellular recordings (using sharp or patch electrodes) give a more microscopic view of individual cell function (Bernard, 2006).

Understandably, proper slice preparation is of critical importance in determining tissue viability as well as the applicability of experimental results. Once the animal is anaesthetized, the brain must be removed as quickly and gently as possible and placed immediately in ice-cold, oxygenated (95% O_2 / 5% CO_2) artificial cerebral spinal fluid (aCSF). Slices are normally cut at a predetermined thickness between 200μm and 600μm. Cutting orientation is an important consideration, especially if specific circuitries must remain intact between brain regions (e.g. entorhinal cortex and HC). Following cutting, slices are transferred into a holding chamber and maintained in aCSF at room temperature for at least an hour. Testing is performed in a recording chamber

continually perfused with warmed aCSF (~32° C) at a designated flow rate between 1.5 – 4.5ml/min (Bernard, 2006).

Seizure-like activity with *in vitro* hippocampal slices can be studied acutely (e.g. using $GABA_A$ antagonists, excitatory compounds, or high-frequency electrical stimulation), or in animals that have developed, or are in the process of developing epilepsy (e.g. using chronic models such as kindled rats). However, although many studies have investigated underlying activity in various chronic models, seizure-like discharges have not yet been reported in slices from epileptic animals *in vitro* during physiologic conditions (Bernard, 2006). Therefore, challenges such as those applied to induce acute seizures are often used to compare patterns and properties of ictal-like activity in tissue from both seizure-prone brain and controls (Behr *et al.*, 1996; Lynch and Sutula, 2000; Walther *et al.*, 1986).

The main limitation of the hippocampal slice preparation is the massive loss of intrinsic and extrinsic connectivity. In rats, for example, a 400μm horizontal (transverse) slice represents less than 10% of the complete HC, and requires severing of many longitudinal axons (Freund and Buzsaki, 1996). In addition, while local glutamatergic and GABAergic synaptic pathways are preserved within a slice, important modulatory connections (dopaminergic, serotonergic, etc) are cut. Further, many of the hormones and amino acids present in normal CSF (e.g. CORT, Glu, GABA) are not usually included in aCSF solution. Therefore, caution should be exercised in the interpretation of results from slice preparations. Despite these limitations, however, hippocampal slices remain one of the best ways to analyze the reorganizations that occur within

various hippocampal networks during epileptogenesis, and provide an excellent resource for studying modifications in excitatory and inhibitory activity, particularly in conjunction with other investigative methods (for review, see Bernard, 2006)).

1.6.4 The NIS-L rat model

As previously mentioned, high doses of the Glu agonist DOM can produce seizure in a variety of mammals (Grimmelt *et al.*, 1990; Iverson *et al.*, 1989; Ramsdell and Zabka, 2008; Ramsdell and Zabka, 2008; Scallet *et al.*, 2004; Tasker *et al.*, 1991; Tryphonas *et al.*, 1990a; Tryphonas *et al.*, 1990b) including humans (Cendes *et al.*, 1995; Perl *et al.*, 1990; Teitelbaum *et al.*, 1990; for review, see Lefebvre and Robertson, 2009). Long-term behavioural alterations have also been reported in rat pups exposed to DOM *in utero* (Levin *et al.*, 2005).

Very low, sub-convulsant doses (20μg/kg) of DOM administered to Sprague-Dawley rat pups sub-cutaneously (s.c.) once per day throughout the second postnatal week of life (PND8-14) results in long-term changes in both behaviour (Adams *et al.*, 2008; Adams *et al.*, 2009; Burt *et al.*, 2008a; Burt *et al.*, 2008b; Doucette *et al.*, 2004; Perry *et al.*, 2009) and hippocampal cytoarchitecture (e.g. MFS) and neurochemistry (e.g. increased TrkB receptor expression) (Bernard *et al.*, 2007) that are consistent with many current animal models of TLE, as well as what is found in the human condition. The structural changes in this new model (herein referred to as novelty induced seizure-like; NIS-L) appear to be progressive, and eventually culminate in cell loss at later time points (Doucette *et al.*, 2004).

Behavioural seizure activity in this model is low-grade (equivalent to Stage 2 on the Racine (1972) scale), consisting of hunched posture, vibrissae twitching, mastication, squinting and/or blinking, and head bobbing, and can be triggered in adulthood by exposure to novel tasks such as the water maze or the open field (Doucette *et al.*, 2004), suggesting that individual perception of (and sensitivity to) a given stimulus may contribute to the seizure mechanism. Additionally, not all NIS-L rats respond to all paradigms that have been shown to elicit seizure activity in the model (Doucette *et al.*, 2004; Perry *et al.*, 2009). This is an important feature, since seizure activity in humans with TLE is also variable. Indeed, understanding why an individual may have a seizure at any given point in time is one of the fundamental questions in epilepsy research (Schwartzkroin, 1997).

Interestingly, triggered seizures have also been noted in Mongolian gerbils in an inherited epilepsy model (for review, see Buckmaster, 2006). Like the NIS-L rat, these gerbils experience seizures elicited by external stimuli, and not all gerbils respond to all stimuli. Some seizure-evoking protocols in gerbils include placing the gerbil on an automatic shaker for 30 seconds, moving the gerbil from the home cage to a red plastic shopping basket, or placing the gerbil in an empty plastic cage and blowing compressed air on its back for 15 seconds (see Buckmaster, 2006). However, in contrast to the NIS-L rat, which exhibits only complex partial behavioural seizure responses to stimuli (Doucette *et al.*, 2004), seizure-prone gerbils will progress fairly rapidly from mild seizure activity to more generalized forms (Buckmaster, 2006). Additionally, while the gerbil model is genetically based, the NIS-L rat is an acquired form, with low-grade

seizure activity emerging in adulthood following mild exposure to a Glu agonist in early postnatal development.

1.6.5 EEG investigation in animal models

In humans, EEG is an important tool for the study and diagnosis of epilepsy. Similarly, alterations in EEG in animal models are a vital part of the validation process (Bertram, 2006; Sarkisan, 2001). In the last few years, the study of seizure activity has been greatly facilitated by the use of techniques such as radiotelemetry (Figure 1.16, pg 63), which allows EEG activity to be recorded from freely moving animals during pharmacologically induced and spontaneously recurrent epileptiform activity (Bastlund *et al.*, 2004; Bastlund *et al.*, 2005; Raedt *et al.*, 2009; Williams *et al.*, 2006). The ability to record and analyze EEG in this manner provides a flexible method for the investigation of brain wave activity in rats in an assortment of paradigms, including during pharmacological manipulations.

Preparing an animal for radiotelemetry recording requires a surgical procedure to implant a small, battery-powered transmitter under the skin, and connect it to leads that can be positioned either on the dura of the brain for electrocorticoencephalogram (ECoG) recordings, or stereotaxically positioned within the brain for depth recordings of specific neuronal populations (similar to implanting an electrode for electrical kindling). A receiver plate picks up the radio transmissions and forwards the information to a computer. Specialized software translates the digital signal into traces that may be viewed on the computer and saved for later analysis. The lifespan of the transmitter

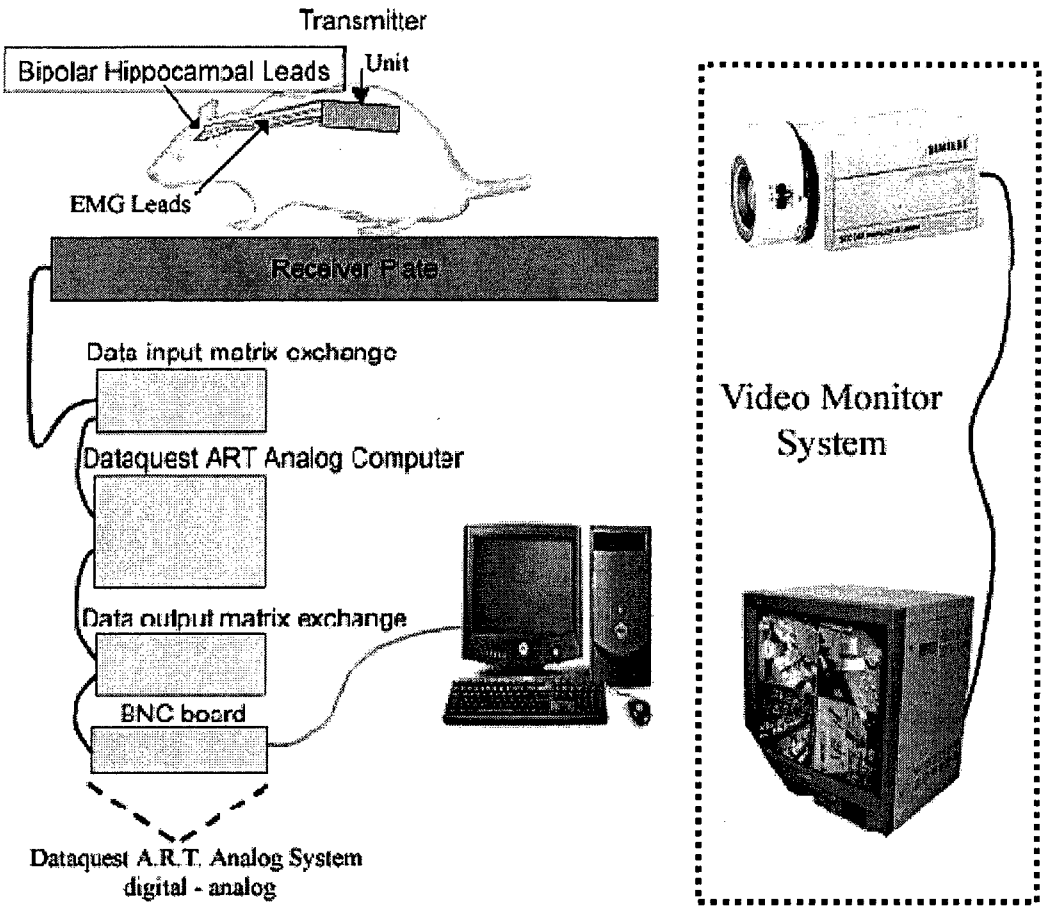

Figure 1.16. Radiotelemetry system for recording EEG / EMG activity in freely moving rats. The video monitoring (quad) system provides simultaneous visual confirmation of corresponding activity.

(Adapted from Williams et al., 2006)

battery is approximately 3 months of continuous use, and it can be switched on and off by running a magnet over the animal's body.

Since there are many movements that can cause EEG alterations in animals (e.g. chewing, grooming, etc), positioning one of the leads in muscle tissue allows for simultaneous electromyogram (EMG) recording, providing easy identification of movement artifacts (Bastlund *et al.*, 2004). In addition, recording behavioural activity using video monitoring further enhances the amount of information available (Figure 1.16, pg 63), and in conjunction with EMG information, ensures that only the desired behaviours are evaluated (Williams *et al.*, 2006).

1.7 Rationale, Hypothesis, and Study Objectives

1.7.1 Rationale for the experiments

Epilepsy is a multifaceted disorder that encompasses many symptoms and involves a multitude of complex neuronal mechanisms (Dudek *et al.*, 2002). At present, two of the greatest challenges in epilepsy research are identification of individuals at risk of developing the disorder, and preventing and/or modifying the epileptogenic process (Pitkänen *et al.*, 2007). Animal models, particularly those that most closely model characteristic human seizure development following an early-life insult that does not normally induce status epilepticus, are crucial components for investigation of alterations inherent in epileptogenesis, as well as for increasing our overall understanding of basic neuronal physiology (Bender and Baram, 2007). Ideally, multiple mechanisms involved in seizure development should be considered together,

from the molecular and cellular levels to neural systems and behaviour, with the understanding that even subtle changes at one level can result in alterations that may become cumulative and profound at another (Dudek *et al.*, 2002).

As a new developmental model of TLE, the NIS-L rat is an ideal candidate for allowing study of alterations that can result from subtle interference in early postnatal brain development, presumably reflecting changes in excitatory/inhibitory circuitry during network formation. Through characterization of this model using a variety of techniques, further validation and a greater understanding of underlying mechanisms and inherent features can be elucidated.

1.7.2 Hypothesis

The overarching hypothesis for this study is that early-life exposure to changes in glutamatergic system activation produce long-term modifications in excitatory/inhibitory circuitry characterized in adulthood through altered electrophysiological, behavioural, and histochemical activity.

1.7.3 Objectives

Using the NIS-L rat model for all investigations, the main objectives of the current thesis were:

1) To characterize ictal and interictal EEG activity in the NIS-L rat model
2) To explore alterations in seizure threshold and seizure propagation
3) To study potential changes in susceptible GABAergic subpopulations in the HC

4) To assess possible electrophysiological changes in hippocampal circuitry

5) To investigate underlying mechanisms potentially responsible for the effects of early DOM exposure

2.0 EEG PATTERNS AND GENERALIZED SEIZURE THRESHOLD IN THE NIS-L RAT

Portions of this chapter have been submitted to Neuroscience (along with sections of chapter 3) as follows: Gill, D.A., Bastlund, J.F., Watson, W.P., Ryan, C.L., Reynolds, D.S., Tasker, R.A. Neonatal exposure to low-dose domoic acid lowers seizure threshold in adult rats.

Additional data from this study can be found in Appendix A.

2.1 Introduction

A critical period for maturation and final organization of excitatory and inhibitory function in the brain occurs during perinatal development when network connections are being formed and refined. In the rat HC, many of these connections reach adult levels by the end of the second postnatal week, following an identifiable developmental progression (Burgard and Hablitz, 1993; Tyzio *et al.*, 1999) which appears to be common to a wide variety of species (Ben-Ari, 2002). Insult or injury to the brain at this time may have far reaching consequences that manifest as changes in behaviour resulting from modifications in underlying brain structure and function (Dobbing and Smart, 1974; Nouws, 1992). For example, it is well known that prenatal exposure to either environmental stress (Hougaard *et al.*, 2005) or chemical toxins (Levin *et al.*, 2005) results in long-lasting behavioural changes. Similarly, exposure to neurotoxic doses of various excitatory compounds during critical windows of early postnatal development reliably produce rats that, as adults, display spontaneously recurrent seizure activity that is apparent both behaviourally and through EEG analysis (Stafstrom and Sutula, 2005), and also creates a hyperexcitable hippocampal network *in vitro* (Galvan *et al.*, 2000; Santos *et al.*, 2000).

Structurally similar to the excitatory amino acids KA and Glu, DOM is a naturally occurring neurotoxin that is a potent agonist for Glu receptors, particularly GluK5 and GluK6 (Sommer *et al.*, 1992), and as such, is a valuable research tool for investigation into excitatory CNS circuitry. Used in high doses, DOM reliably produces a well documented variety of behavioural symptoms that range from impaired learning and

memory function, seizures, coma, and ultimately death in many species (Grimmelt *et al.*, 1990; Iverson *et al.*, 1989; Nakajima and Potvin, 1992; Scallet *et al.*, 2004; Tasker *et al.*, 1991; Tryphonas *et al.*, 1990a; Tryphonas *et al.*, 1990b). Less is known, however, about the possible effects of very low, sub-convulsive doses of this compound, particularly in the developing brain. It has been previously demonstrated that low doses of the Glu agonists domoic or kainic acid administered during the second postnatal week can alter neurobehavioural development in rat pups (Doucette *et al.*, 2003; Tasker *et al.*, 2005). When these animals reach adulthood, many of them display a low-grade seizure-like behavioural response to a variety of maze paradigms (the NIS-L rat model; see Chapter 1, section 1.6.4). In addition, histological analysis has revealed changes in hippocampal structure and function, including increases in both MFS and TrkB expression similar to animal models of TLE (Bernard *et al.*, 2007; Doucette *et al.*, 2004).

Identifiable alterations in EEG patterns are one of the defining criteria for determining whether an animal model is a valid option for use in the study of seizure disorders (Engel and Schwartzkroin, 2006; Fisher, 1989; Sarkisian, 2001). Radiotelemetry, which allows EEG activity to be recorded from freely moving animals during pharmacologically induced and spontaneously recurrent epileptiform activity (Bastlund *et al.*, 2004; Bastlund *et al.*, 2005; Williams *et al.*, 2006), provides a flexible method for the investigation of brain wave activity in rats during behavioural testing in an assortment of paradigms including water maze procedures. Using a non-tethered system, radiotelemetry gives the researcher freedom to manipulate the environment to more closely resemble real-life situations while still allowing the monitoring of underlying brain activity. It is well known that environmental triggers such as stress can

result in a heightened seizure response in humans (Frucht *et al.*, 2000; Koutsogiannopoulos *et al.*, 2009; Pinikahana and Dono, 2009), so requiring seizure-prone rats to perform behavioural tasks that include a mild to moderate stress component (such as swimming), can provide an appropriate precipitant for seizure manifestation that is more closely linked to the human condition, and may help elucidate elements of seizure activity, such as the transition from interictal to ictal waveforms.

Another important aspect of EEG monitoring is its ability to help identify seizure type. While there are only two main seizure categories (generalized and partial), there are many subcategories that are diagnosed based on both clinical characteristics and EEG patterns (Commission on Classification and Terminology of the International League Against Epilepsy, 1981). Absence seizure is a generalized seizure form that can be identified on EEG tracings as short bursts of spike-and-wave-like discharges with high amplitude (Andre *et al.*, 1998; Ono *et al.*, 1990; Willoughby and Mackenzie, 1992). Seizure generation involves both thalamus and cortex (thalamo-cortical) (for review, see Hughes, 2009), with accompanying behavioural expression consisting of sudden, brief pauses in activity that are generally combined with a blank, unfocused stare. In adult rats, this type of seizure can be readily elicited through administration of low-dose PTZ (Andre *et al.*, 1998; Ono *et al.*, 1990; Willoughby and Mackenzie, 1992), an antagonist of the inhibitory $GABA_A$ receptor, along with myoclonic jerks (MCJs) (Ono *et al.*, 1990; Velisek, 2006), another form of generalized seizure activity.

The purpose of the current study was to investigate and characterize EEG patterns and generalized absence seizure activity in the NIS-L rat model. Radiotelemetry was used to

record and quantify cortical EEG and EMG activity during elicited seizure-like behavioural episodes, as well as to investigate the effects of sub-convulsive PTZ administration.

2.2 Materials and Methods

2.2.1 Experimental animals

Offspring born in-house from untimed Sprague-Dawley rats (Charles River, Germany) were culled within 24 hours of birth to 10 pups per litter (5-♀ and 5-♂ where possible). From postnatal day 8-14 (inclusive), male pups were weighed and given a single daily injection (10ml/kg, s.c.) of either 20μg/kg DOM (BioVectra dcl, Canada) or SAL, as described previously (Doucette *et al.*, 2004). On PND22, female rats were humanely euthanized, and males were group housed (2-4 per cage) within a ventilated scantainer unit under a 12h light-dark cycle (lights on at 6 a.m.) in plastic cages (43 cm x 27 cm x 18.5 cm), given a clear plastic tunnel (14 cm x 9 cm x 8.5 cm) and a wooden block (5 cm x 1 cm x 1 cm) as environmental enrichment and left undisturbed, except for normal maintenance, until the commencement of surgeries. Music was supplied to the housing area through a single speaker, and followed the same cycle as the lights. Room temperature was maintained at 21±2°C and relative humidity at 55±5%. Standard rodent food (SDS, UK) and tap water was available *ad libitum*. Following surgery, rats were individually housed for the duration of testing. All surgeries and testing were performed between 09:00h and 18:00h and were carried out under a license from the Danish Ministry of Justice, and in accordance with the EC Directive 86/609/EEC and the Danish law regulating experiments on animals.

2.2.2 Telemetry surgery

At approximately 90 days of age, rats were anaesthetized with a 0.2 ml/100g (s.c.) injection of one part Hypnorm (0.315 mg/ml fentanyl + 10 mg/ml fluanisone, Janssen Inc., USA), and one part Dormicom (5 mg/ml midazolam, F. Hoffmann-La Roche AG, Switzerland) in two parts sterilized water. Radiotelemetry transmitters (TL10M3-F50-EEE or TL10M3-F50-EET, Data Sciences International, St. Paul, MN, U.S.A.) were surgically implanted in a subcutaneous pocket formed on the animal's left flank for continuous cortical (n=20; 10-DOM, 10-SAL) EEG / EMG recording as described previously (Bastlund *et al.*, 2004). Of the 20 cortical placements, 18 consisted of two supradurally placed lead wire held in place by jewelers' screws and positioned 2mm each side of midline and ~2mm anterior to bregma as well as two leads ~2mm anterior to lambda to generate a total of two cortical bio-potentials. Two leads implanted into the musculus cervicoauricularis provided one EMG feed. A ground lead was attached to the anterior sinus. The remaining two rats in this group (1-DOM, 1-SAL) received two leads placed each side of midline with one anterior to bregma and one anterior to lambda, generating one cortical bio-potential, as well as receiving one EMG feed as described above. All rats were treated prior to and for 7 days post surgery with Rimadyl vet. (1 ml/kg s.c., 1:10 dilution, Pfizer, Denmark) and Baytril vet. (2 ml/kg s.c., 1:10 dilution, Bayer Health Care, Denmark) and allowed 3 full weeks to recover. Further pain relief was given immediately following surgery through an s.c. injection of Temgesic (0.3 mg/ml buprenofin, Schering-Plough, USA). Local irritation was treated with 5% Xylocaine crème (lidocaine chloride, AstraZeneca, Norway). Following recovery, transmitters were switched on and rats were recorded for both EEG and video

(see Appendix A, pg 228) for 14 days (24 hours/day) under normal maintenance conditions in the home cage.

2.2.3 Radiotelemetry system

The telemetry system used to record EEG/EMG from animals was composed of TL-10M3-F50-EEE (3 bio-potential) and TL-10M3-F50-EET (2 bio-potential) magnetic activated transmitters, RPC-1 receiver plates, data exchange matrices, and computers installed with Dataquest A.R.T. 2.2. (Data Sciences International, USA) (see Figure 1.16, pg 63). The sampling frequency was set at 250 Hz for all recordings.

2.2.4 Water maze testing

On approximately PND150, rats were tested in the Morris water maze (MWM) to induce seizure-like (NIS-L) behaviour (Doucette *et al.*, 2004). In brief, each rat received 8 consecutive trials (maximum 60s / trial, 60s on platform between trials, and a 20s inter-trial interval in drying cage) in a 1.2m black circular pool with a hidden escape platform submerged ~2cm below water level (see Appendix A (pg 232) for further details). EEG / EMG outputs were recorded from the platform between trials, as well as for 1 hour in the drying cage following completion of testing. All trials were video-recorded (Sony digital camera w/3.6mm Compunar f/5.6 lens), as was drying cage activity (Monicor TVSP-42 B/W Quad cameras; Panasonic NV-HS870 VCR). Swim speed and latency to platform were monitored through Noldus EthoVision (v.2.3 Noldus Information Technology, The Netherlands) (Results presented in Appendix A, pg 233). Presence or absence of the NIS-L behavioural syndrome was scored with experimenter blind to condition.

2.2.5 PTZ challenge

Ten days following water maze testing, rats were administered an intraperitoneal dose (25mg/kg) of PTZ (Nomeco, Denmark), and subsequently monitored for 30 minutes in the home cage. This acute dose of PTZ was chosen based on previous literature as being sub-convulsive in normal rats (Andre *et al.*, 1998; Arrieta *et al.*, 2005; Bonan *et al.*, 2000; Hassan *et al.*, 2000; Schmoll *et al.*, 2003), yet able to induce absence seizure activity as identifiable in EEG analysis (Andre *et al.*, 1998; Schmoll *et al.*, 2003). Seizure behaviours were hand-scored using a 5-point scale (Racine, 1972a) with myoclonic jerks indicated separately (indicative of seizure induction). EEG / EMG activity was recorded, and rats were also video-recorded (Monicor TVSP-42 B/W Quad cameras; Panasonic NV-HS870 VCR) for later analysis if required. Two days later, a subsequent treatment of PTZ was administered at a higher dosage (32mg/kg i.p.). Results from this treatment may be found in Appendix A, pg 235.

2.2.6 Analysis of electroencephalogram

All traces generated by radiotelemetry EEG and EMG bio-potentials were imported in Somnologica 3.1.0.1171 software (Flaga Medical Devices, Iceland) for visualization and analysis using fast Fourier transform (FFT). For recordings made during water maze testing, overall frequency power was determined through power spectrum analysis for each rat for one hour in the drying cage following testing, and the percent of activity occurring in each wave band was analyzed for the same period of time. Wave band activity was defined as follows: delta 0.5-3.99 Hz ; theta 4.0-7.99 Hz ; alpha 8.0-11.9Hz; sigma 12.0-13.9 Hz ; beta 14.0-24.9 Hz ; gamma 25.0-90 Hz. The presence of

NIS-L activity in the drying cage was scored from video recordings (experimenter blind to condition), and if present, was subsequently matched to the corresponding EEG tracing. A 10 sec interval during identified NIS-L activity was quantified using power spectrum analysis, then compared to 10 sec intervals immediately preceding and following the episode. Electromyogram tracings and video recordings were used to identify possible artifacts in the EEG. For PTZ testing, absence seizure was defined on EEG as short bursts of spike-and-wave-like discharges with high amplitude combined with a reduction in EMG activity (Velíšek, 2006; Willoughby and Mackenzie, 1992), while MCJs were confirmed through EEG as sharp, high amplitude, high frequency events involving both anterior and posterior brain regions, along with corresponding action on the EMG lead. Latency to the first absence seizure episode and myoclonic movements as well as frequency of episodes were also measured.

2.2.7 Data analysis

Parametric data were analyzed using either paired or independent t-tests, while non-parametric measures were examined using Chi Square (X^2) Crosstabulation. Results are expressed as the mean ± SEM. Analyses were performed using SPSS (v.10.0.5 SPSS Inc., Chicago, IL), and the significance level for all tests was set at $\alpha \leq 0.05$.

2.3 Results

Two of 20 rats did not survive surgery (1 DOM and 1 SAL), and 2 rats had to be euthanized prior to water maze testing (1 DOM and 1 SAL) due to complications arising from transmitter implantation, leaving 16 rats (8 DOM and 8 SAL) in this study. In

some recordings, power spectrum information could not be obtained from the EEG, so the data from those tracings were not included in the relevant statistical analyses.

2.3.1 Water maze testing

Of 16 rats scored for seizure-like behaviours (8 Sal / 8 DOM), 62.5% of DOM-treated rats exhibited the NIS-L syndrome [$X^2_{(1)} = 7.27$, p=0.007] with no false positives in the SAL -treated group. Rats treated neonatally with DOM (n=8) tended to have increased measures of total power, although this effect was not statistically significant [$t_{(7.036)} = -2.085$, p=0.075]. Electroencephalogram data was analyzed immediately prior to, during, and after behavioural expression of the NIS-L syndrome, and revealed changes in power band spectral patterns (Figure 2.1, pg 77) as well as significant increases in peak frequencies in anterior [before: $t_{(3)} = -10.038$, p=0.002; after: $t_{(3)} = 11.491$, p=0.001] (Figure 2.1B, pg 77) and posterior [before: $t_{(4)} = -2.336$, p=0.08; after: $t_{(3)} = 5.74$, p=0.01] (Figure 2.1D, pg 77) leads compared to baseline measures. This increase is identifiable on EEG tracings as recurrent episodes of fast wave activity in both anterior and posterior leads, accompanied by an immediate response in EMG activity (see Figure 2.2, pg 78 for a representative trace).

Domoate-treated rats also showed a definite tendency toward increased beta band (14.0-25Hz) activity in the posterior brain region [$t_{(11)} = 2.110$, p=0.059] (Table 2.1, pg 79), a predisposition that was further confirmed by analysis of a small sub-population of DOM-treated rats that received hippocampal placements (n=3; not included in study; see Appendix A, pg 237) revealing significant increases in beta activity compared to both DOM cortical counterparts and SAL controls.

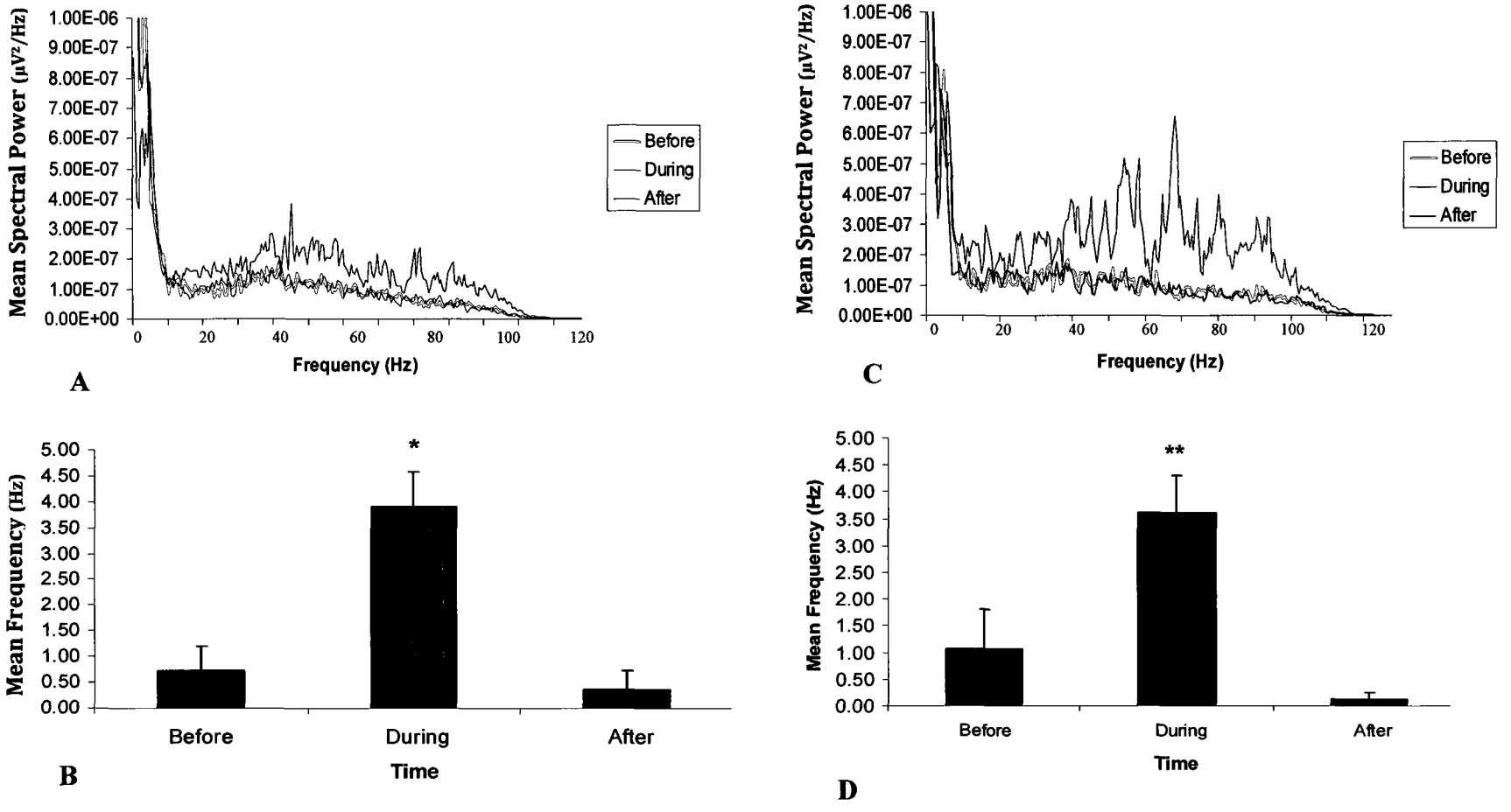

Figure 2.1 Mean spectral power band activity and peak frequencies before, during, and after seizure-like activity in DOM treated rats for anterior (A&B) and posterior brain (C&D). Error bars represent SEM. The single asterisk indicates a significant difference from all other time points, while the double asterisk denotes a significant difference from the "after" time point only ($p<0.05$).

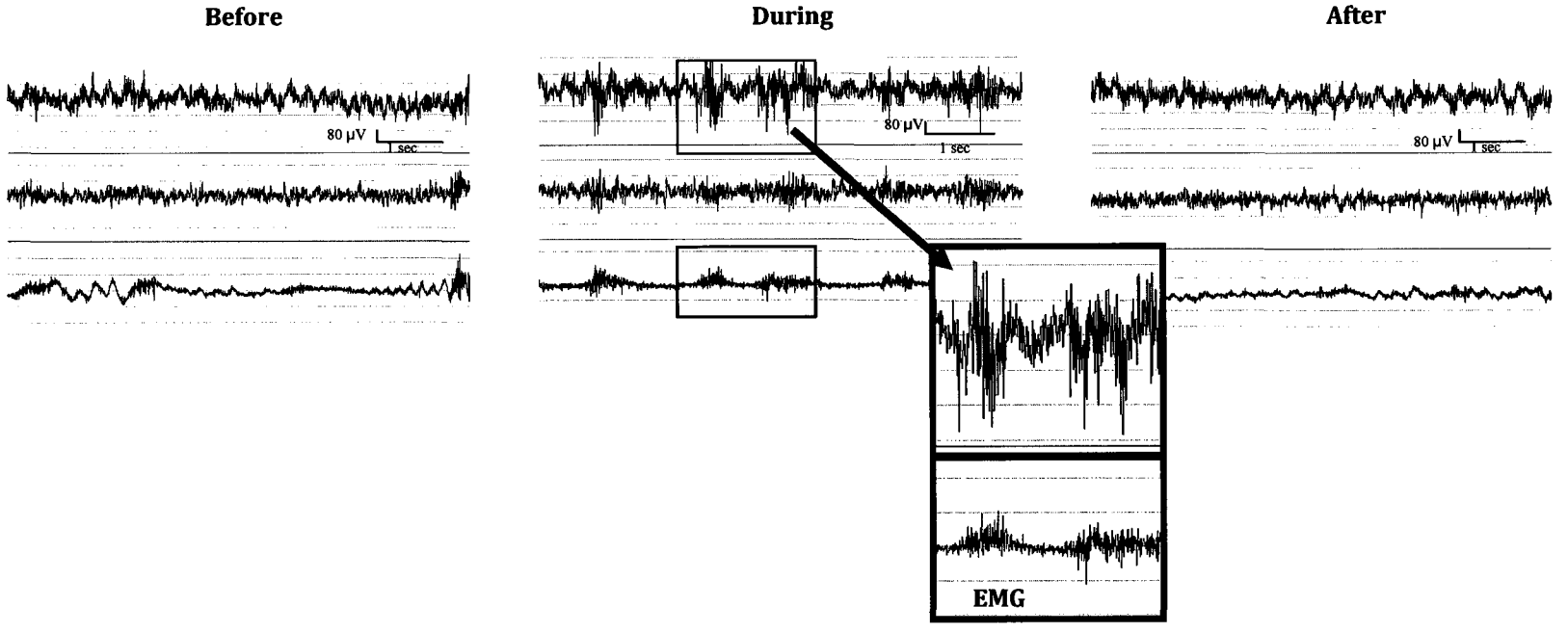

Figure 2.2 EEG from a rat displaying NIS-L. The top recording in each trace is the anterior lead, the middle is the posterior lead, and the bottom is the EMG. **Inset:** Magnified image during NIS-L (EEG anterior and EMG only) to show initial onset in EEG (approximately 2 second duration).

Table 2.1 Overall power band activity for SAL and DOM treated rats during post-swim period.

	SAL		DOM	
	Anterior	**Posterior**	**Anterior**	**Posterior**
Frequency	(% activity ±SEM)		(% activity ±SEM)	
Delta	14.14 (±1.5)	10.17 (±1.4)	12.75 (±2.6)	11.29 (±2.8)
Theta	8.14 (±0.6)	9.50 (±0.9)	8.25 (±0.6)	9.14 (±0.7)
Alpha	4.43 (±.0.3)	5.00 (±0.3)	4.75 (±0.3)	5.14 (±0.3)
Sigma	2.00 (±0.0)	2.17 (±0.2)	2.00 (±0.0)	2.29 (±0.2)
Beta	10.57 (±0.2)	11.50 (±0.2)	10.75 (±0.2)	12.29 (±0.3) #
Gamma	60.43 (±2.1)	61.83 (±1.9)	61.88 (±3.2)	60.00 (±3.6)

tendency toward increased activity (p=0.059)

2.3.2 PTZ Challenge

To determine if neonatal treatment with low dose DOM results in a permanent reduction in generalized seizure threshold, behavioural response to systemic injection of the convulsant PTZ was investigated. Groups of adult rats treated neonatally with either SAL or DOM (n=8 for each) and challenged with a single, normally subconvulsive dose (25 mg/kg) of PTZ demonstrated no differences in latency to absence seizure [$t_{(14)}$ = 0.755, p=0.463] or in the number of absence seizures experienced [$t_{(14)}$ = 1.525, p=0.149]. However, an evaluation of myoclonic activity revealed that treated rats had a decreased latency to the first MCJ [$t_{(11)}$ = 5.091, p = 0.041] and a tendency toward an increase in the total number of MCJs [$t_{(7)}$ = -1.999, p = 0.085]. The lack of statistical significance may be due to the high variability in the DOM group (see Table 2.2, pg 81 for a summary of these data).

In addition, an assessment of the maximum behavioural seizure level exhibited during the observational period revealed that a statistically significant number of DOM-treated rats [$X^2_{(1)}$ = 5.33, p=0.021] experienced Stage 5 (tonic-clonic) convulsions within 30 minutes of acute i.p. injection, a response that did not occur in controls at this dose (Figure 2.3, pg 82).

2.4 Discussion

The present study has shown that treatment with sub-convulsive doses of DOM during the second postnatal week of life produces identifiable alterations in EEG activity and an enhanced sensitivity to PTZ in the adult rat. The EEG alterations are characterized

Table 2.2 Total number of absence seizures and myoclonic jerk (MCJ) activity (mean ±SEM) exhibited during the 30 minute period following acute penylenetetrazol (25mg/kg) administration.

	SAL	DOM	
Measure:			(p value)
Absence (total #)	61.00 (±14.3)	34.88 (±9.4)	0.149
Absence latency (sec)	442.50 (±201.2)	255.00 (±152.4)	0.470
MCJ (total #)	0.63 (±0.5)	14.75 (±7.1)	0.085 #
MCJ latency (sec)	1560.00 (±176.0)	753.75 (±306.4)	0.043 *

tendency toward increased activity
*statistically significant decrease from controls

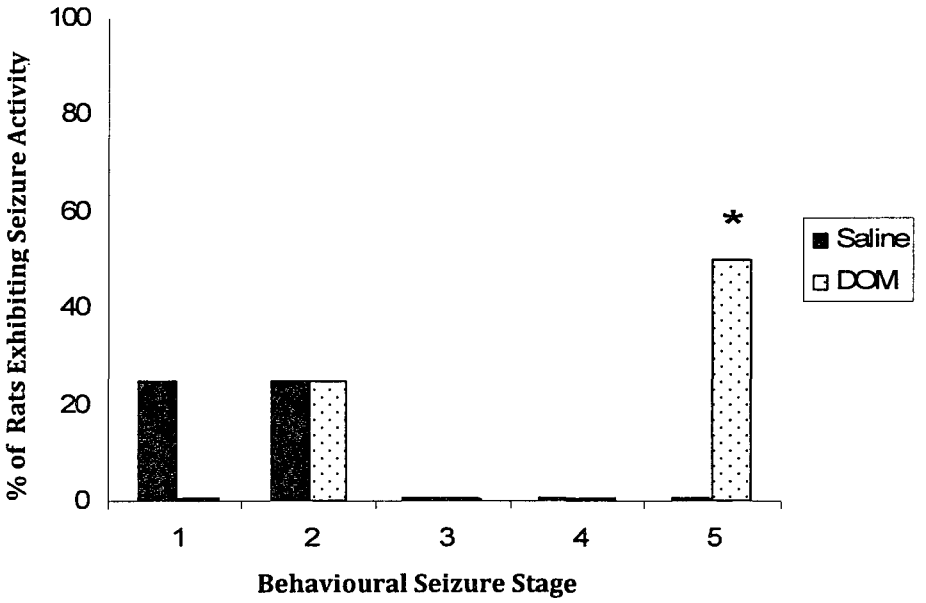

Figure 2.3 Maximum behavioural seizure stage (Racine, 1972a) exhibited during the 30 minute period following acute penylenetetrazol (25mg/kg) administration. Asterisk indicates a statistically significant difference from controls.

by two separate phenomena: 1) increased frequency output occurring in all recorded brain areas during NIS-L behaviours compared to baseline (Figure 2.1B and D, pg 77), and 2) a tendency toward increased power in the beta range (14-25Hz) in posterior brain regions compared to controls (Table 2.1, pg 79). The augmented response to acute PTZ exposure in DOM-treated rats (Figure 2.3, pg 82) is indicative of changes in excitatory / inhibitory tone at the generalized level.

Behaviours characteristic of the NIS-L phenomenon have been previously detailed by Doucette and colleagues (2004) as a combination of activities including hunched body posture, mastication, head bobbing, and repetitive eye blinking/squinting that appear equivalent to a Stage 2 seizure (Racine, 1972a). In the current study, this behavioural repertoire was manifested in both the anterior and posterior EEG leads as recurrent bursts of fast wave activity, accompanied by a well-defined response in the EMG lead (Figure 2.2, pg 78). The EMG activity is believed to be a result of the head bobbing behaviour, as the leads were positioned on the neck muscle (cervico-auricularis), and would therefore be particularly sensitive to this movement. Power spectra analysis of the peak frequency output during NIS-L activity revealed a significant increase during these episodes compared to baseline measures taken immediately prior to and following behavioural manifestation (Figure 2.1B and D, pg 77). This increase appears to be solely a result of the seizure-like activity itself and is distinct from normal behaviours, as baseline EEG measures often included grooming, walking around the cage, and rearing/exploring. The phenomenon is further exemplified in Figure 2.1A and C (pg 77), which shows the shift in brain activity from the lower frequencies displayed before

and after the seizure-like events, to those in the gamma range during NIS-L behavioural expression.

A strong tendency to an overall increase in beta activity in posterior brain regions was found in DOM-treated rats following water maze exposure (Table 2.1, pg 79). In humans, increases in beta band frequencies have been linked to heightened fear and/or anxiety levels (Aftanas *et al.*, 2006; Sachs *et al.*, 2004), while in rats, beta bands are considered to be a relevant measure of pharmacological effects of both benzodiazepines and non-BZP receptor modulators at the GABA receptor complex (Mandema and Danhof, 1992; van Lier *et al.*, 2004; Visser *et al.*, 2003a; Visser *et al.*, 2003b), with increases representing higher levels of alertness. The alteration in beta activity found in the current study is especially interesting given the interdependency between GluK5 receptors (for which DOM has high affinity), and GABA interneuron function and development (Ben-Ari and Cossart, 2000; Braga *et al.*, 2003; Lerma *et al.*, 2001). One region with exceptionally high GluK5 expression is the amygdala (Braga *et al.*, 2003), an area that is also well-known to play a central role in emotional processing (Sah *et al.*, 2003), particularly for stress and anxiety responses (Berretta, 2005; Goldstein *et al.*, 1996; Shekhar *et al.*, 2005). In addition, the amygdala has been shown to operate under tight inhibitory control through GABA-mediated pathways (Aroniadou-Anderjaska *et al.*, 2007; Ehrlich *et al.*, 2009). The GluK5 receptor subunit, which is often situated presynaptically on GABA interneurons in both the amygdala and the HC (e.g. Braga *et al.*, 2003; Lerma, 2006 for review), is thus in an unique position to provide modulatory activity throughout this region.

In humans, stress is reported to be the most common precipitant for seizure activity (Frucht *et al.*, 2000; Koutsogiannopoulos *et al.*, 2009; Pinikahana and Dono, 2009), thus strongly implicating amygdalar involvement in seizure generation, while further association is suggested through the high sensitivity of the amygdala to kindling procedures in the production of animal seizure models such as TLE (for review, see McIntyre, 2006). Tied closely to the amygdala, both functionally and anatomically, the HC is also very susceptible to the kindling procedure (McIntyre, 2006). Recent *in vitro* studies have shown that beta rhythms can also result from increased excitability in principal cells from area CA1 of the HC that receive perisomatic innervation from fast-spiking GABAergic interneuronal populations (Bibbig *et al.*, 2007). It is therefore possible that the increase in beta activity seen in this study may be indicative of subtle changes in GABAergic regulation within the amygdala and/or HC of NIS-L rats as a consequence of postnatal DOM exposure, manifesting as both a heightened stress/anxiety response, as well as low-grade seizure activity. While these results are subtle, they do raise intriguing questions regarding the possible role of these structures in the generation of NIS-L effects, and definitely warrant further investigation.

Since the administration of DOM in the NIS-L model is systemic, and since DOM is an analog of Glu, a neurotransmitter with ubiquitous activity throughout the CNS, it is reasonable to expect that early exposure to this excitotoxin could potentially affect the balance of excitation/inhibition in whole brain systems as well. Recent studies have highlighted the myriad changes that can occur in the balance between excitatory and inhibitory function during development (Brooks-Kayal, 2005; Gubellini *et al.*, 2001; Levitt, 2005), especially within the critical time window when GABA, an inhibitory

neurotransmitter in the adult brain, is undergoing its conversion from a depolarizing to a hyperpolarizing role as the system matures (Ben-Ari, 2002; Lee *et al.*, 2005; Sipila *et al.*, 2005; Tyzio *et al.*, 1999). During this switch, Glu receptors gradually come online and begin to assume the excitatory functions that they will continue to control throughout adulthood. Interestingly, GluK5 receptors in particular are believed to be tightly linked to the GABA/ Glu switch, as these receptors function both postsynaptically and presynaptically, where they have been shown to modulate synaptic transmission in excitatory and inhibitory terminals in the HC (Breustedt and Schmitz, 2004; Fisahn *et al.*, 2004; Jiang *et al.*, 2001) and amygdala (Braga *et al.*, 2003; Braga *et al.*, 2004; Rogawski *et al.*, 2003).

In the current study, a decrease in generalized seizure threshold was observed, as indicated by a significant number of DOM-treated rats experiencing Stage 5 tonic-clonic behavioural and electrographic seizure following a single sub-convulsant (i.p.) dose (25mg/kg) of PTZ. This was completely unexpected, and was not seen in SAL controls. There was also a decrease in latency to MCJs in DOM-treated rats, indicating an overall increase in seizure induction rate (Ahern *et al.*, 2006; Szot *et al.*, 1999), as well a tendency for treated rats to display increased MCJ (generalized) behaviours (Table 2.2, pg 81). Additionally, the shifting of the spectral power band patterns toward the gamma range may be seen in both anterior and posterior brain regions (Figure 2.1A and C, pg 77), and peak frequencies are similarly increased over all cortical areas (Figure 2.1B and D, pg 77) during the manifestation of seizure behaviours. However, an inspection of the power band graphs reveals that more activity still seems to be occurring in posterior (hippocampal/amygdalar) regions, although this difference has not been quantified. As

well, it appears that the seizure activity is probably not mediated by a thalamo-cortical process, since latency to absence seizure and the number of absence seizures in response to acute PTZ did not differ between the groups, even though that same low dose did elicit Stage 5 seizure in treated animals (Table 2.2, pg 81).

Insult or injury to the developing brain during critical periods of maturation and final organization of excitatory and inhibitory function may have far reaching consequences, including altered responses to stress and/or seizure genesis. The current study has investigated and provided a characterization of changes in EEG output from adult rats following low-dose perinatal DOM exposure during an important window of postnatal development. Using radiotelemetry to record EEG in freely moving rats during a behavioural task that is considered to be moderately stressful, seizure-like behaviours were observed in treated animals, and visible and quantifiable alterations in EEG activity were present during these episodes compared to baseline activity in the same rats. DOM treated rats also showed an overall heightening of beta activity for at least one hour following water maze exposure, whether NIS-L behaviours were exhibited or not, which may indicate an altered response to stress and/or novelty. And finally, NIS-L rats have a lowered seizure threshold for acutely administered PTZ. Based on the novel data presented here, it is evident that early life exposure to even low levels of excitatory neurotoxins may be associated with permanent modifications in seizure susceptibility. In this respect, the NIS-L model fills an important niche in the study of developmentally generated seizures.

3.0 FOCAL SEIZURE THRESHOLD AND SEIZURE PROPAGATION IN THE NIS-L RAT MODEL

Portions of this chapter have been submitted to Neuroscience as follows: Gill, D.A., Bastlund, J.F., Watson, W.P., Ryan, C.L., Reynolds, D.S., Tasker, R.A. Neonatal exposure to low-dose domoic acid lowers seizure threshold in adult rats.

Additional information pertaining to this study can be found in Appendix B.

3.1 Introduction

Exposing Sprague-Dawley rat pups to very low, sub-convulsant doses of DOM during perinatal development has been previously shown to result in seizure-like behaviours (NIS-L) in adulthood that are similar to those of partial complex epilepsy (e.g. TLE) in humans, as well as cellular changes in the DG and area CA-3 of the HC (Bernard *et al.*, 2007; Doucette *et al.*, 2004). In addition, *in vivo* electrophysiological studies of this model using radiotelemetry have revealed alterations in EEG patterns during low-grade behavioural seizure episodes, as well as a reduction in generalized seizure threshold levels (see Chapter 2).

Currently, one of the most widely used animal models for TLE is the electrical kindling model (Goddard, 1967), which normally involves daily exposure to a short duration, low amplitude focal brain stimulation via a stereotaxically placed depth electrode (McIntyre, 2006). Commonly targeted limbic brain structures are either the amygdala or HC, with each site displaying a distinctly identifiable profile during kindling development. The behavioural progression of seizures during amygdala kindling is frequently measured using a five-point scale (Racine, 1972a), and progression through these stages has been shown to correspond well with neuronal seizure propagation (Hewapathirane and Burnham, 2005). The predictability of seizure progression makes this protocol a useful tool for studies involving focally generated seizure activity, and the ability to control the amplitude of the stimulation allows for a graded assessment of basal sensitivity in the targeted region, a concept most often referred to as seizure threshold.

Functional changes underlying kindling in the brain are often confirmed using Timm staining, a histological method that allows for visualization of the mossy fibre pathway (axons running from the granule cells in the DG to pyramidal cells in area CA-3) in the HC. Under normal conditions, moderate increases in MFS are associated with learning and memory, reflecting the increased connectivity required in this region to support its enhanced function (Adams *et al.*, 1997; Holahan *et al.*, 2006; Ramirez-Amaya *et al.*, 1999; Ramirez-Amaya *et al.*, 2001). However, following seizure activity, excessive and aberrant MFS occurs, and this inappropriate sprouting is considered to be one of the defining hallmarks for seizure pathology (for review, see Cavazos *et al.*, 1991; Represa and Ben-Ari, 1992; Sutula *et al.*, 1988). Consequently, sprouting of mossy fibres is often used as a direct measure of kindling development and progression (Sutula and Dudek, 2007).

As a known trigger for seizure in humans (Frucht *et al.*, 2000; Koutsogiannopoulos *et al.*, 2009; Temkin and Davis, 1984), as well as having been shown to accelerate kindling in animals (Kumar *et al.*, 2007), stress may also be an important factor in generating NIS-L activity. While previous studies in our lab have shown no differences in CORT or its precursor, adrenocorticotropic hormone (ACTH) levels as a measure of physiological stress in response to mild to moderately stressful events (Perry *et al.*, 2009), to date, no investigation of these indicators following highly stressful activities has been performed.

The primary purpose of the current study was to investigate possible long-term changes in focal seizure susceptibility and propagation in the NIS-L rat model using an electrical

kindling paradigm. In addition, the consequences of acute, high-level stress on both kindling development and CORT/ACTH response in the model were examined. A subsequent analysis of MFS to explore potential underlying structural modifications within the groups will also be presented.

3.2 Materials and Methods

3.2.1 Experimental animals

Male offspring born in-house from untimed Sprague-Dawley rats (Charles River, Germany) were culled within 24 hours of birth to 8 pups per litter. From postnatal day 8-14 (inclusive), pups were weighed and given a single daily injection (10ml/kg, s.c.) of either 20μg/kg DOM (BioVectra dcl, Canada) or SAL (Doucette *et al.*, 2004). All other procedures for postnatal handling were as described in Chapter 2. Surgeries and testing were performed between 09:00h and 18:00h and were carried out under a license from the Danish Ministry of Justice, and in accordance with the EC Directive 86/609/EEC and the Danish law regulating experiments on animals. A timeline for all experimental manipulations used in this study can be found in Figure 3.1 (pg 92).

3.2.2 Kindling surgery

Rats approximately 60 days old (n=54; 28-DOM, 26-SAL) were anaesthetized as described for the telemetry surgeries (Chapter 2) and stereotaxically implanted with a polyimide-insulated, twisted stainless steel bipolar electrode (Plastics One, Inc) for stimulation and recording in the right amygdala (3.0 mm posterior, 4.8 mm lateral

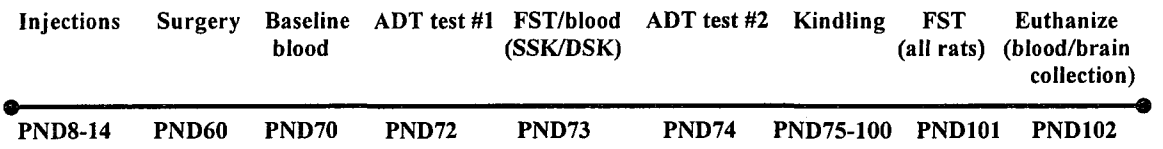

Figure 3.1. Time line for experimental manipulations. ADT - afterdischarge threshold; PND - postnatal day; SSK - saline stress/kindle group; DSK - DOM stress/kindle group; FST - modified forced swim task.

to bregma and 7.2 mm ventral from dura). Prior to and for 5 days following surgery, all rats were treated with Rimadyl vet® (5mg/kg s.c., Pfizer, Denmark) and Baytril vet® (5mg/kg s.c., Bayer Health Care, Denmark) and allowed two weeks to recover before the commencement of testing.

Further pain relief was given immediately following surgery through an s.c. injection of Temgesic (0.3 mg/ml buprenofin, Schering-Plough, USA). Local irritation was treated with 5% Xylocaine crème (lidocainechloride, AstraZeneca, Norway).

3.2.3 Acute stress paradigm

Two days prior to the commencement of any other manipulations, tail vein blood samples (~1.5ml) were taken from all rats, collected in sterile 2ml containers (Vacuette K_3 EDTA) and stored on ice until microcentrifugation (Megafuge 1.0R (Thermo Scientific) @3274xg for 15 minutes @4°C) to provide serum for baseline CORT/ACTH levels. Serum samples were then frozen and stored at -80°C until assayed.

To assess the physiological effects of an acute, high-level stressor in DOM-treated rats, 2 sub-groups were selected (SAL STRESS + kindle (SSK; n=8), DOM STRESS + kindle (DSK; n=8)) to swim in a modified forced swim task (FST) between threshold testing days (see section 3.2.4 for details regarding ADT testing). The modified FST is a highly stressful behavioural test that has been previously utilized for studies with this model (see Appendix A, section A.6, pg 242 for details). During FST, rats were monitored for NIS-L behaviours by an experimenter blind to condition. Within 20 minutes of FST exposure, blood was again sampled from the stress groups as described above.

At the conclusion of the kindling process, rats from all groups were swum in the modified FST to assess spontaneous behavioural seizure activity. Twenty-four hours later (at time of euthanization) trunk blood was collected as a final baseline measure. Care was taken during all blood collections to control for time-of-day sampling effects.

Corticosterone radio immunoassays (RIAs) were performed using Coat-A-Count Rat CORT kits (TKR-C1; Diagnostic Products Corporation, USA), while ACTH (R,M) RIA kits (Phoenix Pharmaceuticals, Inc., USA) were used for ACTH assays. All counts were obtained through RiaCalc WIZ (v3.6). Intra-assay co-efficient of variance values for CORT ranged from 0.21 to 7.18, with a mean value of 2.05, while values for ACTH ranged from 0.34 to 11.23, with a mean value of 4.16.

3.2.4 Focal seizure susceptibility and seizure propagation

Rats with implanted electrodes for kindling were stimulated via a custom made stimulator (Ellegaard systems, DK), and the resultant EEG was recorded unfiltered using an amplifier (model 1902, CED, UK), a digitaliser (micro1401, CED, UK) and Spike2 software (version 4.21, CED, UK).

Prior to the commencement of kindling, rats were tested once per day for two days (one day between electrical stimulations) to determine after discharge threshold (ADT) according to the following paradigm. Stimulations consisted of 1sec trains of 50 Hz, 1ms biphasic square-wave pulses; the first day stimulations started at 100μA and were increased in 10μA increments every 60 sec until an AD was evoked, or until an intensity of 500μA was reached. On the subsequent day of threshold testing, stimulations were

initiated 100μA below the level that had previously elicited an AD and increased in 10μA increments every minute until AD was achieved, but at no time were rats given a stimulation below the 100μA baseline level. Rats that exhibited a response at the initial stimulation level (100μA) were scored as 100 (n=2), while rats that failed to respond by 500μA (n = 3) were arbitrarily classified as shams, and no further stimulation was delivered. In addition, since they had no measured response level, they were not included in the ADT analysis. Intensity of stimulation required to produce an AD, duration of AD (ADD), and behavioural seizure stage achieved (Racine *et al.*, 1972a) were all recorded.

Following threshold testing, rats were quasi-randomly divided into six groups: SAL + kindle (SK; n=9), SAL STRESS + kindle (SSK; n=7), SAL sham (SS; n=9), DOM + kindle (DK; n=12), DOM STRESS + kindle (DSK; n=8), and DOM sham (DS; n=8). For those animals in kindle groups, kindling was initiated 24 hours following the final ADT testing, and consisted of one stimulation per day (7 days/week) for 25 days at an intensity 25μA higher than that required to produce an AD on testing day 2. Duration of AD, maximum behavioural seizure stage evoked (Racine, 1972a), and duration of Stage 5 seizure (if exhibited) was recorded each day by an experimenter blind to perinatal treatment. Rats were considered to be fully kindled after experiencing 5 consecutive stage 5 seizures, as manifested both behaviourally and electrographically.

3.2.5 Analysis of kindling data

Delivery of electrical stimulus was confirmed via EEG tracings (Spike2 software v. 4.21, Cambridge Electronic Design, UK) as a "flat line" recording. The AD was

identified as an alteration in waveform consisting of a simple spike or spike and wave pattern lasting for a minimum of 3 seconds following the stimulus. Behavioural seizure stages were recorded according to the (Racine, 1972a) 5-point scale. Only animals subsequently confirmed by histology to have electrode placements in the amygdala were included in statistical analyses.

3.2.6 Timm staining and electrode verification

Timm staining was used to provide visualization and quantification of the mossy fibre pathway in the HC of rats from the kindling groups. Within 48 hours of the final kindling stimulation (24 hours following forced swim testing; see Figure 3.1, pg 92), rats were euthanized with pentobarbital (Unikem, Denmark) and immediately decapitated. Electrodes were removed, and brains were cut into hemispheres and immersed in a 0.4% sodium sulphide solution for 20 minutes (Sperber *et al.*, 1991). Each hemisphere was then placed in 50ml of 30% (w/v) sucrose in 10% buffered neutral formalin (BNF) for 36 hours. Tissue was frozen in Cryo-Matrix using dry ice and stored individually in air-tight aluminum freezer bags at -80°C until sectioning with a cryostat.

Sections used for Timm staining were cut in the coronal plane at 20μm on 0.5% gelatin coated slides and allowed to dry overnight. Each slide contained slices at 3 hippocampal levels from either SO or SL (dorsal, intermediate, ventral), while the inner molecular layer of the DG was examined at dorsal and ventral levels only. Dorsal was delineated as -3.50mm relative to Bregma, intermediate was -4.50mm relative to Bregma, and the ventral level was considered as -5.50 relative to Bregma. Timm staining was performed

according to a previously validated protocol (Bernard *et al.*, 2007), with slight modifications. On the morning of staining, 0.5% gelatin was gently pipetted over each section of tissue, and allowed to sit for 1-2 minutes before removal. Tissue was then oven dried at ~32°C for 3 hours, during which time the Timm's mixture was prepared in a glass staining dish using the following ingredients: 120ml of 50% gum Arabic (in dH_20), 10 ml citric acid (5.1g per 10ml dH_20), 10ml sodium citrate solution (4.7g per 10 ml dH_20), 50ml hydroquinone in 50ml (3.47 g per 50ml dH_20), 10ml Silver Nitrate (212.25 mg in 10ml dH_20), for a total volume of 200ml. All chemicals were supplied by Sigma-Aldrich (Oakville, Ontario, Canada). The final 2 ingredients were mixed, but not added to the solution until immediately before use. To avoid the possibility of any metal contamination, all utensils and containers consisted of freshly washed glassware. Tissue was developed in total darkness (~80-100 minutes) with the solution constantly stirred at 200rpm. Once developed, slides were washed for 45 minutes in tap water, serial dehydrated in ethanol (70%, 95%, 100%, 100%; 3 minutes each), cleared twice in xylene, and cover-slipped with Permount.

Mossy fibre images were blind-scored using Image J software (National Institutes of Health) using images obtained through a Zeiss Axioplan2 Imaging microscope (2.5x objective) equipped with an AxioCam HR digital camera and utilizing the density analysis method described by Bernard *et al.* (2007). The nine areas of the inner molecular layer (IML) of the DG, and six in both SL and SO of CA3 that were analyzed for the current study are demarcated in Figure 3.2 (pg 98), along with the locations of the corresponding background measurements.

Figure 3.2. Scoring points used for quantification of mossy fibre sprouting. Dentate gyrus: black circles represent the nine areas sampled in the inner molecular layer, while the red circles (outer molecular layer) show areas used for background measurement. Hippocampus proper: yellow circles show the position of stratum lucidum samples, green delineates areas recorded for stratum oriens, and blue show background measurements. (Tissue silver-labeled for heavy metals using Timm stain, and cell bodies counter-stained with 0.1% cresyl-violet).

Electrode placements for kindled animals were verified using 20μm sections (cut in the coronal plane) on charged slides (Superfrost Plus; Fisher Scientific, U.S.A.), stained with cresyl violet and compared to the Paxinos and Watson (2007) brain atlas for location confirmation (see Figure 3.3, pg 100 for representative image).

3.2.7 Data Analysis

Parametric data were analyzed using either paired or independent t-tests or ANOVAs with repeated measures when required, while non-parametric measures were examined using Chi Square (X^2) Crosstabulation and Mann Whitney U tests for rank ordered data. Results for behavioural data are expressed as mean ±SD, while all other results are mean ±SEM. Analyses were performed using SPSS (v.10.0.5 SPSS Inc., Chicago, IL), and the significance level for all tests was set at

$\alpha \leq 0.05$.

3.3 Results

At various time points during the kindling procedure, several rats (n=6) had to be euthanized due to loosened electrodes, leaving 48 rats at the conclusion of the study.

To determine if early-life exposure to low dose DOM results in a permanent reduction in focal seizure threshold, neonatally-treated DOM and SAL rats implanted with a single, bipolar electrode in the right basolateral amygdala at PND90, were tested to determine the minimum amplitude required to elicit an AD over two separate days. Subsequent analysis revealed that DOM-treated rats have a significantly lower ADT [$F_{(1,36)} = 4.688$, $p=0.037$] in response to electrical stimulation of this area (see Figure 3.4, pg 101).

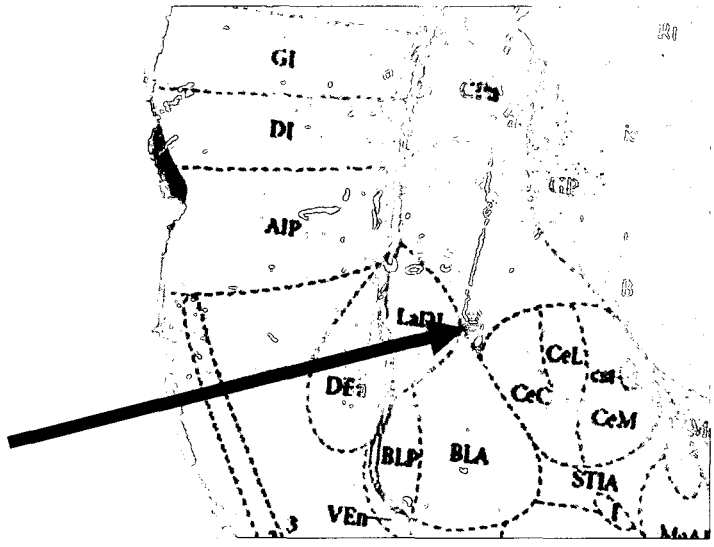

Figure 3.3. Representative example of a correctly placed electrode for amygdala kindling. Tissue stained with 0.5% cresyl-violet for visualization, and overlaid with appropriate template co-ordinates from the Paxinos and Watson (2007) rat brain atlas.

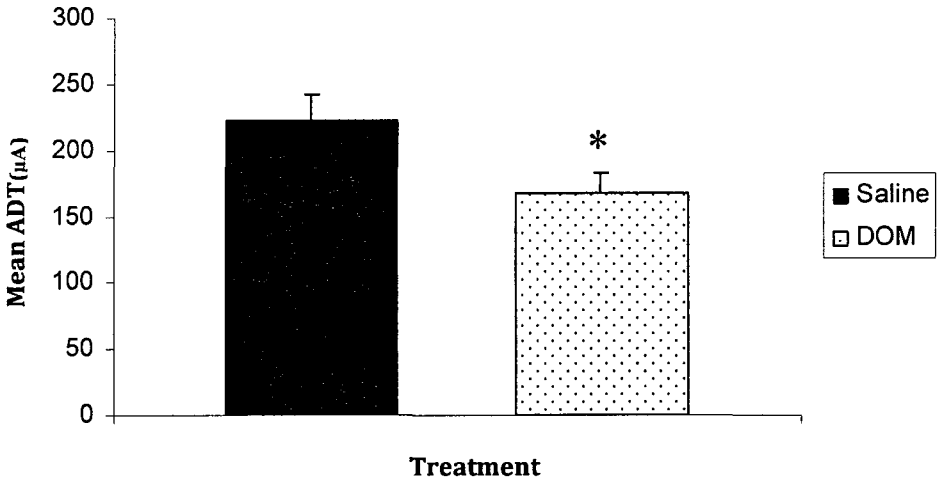

Figure 3.4. Mean after-discharge threshold (ADT) in the amygdala over two testing days (repeated measures – focal seizure threshold) for DOM and saline treated rats. Error bars indicate SEM and the asterisk denotes a significant difference from controls ($p<0.05$).

In response to an acute exposure to the modified FST, a statistically significant number of DOM-treated rats displayed the NIS-L syndrome (62.5% DOM; 0% SAL) [$X^2_{(1)}$ = 6.563, p = 0.010]. However, RIA analysis revealed no differences between the groups in CORT or ACTH levels at any time point (see Table 3.1, pg 103 for a summary of these data), although counts were definitely elevated for all rats during the first 20 minutes following FST exposure.

Following threshold testing, rats from each treatment group received one electrical stimulation a day for 25 consecutive days at 25μA above their individual ADT level, with the subsequent AD duration, maximal behavioural seizure (MBS) stage, and duration of Stage 5 seizure (if present) recorded. Since there were no statistically significant differences noted for these measures between stress and non-stress groups in each treatment (SAL ADD [$F_{(1,8)}$=0.853, p =0.383]; mean behavioural seizure stage SK – 3.5±0.28 versus SKS – 3.4±0.31; DOM ADD [$F_{(1,11)}$=3.789, p = 0.078]; mean behavioural seizure stage DK – 3.0±0.26 versus DKS – 3.6±0.34) (see Appendix B.2, pg 248 for graphical presentation over days), groups were collapsed for further analysis. As depicted in Figure 3.5A (pg 104), there were no differences noted in behavioural seizure progression, and no change in ADD between DOM and SAL kindled rats overall (Figure 3.5B, pg 104). In addition, latency to the first Stage 5 seizure, latency to the fully kindled state (defined as 5 consecutive Stage 5 seizures), total number of Stage 1-3 seizures, total number of Stage 4-5 seizures, and total number of behavioural seizures overall did not differ, nor did the duration of the Stage 5 seizures (Table 3.2, pg 105; Appendix B3.1, pg 249).

Table 3.1. Summary of corticosterone (CORT) and adrenocorticotropic hormone (ACTH) counts (mean ±SEM) prior to any manipulations (pre-baseline: n=47; 19-SAL, 28-DOM), after exposure to the forced swim task (FST: n=15; 7-SAL, 8-DOM), and at the end of the study (post-baseline: n=42; 18-SAL, 24-DOM).

	CORT(ng/ml)		ACTH (pg/ml)	
	SAL	DOM	SAL	DOM
	(Mean ±SEM)		(Mean ±SEM)	
Measure				
Pre-Baseline	374.59 (±35.1)	332.26 (±28.8)	474.76 (±22.1)	459.00 (±17.7)
After FST	654.86 (±47.6)	681.91 (±31.8)	514.64 (±51.0)	502.79 (±34.7)
Post-Baseline	148.47 (±67.4)	148.99 (±12.7)	447.01 (±19.9)	453.73 (±23.4)

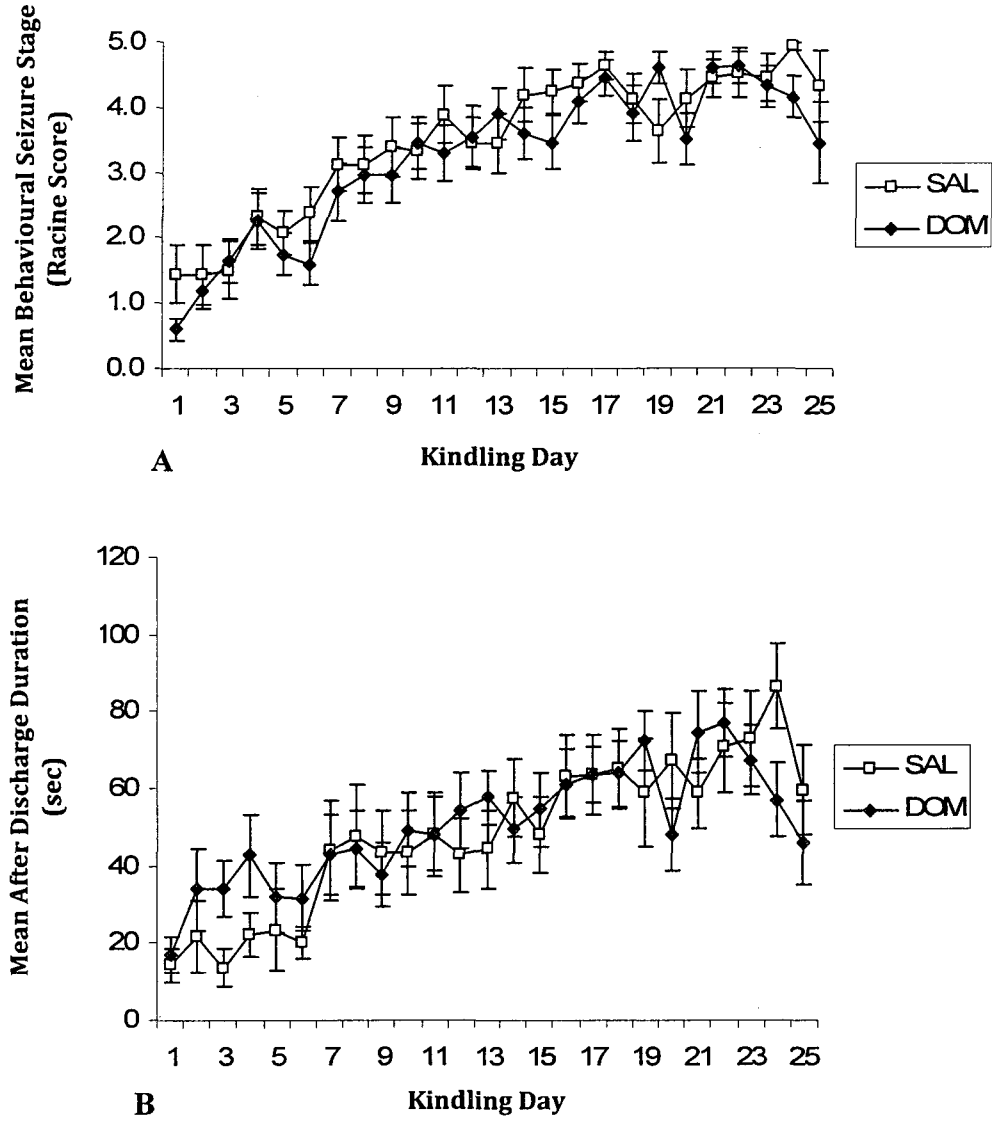

Figure 3.5. Seizure progression over kindling days for DOM and SAL treated rats. A) Behavioural seizure scores B) Mean after discharge durations. Error bars indicate ±SEM.

Table 3.2. Summary of behavioural seizure progression and total behavioural seizures (mean ±SD) exhibited by DOM-treated and control rats during kindling.

Measure	SAL	DOM
Latency to 1st Stage 5 seizure (days)	9.38 (±5.57)	8.79 (±4.88)
Latency to fully kindled (days)	17.50 (±8.13)	18.74 (±6.03)
Duration of Stage 5 seizures (sec)	8.24 (±2.30)	9.56 (±3.52)
Total # Stage 5 seizures	12.00 (±4.87)	12.22 (±3.64)
Total # Stage 1 / 2 / 3 seizures	8.63 (±4.47)	9.11 (±3.88)
Total # Stage 4 / 5 seizures	13.81 (±5.10)	13.78 (±4.32)
Overall seizure total	22.44 (±1.79)	22.89 (±.963)

To assess whether exposure to high-stress following the completion of kindling would induce or increase the severity of seizure activity in any of the kindled groups, all rats were run in the modified FST. As a physical measure of stress level, the presence of porphyrin during the testing period was also recorded as a 'yes' or 'no' response. In the stress groups, 66.6% of DOM-treated rats (4 of 6) exhibited NIS-L behaviours compared to 0% in the SKS group [$X^2_{(1)} = 6.741$, $p = 0.009$]. Since this was the second exposure to this task for these rats (and was thus presumably no longer novel), it is notable that 3 of the 4 animals that showed this behavioural sequelae had also exhibited it during the first FST exposure as well. In addition, an analysis of behavioural response to FST exposure following kindling revealed a difference in NIS-L expression between kindled groups overall [$X^2_{(1)} = 13.092$, $p < 0.001$] (Figure 3.6A, pg 107 provides a graphical representation of the percentage of rats displaying NIS-L during FST). However, no sign of seizure activity above the Racine (1972) Stage 2-3 level was seen in any group at any time.

There was no difference between stress groups for porphyrin secretion [$X^2_{(1)} = 0.066$, $p = 0.797$]. However, an assessment of the no-stress groups showed a statistically significant increase in porphyrin expression in DOM-treated, kindled rats [$X^2_{(1)} = 7.875$, $p = 0.005$] compared to their SAL counterparts, a difference that resulted in a significant increase in DOM-treated groups overall [$X^2_{(1)} = 4.153$, $p = 0.042$] (see Figure 3.6B, pg 107).

Mossy fibre sprouting has been shown to increase in both animal (Dudek and Sutula,

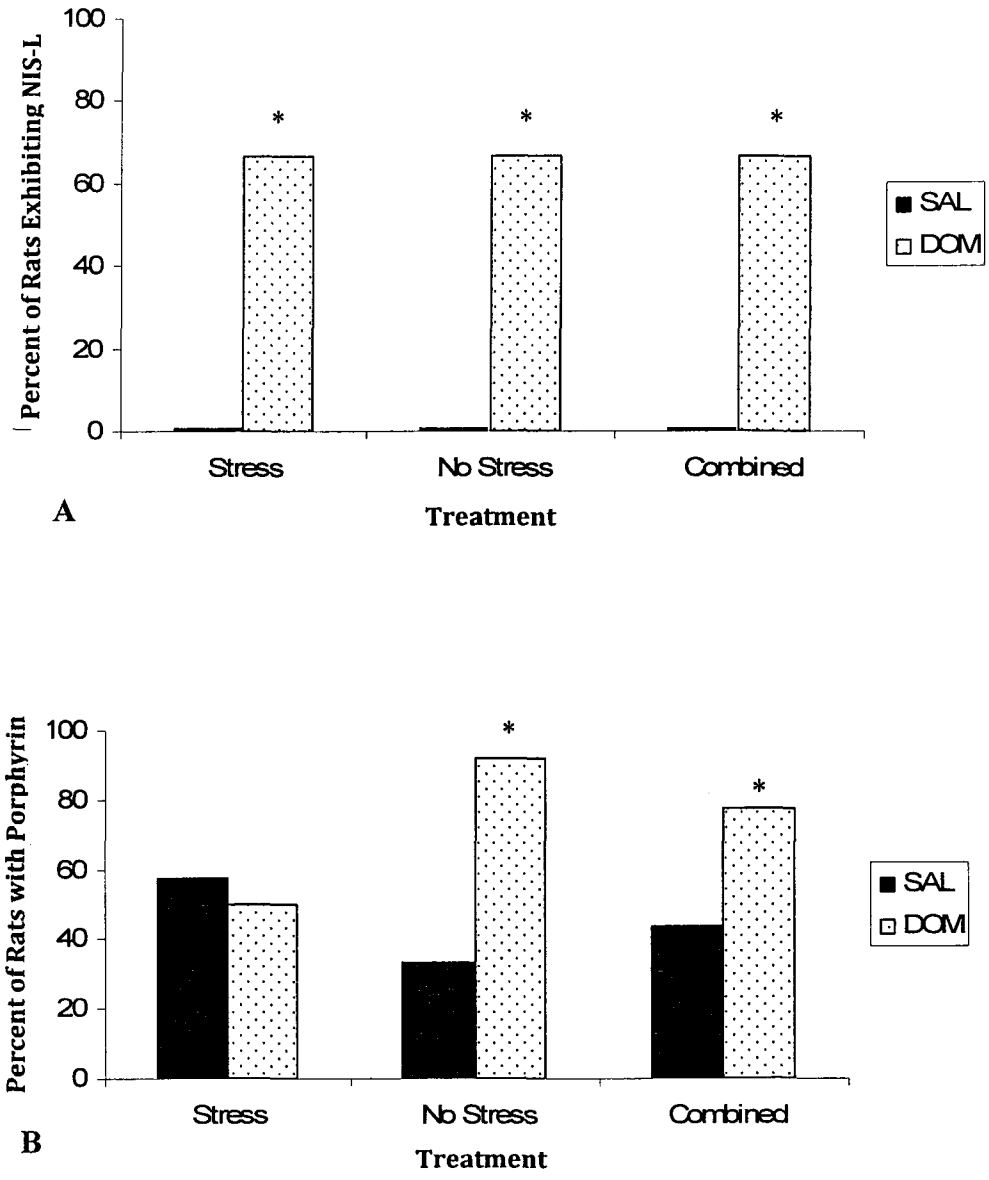

Figure 3.6. Differences between stressed, non-stressed, and combined groups of DOM-treated and control rats in the modified forced swim task following 25 days of electrical amygdala kindling. A) Percentage of rats in each group showing NIS-L behaviours during testing B) Percentage of rats expressing porphyrin during the testing period. Asterisks represent a significant difference from the appropriate control group ($p<0.05$).

2007; Frotscher *et al.*, 2006; Nadler, 2003; Sutula *et al.*, 1988; Tauck and Nadler, 1985) and human (Babb, 1991; de Lanerolle *et al.*, 1989; Houser, 1990; Sutula *et al.*, 1989) HC following seizure activity. Previously, our lab has reported a significant increase in MFS in the ventral IML of adult rats as a result of perinatal DOM administration in the absence of any other extrinsic manipulation (Bernard *et al.*, 2007). In the current study, an assessment of MFS for both the stimulated and the non-stimulated hemisphere was performed using Timm staining to assess changes that might have occurred in hippocampal cytoarchitecture for DOM-treated and control rats as a result of the kindling process and/or the acute behavioural stressor experienced by DKS and SKS rats prior to kindling. In agreement with previous findings, all treated rats (kindled, kindled stress, and sham) showed increases in MFS, with dramatic changes occurring in the IML at the ventral level in both left [$F_{(1,46)} = 12.455$, $p = 0.001$] and right [$F_{(1,43)} = 13.056$, $p = 0.001$] hemispheres (Figure 3.7, pg 109). This increase remained consistent with or without the inclusion of sham kindled rats, indicating that the sprouting in this region was inherent in the treated group. As an evaluation of the stress groups compared to their kindled counterparts (i.e. DOM-stress versus DOM kindled; SAL-stress versus SAL kindled) revealed no statistically significant differences between the groups, their data was collapsed into the appropriate treatment condition for the remainder of the analysis.

Mossy fibre sprouting in the dorsal SO in the hemisphere contralateral to electrode placement was also significantly increased in DOM-treated animals [$F_{(1, 46)} = 5.331$, $p = 0.025$] (Figure 3.8, pg 110). Results from all measured hippocampal areas are shown in Table 3.3 (pg 111). As expected, an analysis of MFS between all sham and

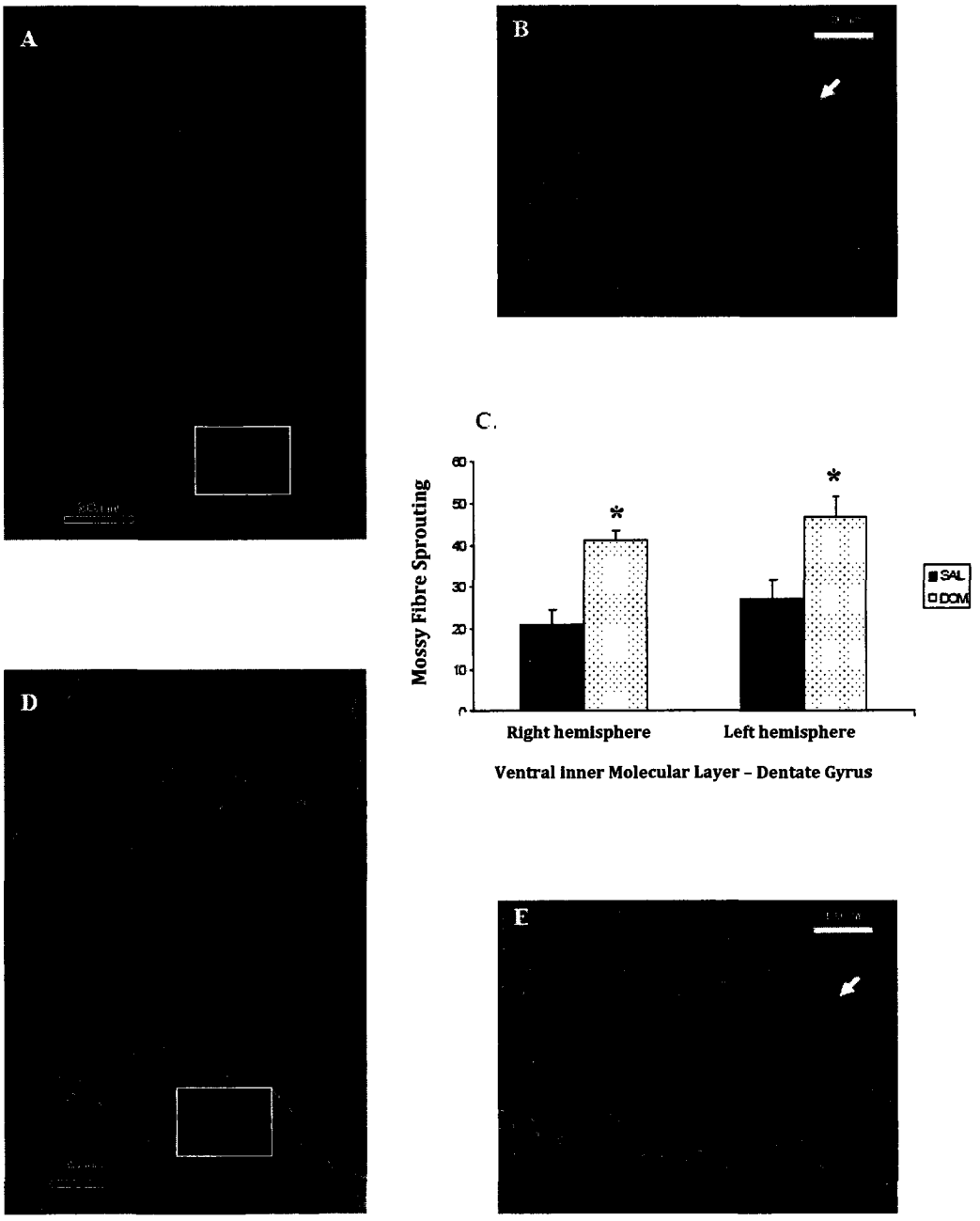

Figure 3.7. Mossy fibre sprouting at -5.5mm bregma in kindled rats. DOM-treated rats show increased sprouting in the inner molecular layer at the ventral level. White boxes in A & D delineate areas shown in greater detail in B & E. A) SAL hippocampus (right hemisphere) B) SAL inner molecular layer. Some small zinc deposits throughout the granule cell layer and inner molecular layer are indicated by the white arrow. C) Graphs showing group differences in MFS for both right and left hemispheres. Error bars indicate SEM and asterisks denote a significant difference from controls ($p<0.01$). D) DOM hippocampus (right hemisphere) E) DOM inner molecular layer. Note the heavy band of zinc (MFS) running throughout the inner molecular layer (white arrow) compared to deposits in B.

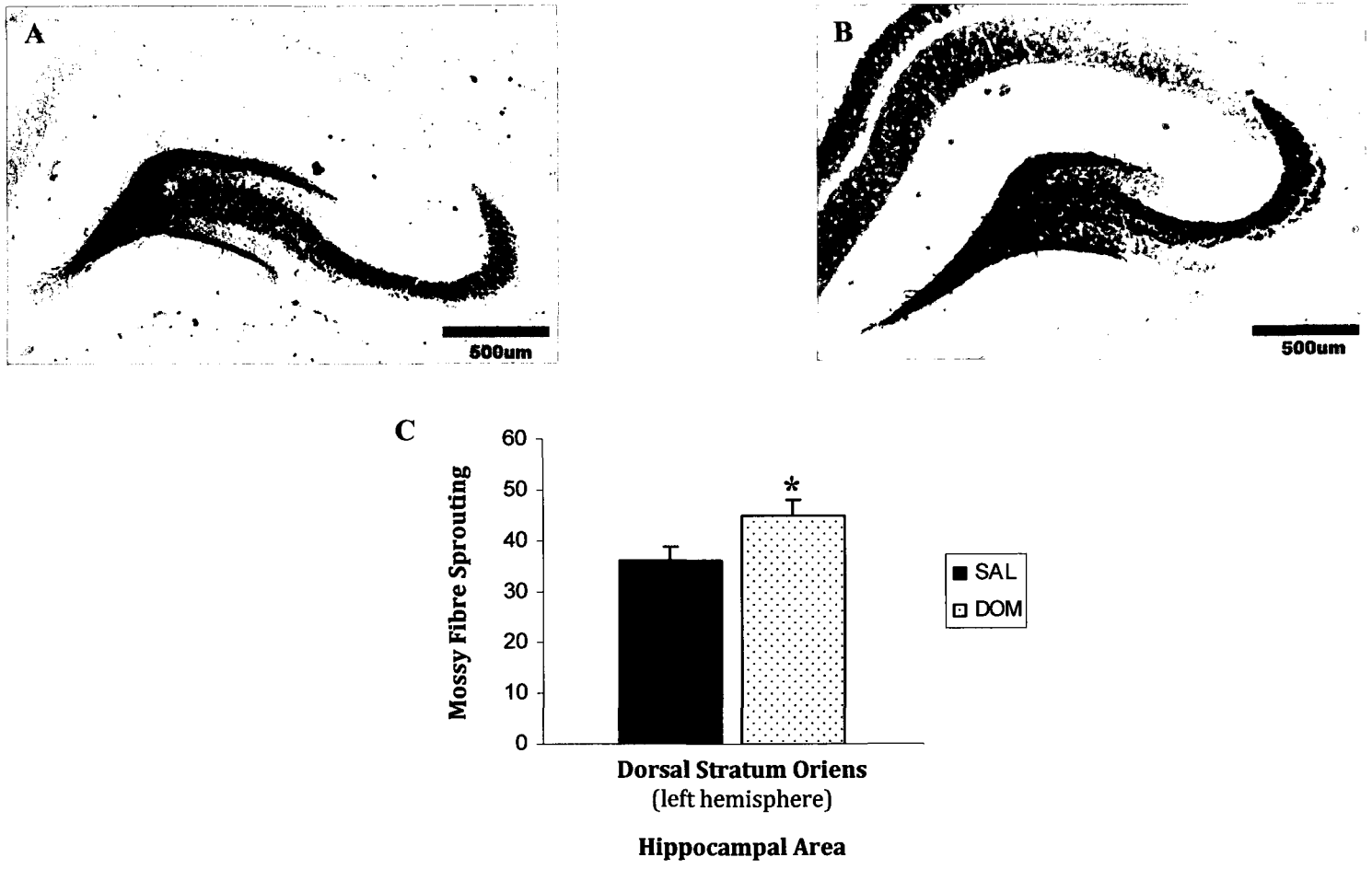

Figure 3.8. Mossy fibre sprouting in dorsal CA3. A) SAL B) DOM C) Graph of group differences in MFS in left stratum oriens. Error bars represent SEM and the asterisk indicates a significant difference from controls ($p<0.05$).

Table 3.3. Mean (±SEM) mossy fibre sprouting scores for SAL and DOM-treated kindled rats.

Hippocampal Region	SAL		DOM	
	Left	Right	Left	Right
Dentate gyrus:				
IML – dorsal	4.4 (±0.58)	4.9 (±2.30)	3.8 (±0.41)	3.7 (±0.44)
IML – ventral	21.1 (±3.45)	27.2 (±2.39)	41.1 (±4.50) *	46.7 (±5.08) *
Stratum oriens:				
Dorsal	36.3 (±2.66)	40.7 (±2.38)	45.2 (±2.79)*	42.5 (±2.82)
Mid	6.3 (±1.65)	10.4 (±1.63)	8.5 (±2.61)	7.9 (±2.14)
Ventral	17.9 (±1.76)	18.6 (±1.77)	17.7 (±1.79)	17.0 (±1.44)
Stratum lucidum:				
Dorsal	86.1 (±3.86)	91.5 (±2.77)	92.4 (±3.20)	87.8 (±3.65)
Mid	92.1 (±2.95)	88.0 (±2.14)	91.8 (±3.95)	93.9 (±3.92)
Ventral	61.5 (±3.34)	60.2 (±2.81)	65.4 (±4.05)	64.0 (±3.75)

* significantly different from controls

kindled rats revealed a significant increase in sprouting for those animals who received daily stimulation, regardless of perinatal treatment (data not shown).

3.4 Discussion

The major finding of this study is that treatment with sub-convulsive doses of DOM during the second postnatal week of life produces an enhanced sensitivity to electrical stimulation and increases in MFS in the adult rat in the absence of an increase in electrically-induced seizure propagation. Enhanced amygdalar AD response to stimulation in adulthood in these rats is indicative of changes in excitatory/inhibitory tone in focal networks (Figure 3.4, pg 101), and in combination with increases in hippocampal MFS (Table 3.3, pg 111, Figure 3.7, pg 109, and 3.8, pg 110), suggest that this alteration results from a permanent restructuring of neuronal circuitries. Because alterations in seizure threshold can have a significant impact on the development of pathological disorders such as epilepsy, the observation that low dose neonatal DOM administration causes apparently permanent reductions in seizure threshold may be important for understanding the etiology of seizure disorders.

Long-term reductions in seizure threshold following perinatal electrically- or chemically-induced status epilepticus have been reported previously (Brooks-Kayal, 2005; Dakshinamurti *et al.*, 1993; Moshe and Albala, 1983; Porter, 2008; Zhang *et al.*, 2004). The consequences of more subtle insults during early development, however, are not well known. In the current study, we chose to investigate seizure susceptibility and propagation in adult rats that were treated postnatally with low (sub-convulsive) doses of DOM because our previous investigations of this model have reported both behavioural

and histopathological (Bernard *et al.*, 2007; Doucette *et al.*, 2004; Doucette *et al.*, 2003) changes consistent with other animal models of epilepsy. Since stress can be a precipitating factor in seizure induction, we also examined the effects of an acute, highly stressful task on behavioural (NIS-L) and physiological (CORT and ACTH) responses, as well as on kindling propagation as measured through ADD and behavioural seizure stage progression.

Results obtained during a classic amygdala kindling paradigm demonstrate that early DOM treatment produced animals that exhibit a lowered focal seizure threshold in adulthood as evidenced by a decrease in the amount of current required to elicit an AD following electrical stimulation (Figure 3.4, pg 101). This increase in sensitivity, however, did not translate to a faster seizure propagation to the rest of the brain (Figure 3.5, pg 104) in any group, at most resulting in a mild tendency toward increased ADDs in DOM-treated, stressed rats compared to their kindled-only counterparts [$F_{(1,11)} = 3.789$, $p = 0.078$] (Appendix B, Figure B2.1, pg 248). One possible explanation for these findings may be related to the mild nature of the initial insult in this model. In a recent study, Flynn and Teskey (2007) show that 20 days of electrical stimulation to the corpus callosum at very low levels (50μA) will produce a permanent reduction in seizure threshold without any signs of overt seizure activity, while high intensity currents increase the ADT temporarily, with a subsequent return to baseline after several days of no stimulations (Flynn and Teskey, 2007; Pinel *et al.*, 1976; Racine, 1972b). Repetitive injections of subconvulsant doses of DOM during development may be a comparable phenomenon, acting as a form of low-grade chemical kindling when administered early in life, and resulting in a permanently reduced ADT in adulthood. In

addition, studies in other labs have shown that reduced focal ADT, while providing an overall indication of neuronal excitability in a measured region, does not appear to be the physiological basis for progression to motor seizure during electrical kindling (Pinel *et al.*, 1976; Racine, 1972b). In fact, investigations of the "transfer" effect of ADT levels in the limbic system have actually shown increased ADT in contralateral hemispheres or in other structures (Bragin *et al.*, 2002; Racine, 1972b), a phenomenon which may be responsible for the reported delay in contralateral recruitment in a study measuring seizure progression throughout the HC (Hewapathirane and Burnham, 2005). In the current study, this inhibitory mechanism appears to have remained intact.

The pattern of MFS seen in the current study (Figure 3.7, pg 109) for DK rats, showing increased sprouting in ventral IML regions only, is in agreement with the finding that seizure progression from partial (Stage 1-2) to generalized (Stage 3-5) did not differ between the treatment groups (Table 3.2, pg 105). It has been previously shown that seizure activity originating in the amygdala will manifest behaviourally only after propagation to the HC (Hewapathirane and Burnham, 2005). Low level behavioural seizure has been shown to result from synchronous neuronal activity in the HC, and if seizure progression occurs, it proceeds in a predictable manner throughout the region; ventral to dorsal on the side ipsilateral to stimulation (Stage 1-2), then crosses over and continues from dorsal to ventral on the contralateral side (Stage 2+). As mentioned previously, recruitment of the dorsal region of the contralateral HC happens at a significantly slower pace than does ipsilateral progression, although direct activity transfer to both hippocampal hemispheres has been seen simultaneously at ventral levels, indicative of the heightened susceptibility in this region (Hewapathirane and

Burnham, 2005). Generalization of seizure activity, however, requires the recruitment of structures external to the HC that have widespread, bilateral connections (e.g. thalamus) (Bertram *et al.*, 1998; Bertram *et al.*, 2001). Therefore, if increased MFS in the DG at a particular hippocampal level is considered indicative of structural, and subsequent functional, reorganization in response to a given stimuli (in this case, perinatal DOM administration), the lack of increased sprouting in DG regions that are not as sensitive to seizure activity (i.e. intermediate and dorsal HC) may provide a possible rationale for a resulting lack of seizure propagation to brain regions outside the limbic system (Table 3.2, pg 105).

Further, we have previously reported that NIS-L rats do not experience any increase in absence-like seizures (a form of generalized seizure that is mediated through thalamo-cortical reverberations) following an acutely administered low (25mg/kg) dose of pentylenetetrazol (see Chapter 2). If, as Bertram and colleagues suggest, the thalamus is an instrumental structure for orchestrating generalized seizure activity, this previously noted lack of thalamic response may also help explain why seizures in NIS-L rats did not generalize any faster than those in control animals. Lack of an increased seizure propagation rate in systems that, in other respects, have enhanced excitability is also not an uncommon event in the literature. Studies of kindling transfer and kindling antagonism in experimental animals have reported this effect (Duchowny and Burchfiel, 1981; Haas *et al.*, 1990; Haas *et al.*, 1992; Kirkby *et al.*, 1993; Kirkby *et al.*, 1995; Racine, 1972b), and indeed, human complex partial seizures (particularly those of limbic origin) also do not always generalize to produce motor convulsions (Blume, 2006; Klass, 1975).

The other intriguing aspect of the seizure propagation results is that there was no difference between DOM-treated rats and controls in the latency to low-grade behavioural seizure in response to amygdalar stimulation, although it has been repeatedly demonstrated that these treated rats have a greater propensity to display NIS-L behaviours during novel challenges (Bernard *et al.*, 2007; Doucette *et al.*, 2004; Perry *et al.*, 2009). In the current investigation, exposure to the highly stressful forced swim test resulted in DOM-treated rats exhibiting NIS-L behavioural responses both during initial task exposure, as well as in a second exposure 3 weeks later (Figure 3.6A, pg 107), demonstrating both a definite susceptibility to respond as well as suggesting that the perceived stress of the task, not its novelty, might somehow be involved in creating the necessary conditions for NIS-L manifestation. Interestingly, in a study investigating how pre-existing epileptic conditions affect kindling rates, Bragin and colleagues (2002) discovered that rats treated with intrahippocapal kainic acid (KA—a close analogue of DOM) to produce recurrent spontaneous seizures actually exhibited a progressively increased ADT and suppressed spontaneous seizure expression during subsequent electrical kindling of the perforant path, suggesting that some sort of seizure suppressing mechanism might have been activated to maintain homeostatis (Pinel *et al.*, 1976; Stripling and Russell, 1989; Weiss *et al.*, 1998). It is possible that a similar effect may be taking place in the current study. However, since ADT was not measured at the conclusion of this study, nor were ADT levels recorded in other brain regions, this question remains unanswered to date. In addition, the slight tendency noted in the DKS group toward increased AD duration (Appendix B, Figure B2.1, pg 248) may be worth investigating further using a daily stress paradigm during kindling to examine whether stress does indeed play a key role in NIS-L induction.

In the current investigation, other than behavioural and physical indicators of heightened sensitivity to stress (Figure 3.6, pg 107), no definitive proof that early exposure to low-dose DOM leads to an altered stress response in adulthood as measured either by CORT or ACTH levels (Table 3.1, pg 103), increased AD durations, or behavioural seizure stage response (see Appendix B2.1, pg 248 for details) was found.

In previous studies in the DOM model, rats that received no treatment other than postnatal DOM administration have shown alterations in neuronal structure, including increased MFS in the IML of ventral and intermediate regions of the HC (Bernard *et al.*, 2007; Doucette *et al.*, 2004). The dramatically increased MFS in the DOM-treated group in both left and right IML at the ventral level (Figure 3.7, pg 109) in the current study substantiates this previous work, demonstrating that structural reorganization of the hippocampal mossy fibre pathway occurs in response to treatment. Combined with the increased sensitivity seen in the amygdala (Figure 3.4, pg 101), these results suggest that both of these limbic areas are altered by DOM treatment. It is therefore possible that the lack of difference between groups in amygdala to hippocampal seizure propagation may simply be an indication that the circuitry *between* these two regions has not been affected, even though each area on its own displays heightened excitability; a disconnect that has been reported previously in kindling studies (Pinel *et al.*, 1976; Racine, 1972b). This seems particularly feasible given that the stimulation intensity used to kindle each rat was arbitrarily assigned (+25μA) based on the individual threshold value of each rat. If this is indeed a factor, then further studies using one standardized stimulation level for both groups (e.g. 350μA), or a level determined as a

percentage increase from threshold might unmask differences in seizure propagation that were not evident using the current paradigm.

While the current study does not provide definitive proof regarding whether the low-grade seizure behaviours exhibited under everyday conditions by DOM-treated rats are of limbic origin, several past and present observations do suggest that this region is intimately involved in the process. Firstly, as already noted, increased MFS in the HC is a well-recognized indication of functional reorganization following seizure activity in the brain. Additionally, other changes in the HC have been noted in the DOM model, including increased TrkB protein expression, upregulation of brain derived neurotrophic factor (BDNF) mRNA, and hippocampal cell loss in aged animals (Bernard *et al.*, 2007; Doucette *et al.,* 2004). The fact that increased MFS is evident in both hippocampal hemispheres in DK rats in the current study indicates that alterations resulting from postnatal DOM injection appear to be affecting the highly susceptible ventral region in its entirety (Figure 3.7, pg 109). As well, the customary behavioural expression of seizure-like activity seen in NIS-L rats under normal (non-kindled) conditions are consistently low-grade, Stage 1-2 level events (Racine, 1972a), which are thought to be hippocampally-mediated (Hewapathirane and Burnham, 2005).

The current study has also shown increased MFS in treated rats for area CA3 in the SO contralateral to electrode placement (Figure 3.8, pg 110), but in no other CA3 hemisphere or level (Table 3.3, pg 111). Since this region has been previously noted as particularly susceptible to kindling-induced changes in MFS (Represa and Ben-Ari, 1992), it is reasonable to suggest that the combination of pre-existing modifications from

perinatal DOM exposure, along with the kindling paradigm itself, provided sufficient stimulation in this area to produce the subsequent increase seen in the treated group. Additionally, although increased MFS in the SO has not previously been reported to occur in non-kindled DOM-treated rats at this age (~PND120-150), it has been noted in much older rats (Doucette *et al.,* 2004), suggesting that the kindling procedure used in the current study may be accelerating the sprouting process in treated animals. The lack of difference in the hemisphere ipsilateral to the stimulating electrode is more puzzling, but may be a result of a masking effect from the kindling procedure, or due to cell loss from the electrode placement, whereas the contralateral hemisphere was distant enough from the initiating stimuli to allow for differences to be observed. However, further study will be required to examine the underlying mechanisms that may be responsible for the alterations in MFS in this region.

Insult or injury to the developing brain during critical periods of maturation may have far reaching consequences. The current study has revealed that administration of low-dose DOM during postnatal development results in an increase in neuronal excitability during adulthood that may predispose the organism to seizure-related pathologies. This increased sensitivity manifests as a lowered seizure threshold for focal stimulation as well as through augmented MFS in highly susceptible regions of the HC. Based on the novel data presented here, it is evident that early life exposure to even low levels of excitatory neurotoxins may be associated with permanent modifications in seizure susceptibility.

4.0 EARLY EXPOSURE TO DOMOIC ACID PRODUCES LONG-TERM REDUCTIONS IN PARADOXICAL SLEEP

A slightly modified version of this chapter has been published as: Gill, D.A., Bastlund, J.F., Anderson, N.J., Tasker R.A. Reductions in Paradoxical Sleep Time in adult rats treated neonatally with low dose domoic acid. *Behavioural Brain Research* (2009), doi:10.1016/j.bbr.2009.07.018.

4.1 Introduction

In the rat brain, the first few postnatal weeks are a critical period for the development of appropriate neuronal connectivity, and a disruption to this process may result in far-reaching alterations that persist well into adulthood. It has been previously demonstrated that exposing rat pups to very low, sub-convulsant doses (20μg/kg) of DOM during the second postnatal week of life results in long-term changes in both behaviour (Doucette *et al.*, 2004) and hippocampal cytoarchitecture and neurochemistry (Adams *et al.*, 2008; Adams *et al.*, 2009; Burt *et al.*, 2008a; Burt *et al.*, 2008b; Doucette *et al.*, 2004; Perry *et al.*, 2009) that are consistent with many current animal models of temporal lobe epilepsy as well as other forms of neurological disease. The changes in this new model appear to be progressive, eventually culminating in cell loss at later time points (Bernard *et al.*, 2007). Additionally, decreases in both generalized and focal seizure threshold using chemical (Chapter 2) and electrical (Chapter 3) paradigms have also been reported in NIS-L rats, further linking early DOM exposure with modified excitatory function in adulthood.

A naturally-occurring marine toxin that is structurally similar to kainic acid, DOM is believed to exert its excitatory effects primarily through an agonist action at the kainate sub-family of Glu receptors, although it can also activate all members of the Glu receptor group at varying concentrations (for review, see Novelli *et al.*, 2000). Therefore, in addition to the importance of understanding the possible consequences of DOM ingestion from a clinical perspective, the compound is also a valuable tool for investigation into neuronal alterations that can result from disruptions to the Glu system either during adulthood, or at various time points during CNS development.

The connection between sleep and seizure has been well documented in epilepsy literature (Bazil, 2000; Kotagal and Yardi, 2008; Malow, 2007; Touchon *et al.*, 1991), and many studies have further defined specific correlations between the duration of particular sleep stages and seizure incidence (Jaseja, 2004; Manni *et al.*, 2006; Miller *et al.*, 1994; Shouse *et al.*, 2000). In most reports, two main sleep stages are evaluated; slow wave sleep (SWS), sometimes referred to as non-REM (NREM) sleep, that consists mainly of waveforms in the lower frequency range with no appreciable EMG activity, and rapid eye movement (REM) sleep, defined as sleep consisting of higher frequency (e.g. beta) EEG, again with no appreciable accompanying EMG. This latter form of sleep is also known as paradoxical sleep (PS) due to the striking similarity of its waveforms to those of an awake brain, and it is this terminology that will be employed in the current study. Altered sleep patterns have long been recognized as symptomatic of many forms of neurological dysfunction including epilepsy (Bazil, 2000), stroke (Bassetti and Aldrich, 2001), demyelinating disease (Anch and Laposky, 2000) and schizophrenia (Monti and Monti, 2005). In this respect, changes in PS can be an important indication for the relevance of an animal model to specific pathological disorders.

In the last few years, the study of both seizure activity and sleep patterns has been greatly enhanced through the use of techniques such as radiotelemetry, which allows EEG waveforms to be recorded from freely moving rats (Bastlund *et al.*, 2004; Bastlund *et al.*, 2005; Williams *et al.*, 2006). This approach provides a flexible method for the investigation of brain wave activity without requiring tethering, or other similar on-

going experimenter manipulations that could interfere with the animal's normal, day-to-day activities. Additionally, the procedure allows for even more versatility through the simultaneous recording of an EMG lead, providing valuable information for studies such as those involving sleep, which rely on a moment by moment analysis of activity levels for conducting accurate assessments.

In the current study, PS time was evaluated in both treated and control rats using home cage analysis of cortical EEG and EMG waveforms from adult animals implanted with radiotelemetry instrumentation. Since the NIS-L model is considered to be characteristic of temporal lobe epilepsy, it was hypothesized that treated rats would experience decreased PS sleep, consistent with both current animal models of epilepsy, as well as the human condition.

4.2 Materials and Methods

4.2.1 Preparation of experimental animals

Animals in this study were part of a larger investigation looking at EEG alterations in DOM-treated rats following water maze exposure (see Chapter 2 for details regarding postnatal treatment and telemetry surgery).

4.2.2 Radiotelemetry system

The telemetry system used to record EEG/EMG from animals was composed of TL-10M3-F50-EEE (3 bio-potential) and TL-10M3-F50-EET (2 bio-potential) magnetic activated transmitters, RPC-1 receiver plates, data exchange matrices, and computers installed with Dataquest A.R.T. 2.2. (Data Sciences International, USA) (see Figure

1.16, page 21). The sampling frequency was set at 250 Hz for all recordings. The data for the current study represent one discrete 24 hour continuous EEG monitoring of home cage activity for all animals with care taken to minimize and/or eliminate any possible environmental confounds.

4.2.3 Analysis of electroencephalogram

All traces generated by radiotelemetry EEG (both anterior and posterior leads) and EMG bio-potentials were imported in Somnologica 3.1.0.1171 software (Flaga Medical Devices, Iceland) for visualization and analysis through the Animal Sleep Report Rodent Scoring Module (v3.3.1). Measurements included duration and number of episodes for the following stages: 1) wake (moderate to high frequency EEG with EMG activity); 2) SWS (predominant waveforms in the lower frequency range and no EMG activity) and 3) PS, (higher frequency (e.g. beta) EEG with no EMG activity) (Figure 4.1, pg 125).

4.2.4 Data analysis

The presence of artifacts in EEG and/or EMG signals can lead to faulty scoring of affected epochs when using automated scoring algorithms. To ensure that only robustly scored recordings were included in the final analysis, an operator experienced in manual EEG/EMG analysis discarded traces in which artifact levels would produce unreliable scoring. In total, 8 out of 18 recordings were discarded in this manner, such that N=10 (5-DOM, 5-SAL). Between groups differences were analyzed using independent t-tests

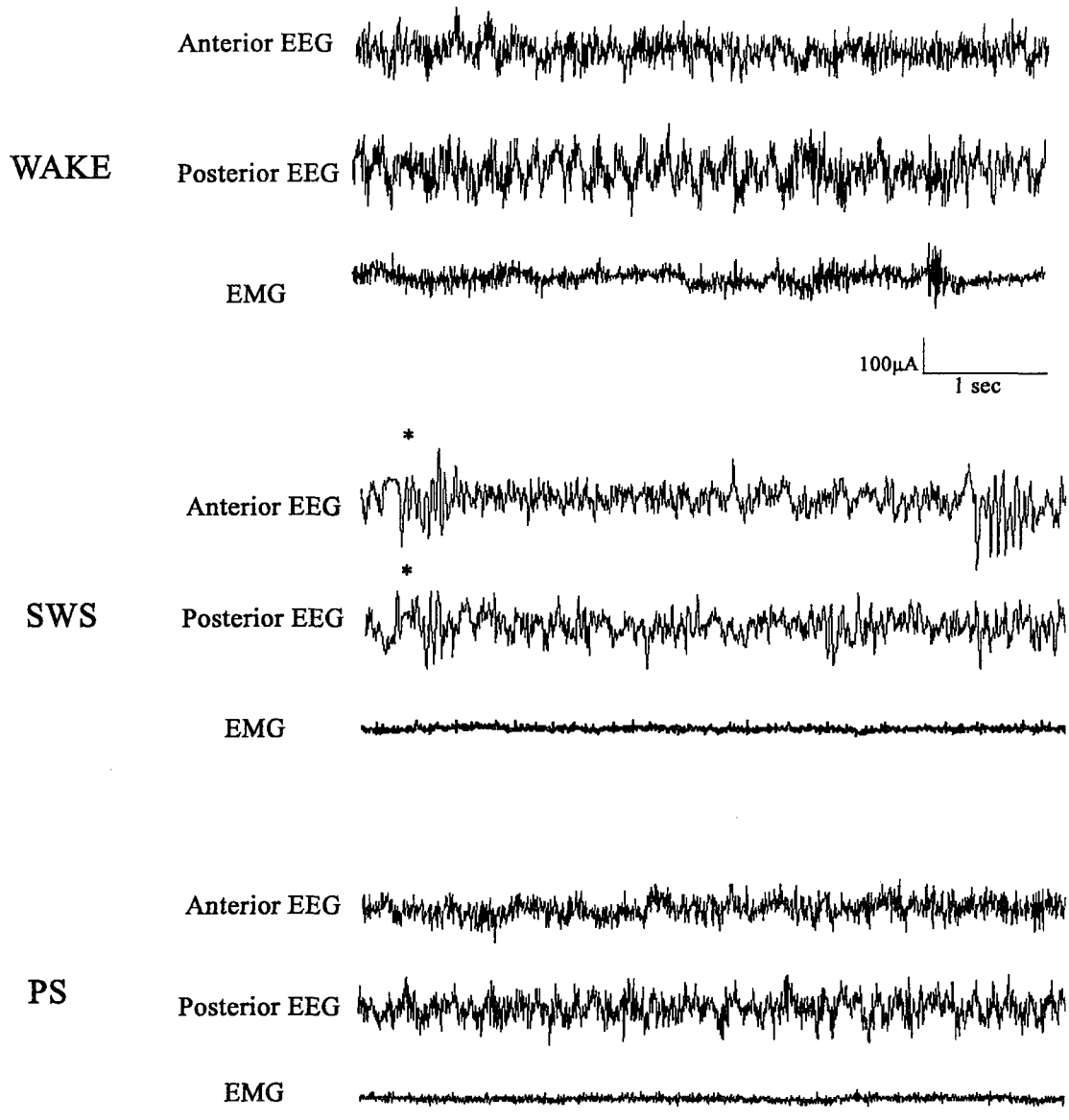

Figure 4.1 EEG/EMG tracings showing a representation from the same rat for each of the three defined stages used for analysis: wake, slow-wave sleep, and paradoxical sleep. Note the rhythmic EEG activity and characteristic sleep spindles in both anterior and posterior leads (indicated by asterisks) and lack of EMG activity during slow-wave sleep, while EEG patterns in paradoxical sleep revert back to waveform similar to that of the awake animal, and the EMG remains quiet.

(one-tailed), and results are expressed as mean ± SEM. Analyses were performed using SAS (v.6.11), with $\alpha \leq 0.05$.

4.3 Results

This study was conducted to explore possible alterations in sleep duration in the NIS-L rat model. The first parameter measured was total sleep time. All rats slept an equivalent total amount during the 24 hours analyzed, with treated rats sleeping an average of 841.7 minutes (SEM ±59.9), and controls experiencing 804.4 minutes (SEM ±40.8) of total sleep time. This similarity in total sleep remained when the time period was divided into two 12 hour sessions representing daylight (when nocturnal animals such as rats would normally sleep), and night (when the majority of time would be spent awake) (see Figure 4.2, pg 127).

To determine whether postnatal DOM treatment produced long-term effects on the amount of time spent in each sleep stage, the mean duration of SWS and PS was examined. An evaluation for time spent in SWS showed no differences between the groups, regardless of the period analyzed. However, as predicted, a comparison of mean time spent in PS during daylight hours revealed that NIS-L rats experienced 39.1% less PS than controls [$t_{(8)} = 1.926$, $P = 0.04$]. Figure 4.3 (pg 128) provides a graphical comparison of the average amount of time spent in each stage for this 12 hour period.

Previous studies have used the number of stage shifts into PS to measure sleep organization, with the number of shifts into PS decreasing in conjunction with the

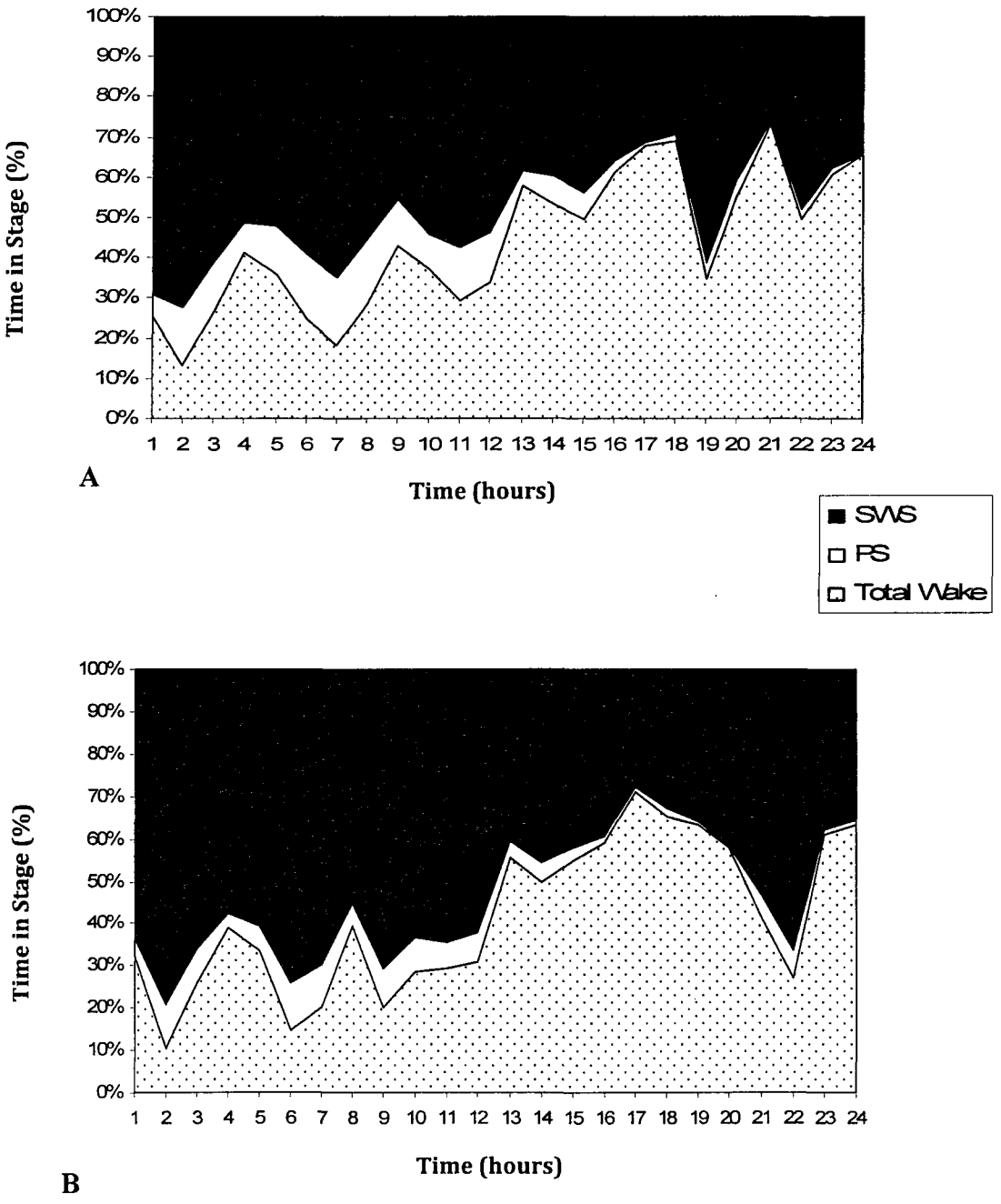

Figure 4.2. Percentage of time each group (A- SAL and B- DOM) spent in slow wave sleep (SWS), paradoxical sleep (PS), and awake.

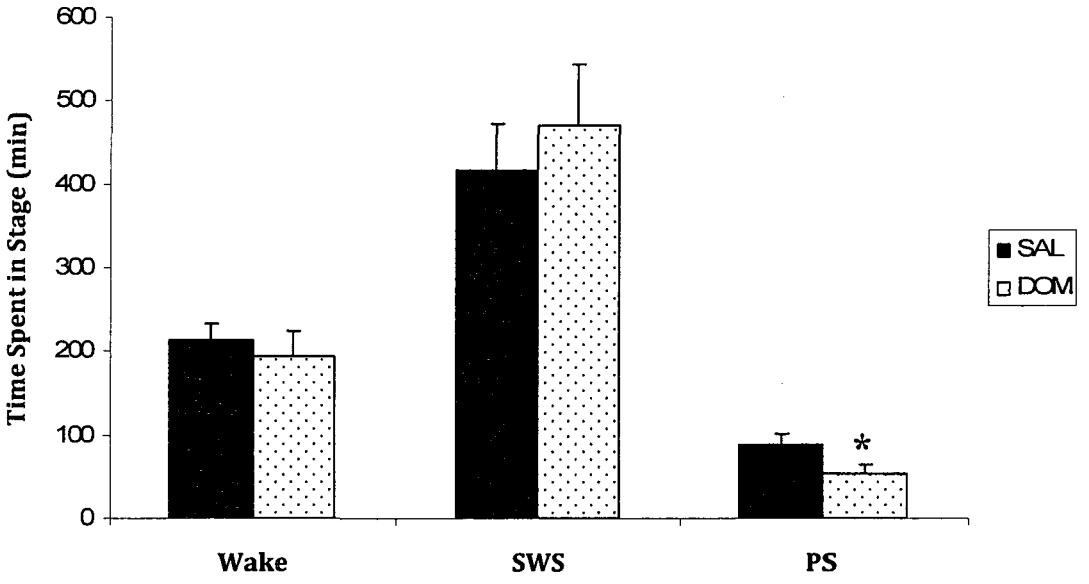

Figure 4.3. Mean amount of time rats spent awake, in slow wave sleep, and in paradoxical sleep during the 12 daylight hours. Error bars indicate SEM, and the asterisk indicates a significant difference from the appropriate control group ($p < 0.05$).

amount of PS experienced (Gigli and Gotman, 1992; Stone and Gold, 1988). In the current study, there was no equivalent decrease noted in stage shifts (Figure 4.4, pg 130), suggesting that treated rats entered PS similarly to controls, but were unable to maintain the appropriate duration for this stage.

4.4 Discussion

The current study has shown that early postnatal treatment with DOM results in altered PS patterns during adulthood. While treated rats maintain similar levels of total overall sleep time in comparison with controls, the amount of time they spend in PS is significantly decreased (Figure 4.1, pg 125). This finding is in agreement with the PS alterations found in other animal models of epilepsy, where decreases have been seen following a variety of treatment paradigms, including pentylenetetrazole (PTZ) administration (Schilling *et al.*, 2006), electrical kindling in both rats (Kumar and Raju, 2001; Raol and Meti, 1998; Stone and Gold, 1988) and cats (Gigli and Gotman, 1992; Hiyoshi *et al.*, 1989; Shouse and Sterman, 1981a; Shouse and Sterman, 1981b), as well as in spontaneous epileptic rats (SER) (Bastlund *et al.*, 2005).

Interestingly, in kindling studies, cessation of electrical stimulation was often reported to result in the return of PS to normal values in as little as 48 hours (Raol and Meti, 1998) to one month (Kumar and Raju, 2001). This is in contrast to SER rats, which, following an initial 2 hour bout of electrical stimulation in adulthood, were left undisturbed until six weeks later, during which time spontaneous seizures had developed and decreases in PS were subsequently noted (Kumar and Raju, 2001). In the NIS-L model, precipitating

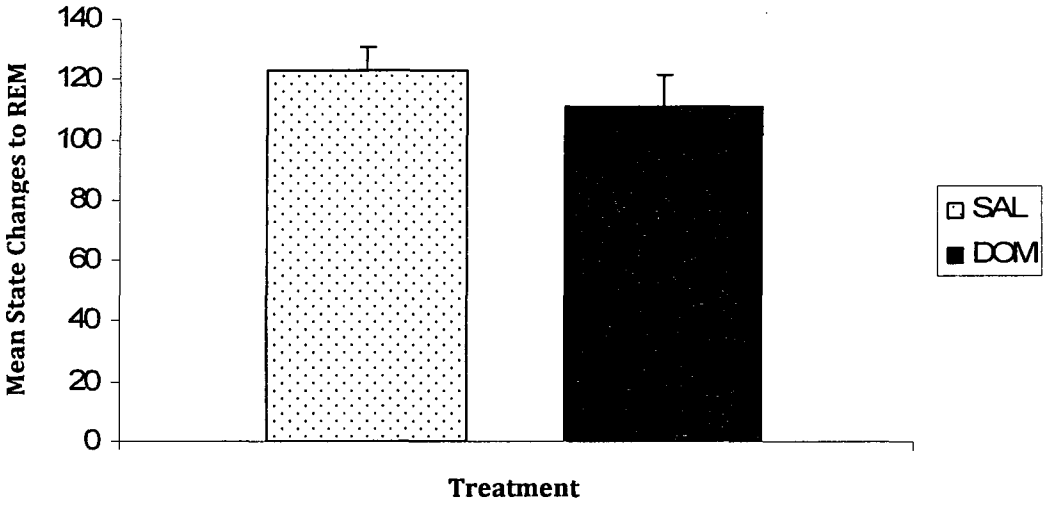

Figure 4.4. Mean number of stage shifts to paradoxical sleep in adult rats treated neonatally with DOM or saline. DOM treated rats did not differ from controls in number of stage shifts to paradoxical sleep.

treatment had occurred more than 4 months prior to testing, strongly suggesting that the reduction in PS in these rats is a permanent, long-term disruption.

One of the most intriguing aspects of the current study is the discovery that, while NIS-L rats do have decreased PS durations, they do not differ from controls in the number of times they enter the paradoxical sleep stage (Figure 4.4, pg 130). A previous study investigating this parameter in kindled rats has found that state changes from SWS to PS tend to decrease along with the total amount of time spent in the PS stage (Stone and Gold, 1988), while in the human condition, the number of sleep stage shifts may actually be increased (Touchon *et al.*, 1991). The current finding suggests that the difficulty for NIS-L rats is not in their ability to achieve paradoxical sleep, but rather in their capacity to maintain it. One possible explanation for this phenomenon may be related to the developmental nature of the model. It is now known that the brain region responsible for controlling sleep stages and stage shifts (the pedunculopontine (PPN) of the reticular activating system) undergoes a massive neuronal reorganization during the second and third postnatal week in the rat (for review, see Garcia-Rill *et al.*, 2008) in conjunction with a developmental overshoot of Glu receptors as the brain switches from a primarily GABA and NMDA-mediated system to its more complex adult configuration (Ben-Ari, 2006a). In short, a shift in PPN neuronal depolarization occurs, changing from a reliance on NMDA function to one utilizing KARs. Under normal circumstances, this reorganization is believed to be responsible for the sharp decrease in PS that is seen in rat pups in their first 30 days, subsequently leveling off to adult values (Garcia-Rill *et al.*, 2008). In the NIS-L rat, postnatal DOM treatment coincides with this developmental shift, and due to its putative actions at AMPA/KARs, may somehow modify the system

enough to either result in, or contribute to the PS deficits seen during adulthood. Since the model is already associated with seizure activity, it is likely that the latter explanation is most probable. However, investigation into the NIS-L model with respect to the possible effects of DOM on PPN development might also be enlightening from a developmental sleep perspective.

In conclusion, the present results demonstrate that exposing rat pups to very low, sub-convulsant doses of DOM during the second postnatal week of life results in reductions in PS duration, but not total sleep time or stage shifts into the PS stage once the rat has reached adulthood, providing further evidence of physiological alterations in the NIS-L rat model similar to those found under neuropathological conditions such as epilepsy, and giving additional insight into the critical role of appropriate glutamatergic signaling during brain development. Following previous studies showing reductions in seizure threshold, and alterations at both the cellular and the molecular level, as well as behavioural manifestations equivalent to low-grade seizure, these results further strengthen the NIS-L model as a valuable and relevant tool for the study of seizure genesis.

5.0 POSTNATAL EXPOSURE TO LOW-DOSE DOMOIC ACID PRODUCES SELECTIVE REDUCTIONS IN HIPPOCAMPAL GABAergic SUBPOPULATIONS

A modified version of this chapter has been submitted to Brain Research as follows: Gill, D.A., Ramsay, S.L., Tasker, R.A. Selective reductions in subpopulations of GABAergic neurons in adult rats following postnatal exposure to domoic acid.

Additional information relating to this study can be found in Appendix C.

5.1 Introduction

In the rat, early postnatal development is a critical period for neuronal migration, differentiation and network formation, equivalent to changes that occur during the third gestational trimester in humans (Clancy *et al.*, 2001; Dobbing and Smart, 1974; Dobbing and Sands, 1979). Central to these processes is GABA, a neurotransmitter which in adulthood is inhibitory, but during development, serves an excitatory role (for reviews, see Ben-Ari, 2002; Ben-Ari, 2006a; Ben-Ari *et al.*, 2004; Ben-Ari *et al.*, 2007; Gubellini *et al.*, 2001). However, while GABAergic input is instrumental to the progression of neuronal maturation, appropriate and timely Glu signaling is also of vital importance during this crucial organizational period (see Ben-Ari, 2006a; Lujan *et al.*, 2005 for reviews). Subsequently, insults that affect either the GABA or the Glu system during sensitive developmental stages readily result in increased excitatory activity, potentially leading to a variety of alterations that can include changes in neuronal proliferation and/or connectivity, and may ultimately affect proper maturation of excitatory or inhibitory systems.

To date, most neurodevelopmental studies have focused on the consequences of severe trauma, often using high doses of excitatory compounds to induce massive neuronal events such as status epilepticus (Dugich-Djordjevic *et al.*, 1992; Schreiber *et al.*, 1992; Thurber *et al.*, 1994). This research has contributed greatly to our understanding of the factors that can lead to the development of neuropathological disorders such as epilepsy, as well as providing information regarding some of the underlying changes that may occur in the brain following such excitotoxic events. In adult rats, excess excitatory activity has been shown to produce reductions in overall GABAergic availability in the

HC (Kobayashi and Buckmaster, 2003), as well as a significant decrease in the immunoreactivity of susceptible interneuronal subpopulations such as those containing the neuropeptide somatostatin (SST) (Buckmaster and Dudek, 1997b; Kobayashi and Buckmaster, 2003; Sperk *et al.*, 1992) and the calcium-binding protein parvalbumin (PV) (Kobayashi and Buckmaster, 2003; Sloviter, 1989b), both closely linked with seizure activity. In addition, decreases in mossy cells, a vulnerable population of excitatory neurons in the hippocampal hilar region, are also noted (for review see, (Buckmaster and Schwartzkroin, 1994). However, much less is known about comparable alterations that may result from more subtle neurotoxic exposures during critical developmental periods.

It has been previously shown that low doses of the Glu agonist DOM administered to rats during the second postnatal week produces a low-grade seizure-like behavioural response in a variety of maze paradigms (Doucette *et al.*, 2004), as well as reductions in seizure threshold (see Chapters 2 and 3). In addition, histological analysis has revealed changes in hippocampal structure and function in this model, including increases in both MFS and TrkB expression (Bernard *et al.*, 2007; Doucette *et al.*, 2004). All of these changes are similar to those seen in other animal models of TLE, as well as in the human condition (Buckmaster, 2004). In the current work, alterations in both GABAergic and non-GABAergic cell expression that result from early DOM exposure were investigated using immunohistochemical techniques, with the hypothesis that administration of low-dose DOM during postnatal days (PND) 8-14 will decrease overall GABA availability and mossy cell counts in adult animals, as well as reduce immunoreactivity in susceptible SST and PV interneuronal subpopulations.

5.2 Materials and Methods

5.2.1 Experimental Animals

Offspring born in-house from untimed Sprague-Dawley rats (Charles River, Quebec) were culled within 24 hours of birth to 10 pups per litter (5-♀ and 5-♂ where possible). From postnatal day 8-14, pups were weighed and given a single daily injection (10ml/kg, s.c.) of either 20μg/kg DOM (BioVectra dcl, Canada) or SAL, as described previously (Bernard *et al.*, 2007; Doucette *et al.*, 2004). Following weaning on PND21, rats were group housed (2-3 per cage) under a 12h light-dark cycle (lights on at 06:00h) and were left undisturbed, except for normal maintenance, until PND90. Room temperature was maintained at 21±2°C. Rodent chow (5001 Ralston Purina) and tap water were available *ad libitum*. Studies were carried out under approval from the University of Prince Edward Island Animal Care Committee, and in accordance with the Canadian Council on Animal Care guidelines.

5.2.2 Fixation and tissue preparation

To assess changes in interneuron populations, 18 adult rats (PND90; 8 DOM, 10 SAL; 9-♀ and 9-♂) were euthanized with CO_2 and immediately decapitated. Brains were hemisected and each hemisphere was submerged in 50ml of 30% (w/v) sucrose in 10% buffered neutral formalin (BNF) for 36 hours. Tissue was frozen in Cryo-Matrix using liquid nitrogen and stored at -80°C until sectioning with a cryostat.

All sections were cut from the right hemisphere at 10μm using a protocol designed to provide optimal hippocampal access at 3 levels: dorsal (cut coronally at -3mm Bregma), mid (cut horizontally 4mm ventral from top of brain), and ventral (cut horizontally 900μm ventral from mid level) (see Figure 5.1, pg 138), and mounted on Superfrost Plus slides (Fisher Scientific, USA). Tissue from both treatment groups were run simultaneously by an experimenter blind to condition to ensure consistent processing. Negative controls for all primary and secondary antibodies were included in every run and displayed no specific staining. Prior to antibody application, antigenic sites for all immunohistochemical procedures were opened using a standard heat-induced epitope retrieval (HIER) protocol consisting of 20 minutes in a 95°C sodium citrate buffer (pH 6.0) solution followed by a 20 minute cool down. For SST and PV, 0.05% Tween 20 was added to the buffer to provide additional cellular permeabilization.

5.2.3 Immunohistochemistry for GABAergic markers

Overall GABA availability was evaluated using a rabbit polyclonal antibody against GAD65/67 (1:100 Abcam #11070). Because GAD65 is a membrane associated enzyme, digitonin (100μM) was used for permeabilization to minimize membrane degradation while still allowing the antibody cellular access to target GAD67, which is located in the cytoplasm. Following the permeabilization step, tissue was blocked with 1% bovine serum albumin (BSA) in phosphate buffered saline (PBS) mixed with Tween 20 (0.05%) (PBST), then incubated overnight at 4°C with the primary antibody in 1% BSA/PBST. After incubation, tissue was rinsed with PBS, and labeled using Alexa Fluor 488 goat anti-rabbit IgG (1:200, Invitrogen #-11008) for 1 hour at room temperature (RT).

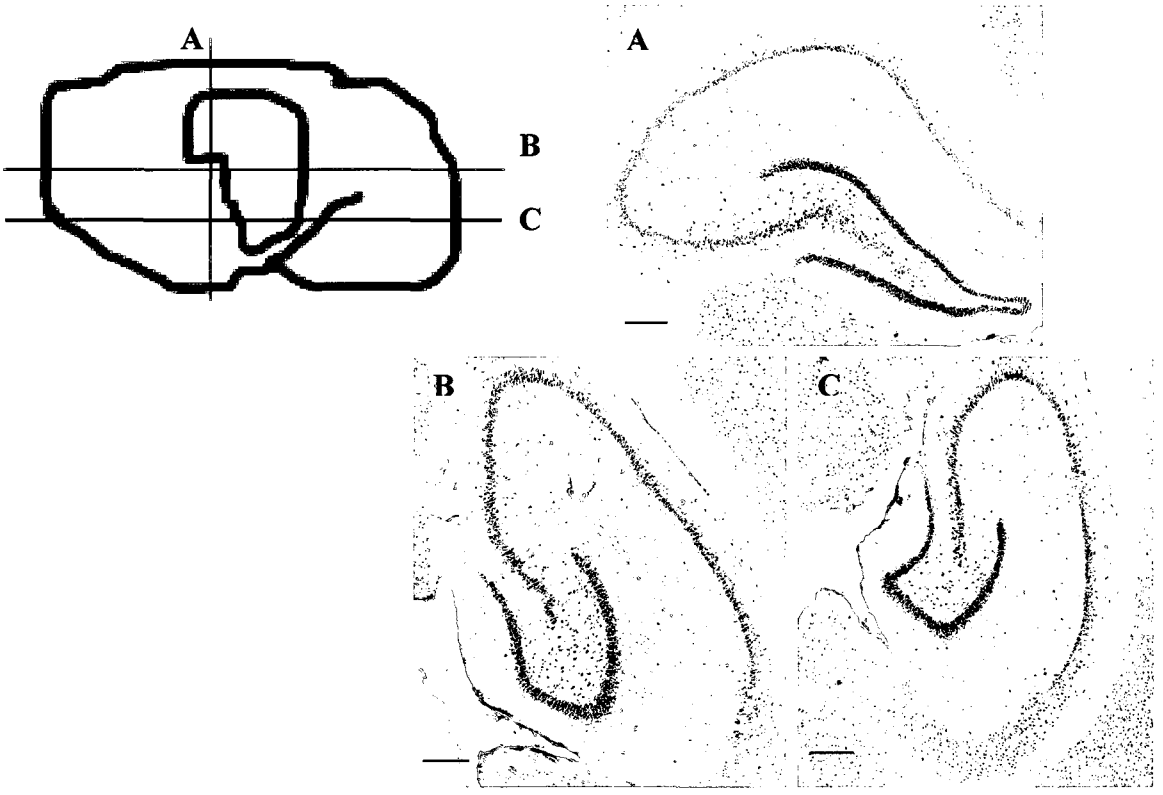

Figure 5.1. Schematic drawing of the hippocampus indicating the three levels analyzed, with representative cresyl stained micrographs corresponding to each septo-temporal location. A) dorsal B) mid C) ventral. See text for further details. Scale bar = 250μm.

Following a final rinse with PBS, Citifluor (Canemco-Marivac, P.Q.) was applied, and slides were cover-slipped and sealed using nail polish.

Somatostatin was visualized using a protocol modified from Buckmaster and Dudek (1997). Following HIER, tissue was exposed to 1% peroxide in 0.1M phosphate buffer (PB) and then to a standard blocking solution (3% goat serum, 2% BSA, 0.3% Triton X in tris buffered saline (TBS) pH 7.4) at room temperature (RT) for 2 hours. After rinsing with TBS (2x15 min), sections were incubated using a rabbit polyclonal antibody against somatostatin (1:4000, Peninsula Labs #T-4103) for 20 hours at 4°C. Secondary binding using biotinylated anti-rabbit IgG (Vector Laboratories Inc. #BA1000; 1:500 in 2% BSA and 0.3% Triton X-100 for two hours at RT) was amplified using an avidin-biotin complex (ABC; Vectastain Elite kit - Vector Laboratories Inc., Burlingame, CA) for 30 minutes. Secondary labels were visualized using a DAB peroxidase substrate kit (SK-4100, Vector Laboratories Inc.), with a reaction time of ~4-5 minutes stopped with TBS rinses and a 2 minute wash in running tap water. Tissue was then dehydrated, cleared, and cover-slipped with Permount.

Tissue for PV evaluation was blocked (3% goat serum, 2% BSA, 0.3% Triton X in TBS (pH 7.4) at RT for 2 hours and rinsed with TBS (2x15 min), then incubated at 4°C for 68 hours with a mouse monoclonal antibody (1:2000, Abcam #ab50338) mixed with 1% goat, 0.2% BSA, 0.3% Triton-X and TBS. The secondary antibody consisted of 1:200 Alexa Fluor 594 (Invitrogen #A-20004) goat anti-mouse in 2% BSA, 0.3% Triton X and

TBS, incubated for 3 hours at RT. Following a PBS rinse, slides were cover-slipped with Citifluor (Canemco-Marivac, P.Q.) and sealed with nail polish.

5.2.4 Cresyl violet (Nissl) staining

Tissues for total cell counts (one slide per animal) were submerged in 0.5% cresyl violet for 90 seconds, rinsed in tap water, dehydrated through a series of ethanol (70-100%) baths (3 min each), cleared with xylene (2x3 min), and coverslipped using Permount.

5.2.5 Image analysis and quantification protocol

All fluorescent labels were obtained using a Fluroarc exciter lamp with a Zeiss Axioplan2 microscope (10x planar objective), and recorded using an attached AxioCam HR digital camera set manually to ensure image consistency. Cell profile counts for PV and GAD65/67 were performed on micrographs, while DAB labeled SST cells and cresyl-violet stained cells were quantified using an Olympus BH-2 microscope equipped with a 10x objective lens. Counts in the HC (SST and PV) were conducted in both the hilus and SL / SR while non-GABAergic (Nissl) cell counts were from the hilus only (Figure 5.2, pg 141). An estimation of alterations in mossy cell profile numbers was obtained by subtracting GAD65/67 counts from total cell counts. In the amygdala, PV counts were obtained from the BLA region on coronal slices only (-3mm bregma), using the external capsule and optic nerve as positioning guides. To ensure that all cell counts were assessed from equivalently sized regions, an initial analysis of region volume was performed at each hippocampal level using Image J (National Institutes of Health), and no differences were noted (data not shown). All quantification was performed with the experimenter blind to condition.

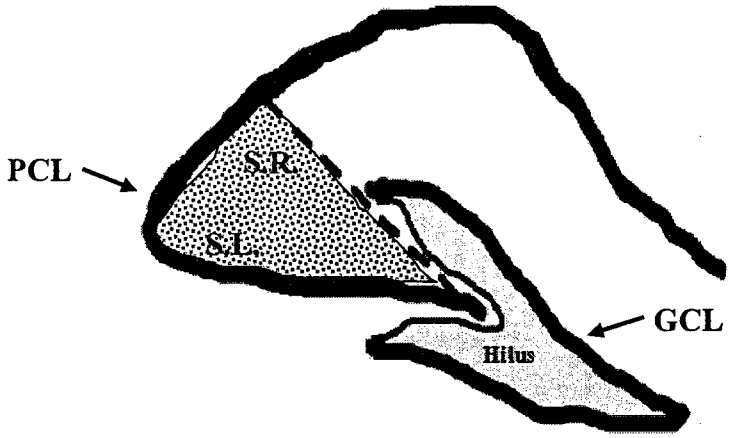

Figure 5.2. Shaded regions delineate hippocampal regions analyzed for glutamic acid decarboxylase 65/67, somatostatin, and parvalbumin immunoreactivity. S.L.–stratum lucidum; S.R.–stratum radiatum; PCL –pyramidal cell layer; GCL –granule cell layer.

5.2.6 Data analysis

Data were analyzed using two-way (SEX x COND) ANOVAs (v.10.0.5 SPSS Inc., Chicago IL), with t-tests for independent means utilized to evaluate interactions. Results are expressed as the mean ± SEM. The criterion for statistical significance was set at $p \leq 0.05$.

5.3 Results

The results for each individual marker are presented below. Representative micrographs of the differences seen between groups for each of the three antibodies is provided in Figure 5.3 (pg 143), and a summary of the mean data for both males and females in all measured regions can be found in Table 5.1 (pg 144).

Overall GABAergic availability was assessed in the current study using a marker for both membrane bound (GAD65) and cytosolic (GAD67) glutamic acid decarboxylase. In the hilus of the DG (Figure 5.4A, pg 145, and Table 5.1, pg 144), no significant differences were noted at either dorsal or mid levels, although there was an interesting reversal in mean counts between male and female groups in the mid DG, where DOM treated males showed decreased counts (SAL: 57.80±4.71; DOM: 45.00±9.56), while counts for DOM females actually increased (SAL: 41.20±9.79; DOM: 53.00±2.44). At the ventral level, there was a significant main effect for both condition [$F_{(1,14)} = 18.795$, $p = 0.001$] and sex [$F_{(1,14)} = 18.972$, $p = 0.001$], with DOM treated animals showing decreased GAD immunoreactivity (ir) overall compared to controls, and females displaying a greater decrease in counts between groups than males (Table 5.1, pg 144).

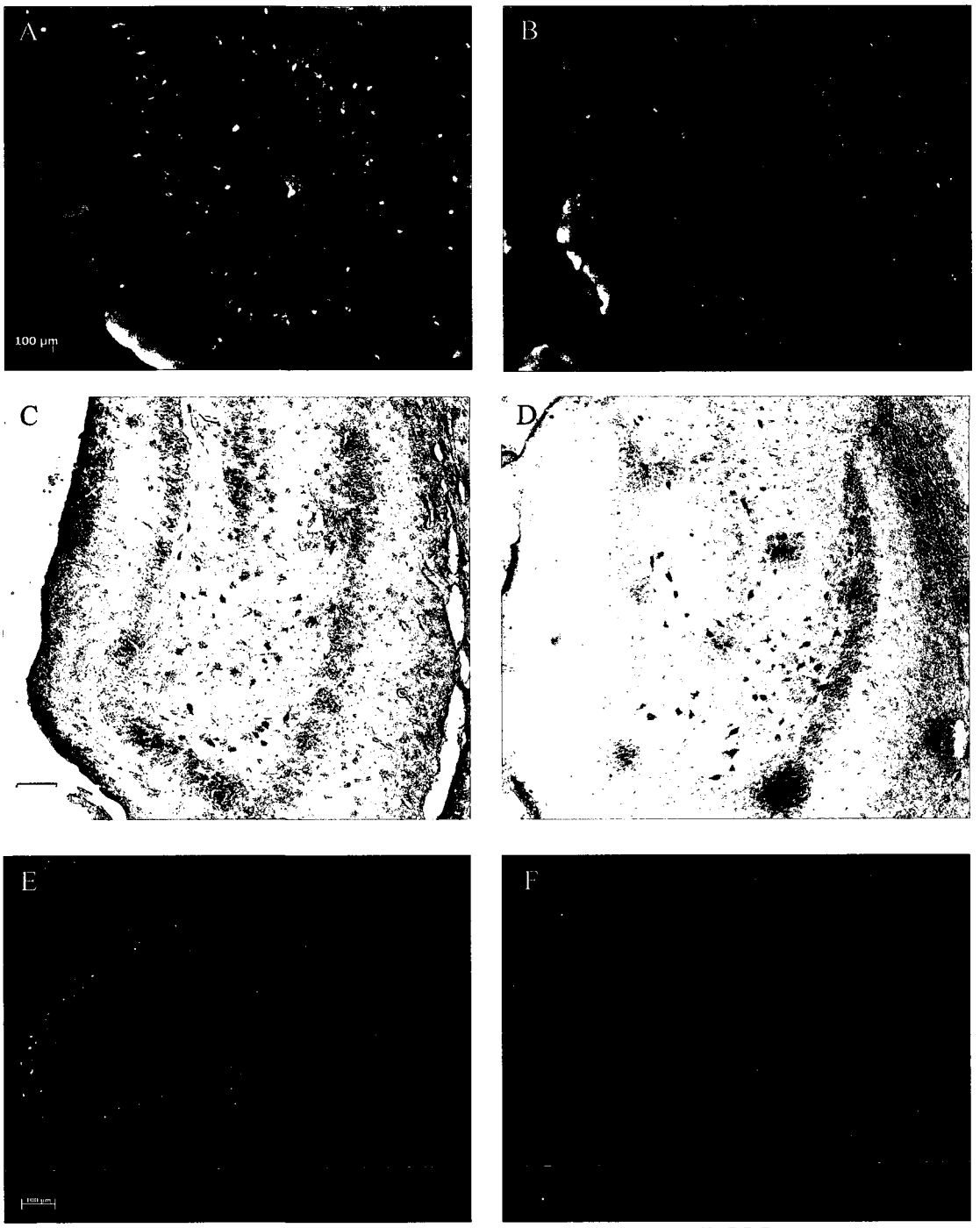

Figure 5.3. Representative micrographs of differences seen between groups for each of the three antibodies measured. A) GAD65/67 control and B) GAD65/67 DOM in the ventral dentate gyrus. C) SST control and D) SST DOM in mid dentate gyrus E) PV control and F) PV DOM in dorsal dentate gyrus.

Table 5.1. Summary of the mean (±SEM) data for both males and females in all measured hippocampal and amygdalar regions.

	Control		DOM	
	Female	Male	Female	Male
GAD65/67				
Dentate Gyrus				
Dorsal	60.60 (±4.24)	58.20 (±6.81)	60.75 (±8.29)	53.25 (±6.80)
Mid	41.20 (±9.79)	57.80 (±4.71)	53.00 (±2.44)	45.00 (±9.56)
Ventral	70.60 (±3.23)	55.20 (±1.29)	55.25 (±0.99)	49.25 (±4.38)
CA3				
Dorsal	35.20 (±3.66)	36.40 (±3.21)	31.75 (±2.88)	32.50 (±3.28)
Mid	35.20 (±4.62)	38.20 (±2.75)	43.00 (±3.42)	27.25 (±4.33)
Ventral	32.80 (±3.38)	36.00 (±3.12)	33.00 (±1.70)	26.25 (±3.78)
Somatostatin				
Dentate Gyrus				
Dorsal	16.40 (±2.54)	22.80 (±0.98)	14.75 (±1.55)	16.25 (±3.35)
Mid	18.20 (±2.63)	17.40 (±2.27)	20.75 (±2.78)	12.50 (±2.06)
Ventral	19.40 (±3.88)	18.20 (±1.59)	19.25 (±3.09)	18.25 (±3.28)
CA3				
Dorsal	5.00 (±0.55)	7.40 (±1.44)	5.00 (±1.47)	5.25 (±1.65)
Mid	4.20 (±0.37)	3.00 (±0.32)	4.75 (±2.18)	4.50 (±1.32)
Ventral	3.00 (±0.63)	3.80 (±0.92)	3.00 (±0.58)	4.25 (±0.48)
Parvalbumin				
Dentate Gyrus				
Dorsal	10.40 (±1.12)	10.20 (±1.46)	5.75 (±2.39)	6.75 (±1.32)
Mid	8.40 (±0.75)	11.60 (±1.03)	7.50 (±1.89)	5.25 (±1.44)
Ventral	8.00 (±1.08)	10.00 (±1.27)	4.50 (±3.20)	7.50 (±1.94)
CA3				
Dorsal	8.60 (±0.93)	17.00 (±4.37)	12.50 (±3.28)	12.50 (±2.26)
Mid	12.20 (±3.02)	19.40 (±1.54)	15.00 (±2.12)	10.00 (±1.58)
Ventral	14.25 (±0.85)	15.80 (±2.35)	12.00 (±4.18)	14.25 (±0.85)
Amygdala	31.80 (±3.92)	31.00 (±2.68)	34.40 (±3.34)	25.00 (±2.52)

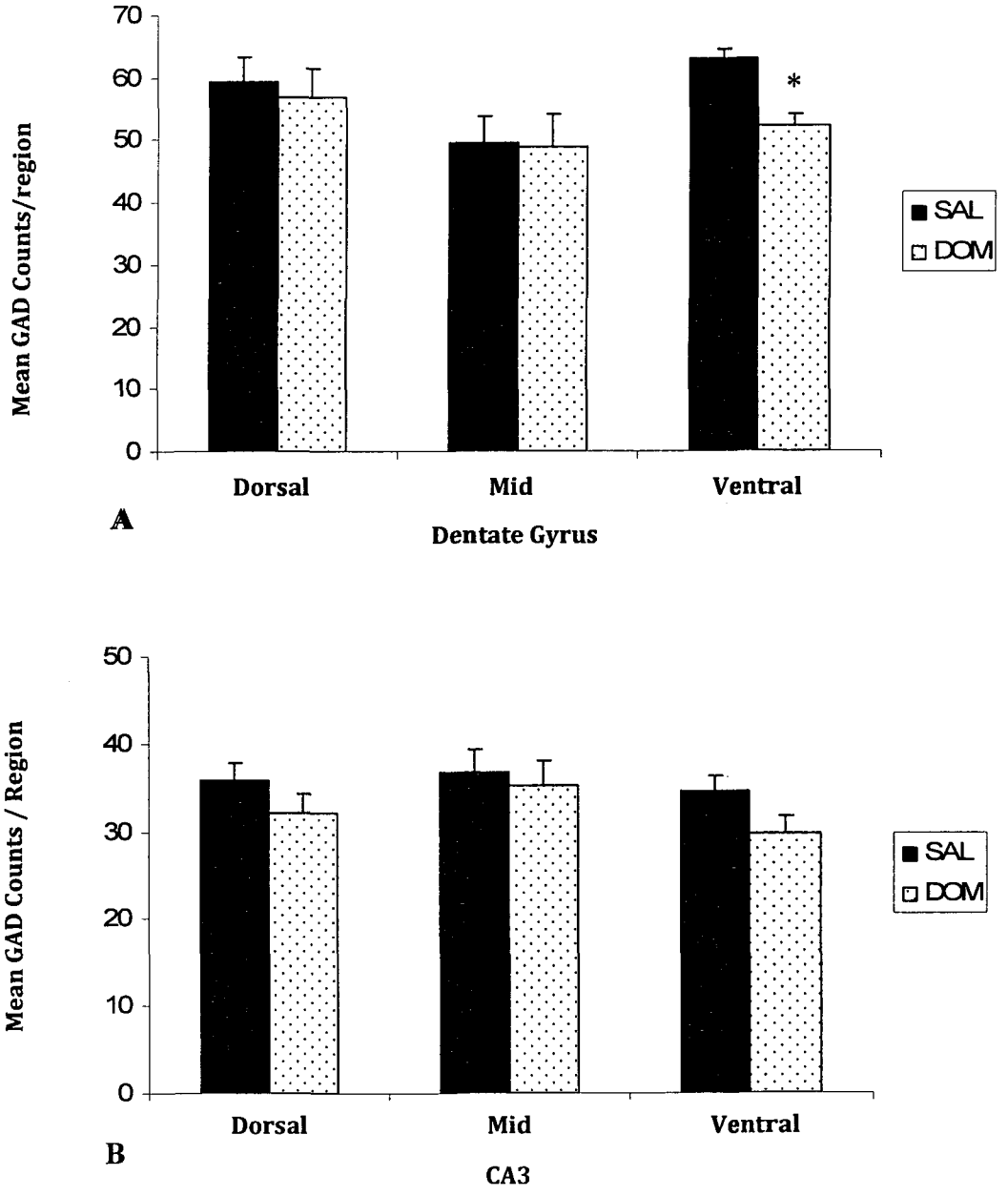

Figure 5.4. Mean GAD65/67 counts for all hippocampal levels. A) Dentate gyrus: asterisk indicates a significant difference from controls. B) Area CA3. In both graphs, error bars denote SEM.

In area CA3 (Figure 5.4B, pg 145 and Table 5.1, pg 144), there was no significant main effect at any hippocampal level (dorsal, mid, or ventral) analyzed, but there was a sex by condition interaction noted [$F_{(1,14)} = 5.803$, $p = 0.03$] at the mid level. Further investigation evaluating each sex individually uncovered a trend toward decreased GAD65/67-ir for treated male rats (see Figure 5.5A, pg 147) compared to their untreated counterparts [$t_{(7)} = 2.229$, $p = 0.06$]. No significant difference was seen in females alone for this region, although again, the mean counts for DOM females tended to be slightly higher than those for female controls (SAL: 35.20±4.62; DOM 43.00±3.42), a pattern that was noted in other hippocampal regions as well.

No difference was found in SST cell counts in any region at any hippocampal level measured (Figure 5.6, pg 148 and Table 5.1, pg 144), although DOM treated males did show a tendency toward less immunoreactivity in the hilar dorsal region [$t_{(7)} = 2.085$, $p = 0.076$] (see Figure 5.5B, pg 147).

In the DG, there was a statistically significant main effect in PV-ir for condition at the dorsal level [$F_{(1,14)} = 6.48$, $p = 0.02$] (Figure 5.7A, pg 149). At the mid level, there was a main effect for condition ($p=0.01$), as well as a sex by condition interaction [$F_{(1,14)} = 4.613$, $p = 0.05$]. Further investigation into this interaction revealed that DOM treated males had significantly decreased PV-ir at this level [$t_{(7)} = 3.695$, $p = 0.008$] compared to controls. These differences are depicted graphically in Figure 5.5C (pg 147). There was no difference noted for PV counts between groups or sexes at the ventral level of the hilar region. However, in area CA3, while there was no difference at either dorsal or ventral locations, there was a sex by condition interaction at the mid level

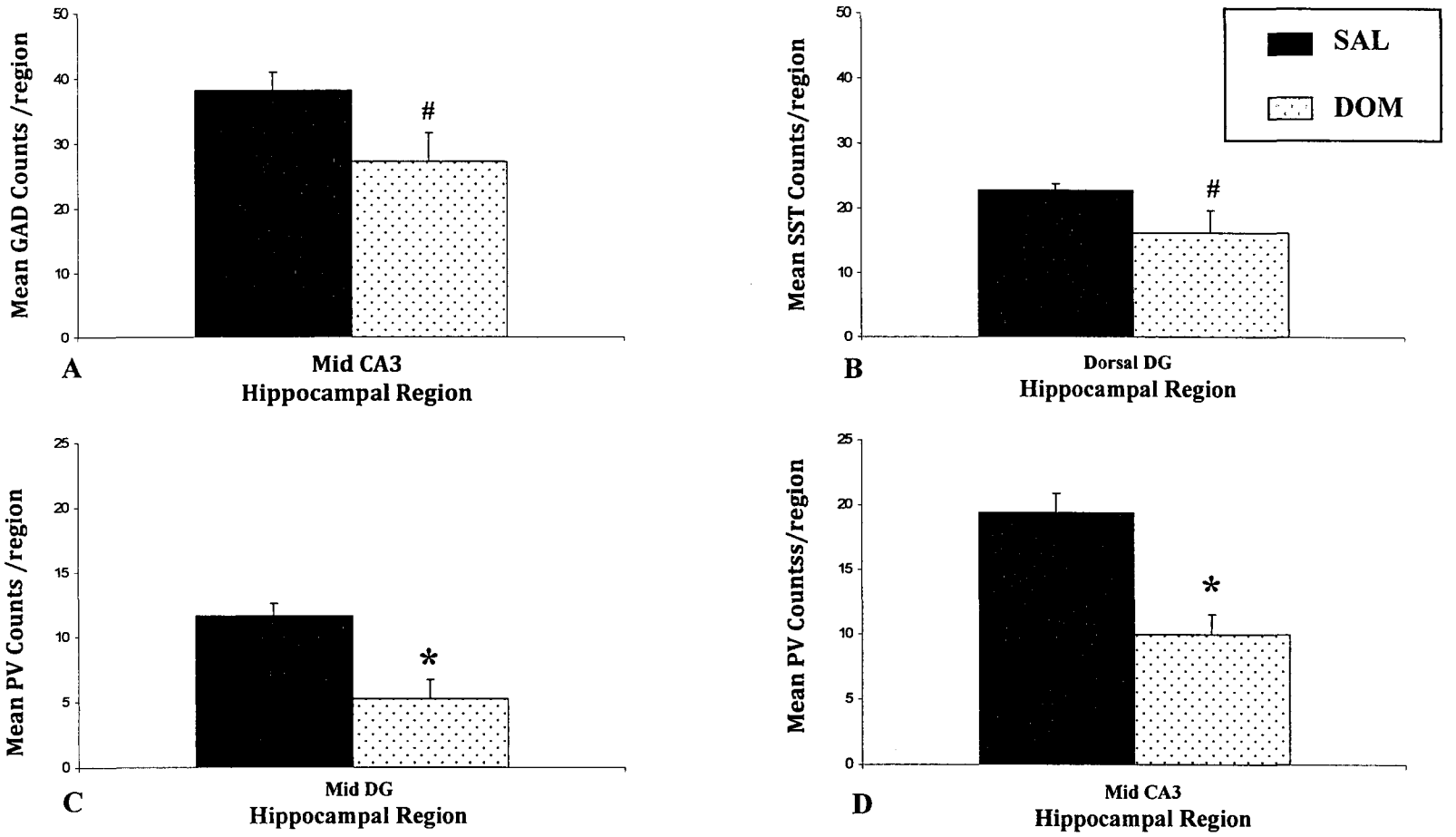

Figure 5.5. Differences noted for male-only groups in immunoreactivity. A) A trend toward a decrease in overall GAD expression was noted at the mid CA3 level (p=0.06), as well as B) in the dorsal dentate gyrus for decreases in somatostatin (p=0.076). Parvalbumin immunoreactivity was reduced in both mid dentate gyrus (C) and mid CA3 (D). Asterisks indicate a statistically significant difference from controls, the pound signs indicate a tendency toward significance, and error bars denote SEM.

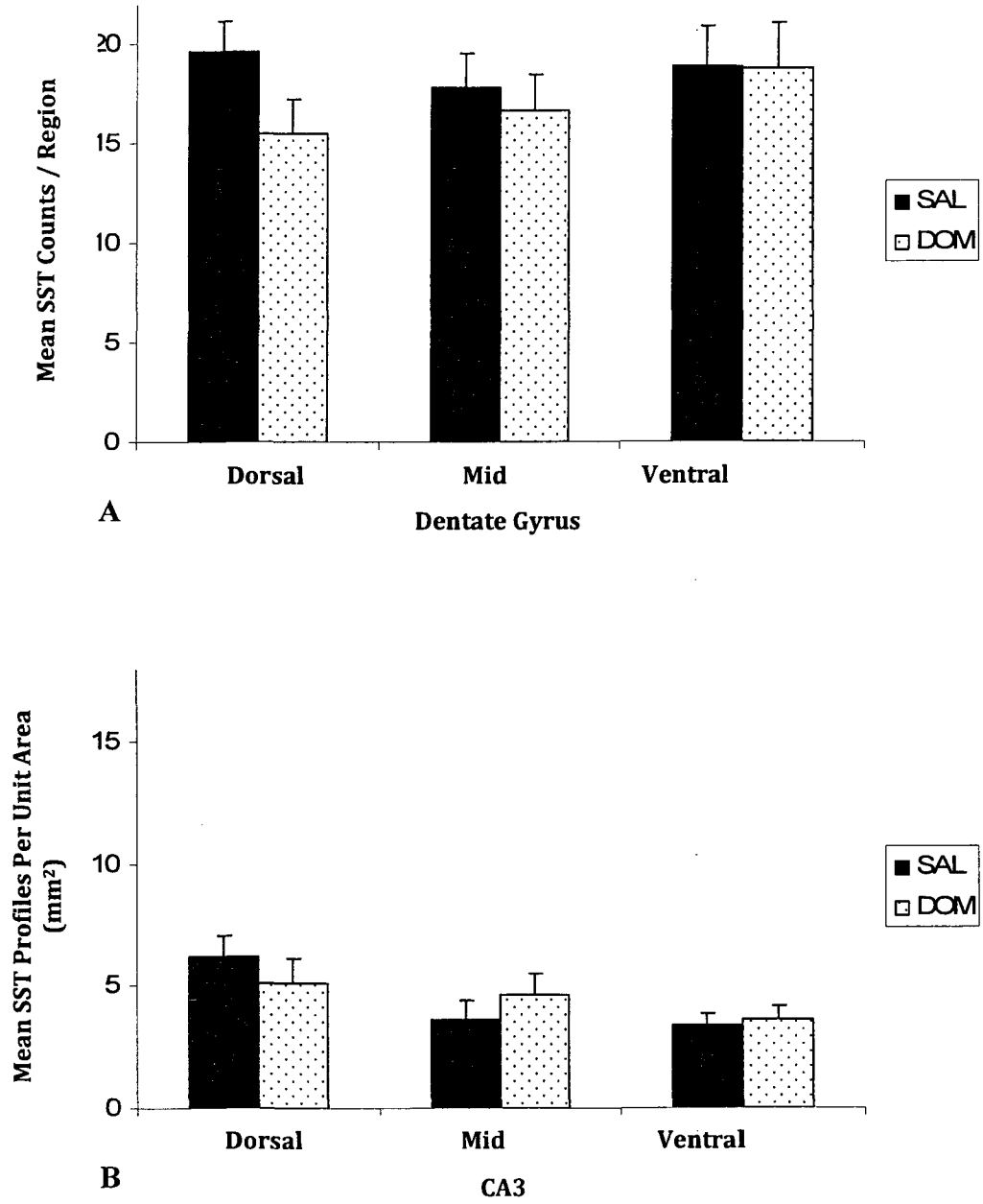

Figure 5.6. Mean somatostatin (SST) counts for all hippocampal levels. A) Dentate gyrus. B) Area CA3. In both graphs, error bars denote SEM.

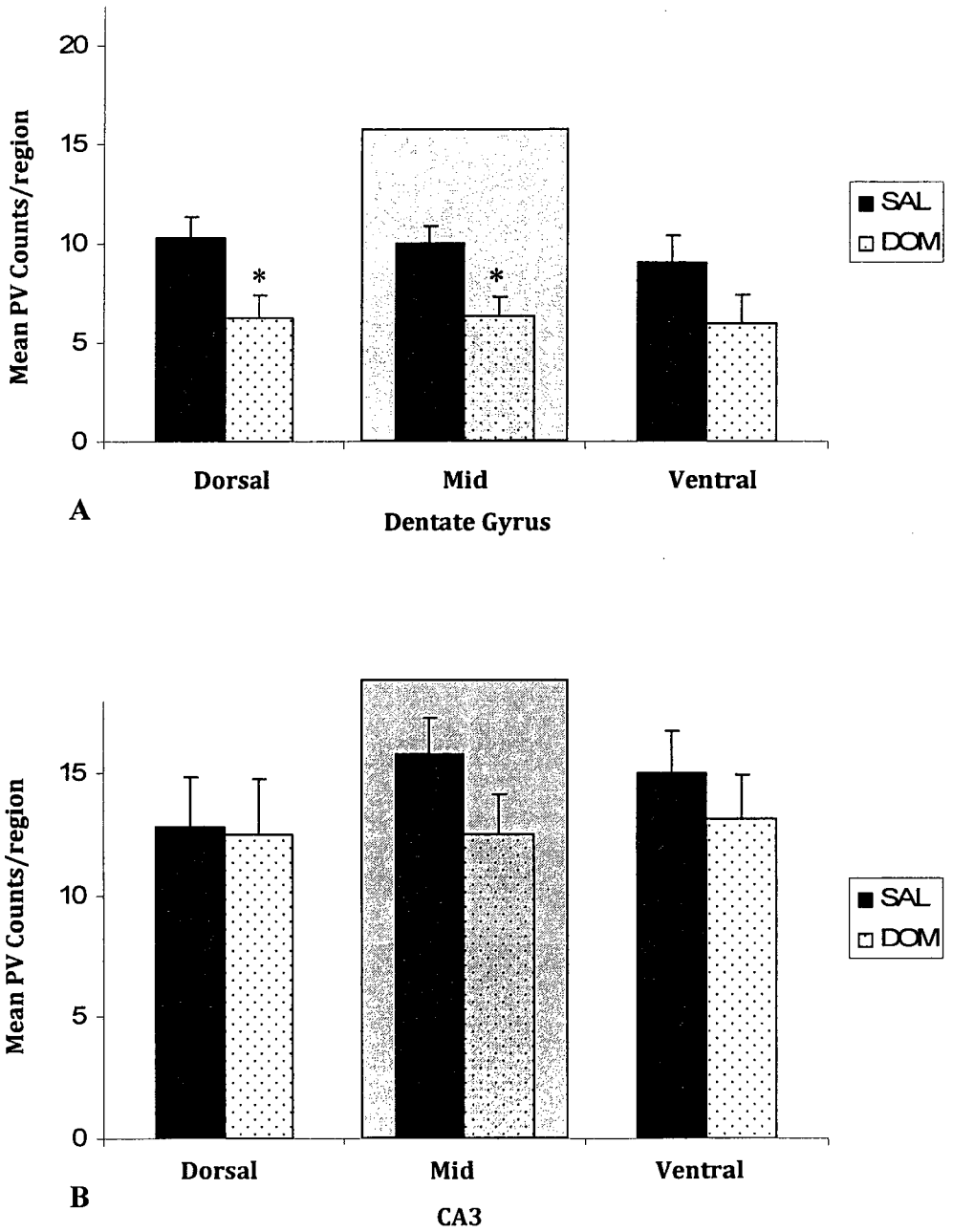

Figure 5.7. Mean parvalbumin counts for all hippocampal levels. A) Dentate gyrus: asterisk indicates a significant difference from controls. B) Area CA3. Error bars in both graphs indicate SEM, and shaded regions denote levels that showed interactions.

[$F_{(1,14)} = 7.374$,$p = 0.017$], and again, DOM treated male rats were the ones affected, with significantly less PV-ir recorded [$t_{(7)} = 4.22$, $p = 0.004$] (Figure 5.5D, pg 147).

There was no difference between controls and treated animals for PV-ir in the BLA [$F_{(1,14)} = 2.339$, $p = 0.148$] when the sexes were combined. However, when examined individually, DOM treated males did exhibit a trend toward decreased PV counts compared to controls (DOM: 25 ±2.52; SAL: 34 ±3.34), although this result did not quite reach significance [$t_{(7)} = 2.143$, $p = 0.069$]. Data are summarized in Table 5.1 (pg 144).

For differences in excitatory cell expression (e.g. mossy cells), we looked at neuronal profile counts at three levels of the hilar region using cresyl staining, and subtracted the GAD65/67 (inhibitory cell) profile counts. At dorsal and ventral levels, there was no difference noted, but at the mid level (Figure 5.8, pg 151), DOM treated rats showed a slight decrease in non-GABAergic cells [$F_{(1,14)} = 4.742$, $p = 0.047$]. There were no interactions noted at any level for this measure.

5.4 Discussion

This study has shown that, in rats, perinatal exposure to low doses of the Glu agonist DOM during the second postnatal week produces decreases in overall GABA availability (Figure 5.4A, pg 145) and parvalbumin-containing interneuronal immunoreactivity (Figure 5.7A, pg 149) in the HC, but does not appear to affect somatostatin levels to the same degree (see Figure 5.6, pg 148). Furthermore, many of the noted alterations appear to be more prevalent in males than females (Figure 5.5,

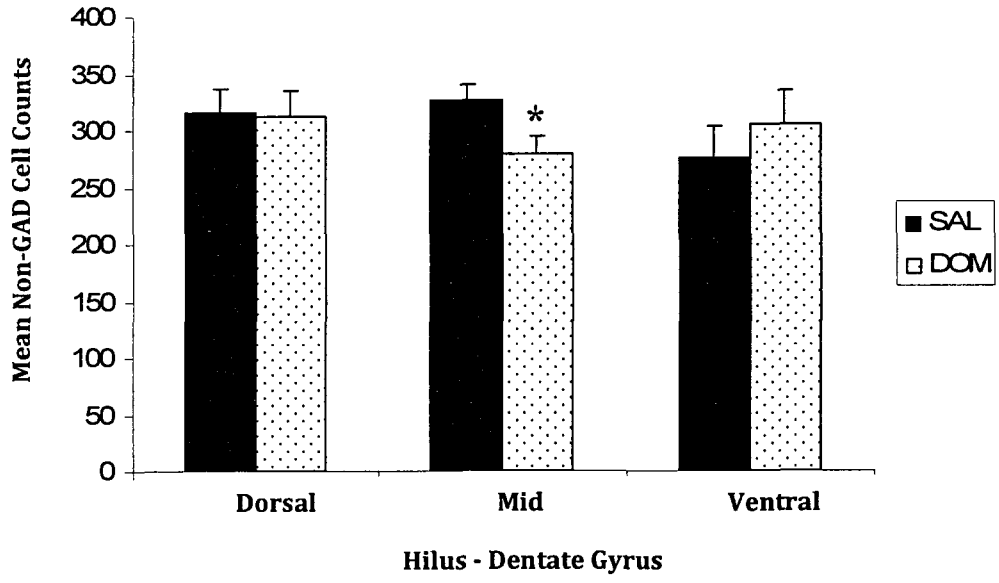

Figure 5.8. Mean non-GABAergic cell counts in the dentate gyrus. The asterisk indicates a significant difference from the appropriate control group ($p<0.05$).

pg 147). In the amygdala, PV-containing interneurons were unchanged overall when both sexes were combined, but when investigated separately, DOM-treated males again demonstrated a strong tendency for less immunoreactivity (Table 5.1, pg 144). Additionally, non-GABAergic (mossy) cells also appear to be affected, with a decrease noted at the mid level in the hilar region (Figure 5.8, pg 151).

Studies in animals investigating the effects of SE have found that decreases in interneuronal populations are often more pronounced at the ventral (temporal) hippocampal level (Kobayashi *et al.*, 2003). The decreases seen in overall GAD65/67 counts in ventral DG for the current investigation (Fig 5.4A, pg 145) are in line with this propensity. However, in area CA3, a more complex picture emerges, with DOM males showing a marked decrease in counts at the mid region (Figure 5.5A, pg 147), as well as a tendency toward a decrease ventrally, while DOM females tend toward an increase in expression. A similar pattern occurred at the mid level of the DG as well (see Table 5.1, pg 144). This intriguing reversal in immunoreactivity levels between males and females, which re-emerges again in the PV data, may be a result of the developmental timeframe during which DOM is administered combined with the specific physiologic function of the proteins measured. It has recently been shown that developmental time-points may not be equivalent between the sexes. Females appear to mature faster than males (Lemmens *et al.*, 2005), particularly with regard to the development of GABAergic systems, and the subsequent formation of functional excitatory/inhibitory networks (Galanopoulou, 2008a; Kyrozis *et al.*, 2006) . In fact, in the substantia nigra, the GABA switch from an immature, depolarizing activity to the mature, hyperpolarizing version has been shown to occur as much as 7 days earlier in females

than in males (Kyrozis *et al.*, 2006), and thus can have a significant impact on maturational processes, particularly with regard to the timing of excitatory insults and subsequent seizure susceptibility (Galanopoulou, 2008b). In light of this knowledge, the differences in interneuronal expression seen between males and females in the current study are especially intriguing. Additionally, the marker chosen for GAD may also be an important factor in these results, since it has recently been reported that, in mice, GAD65 is functional under normal physiological conditions, while GAD67 appears to be more highly expressed during pathological events (Wu *et al.*, 2007). To date, most investigations of GABA availability following seizure activity have evaluated only one GAD isoform. It is therefore possible that the tendency toward increases found in females in mid DG and CA3 hippocampal levels may be due to increased GAD67 production in response to heightened regional activity, while males, having a less mature system at the time of initial insult, did not develop this system to the same extent. However, much more work is required before the answer to these intriguing questions is revealed.

The decreases seen in the current study for PV-ir are also interesting, showing an overall effect of DOM treatment at the dorsal level of the DG (Figure 5.7, pg 149), as well as a male-only effect for treatment at the mid region, a reduction that is also mirrored at mid CA3 (Figure 5.5C and D, pg 147), and in the basolateral amygdala (Table 5.1, pg 144). Again, the decreases seen predominantly in males are in line with the concept of a differential maturation schedule for the GABAergic system between the sexes. These differences may be further explained by the fact that PV-containing interneurons do not develop in (male) rats until PND8-14 (Nitsch *et al.*, 1990; Solbach and Celio, 1991),

which is exactly the time frame during which we administer DOM. While the role of PV in epilepsy is not yet well characterized, it is known to be a key player in the epileptogenic process in humans, with a diversity of alterations in PV-ir described (Arellano *et al.*, 2004; Sloviter *et al.*, 1991; Wittner *et al.*, 2005; Zhu *et al.*, 1997). In animal models, it has been shown that seizure activity may down-regulate PV expression within the cell (Scotti *et al.*, 1997). Thus, a decrease in PV-ir may not necessarily indicate an actual decrease in PV-containing interneurons, but simply a decreased PV expression. However, as a protein responsible for buffering intracellular calcium, reductions in PV immunostaining, whether due to decreased expression or actual cell loss, are still indicative of important alterations in PV-mediated circuitry.

In SE models, SST is considered to be one of the most consistently vulnerable interneuronal populations (Buckmaster and Dudek, 1997b; Kobayashi and Buckmaster, 2003) in the hippocampus, and SST is also a known anticonvulsant neuropeptide (Braun *et al.*, 1998). However, while a decrease in this subpopulation of interneurons is now considered to be a hallmark of epilepsy, the functional consequences of their loss have yet to be elucidated, as no equivalent decrease in inhibition has as yet been discovered (for review, see Tallent, 2007). In fact, increased inhibition has often been reported (Buckmaster and Dudek, 1997a; Haas *et al.*, 1996). In the DOM rat, no significant decreases were seen in SST-ir, although there was a trend noted in DOM males in the dorsal hilar region (see Figure 5.5B, pg 147). While not consistent with the SE models, these results are in line with what is noted during kindling progression, where no real loss of SST-ir is seen during the early stages of stimulation (Csaba *et al.*, 2004;

Schwarzer *et al.*, 1996), with the system requiring much more activity before SST-ir is significantly reduced (Schwarzer *et al.*, 1996).

Previous work looking at hilar mossy cells has reported that this excitatory population is perhaps the single most vulnerable in the HC (Buckmaster and Schwartzkroin, 1994) and as such, is a logical place to examine the possible effects of subtle neurotoxic insults. However, positive identification of these neurons continues to be limited by the paucity of selective markers, and as a result, their presence is difficult to quantify, often being estimated through a subtractive method similar to that employed in the current study (for review, see Ratzliff *et al.*, 2002). The most obvious confound for this type of protocol is the possibility for inclusion of all cell types, including glia and ectopic granule cells thus creating a risk of underestimating actual mossy cell loss as a result of treatment. In an attempt to examine overall cell expression in as unbiased a manner as possible, we counted all stained cells in the region of interest, subtracted the GAD65/67 interneurons from the mix, and still found an ~15% decrease for the DOM treated group at the mid hilar level (Figure 5.8, pg 151). However, whether this decrease is due to a reduction in mossy cell counts, glial counts, or some combination therein cannot be ascertained from these data. Additionally, this result is in conflict with previous work on the NIS-L model, which reported an increase in both glia and neuronal counts at this level for this age (MacDonald *et al*, 2008), although a more traditional cell loss was subsequently seen at a later time point (Doucette *et al.*, 2004). This discrepancy may be due, at least in part, to the differing assessment methods utilized, but nevertheless raise some interesting questions regarding changes in hilar cell populations that appear to be occurring in the DOM rat at this particular hippocampal level in both studies.

Additionally, it would seem that the alterations seen in the current study are primarily affecting excitatory populations, as there was no corresponding difference noted between NIS-L rats and controls in overall GAD65/67 expression in this area.

In conclusion, the results of this study show alterations in GABAergic expression resulting from early postnatal administration of low-dose DOM that are similar, but not identical to those seen in more severe models, such as those produced through SE induction. Additionally, we have shown that in the DOM model, females appear to be somewhat more resistant than males to these alterations, possibly due to an earlier maturation of the GABA system (Galanopoulou, 2008b). In non-GABAergic populations, a decrease was seen at the mid region of the dentate hilus, perhaps due to a decline in mossy cell numbers in this area, although further study is required to determine the exact populations affected. Overall, this work further adds to the existing body of knowledge regarding seizure development, as well as highlights the importance of understanding how even subtle insults may be detrimental to the intricate interplay between Glu and GABA systems during critical developmental stages.

6.0 ALTERATIONS IN HIPPOCAMPAL CIRCUITRY RESULTING FROM EARLY GLUTAMATE RECEPTOR ACTIVATION

6.1 Introduction

As one of the most excitatory structures in the limbic system, the HC has long been implicated in seizure generation, and has recently been shown to have a primary involvement in low-grade (Stage 1-2) seizure expression (Hewapathirane and Burnham, 2005) as seen in TLE. With a highly organized, laminar arrangement, this area is particularly prone to synchronous activity that can be readily observed through electrophysiological recordings as large amplitude, extracellular field potentials. As a main entry point into the HC proper, the DG serves an unique role in the traditional 'trisynaptic circuit', hypothesized to function by blocking or filtering information from the entorhinal cortex, and thus governing subsequent activity within the highly excitable CA3-CA1 region (for review, see Hsu, 2007).

The ability of the DG to modulate transmission of excitatory activity is dependent upon important characteristics inherent in the principal cells found within its structure. The first is the minimal direct interconnectivity between DG granule cells under normal conditions (for review, see Witter, 2007), which serves to limit recurrent action potential generation. This, along with a relatively negative resting membrane potential, high action potential threshold (Lambert and Jones, 1990; McNaughton *et al.*, 1981) and strong GABAergic inhibition (for review, see Magloczky and Freund, 2005) all combine to make this area extraordinarily resistant to synchronous discharge. However, in circumstances where one or more of these conditions fail, the DG may allow enhanced excitatory transfer into area CA3, where synchronous activity can be more readily generated. Processes such as the loss of hilar interneurons (e.g. Buckmaster and Dudek, 1997b; Kobayashi and Buckmaster, 2003) and the excitatory mossy cells that are

purported to innervate them (for review, see Buckmaster and Schwartzkroin, 1994; Hsu, 2007), as well as MFS into the IML (e.g. Sutula, 2002; Sutula and Dudek, 2007) which involves the redirection of granule cell axons to form an excitatory GC to GC loop, are both seen in TLE. Under these pathologic conditions, the possibility of altered DG modulation creating a hyperexcitable response following EC perforant path stimulation has been the subject of much investigation in the epilepsy research field (for review, see Dudek and Sutula, 2007).

The NIS-L rat model, produced through systemic administration of low-dose DOM during a critical period of early postnatal development, displays many of the features of TLE, including behavioural Stage 1-2 seizure-like activity (Doucette *et al.*, 2004), increases in IML mossy fibre sprouting under both normal conditions (Bernard *et al.*, 2007) as well as in response to electrical kindling (Chapter 3), and decreases in PV-immunoreactive interneurons and hilar mossy cells within the DG (Chapter 5). Since both MFS and selective neuronal loss in the hilus may impact DG and/or CA3 function, an investigation of possible functional alterations in these regions using *in vitro* electrophysiological field-recording techniques was conducted, with the hypothesis that DG transmission would be increased in DOM-treated rats.

6.2 Materials and Methods

6.2.1 *Experimental animals*

Offspring born in-house from untimed Sprague-Dawley rats (Charles River, Quebec) were culled, injected, and weaned as described previously for the NIS-L model (see methods, Chapter 5) and left undisturbed until PND150. All studies were carried out

under approval from the University of Prince Edward Island Animal Care Committee, and in accordance with the Canadian Council of Animal Care guidelines.

6.2.2 Slice preparation and maintenance

At approximately PND150, each rat (n=24; 6♂ DOM, 6♂ SAL, 6♀ DOM, 6♀ SAL) was anesthetized with isofluorane, and the heart stopped with a quick blow to the thorax. Following immediate decapitation, the brain was rapidly removed and stored for 1 minute in ice-cold aCSF (composition (in mM): 124 NaCl, 4 KCl, 1.24 NaH_2PO_4, 1.3 $MgSO_4$, 2 $CaCl_2$, 26 $NaHCO_3$, and 10 glucose) equilibrated with 95% O_2-5% CO_2, pH 7.4. During this time, the cerebellum and ~1cm of the frontal cortex were removed, as well as a small portion of tissue from the dorsal surface so the brain could be oriented to provide horizontal slices containing the HC, the subicular complex, the EC and parts of the temporal cortex (Gloveli *et al.*, 1998; Zhang *et al.*, 1994). Maintaining these connections was necessary to allow electrophysiological investigation of synaptic transmission (Boulton *et al.*, 1992) under normal conditions, as well as during acute exposure to excitatory compounds. Using a vibratome (Leica VT1000s), 400μm thick slices were cut from the ventral portion of the brain and divided at midline, with only slices from the ventral region (~6.3 to 7.5mm ventral from bregma; (Paxinos and Watson, 2007)) included in the study. Slices were allowed to equilibrate to room temperature (~21 °C) for at least 1 hour in oxygenated aCSF, and then transferred to a submersion type recording chamber where they were maintained with a constant flow (gravity fed; 2.5ml/min) of the perfusion medium at 32°C (Warner Instrument Corp #TC-344B) for a minimum of 15 minutes prior to recording.

6.2.3 Electrophysiological recording and stimulation

Extracellular recordings were made using borosilicate glass electrodes (KG-33; Garner Glass Co.) filled with aCSF and pulled to 4-6MΩ resistance. An amplifier (Axopatch 700B configured with aCV7B headstage, Axon Instruments Inc) connected to an MP-285 micromanipulator (Sutter Instruments Co) and interfaced via an A/D converter (Digidata 1300, Axon Instruments Inc) to a computer equipped with PClamp 9.2.1.9 software, allowed the collection and storage of realtime digitized data (10kHz sampling rate) for future analysis.

Stimulation was performed through bipolor microelectrodes connected to an Iso-Flex isolated stimulus unit (A.M.P.I.) and was triggered via a TTL pulse driven by PClamp software. Continuous recordings were obtained using an electrical stimulus (square-wave, single stimulus, 0.5μA) delivered every 5 seconds to the presubicular region of the EC (layer II) to activate perforant pathway (PP) inputs through the DG and into area CA3 of the HC proper (Teyler and Alger, 1976). For input-output (I/O) recordings, the stimulus intensity was varied from 0 to 1.0μA in 0.1μA intervals to measure changes in maximum amplitude of evoked responses. The stimulation levels used in this paradigm were chosen based on pilot study data to provide a consistently measurable response (field inhibitory postsynaptic potential – fIPSP or field excitatory postsynaptic potential – fEPSP: Schneiderman *et al.*, 1992; Trevelyan, 2009; Uva *et al.*, 2009) without driving the tissue to exhibit population spike activity, and were uniform for all slices tested. In addition, recordings were always obtained in the same manner, with 3 initial I/O measurements (DG, hilus, CA3; see below for details) followed by 15 minutes of drug treatment and 10 minutes of wash out in CA3 interspersed with I/O testing every 5

minutes, then a final I/O measurement from the hilus and DG. Input-output activity in the DG was recorded in the molecular layer (proximal to granule cells of the suprapyramidal blade), hilus recordings were obtained from the polymorphic layer immediately below that taken in the DG, and CA3 was assessed from the SL of CA3b (defined as the length of the pyramidal layer that extends beyond the blades of the DG up to the fimbria; see Figure 1.9, pg 34) (Masukawa *et al.*, 1982).

6.2.4 Drug application

For acute drug exposure, DOM (BioVectra dcl, Canada) was added to the perfusion solution to provide a concentration of either 100nM or 250nM. For the low magnesium treatment, $MgSO_4$ was omitted from the aCSF solution. At no time were slices exposed to more than one drug treatment, and a 10 minute wash-out period (using normal aCSF) was conducted following each exposure.

6.2.5 Data analysis

To assess I/O differences, 2-way (SEX x COND) repeated measures ANOVAs were utilized (within-subjects factor: stimulation level), with any interactions investigated separately for sex. Data for changes from baseline measures throughout acute treatments were obtained through subtraction of baseline response from each appropriate time point. For latency to population spike (PSp) response measures, a 'no response' time was arbitrarily assigned the maximum score (1020sec), and data were analyzed using 1-way ANOVA. Non-parametric data were compared through the Chi-Square test for independence (Crosstabs), or Mann-Whitney U for rank-ordered data. SPSS 15.0 for

windows (SPSS Inc.) software was used for all analyses, and the alpha level for all tests set at $\alpha \leq 0.05$.

6.3 Results

To determine whether there were any underlying differences in treated and control tissue following perforant path stimulation, baseline I/O responses in the DG, hilus, and area CA3 were assessed for maximal fIPSP amplitude achieved, response duration (i.e. rise and decay time), and slope (i.e. rise and decay slope). Analysis revealed no differences between treatment groups in any region measured (Table 6.1, pg 164), but there were significant sex effects noted. In the DG, slices from all female rats demonstrated a heightened inhibitory response to stimulation compared to slices from males (mean fIPSP amplitude (mV): females 0.722±0.06; males 0.533±0.06, p=0.038) (Figure 6.1A, pg 165), and while no alterations were seen in rise time or slope in this region, there was a definite propensity toward longer decay times in females as well (decay time (ms): females 3.357±0.24; males 2.650±0.24, p=0.052). In the hilar region, females again showed a greater inhibitory potential (mean fIPSP amplitude (mV): females 0.732; males 0.529, p=0.013) (Figure 6.1B, pg 165), as well as increased response duration demonstrated by a strong tendency toward increased rise time (females 1.808±0.09; males 1.580±0.09, p=0.088) and rise slope (females 0.304±0.03; males 0.210±0.03, p=0.070), and a statistically significant increase in decay time (females 4.791±0.23ms; males 3.506±0.23ms, p=0.001) compared to their male counterparts. Ultimately, these differences in upstream responses did not translate to alterations in fIPSP amplitude in area CA3, as slices from both male and female rats showed equivalent inhibitory potentials in this region (Figure 6.1C, pg 165). However, there was a striking difference

Table 6.1. Summary of mean values (±SEM) for baseline responses in the dentate gyrus, hilus, and CA3.

	Baseline Response		
Measure	**SAL** (mean ±SEM)	**DOM** (mean ±SEM)	p-value
Dentate Gyrus			
fIPSP amplitude (mV)	0.647 (±0.06)	0.640 (±0.06)	0.644
Rise time (ms)	1.675 (±0.12)	1.629 (±0.12)	0.791
Decay time (ms)	3.178 (±0.24)	2.829 (±0.24)	0.319
Rise slope (ms/mV)	0.204 (±0.04)	0.230 (±0.04)	0.637
Decay slope (ms/mV)	-0.314 (±0.09)	-0.279 (±0.09)	0.778
Hilus			
fIPSP amplitude (mV)	0.599 (±0.05)	0.661 (±0.05)	0.416
Rise time (ms)	1.639 (±0.09)	1.749 (±0.09)	0.400
Decay time (ms)	4.037 (±0.23)	4.249 (±0.23)	0.522
Rise slope (ms/mV)	0.251 (±0.03)	0.263 (±0.03)	0.818
Decay slope (ms/mV)	-0.280 (±0.04)	-0.276 (±0.04)	0.939
CA3			
fIPSP amplitude (mV)	0.237 (±0.03)	0.286 (±0.03)	0.227
Rise time (ms)	0.873 (±0.16)	1.031 (±0.17)	0.509
Decay time (ms)	1.055 (±0.20)	1.499 (±0.20)	0.126
Rise slope (ms/mV)	0.033 (±0.11)	0.282 (±0.11)	0.137
Decay slope (ms/mV)	-0.612 (±0.06)	-0.577 (±0.06)	0.697

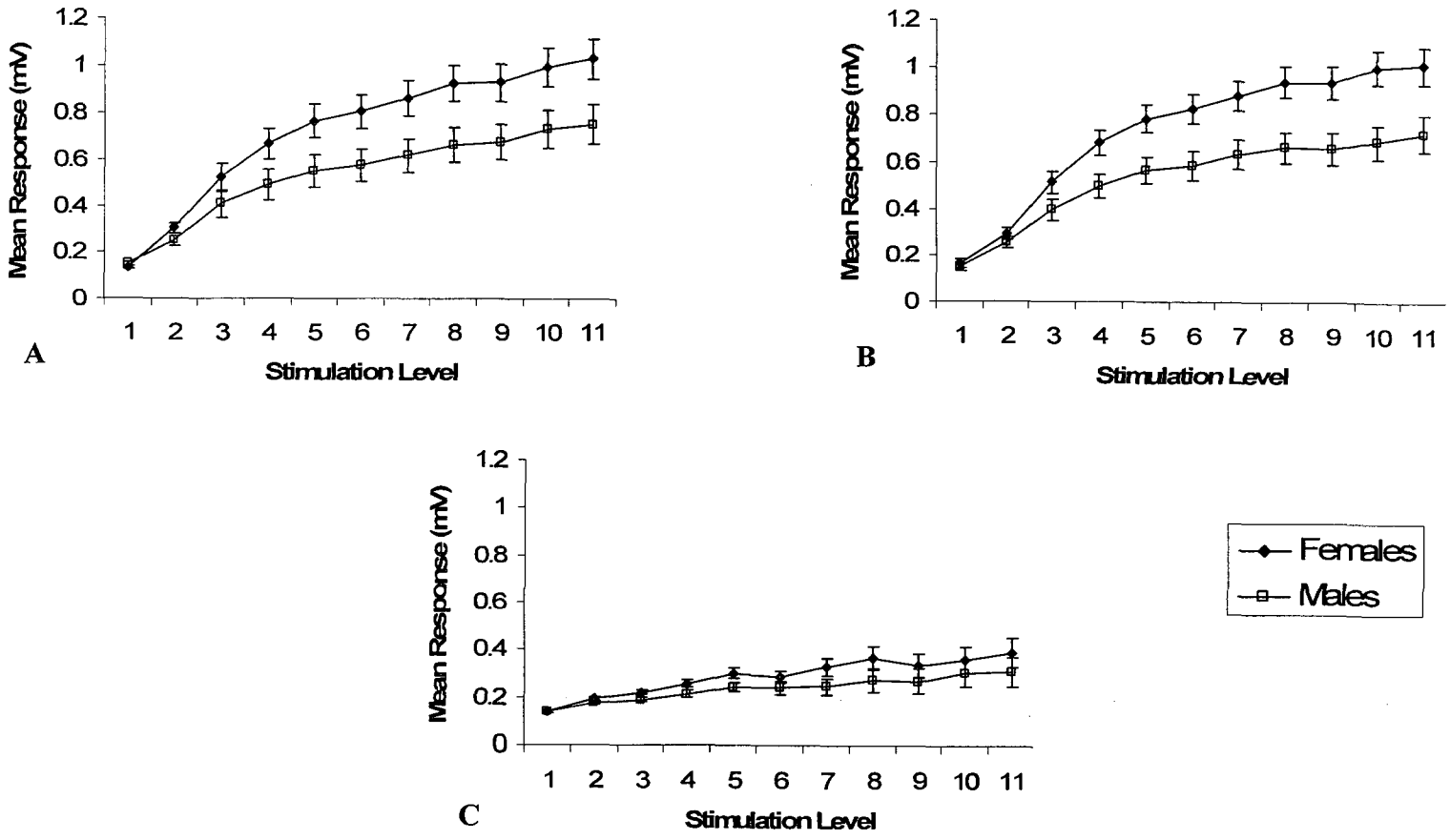

Figure 6.1. Baseline input-output response curve for all female and male rats stimulated in the perforant path and recorded in various regions of the hippocampal formation: A) Dentate gyrus B) Hilus C) CA3. In all graphs, error bars indicate SEM.

in the overall response duration, with females exhibiting substantial increases in both rise (females 1.307±0.18; males 0.598±0.15, p=0.008) and decay times (females 1.762±020; males 0.791±0.20, p=0.002) in CA3 as well.

Previous *in vitro* studies have demonstrated that underlying pathologies may not present unless the slice is challenged through the use of a stressor (e.g. Bernard *et al.*, 2001; Hardison *et al.*, 2000; Patrylo and Dudek, 1998). To this end, slices from treated and control rats were exposed to either 100nM DOM, 250nM DOM or a $0Mg^{++}$ aCSF solution. A fresh slice was used for each exposure, with no slice used for more than one treatment. As in the baseline assessment, I/O responses were evaluated for peak fIPSP (or fEPSP) amplitude, response duration, and slope, but for this portion of the analysis, the focus was on changes in response in area CA3 from the appropriate baseline measure after 5, 10, and 15 minutes of treatment, followed by 5 and 10 minutes of wash-out using normal aCSF perfusion. Additionally, changes in DG and hilus were also assessed as the difference between baseline (prior to treatment) and post treatment (after wash-out) responses. Representative images of various responses in the different regions can be found in Figure 6.2 (pg 167).

There were no statistically significant differences for either condition or sex for changes from baseline responses following 100nM DOM in any of the three regions measured (Table 6.2, pg 168), but there were a few notable tendencies. In the DG, slices from postnatal DOM treated (PDT) animals appeared to show a decrease in rise slope compared to their baseline (-0.064±0.043), while controls apparently experienced an increase in the same region (0.064±0.045; p=0.059) (Figure 6.3A, pg 169). Controls

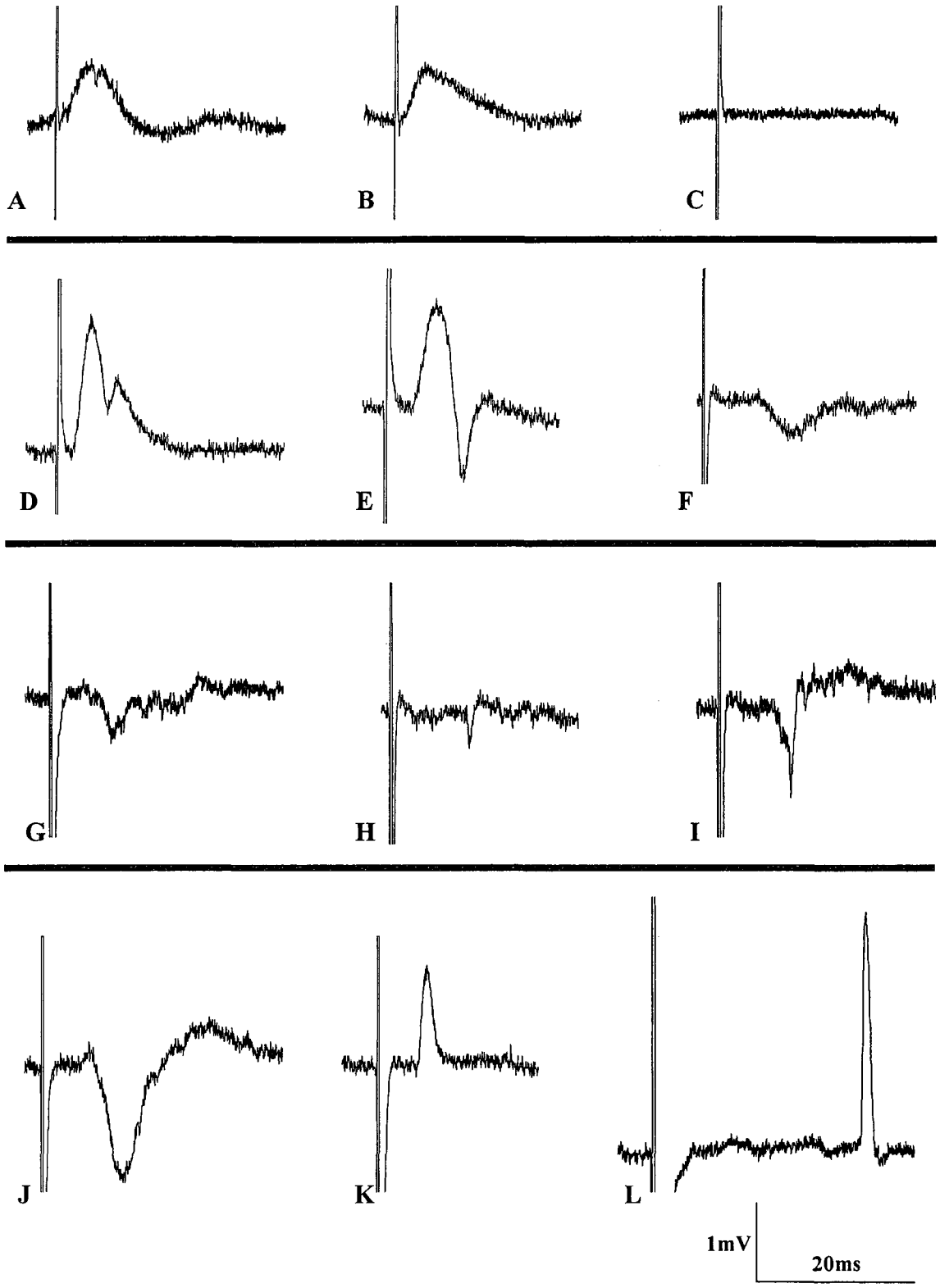

Figure 6.2. Representative tracings during *in vitro* recordings. First row: typical response to stimulation in A) dentate gyrus B) hilus C) hippocampal area CA3. Image D and E: alternative dentate/hilar region and (F through L) CA3 samples of responses noted during drug perfusion. An upward inflection indicates an inhibitory response.

Table 6.2. Summary of mean values (±SEM) for differences from baseline in the dentate gyrus, hilus, and CA3 during and following 100nM DOM.

	100nM DOM		
Measure	**SAL** (mean ±SEM)	**DOM** (mean ±SEM)	p-value
Dentate Gyrus			
fIPSP amplitude (mV)	0.152 (±0.08)	-0.046 (±0.07)	0.072
Rise time (ms)	-0.202 (±0.24)	-0.444 (±0.21)	0.490
Decay time (ms)	1.253 (±0.51)	-0.198 (±0.56)	0.078
Hilus			
fIPSP amplitude (mV)	-0.016 (±0.11)	-0.068 (±0.10)	0.732
Rise time (ms)	-0.665 (±0.38)	-0.192 (±0.27)	0.349
Decay time (ms)	-0.169 (±0.56)	-0.043 (±0.61)	0.881
CA3			
Run 1			
fIPSP amplitude (mV)	0.040 (±0.02)	-0.014 (±0.02)	0.109
Rise time (ms)	0.095 (±0.20)	0.047 (±0.17)	0.862
Decay time (ms)	0.178 (±0.18)	0.172 (±0.22)	0.983
Run 2			
fIPSP amplitude (mV)	-0.024 (±0.06)	0.042 (±0.06)	0.405
Rise time (ms)	-0.265 (±0.11)	-0.143 (±0.09)	0.405
Decay time (ms)	-0.151 (±0.15)	-0.189 (±0.17)	0.870
Run 3			
fIPSP amplitude (mV)	0.071 (±0.05)	-0.005 (±0.05)	0.286
Rise time (ms)	-0.196 (±0.16)	-0.402 (±0.16)	0.389
Decay time (ms)	-0.039 (±0.23)	-0.315 (±0.26)	0.438
Washout 1			
fIPSP amplitude (mV)	0.038 (±0.05)	-0.070 (±0.05)	0.121
Rise time (ms)	-0.368 (±0.16)	-0.104 (±0.14)	0.251
Decay time (ms)	-0.088 (±0.30)	-0.256 (±0.29)	0.693
Washout 2			
fIPSP amplitude (mV)	0.061 (±0.05)	-0.042 (±0.05)	0.168
Rise time (ms)	-0.118 (±0.23)	-0.387 (±0.20)	0.389
Decay time (ms)	0.422 (±0.33)	-0.186 (±0.33)	0.215

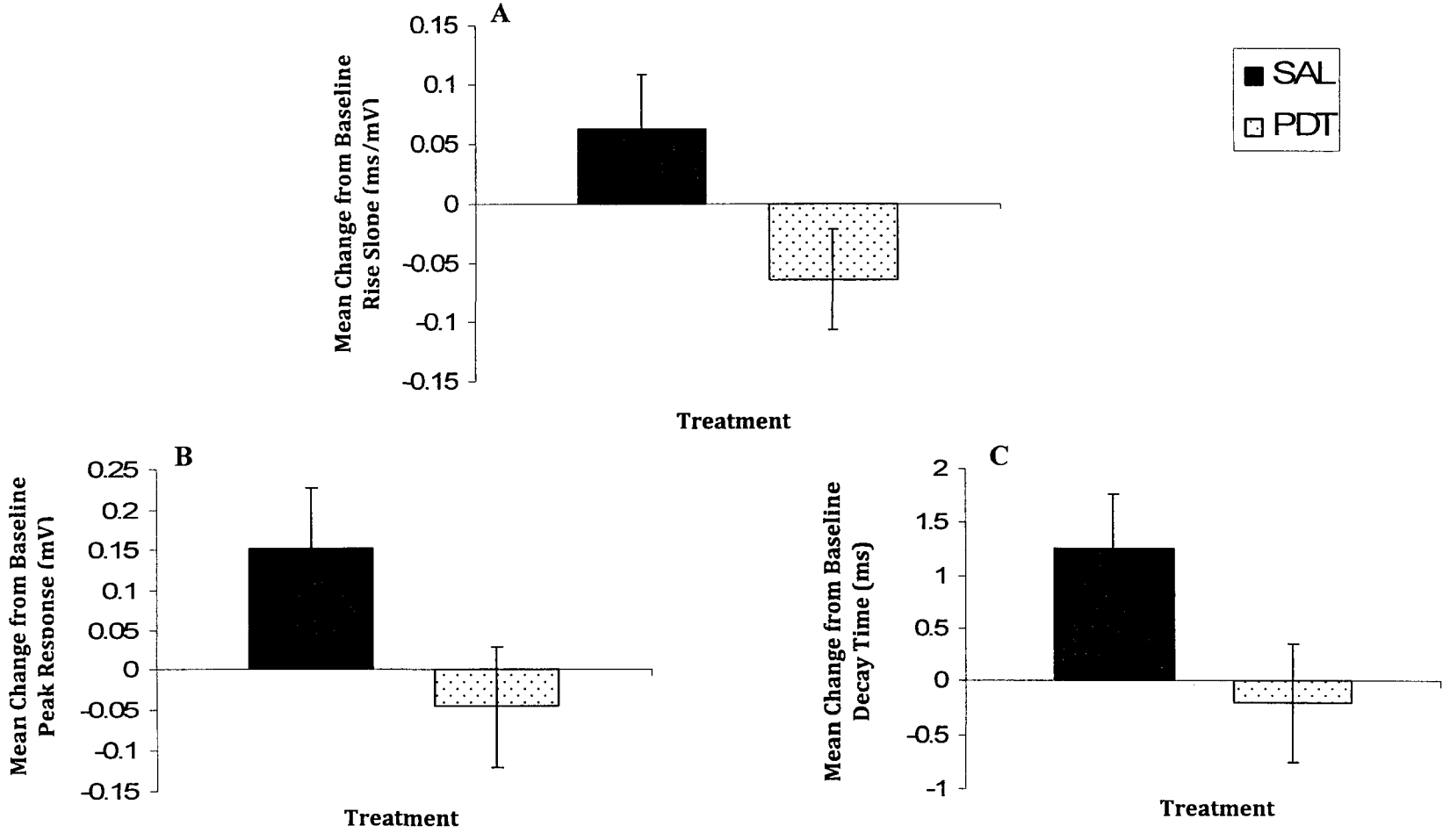

Figure 6.3. Mean changes from baseline measures in the dentate gyrus for saline control (SAL) and postnatal DOM (PDT) tissue following 15 minute acute perfusion of 100nM DOM and 10 minute washout. A) Rise slope ($p=0.06$) B) Peak fIPSP response ($p=0.07$) C) Decay time ($p=0.08$). Error bars indicate SEM.

also exhibited an increase in peak response after drug perfusion (0.152±0.075), while the PDT group tended toward a decrease in inhibition (-0.046±0.071; p=0.074) (Figure 6.3B, pg 169). As well, the mean decay time of the DG response seemed to increase in control tissue (mean 1.253±0.514), while in PDT tissue it appeared to decrease slightly (-0.198±0.559; p=0.078) (Figure 6.3C, pg 169). Together, these changes indicate a tendency toward a shift to the left from pre-DOM conditions for the fIPSP response in the DG of PDT animals (faster, less inhibitory response), while controls shifted to the right (longer, more inhibitory response). In area CA3 there was no effect for condition, but there was a tendency toward several sex-dependent changes after 15 minute DOM exposure, with females showing an increased rise slope while rise slope in males decreased (p=0.051). In addition, following the second wash-out period, males displayed a higher apparent decay slope (0.696±0.172) compared to the decay slope changes from baseline seen in females (0.198±0.172, p=0.075).

Responses during 250nM DOM perfusion were more pronounced, particularly in area CA3 where controls exhibited a decrease in peak inhibitory amplitude from baseline measures throughout the entire treatment period, while slices from the PDT group remained stable (Figure 6.4, pg 171). Rise time was also decreased (shorter) in controls, but due to an interaction (SEX by COND) during drug exposure and a main effect for SEX during the two wash-out periods, this measure was examined separately for males and females. Subsequent analysis implicated females in this change, displaying an apparent drop in rise time for controls after the first 5 minutes of DOM perfusion (p=0.065), a decrease that reached its maximum level by 10 minutes of exposure and remained consistent until the second wash-out (Figure 6.5A, pg 172).

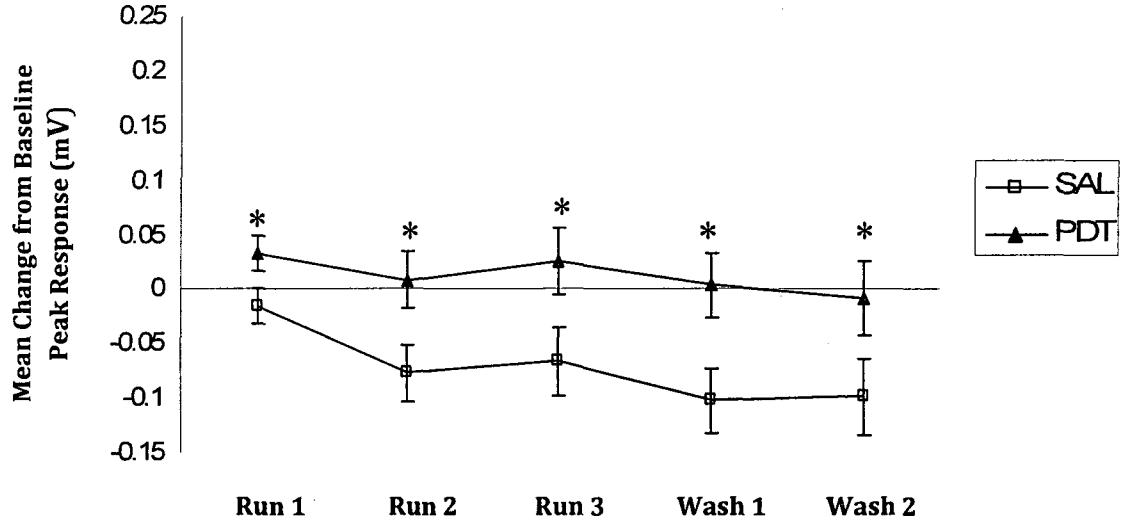

Figure 6.4. Mean changes in peak fIPSP response from baseline measures in hippocampal area CA3 for saline control (SAL) and postnatal DOM (PDT) tissue during acute perfusion with 250nM DOM (Run 1-3), and 10 minute washout. Asterisks denote a significant change from controls ($p<0.05$) and error bars indicate SEM.

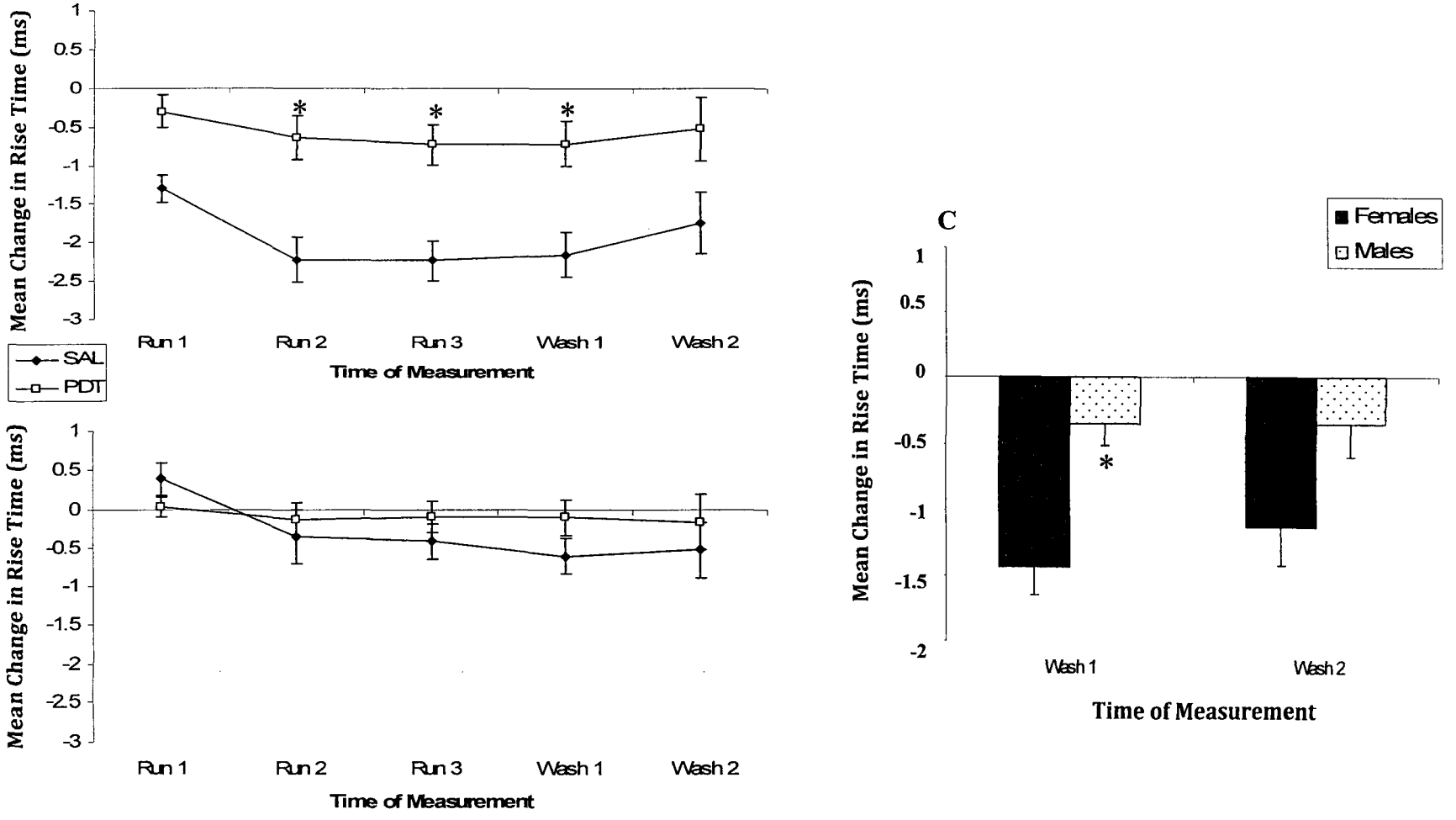

Figure 6.5. Mean changes in rise time from baseline measures in hippocampal area CA3 for A) female and B) male tissue during acute perfusion with 250nM DOM (Run 1-3), and 10 minute washout. C) Comparison of washout period only for sex. Asterisks denote a significant change from controls ($p<0.05$) and error bars indicate SEM.

Males did not exhibit an equivalent difference between groups, although male controls did display a sudden decrease in rise time after 10 minutes of DOM treatment, and this decrease continued throughout the remainder of the exposure (Figure 6.5B, pg 172). These results are similar to what was reported for fIPSP peak amplitude, where neither males or females in the PDT group appeared to experience much alteration during acute 250nM DOM perfusion. A comparison of male to female response during the wash-out period (main effect for SEX) showed that overall, females experienced a greater change from baseline than did their male counterparts, exhibiting a significantly decreased rise time in wash 1 [$F_{(1,12)} = 16.892$, $p=0.001$] and, although not statistically different, a considerable mean decrease in wash 2 as well [$F_{(1,10)} = 4.291$, $p=0.065$] (Figure 6.5C, pg 172). And finally, there were also changes seen in the decay time measure in CA3 in response to 250nM DOM, with a main effect for condition found after 10 and 15 minute exposure, as well as following the first wash (Figure 6.6, pg 174). Again, controls exhibited a decreased decay duration, while slices from the PDT group remained unchanged from their baseline measures. The only difference for slope in area CA3 was one interaction in the decay portion after 5 minutes of treatment. Separation of male and female data at this time point revealed a decreased decay slope compared to baseline measure for PDT females [$F(1,5) = 45.148$, $p=0.001$]. No other interactions or main effects were noted.

In the DG and hilar regions, there were no statistically significant changes seen, although there appeared to be an interaction for rise time in the DG ($p=0.060$). Since this was the measure that had also shown sex differences in CA3, a further investigation was performed. Again, there was a notable change in the female responses, with PDT

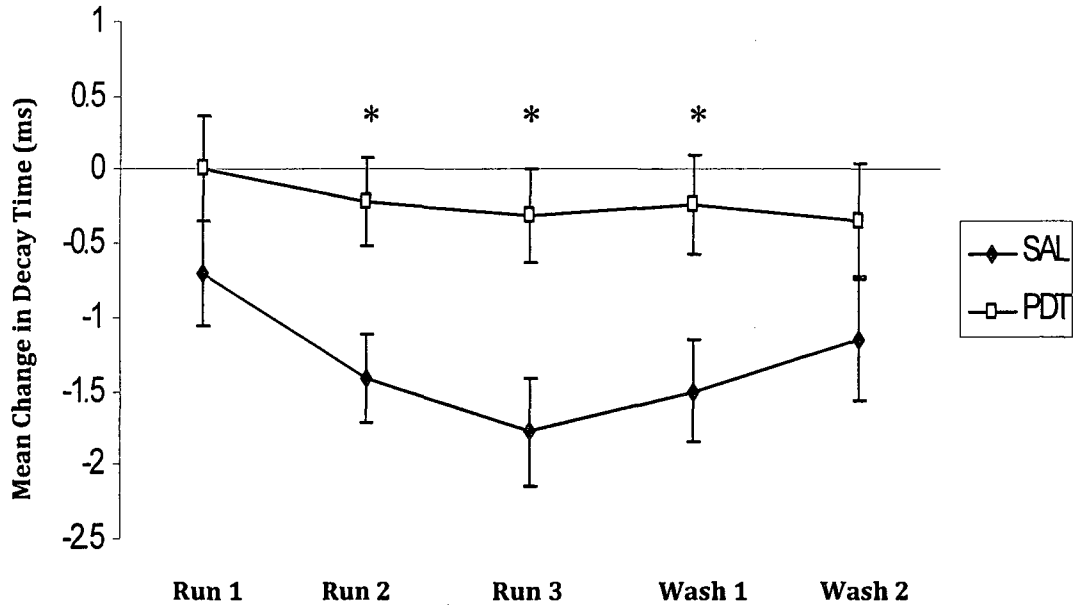

Figure 6.6. Mean changes in decay time from baseline measures in hippocampal area CA3 for saline control (SAL) and postnatal DOM (PDT) tissue during acute perfusion with 250nM DOM (Run 1-3), and 10 minute washout. Asterisks denote a significant difference from controls ($p<0.05$) and error bars indicate SEM.

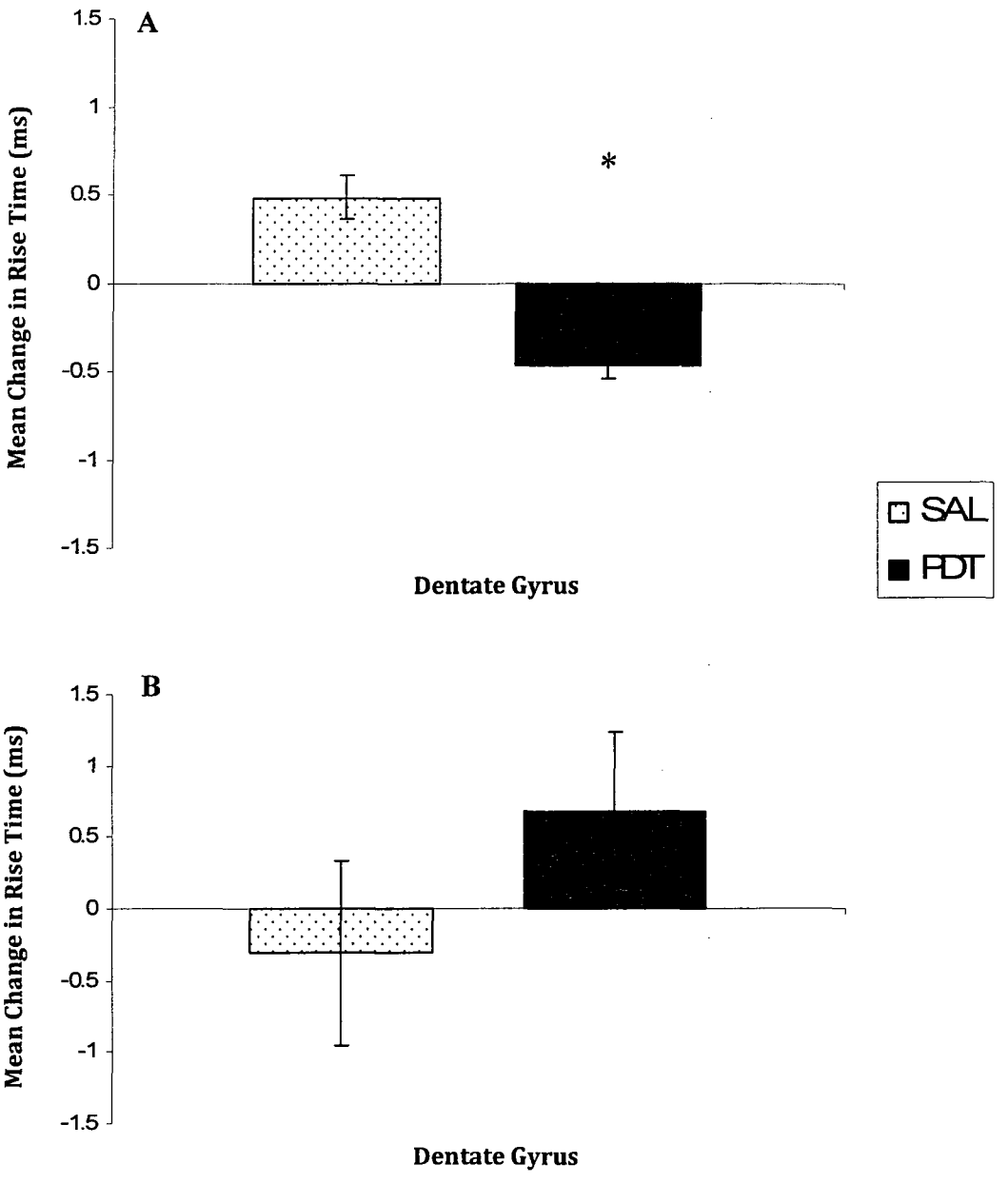

Figure 6.7. Mean rise time changes from baseline measures in the dentate gyrus for saline control (SAL) and postnatal DOM (PDT). A) female, and B) male tissue following 15 minute acute perfusion of 250nM DOM and 10 minute washout. The asterisk denotes a significant difference from controls ($p<0.05$), and error bars indicate SEM.

females experiencing a decreased (shortened) rise time in this region while the rise time for control females increased [$F_{(1,5)} = 14.068$, p=0.002] (Figure 6.7A, pg 175). Males showed no difference between groups in this measure (Figure 6.7B, pg 175).

The final treatment utilized in this study was acute perfusion with a $0Mg^{++}$ aCSF solution to assess possible changes from baseline measures through NMDA-mediated mechanisms. Previous studies using slices from electrically kindled rats have shown spontaneously increased excitability in these animals following 90 minute exposure as measured through duration and amplitude of seizure-like activity bursts (Behr *et al.*, 1996). In the current study, slices were exposed to the $0Mg^{++}$ solution following the same protocol used for the DOM exposure (i.e. 15 minute exposure and 10 minute wash-out with I/O responses recorded at 5 minute intervals). Results showed no differences in any measure in CA3 except for a tendency toward an interaction (SEX x COND) in decay time (p=0.060). However, although not statistically significant [$X^2_{(1)} = 1.815$, p=0.178], it is important to note that during this treatment, 41.7% of tissue in the PDT group switched from an fIPSP in area CA3 prior to the removal of Mg^{++} from the perfusate to an fEPSP, while only 16.6% of controls experienced this shift. There were no differences at all noted in the DG region for the $0Mg^{++}$ treatment (Table 6.3, pg 177), while in the hilus, a closer look at a SEX x COND interaction [$F_{(1,15)} = 5.201$, p=0.038] showed an increased decay time in both control males and PDT females, but neither reached significance due to high variability.

To assess possible differences in evoked activity between PDT and control animals, the following measures were evaluated in response to 0.5mA stimulation during 100nM

Table 6.3. Summary of mean values (±SEM) for differences from baseline in the dentate gyrus, hilus, and CA3 during and following 0 Mg^{++}.

	0 Mg^{++}		
Measure	**SAL** (mean ±SEM)	**DOM** (mean ±SEM)	p-value
Dentate Gyrus			
fIPSP amplitude (mV)	-0.029 (±0.15)	-0.158 (±0.14)	0.538
Rise time (ms)	-0.064 (±0.15)	-0.217 (±0.15)	0.487
Decay time (ms)	0.941 (±0.76)	-0.707 (±0.76)	0.147
Hilus			
fIPSP amplitude (mV)	0.101 (±0.13)	0.029 (±0.13)	0.699
Rise time (ms)	0.161 (±0.21)	-0.064 (±0.17)	0.427
Decay time (ms)	0.906 (±0.91)	0.731 (±0.78)	0.860
CA3			
Run 1			
fIPSP amplitude (mV)	0.034 (±0.02)	0.037 (±0.02)	0.938
Rise time (ms)	0.340 (±0.34)	0.100 (±0.42)	0.873
Decay time (ms)	0.769 (±0.34)	0.695 (±0.34)	0.881
Run 2			
fIPSP amplitude (mV)	0.102 (±0.07)	0.140 (±0.07)	0.710
Rise time (ms)	0.299 (±0.23)	0.061 (±0.23)	0.482
Decay time (ms)	1.205 (±1.03)	1.950 (±1.02)	0.615
Run 3			
fIPSP amplitude (mV)	0.082 (±0.05)	0.081 (±0.06)	0.983
Rise time (ms)	0.023 (±0.38)	0.088 (±0.41)	0.908
Decay time (ms)	0.906 (±1.00)	0.723 (±1.21)	0.909
Washout 1			
fIPSP amplitude (mV)	0.023 (±0.04)	0.096 (±0.04)	0.178
Rise time (ms)	0.480 (±0.48)	0.057 (±0.53)	0.616
Decay time (ms)	0.872 (±0.39)	0.648 (±0.35)	0.435
Washout 2			
fIPSP amplitude (mV)	0.028 (±0.02)	0.038 (±0.02)	0.778
Rise time (ms)	0.169 (±0.22)	-0.186 (±0.22)	0.286
Decay time (ms)	1.357 (±0.73)	0.776 (±0.75)	0.589

DOM, 250nM DOM, and $0Mg^{++}$ treatments: 1) occurrence of population spike (PSp) activity and 2) latency to first population spike. In addition, for the $0Mg^{++}$ treatment, the duration of the spike activity was compared.

During 100nM DOM there was a statistically significant difference in latency to the first PSp ($F_{(1,22)} = 5.626$, $p = 0.027$), with the PDT group responding more quickly (Figure 6.8, pg 179). Increasing the concentration of DOM to 250nM appeared to reverse the 100nM effect on the groups. During this treatment, controls exhibited a shorter latency to PSp response than the PDT animals ($F_{(1,22)} = 5.241$, $p = 0.032$; Figure 6.8, pg 179).

Latency to PSp response between the groups during $0Mg^{++}$ perfusion did not quite reach statistical significance either ($F_{(1,22)} = 3.334$, $p = 0.081$; Figure 6.8, pg 179) nor did population spike occurrence, although there was a definite tendency noted in this measure ($X^2 = 5.867$, $p=0.053$). Compared to the two DOM treatments, exposure to the $0Mg^{++}$ solution often resulted in "epileptiform" activity, with a full 75% of all tissue exhibiting seizure-like waveforms (see Figure 6.9, pg 180, for representative images). However, there was no difference found between the groups for the number of slices that ultimately succumbed to this activity, nor was there any difference in overall duration before a complete return to baseline when they did occur. Interestingly, an analysis of seizure 'consistency' (i.e. the likelihood that seizure-like activity would be continuously evoked in response to stimulation, rank-ordered as: 0- no response, 1- short-term only, 2- intermittently evoked (e.g. every second stimulation), 3- continuous from initiation to wash out, 4- continuous to end of washout period) revealed that the PDT group

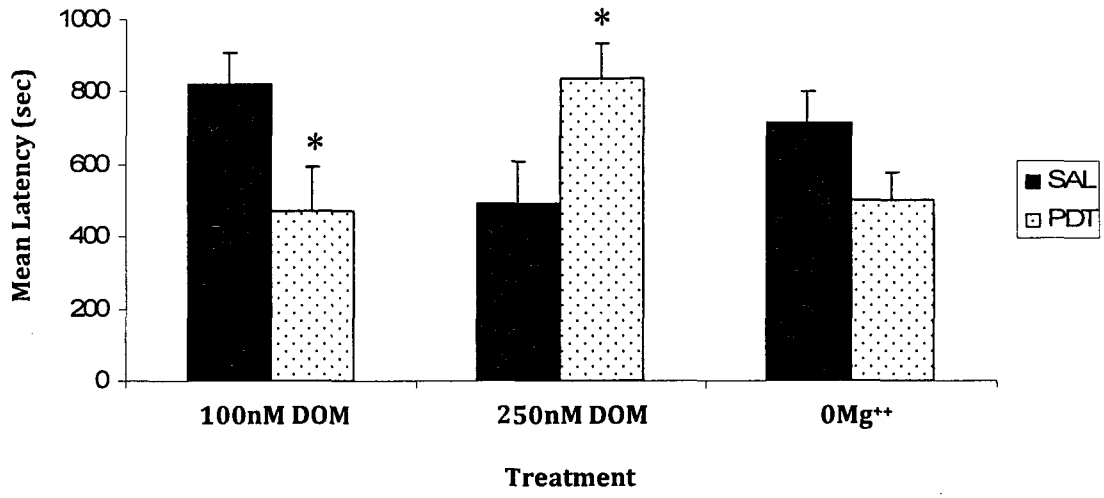

Figure 6.8. Mean latency to population spike activity for saline controls (SAL) and postnatal DOM-treated (PDT) tissue during the various acute excitatory perfusion protocols. Asterisks denote significant differences from the appropriate control group ($p<0.05$), while error bars indicate SEM.

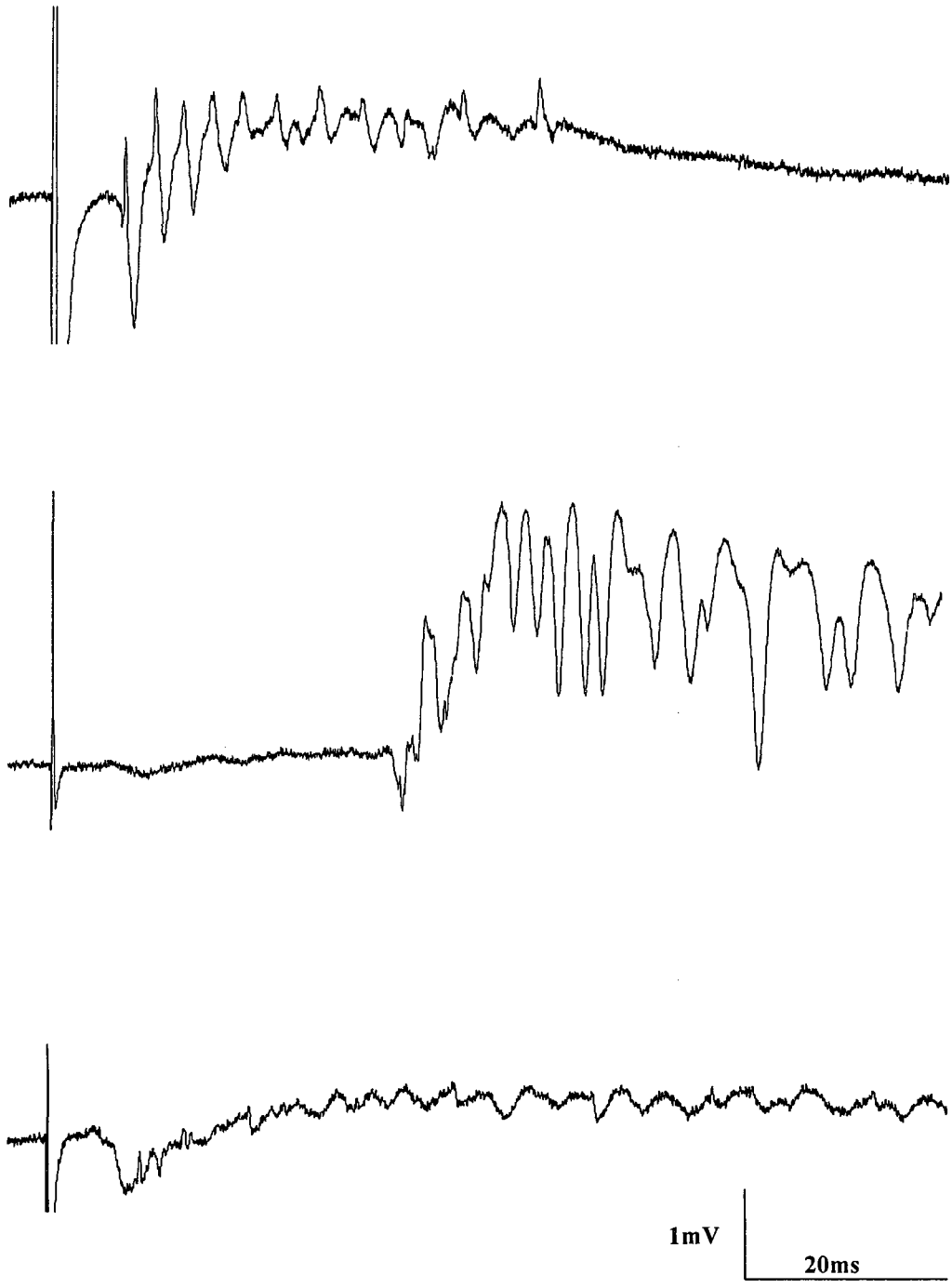

Figure 6.9. Representative images of various seizure-like responses to 0.5μA stimulation in the perforant path during 15 minute perfusion with $0Mg^{++}$ aCSF during *in vitro* recordings in hippocampal area CA3.

experienced more consistent seizure response during the $0Mg^{++}$ treatment than controls ($U = 36.5$, $Z = -2.126$, $p = 0.034$).

6.4 Discussion

There were three main questions addressed in this study. The first was whether postnatal DOM administration altered baseline DG-mediated information transfer to the HC proper in adulthood. The second was to assess the effects of acute DOM perfusion on DG performance and CA3 response in both PDT and control tissue. And finally, DG function and CA3 reactivity to hyperexcitable conditions through NMDA receptor activation was evaluated in each group using a low Mg^{++} aCSF solution.

To measure possible differences in baseline activity, I/O responses to electrical stimulation from the perforant path were assessed in the ventral DG, hilus, and hippocampal area CA3, and no differences were seen between groups in any region measured (Table 6.1, pg 164). This result is not surprising, as a number of previous *in vitro* studies have found no change under baseline conditions when investigating DG-CA3 activity in chronically epileptic tissue from KA- or pilocarpine-induced SE rats (e.g. Ang *et al.*, 2006; Pathak *et al.*, 2007). A similar lack of effect has been noted in studies for area CA1 as well (El-Hassar *et al.*, 2007), with an equivalent pattern of early hyperexcitability followed by a reduction in network output in later (chronic) stages. In humans with TLE, this phenomenon has been attributed to MFS, since tissue with hippocampal sclerosis (which others have shown to be associated with MFS) has been found to be inhibitory after the initial phase of epileptogenesis (Swanson *et al.*, 1998). In the current study, rats were treated during early postnatal development (PND8-14)

and then left until at least PND150 before testing, thus they were well past any initial stages for seizure genesis and also within the time period when MFS has been previously demonstrated to be present in this model (Bernard *et al.*, 2007). Additionally, it is well known that activity in EC, DG and HC proper decline with age (for review, see Gloveli *et al.*, 1998), making it more difficult to assess these regions. Therefore, to eliminate age as a factor, and to target the early phase of possible hyperexcitability seen in other models (Ang *et al.*, 2006; El-Hassar *et al.*, 2007; Pathak *et al.*, 2007), *in vitro* studies at earlier time points (e.g. PND15) should be conducted. The time of initiation of this proposed study may be crucial, since investigations using SE models have shown that, in adult rats, it is the first week following seizure induction that displays the most alteration in DG function (Pathak *et al.*, 2007). For the developmental model used in the current study, which produces no observable seizure during administration of a convulsant compound, this translates into the week starting at PND15. This earliest start point is doubly indicated, as a previous unpublished investigation of fEPSP and population spike activity in area CA1 in the NIS-L rat model following Schaffer collateral pathway stimulation has reported no change in activity in this hippocampal region for animals between PND28-90 (McLeod, 2007).

Interestingly, while baseline DG-CA3 measures in the current study were not found to be altered at this age by treatment, there was a main effect for sex noted, with females showing an increase in fIPSP peak (Figure 6.1A and B, pg 165) as well as a longer response duration in both DG and hilar regions, demonstrated through increased rise and decay times. And while there was no difference in peak fIPSP response in CA3, there was an increase in both rise and decay time for females in this region as well. Although

a full discussion of these intriguing differences is beyond the scope of this thesis, these results do raise questions regarding the possible physiological consequences of the noted changes, and highlight the importance of including both males and females in any study conducted to address issues affecting the population at large.

The second question addressed in this study involved using the same basic paradigm (PP stimulation with responses measured in DG, hilus, and CA3) during acute DOM perfusion to challenge the hippocampal network, allowing for an evaluation of responses obtained in the presence of this highly excitatory (and in the case of the PDT tissue, previously administered) compound. Through subtraction of baseline ('before') I/O responses from results during and after acute treatment, an assessment of alterations was acquired throughout perfusion and washout periods in area CA3, as well as following the complete exposure protocol (drug perfusion and washout) in the DG and hilar regions. Two concentrations of DOM were used in this study (100nm and 250nM), based on previously reported *in vitro* literature (Debonnel *et al.*, 1990; Sari and Kerr, 2001) as well as through pilot investigations in our lab.

Results from the 100nM DOM perfusion showed no statistically significant changes from baseline response (Table 6.2, pg 168). Interestingly, however, in the DG it was noted that animals in the PDT group (NIS-L rats) tended to show responses following acute 100nM DOM exposure that were faster, shorter, and less inhibitory than responses during baseline conditions, while controls displayed a more slowly occurring, prolonged and heightened inhibitory response (Figure 6.3, pg 169). Since this is the region that is responsible for blocking or 'gating' activity through to the HC proper, decreased

inhibitory potential in this region (as seen in PDT tissue) may indicate an increased occurrence of information passage, while control tissue displays an opposite, increased inhibitory effect. Interestingly, however, there was no difference noted between the groups for changes from baseline measures during the 250nM DOM perfusion. Instead, changes were now revealed in area CA3, with controls showing decreases in fIPSP amplitude (Figures 6.4, pg 171) and duration (Figure 6.5, pg 172, and Figure 6.6, pg174) compared to baseline measures, while PDT tissue displayed no alteration from the previous response.

This tendency for control slices to show decreased inhibition in response to DOM is in line with results reported by Sari and Kerr (2001), who found a concentration-dependent increase in excitatory *in vitro* response to Schaffer collateral stimulation of area CA1 during short-term DOM exposure. The same group has also reported a tolerance effect in CA1 for slices that were exposed to DOM, washed for 30-50 minutes, then re-exposed to DOM at concentrations either lower than, equivalent to, or higher than the original exposure (Kerr *et al.*, 2002). Intriguingly, while slices in that study initially responded to DOM in an hyperexcitable fashion, the second application typically produced only small alterations (with the notable exception of the lowest (50nM) concentration, which showed *increased* response to subsequent DOM), a phenomenon that the authors suggest could be attributed to an induced tolerance. The results seen in the current study appear to demonstrate a comparable effect, whereby tissue from rats that have received DOM postnatally displays an apparent tolerance to subsequent DOM exposure compared to control tissue (see Figures 6.4-6.6, pgs 171, 172 and 174). However, while the maintenance of inhibitory balance in hippocampal area CA3 in the

PDT tissue during 250nM DOM perfusion appears to be similar to the tolerance effect noted in previous reports (Kerr *et al.*, 2002), whether it is attributable to an altered DG 'gating' function remains unclear. In the study by Kerr and colleagues (2002), CA3 connections were severed and stimulation was applied to the Schaffer collaterals, indicating that a local alteration was responsible for the tolerance effect, perhaps (as the authors suggest) through a DOM-responsive G-protein-dependent signaling mechanism (see Figure 1.3, pg 11). It is possible that the results seen in the current work are attributable to a similar mechanism, and not to altered DG gating. To further elucidate this question, studies of DG-CA3 function using GABAergic antagonists to 'unmask' the area should be conducted, with results both without (to provide a 'baseline' response in the absence of inhibitory control) and with DOM present (to assess tolerance issues) compared. Nevertheless, whatever the mechanism, the responses seen in PDT tissue in the current study indicate that the postnatal DOM treatment has produced a permanent functional alteration in these rats.

The progressive nature of the alterations reported in this study, with the lower concentration of DOM resulting in DG changes, while the higher DOM concentration affected CA3 responses, is in agreement with previous *in vivo* studies in gerbils showing that increasing stimulation is required for activation of each successive region in the EC-DG-CA3-CA1 loop (Bartesaghi *et al.*, 1995). As well, with both low and high concentration DOM perfusion, there were also small but consistent sex-dependent alterations that often involved differences in female responses to DOM's effects, again reinforcing the necessity for studies that focus on possible male/female response variations when assessing any given manipulation or treatment.

Similar to the effects seen in fIPSP and response duration, latency to population spike activity was also affected by DOM concentration. These measures appear to be in agreement, with the tendency toward faster, less inhibitory potential response in the PDT tissue during 100nM DOM perfusion (Figure 6.3, pg 169) reflected in a shorter latency to the first PSp (Figure 6.8, pg 179), while during 250nM DOM, the effect reversed, and controls showed more excitation in CA3 (Figures 6.4 (pg 171), 6.5 (pg 172), and 6.6, (pg 174)). It is interesting to note that excitation in CA3, particularly in response to pathological conditions, has been hypothesized to be a protective response utilized by an overwhelmed system. Under normal conditions, the dominant response in CA3 is an inhibitory potential (Scharfman, 1993). However, through a CA3 'backprojection' to hilar interneurons, which in turn inhibit granule cells, excitatory activity in area CA3 in response to excessive excitation may actually signal an attempt by pyramidal neurons to stop additional input (for review, see Scharfman, 2007). If the results from the current study are assessed in this way, it could be suggested that the decrease in inhibition for control tissue at 250nM DOM may be indicative of an attempt to activate this protective pathway. To investigate this possibility, recording electrodes placed in both CA3 and the hilar region of the DG would be necessary, to provide simultaneous field responses during DOM perfusion.

The third and final question addressed in this study assessed NMDAR involvement in PDT and control tissue response to the stimulation protocol using a low Mg^{++} aCSF perfusion. While there was no question that this acute exposure was highly excitatory, the removal of the Mg^{++} block from hippocampal NMDA receptors did not result in any alteration between groups for fIPSP response, rise or decay measures, or PSp latency,

indicating that NMDAR function has not been altered in the PDT group. In addition, all groups had an equivalent tendency to display 'epileptiform' activity (Figure 6.9, pg 180) in response to stimulation during acute low Mg^{++} perfusion. Indeed, the only difference noted during this exposure was an increased likelihood for PDT tissue to show a continual and consistent "convulsive-like" activity following stimulation (i.e. every stimulation pulse, $p = 0.034$) along with an increased chance of a shift in direction (fIPSP to fEPSP) indicating that, once activated, the PDT network appeared to be more intensely responsive than that of controls (Bartesaghi *et al.*, 1995). However, while these results suggest that reverberatory activity in the HC of PDT animals has been somehow increased (Stoop and Pralong, 2000), it does not address how this increase in excitation has occurred.

Overall, the current study has presented further evidence of subtle neurological changes in excitatory/inhibitory balance in rats exposed postnatally to low-dose DOM. Previous work in the NIS-L model has shown alterations in many neurophysiological measures, including MFS (Bernard *et al.*, 2007) and interneuronal subpopulations (Chapter 5). However, as reported for many other seizure models during *in vitro* investigations, reorganized circuitry may provide the substrate for dysfunction, but an additional stressor is often still required to reveal underlying alterations (for review, see Sutula and Dudek, 2007; Turner *et al.*, 1998). Consequently, while electrophysiological examination of tissue from PDT and control rats revealed no difference under baseline conditions between the groups in the present work, a concentration-dependent change in inhibitory activity in response to acute DOM perfusion was seen, manifesting as a reduced inhibitory potential (compared to baseline) in the DG for the PDT group

following 100nM DOM exposure and washout, and a tolerance effect in area CA3 during 250nM DOM perfusion. In addition, PDT tissue appeared to exhibit a more intense (persistent) CA3 reaction once inhibitory control was actually lost, as seen during the $0Mg^{++}$ protocol. However, there was no conclusive evidence found implicating altered DG gating function in any of these changes. Further research will be necessary to address several issues raised in this investigation, including (1) the use of longer term low Mg++ exposure (e.g. Behr *et al.*, 1996; Walther *et al.*, 1986) to study possible alterations in spontaneous seizure generation (versus the evoked paradigm used in the current work); (2) evaluation of PDT tissue in the absence of inhibitory 'masking' effects (e.g. Behr *et al.*, 1998; Lynch and Sutula, 2000; Patrylo and Dudek, 1998) with and without DOM application to assess underlying changes in excitatory c ircuitry, and (3) recordings using multiple electrodes for assessing simultaneous effects in different DG-CA3 regions to provide a more comprehensive picture of network activity.

7.0 EFFECTS OF GLUTAMATE RECEPTOR ANTAGONISM DURING EARLY POSTNATAL DEVELOPMENT ON MOSSY FIBRE SPROUTING IN THE ADULT HIPPOCAMPUS

7.1 Introduction

The first few weeks of postnatal development in the rat are critical for neuronal growth and differentiation. In particular, this period is crucial for the shaping and refinement of excitatory and inhibitory networks in the brain, a process that is highly dependent upon appropriate and timely cellular signaling mediated through the excitatory amino acid Glu and the early-excitatory and later-inhibitory roles of GABA neurotransmission (for review, see Ben-Ari *et al.*, 2007). While both Glu and GABA must work in concert to produce a viable network, the focus of this chapter is primarily on the role of Glu signaling during developmental maturation.

The timing of specific receptor development is an important factor for appropriate network organization, and it is now well known that neuronal maturation follows a highly regulated and complex developmental regimen (e.g. Chudotvorova *et al.*, 2005; Tyzio *et al.*, 1999; for review, see Ben-Ari *et al.*, 2004; Ben-Ari, 2006a; McDonald and Johnston, 1990; Molnar *et al.*, 2002). In the earliest stages, GABA and NMDA receptors orchestrate basic developmental processes such as cellular growth and migration (Ben-Ari, 2006a). It is not until the end of the second postnatal week that AMPA receptors become fully functional, concurrent with GABA relinquishing its excitatory role to assume a mature inhibitory function (Khalilov *et al.*, 2005). At this stage, there is a massive over-expression of ionotropic Glu receptors present (for review, see Lujan *et al.*, 2005; McDonald and Johnston, 1990), as well as an excessive proliferation of axonal growth that, during the succeeding weeks, must be selectively pruned to achieve adult levels of functioning (Luthi *et al.*, 2001).

As might be anticipated during such a sensitive developmental period, insults to an immature system can potentially lead to long-term structural and functional alterations that may manifest later in life through a variety of neurologic disorders, and even subtle insults may have far-reaching consequences. Domoic acid, a naturally-occurring excitatory Glu agonist, has been shown to result in long-term alterations in behavior (Doucette *et al.*, 2004), hippocampal morphology (Bernard *et al.*, 2007) and excitatory function (see Chapters 2 and 3) when administered to rats in low doses during the second week of postnatal life (the NIS-L rat model), a pathology very similar to temporal lobe (complex partial) epilepsy. Mechanisms underlying the alterations seen in this model are as yet unknown, although DOM does display a high affinity for KARs, in particular, those containing GluK5 and GluK6 subunits (Clarke and Collingridge, 2004; Debonnel *et al.*, 1990; Lomeli *et al.*, 1992; Sommer *et al.*, 1992; Tasker *et al.*, 1996; Verdoorn *et al.*, 1994). However, DOM has affinity for AMPA and NMDA receptors as well (for review, see Hampson and Manalo, 1998; Pulido, 2008). Since all these Glu receptors are over-abundantly expressed during the time frame of DOM administration in this model (see Lujan *et al.*, 2005; McDonald and Johnston, 1990 for review), the resultant long-lasting alterations may be primarily mediated through any one of the 3 major sub-families. In addition, all are ubiquitously present throughout the HC, a limbic system structure that has long been implicated in TLE pathology.

One way to determine the particular receptor pathway involved in producing long-term alterations is to selectively antagonize the receptor in question and evaluate the consequences. A commonly used measure of hippocampal reorganization in response to excitatory activity is MFS in the IML of the DG as well as in the SL and/or SO of area

CA3 in the HC proper (e.g. Nadler, 2003). Excessive sprouting in any of these areas is considered to be an indicator of possible pathological activity (Sutula *et al.*, 1988), and is often visualized and quantified using Timm staining, a method that silver-labels unbound zinc contained within mossy fibre synaptic boutons (Slomianka, 1992).

The purpose of the current study was to investigate the underlying receptor pathway(s) responsible for mediating long-term alterations seen in adult rats postnatally treated with low-dose DOM. Using a pharmacological approach, I sought to antagonize DOM's effects through blocking either the NMDA or AMPA receptor concurrently with DOM administration in rat pups and, in adulthood, measure MFS density, since aberrant sprouting has been previously identified as one of the defining features of this model. Additionally, possible antagonist-only effects were investigated, since to date, most of the work examining the effects of excitatory blockade in developing systems has been performed in culture, with very few studies looking at consequences *in vivo*.

7.2 Materials and Methods

7.2.1 Experimental Animals

Offspring born in-house from untimed Sprague-Dawley rats (Charles River, Quebec) were culled within 24 hours of birth to 10 pups per litter (5-♀ and 5-♂ where possible). From postnatal day 8-14, pups were weighed and given daily injections (5 ml/kg, s.c. each) of either DOM (20μg/kg) plus SAL, the competitive NMDA receptor antagonist CPP (150μg/kg) plus either SAL or DOM, 600μg/kg or 1mg/kg of the competitive AMPA antagonist NBQX plus either SAL or DOM, or SAL plus SAL. A

comprehensive summary of the treatment groups can be found in Table 7.1 (pg 194). All 8 groups were required to provide both an evaluation of the antagonist effects on DOM treatment, as well as to allow for assessment of possible effects of the antagonist treatment alone. Domoic acid was supplied by BioVectra dcl (Prince Edward Island, Canada) while CPP and NBQX were obtained through Tocris Cookson Inc (Missouri, USA). The CPP dose was chosen based on previous work in our lab using this compound in neonates (Tasker *et al.*, 2005), while the NBQX doses were estimated as a fraction of pharmacologically relevant doses used for studies in adult rats (Hlinak and Krejci, 1994; Lojkova *et al.*, 2006). Following weaning on PND21, rats were group housed (2-3 per cage) under a 12h light-dark cycle (lights on at 06:00h) and were left undisturbed, except for normal maintenance, until PND90. Room temperature was maintained at 21±2°C. Rodent chow (5001 Ralston Purina) and tap water were available *ad libitum*. Studies were carried out under approval from the University of Prince Edward Island Animal Care Committee, and in accordance with the Canadian Council of Animal Care guidelines.

7.2.2 Tissue preparation and Timm staining

Timm staining was used to provide visualization and quantification of the mossy fibre pathway in the HC of rats from the various groups. To this end, 68 adult (PND90) rats from the 8 groups described in Table 7.1 (pg 194) were euthanized with CO_2 and immediately decapitated. Brains were hemisected and the left hemisphere was submerged in a 0.4% sodium sulphide solution for 20 minutes (Sperber *et al.*, 1991), then placed in 50ml of 30% (w/v) sucrose in 10% buffered neutral formalin (BNF)

Table 7.1. Summary of treatment groups and number of rats included in each.

Group	Description (2 injections/day; 5ml/kg (s.c.) each for total volume 10ml/kg)		Number of rats
DOM	20μg/kg	domoic acid plus saline	n= 8; 4♂ 4♀
DCPP	150μg/kg	CPP ((RS)-3-((+/–)-2-carboxypiperazin-4-yl)-propyl-1-phosphonic acid) plus DOM (20μg/kg)	n= 9; 5♂ 4♀
SCPP	150μg/kg	CPP plus saline	n=10; 5♂5♀
DNBQX-6	600μg/kg	NBQX (2,3-Dioxo-6-nitro-1,2,3,4-tetrahyrobenzo[f]quinoxaline-7-sulfonamide disodium salt) plus DOM	n= 6; 3♂ 3♀
SNBQX-6	600μg/kg	NBQX plus saline	n= 6; 3♂ 3♀
DNBQX-1	1mg/kg	NBQX plus DOM	n= 9; 4♂ 5♀
SNBQX-1	1mg/kg	NBQX plus saline	n=10; 5♂ 5♀
SAL		saline only	n=10; 5♂ 5♀

for 36 hours. Tissue was frozen in Cryo-Matrix using liquid nitrogen and stored at -80°C until sectioning with a cryostat.

All sections were cut from the left hemisphere at 20μm using a protocol designed in a previous study (see methods, Chapter 5) to provide optimal hippocampal access at 3 levels: dorsal (cut coronally at -3mm Bregma), mid (cut horizontally 4mm ventral from top of brain), and ventral (cut horizontally 900μm ventral from mid level), and mounted on 0.5% gelatin-coated slides. Tissue from all treatment groups were run simultaneously in the Timm staining process (Bernard *et al.*, 2007; see methods, Chapter 4) by an experimenter blind to condition to ensure consistent processing.

7.2.3 Data acquisition

Mossy fibre images were scored experimenter blind with Image J software (National Institutes of Health) using images obtained through a Zeiss Axioplan2 Imaging microscope (2.5x objective) equipped with an AxioCam HR digital camera and utilizing the density analysis method described by Bernard et al (2007). The nine areas of the inner molecular layer of the DG, and six in both SL and SO of CA3 that were assessed for the current study have been previously described (see Chapter 4, Figure 4.2, pg 127), along with the locations of the corresponding background measurements.

7.2.4 Data analysis

Data were analyzed using two-way (SEX x COND) ANOVA, or one-way ANOVAs or

t-tests as required to assess any interactions. Tukey's post-hoc was used to evaluate COND effects for multiple comparison groups. All data were analyzed in SPSS (v.15 SPSS Inc., Chicago IL). Results are expressed as the mean ± SEM, and the criterion for statistical significance was set at $p \leq 0.05$.

7.3 Results

It has been previously noted (Doucette *et al.*, 2007; Galanopoulou, 2008b; Kyrozis *et al.*, 2006) that developmental manipulations do not always produce equivalent effects in male and female rats, a phenomenon that has been attributed to differing maturational rates. Indeed, Kyrozis and colleagues (2006) have reported that CNS maturation in females may occur as much as one week prior to that in males (for review, see McCutcheon and Marinelli, 2009). In the current study, this developmental variance produced a differing sensitivity to receptor agonism and antagonism for MFS in area CA3 of the HC, seen through two-way ANOVAs as multiple sex by condition interactions. Subsequently, this region was analyzed independently for each sex. The mean results for all groups (separated for sex) can be found in Table 7.2, pg 197-98, and an overall summary is provided in Table 7.3, pg 199.

As reported in previous investigations of the NIS-L rat model (Bernard *et al.*, 2007; Doucette *et al.*, 2004), Timm staining revealed statistically significant increases in MFS for DOM-treated animals. In the IML, increases were seen at both mid [$F_{(1,17)} = 5.020$, $p = 0.042$] and ventral levels [$F_{(1,17)} = 6.320$, $p = 0.025$] (Figure 7.1, pg 200). In CA3,

Table 7.2. Summary of mean MFS density results (±SEM) from dentate gyrus, stratum lucidum, and stratum oriens for all treatment groups and separated for sex.

Dentate Gyrus (IML):

Treatment	Dorsal (mean ±SEM)	Mid (mean ±SEM)	Ventral (mean ±SEM)
Males:			
SAL	3.00 (± 1.2)	4.37 (± 0.8)	4.52 (± 0.8)
DOM	4.32 (± 1.0)	7.08 (± 1.2)	6.83 (± 0.7)
SCPP	0.28 (± 0.6)	9.14 (± 5.4)	9.48 (± 4.7)
DCPP	-1.08 (± 1.2)	5.40 (± 3.0)	10.14 (± 4.3)
SNBQX-6	-1.11 (± 1.7)	-1.87 (± 0.9)	-0.08 (± 1.1)
SNBQX-1	1.18 (± 1.3)	-1.11 (± 1.4)	2.14 (± 1.2)
DNBQX-6	0.55 (± 1.1)	-2.50 (± 2.7)	-0.77 (± 4.9)
DNBQX-1	0.72 (± 1.1)	4.72 (± 2.1)	5.89 (± 3.8)
Females:			
SAL	1.16 (± 1.0)	3.39 (± 0.8)	1.93 (± 1.2)
DOM	3.37 (± 0.3)	5.59 (± 0.5)	5.76 (± 1.3)
SCPP	1.99 (± 0.5)	6.38 (± 0.8)	10.12 (± 2.0)
DCPP	3.08 (± 1.1)	7.23 (± 3.3)	18.51 (± 4.8)
SNBQX-6	-1.79 (± 1.7)	-1.04 (± 1.8)	-0.70 (± 1.5)
SNBQX-1	-1.18 (± 0.9)	1.40 (± 1.3)	0.37 (± 1.1)
DNBQX-6	-1.83 (± 1.3)	-1.02 (± 2.6)	-0.23 (± 4.3)
DNBQX-1	-0.12 (± 1.0)	1.59 (± 2.0)	2.00 (± 3.6)
CA3 – Stratum Lucidum:			
Males:			
SAL	95.47 (± 6.4)	106.09 (± 5.1)	99.52 (± 6.5)
DOM	93.74 (± 4.3)	91.73 (± 5.2)	83.45 (± 5.5)
SCPP	85.02 (± 6.6)	82.45 (± 8.7)	83.41 (± 7.8)
DCPP	81.19 (±17.6)	79.51 (±17.8)	74.88 (±14.5)
SNBQX-6	68.98 (±13.4)	46.93 (± 6.9)	63.78 (± 9.7)
SNBQX-1	44.26 (±17.9)	53.99 (±22.6)	44.92 (±18.0)
DNBQX-6	88.07 (± 1.6)	86.35 (±40.8)	76.78 (±35.6)
DNBQX-1	74.50 (± 9.8)	68.87 (±13.8)	70.56 (± 9.9)
Females:			
SAL	50.89 (±14.9)	46.90 (± 9.7)	44.61 (±10.4)
DOM	82.00 (± 4.6)	86.85 (± 8.6)	84.01 (± 7.7)
SCPP	95.38 (± 4.2)	104.10 (± 8.5)	95.17 (± 6.7)
DCPP	87.48 (± 7.3)	98.05 (± 5.9)	89.87 (± 2.0)
SNBQX-6	21.12 (± 1.2)	23.00 (± 4.7)	19.91 (± 2.1)
SNBQX-1	51.16 (±22.3)	44.03 (±17.5)	47.41 (±17.3)
DNBQX-6	22.30 (± 5.1)	19.74 (± 3.3)	22.02 (± 4.2)
DNBQX-1	44.90 (±17.9)	39.45 (±15.2)	43.40 (±16.7)

Table 7.2. (continued)

CA3 – Stratum Oriens:

Treatment	Dorsal (mean ±SEM)	Mid (mean ±SEM)	Ventral (mean ±SEM)
Males:			
SAL	49.41 (± 6.3)	35.27 (± 4.9)	27.23 (± 3.0)
DOM	46.61 (± 4.4)	35.10 (± 1.1)	28.22 (± 3.3)
SCPP	37.51 (± 7.6)	29.35 (± 8.7)	20.97 (± 6.6)
DCPP	33.72 (± 7.1)	22.09 (± 9.3)	16.99 (± 6.8)
SNBQX-6	50.81 (± 6.9)	27.26 (± 9.0)	32.35 (± 6.8)
SNBQX-1	17.97 (± 9.5)	16.79 (± 9.5)	12.29 (± 7.7)
DNBQX-6	63.66 (± 1.6)	32.18 (±18.3)	17.30 (±12.4)
DNBQX-1	35.36 (± 4.7)	31.46 (± 3.9)	20.89 (± 3.9)
Females:			
SAL	21.10 (± 8.4)	12.26 (± 3.1)	8.21 (± 1.2)
DOM	35.43 (±10.1)	26.17 (± 3.4)	20.93 (± 2.3)
SCPP	33.07 (± 6.4)	30.52 (± 4.1)	21.57 (± 5.9)
DCPP	33.56 (± 4.0)	30.79 (± 6.0)	21.15 (± 2.8)
SNBQX-6	2.56 (± 0.6)	0.96 (± 2.1)	0.44 (± 0.6)
SNBQX-1	28.94 (±15.5)	16.89 (±11.0)	13.27 (± 6.7)
DNBQX-6	6.23 (± 1.6)	1.13 (± 2.1)	2.97 (± 2.2)
DNBQX-1	26.13 (±13.0)	10.73 (± 7.2)	9.92 (± 4.9)

Table 7.3. Compilation of mossy fibre results from the dentate gyrus, stratum lucidum, and stratum oriens for all treatment groups.

Comparison	Dentate Gyrus	CA3 SL	CA3 SO
DOM vs SAL	DOM ↑ MFS	DOM ♀ ↑ MFS No change in ♂	DOM ♀ ↑ MFS No change in ♂
DOM vs DCPP	No difference	No difference	No difference
DOM vs DNBQX	DNBQX ↓ MFS (esp 600µg/kg)	DNBQX ♀ ↓ MFS (600µg/kg) DNBQX ♂ ↓ MFS (1mg/kg) but not sig	DNBQX ♀ ↓ MFS (600µg/kg) DNBQX ♂ no difference
SAL vs SCPP	CPP ↑ MFS	SCPP ♀ ↑ MFS No change in ♂	SCPP ♀ ↑ MFS No change in ♂
SAL vs SNBQX	NBQX ↓ MFS	SNBQX ♂ ↓ MFS (1 mg/kg) SNBQX ♀ ↓ MFS (600µg/kg) but not sig	SNBQX ♂ ↓ MFS (1 mg/kg) SNBQX ♀ ↓ MFS (600µg/kg) but not sig

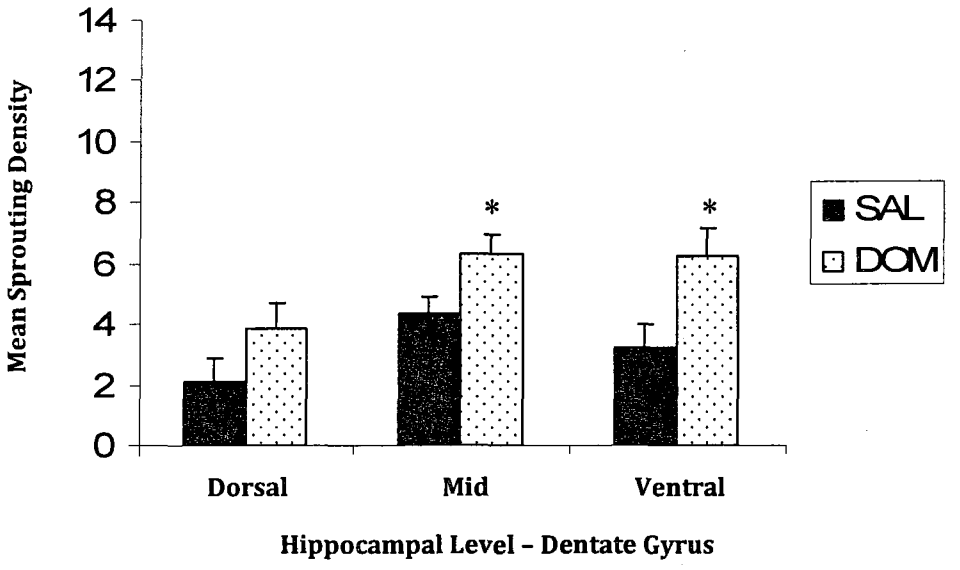

Figure 7.1. Mean mossy fibre sprouting density scores for all DOM-treated and control rats in the inner molecular layer of the dentate gyrus at dorsal, mid, and ventral levels. Asterisks denote a significant difference from the appropriate control group ($p<0.05$), and error bars indicate SEM.

DOM-treated females showed increased sprouting compared to their SAL counterparts at mid and ventral levels in both SL and SO regions (SL mid: [t(7) = 3.003, p = 0.020]; SL ventral: [t(7) = 2.904, p = 0.023]; SO mid: [t(7) = 3.041, p = 0.019]; SO ventral: [t(7) = 5.216, p = 0.001] (Figure 7.2, pg 202), while DOM-treated males exhibited no statistically significant differences for any level or region.

To test the long-term effects of blocking NMDA receptors early in development, as well as concurrent with postnatal DOM administration, we administered daily injections of either DOM (20μg/kg) plus SAL, CPP (150μg/kg) plus DOM (20μg/kg) or SAL, or 2 (5ml/kg volume) injections of SAL alone during PND8-14, and measured MFS density at three hippocampal levels (dorsal, mid, ventral) in both the DG and area CA3.

An assessment of antagonist effects compared to SAL controls revealed several interesting findings. In the DG, a two-way ANOVA showed no statistically significant difference at the dorsal or mid level between SCPP and SAL groups (p=0.259 and p=0.242 respectively), but at the ventral level, a main effect for condition was revealed [$F_{(1,19)} = 6.027$, p =0.026], with SCPP rats showing overall increased sprouting compared to controls (Figure 7.3, pg 203). In the HC proper, investigation of MFS in female rats also showed increases for sprouting in the SCPP group in the SL region at all levels (SL dorsal: [$t_{(4.6)} = 2.871$, p = 0.038]; SL mid: [$t_{(8)} = 4.438$, p = 0.002]; SL ventral: [$t_{(8)} = 4.096$, p = 0.003]), as well as in the mid SO [$t_{(8)} = 3.546$, p = 0.008], and with a strong tendency toward increases in the ventral SO [t(8) = 2.230, p = 0.056]. These results are presented graphically in Figure 7.4 (pg 204), while representative images of MFS group differences can be found in Figure 7.5 (pg 205). Evaluation of male groups

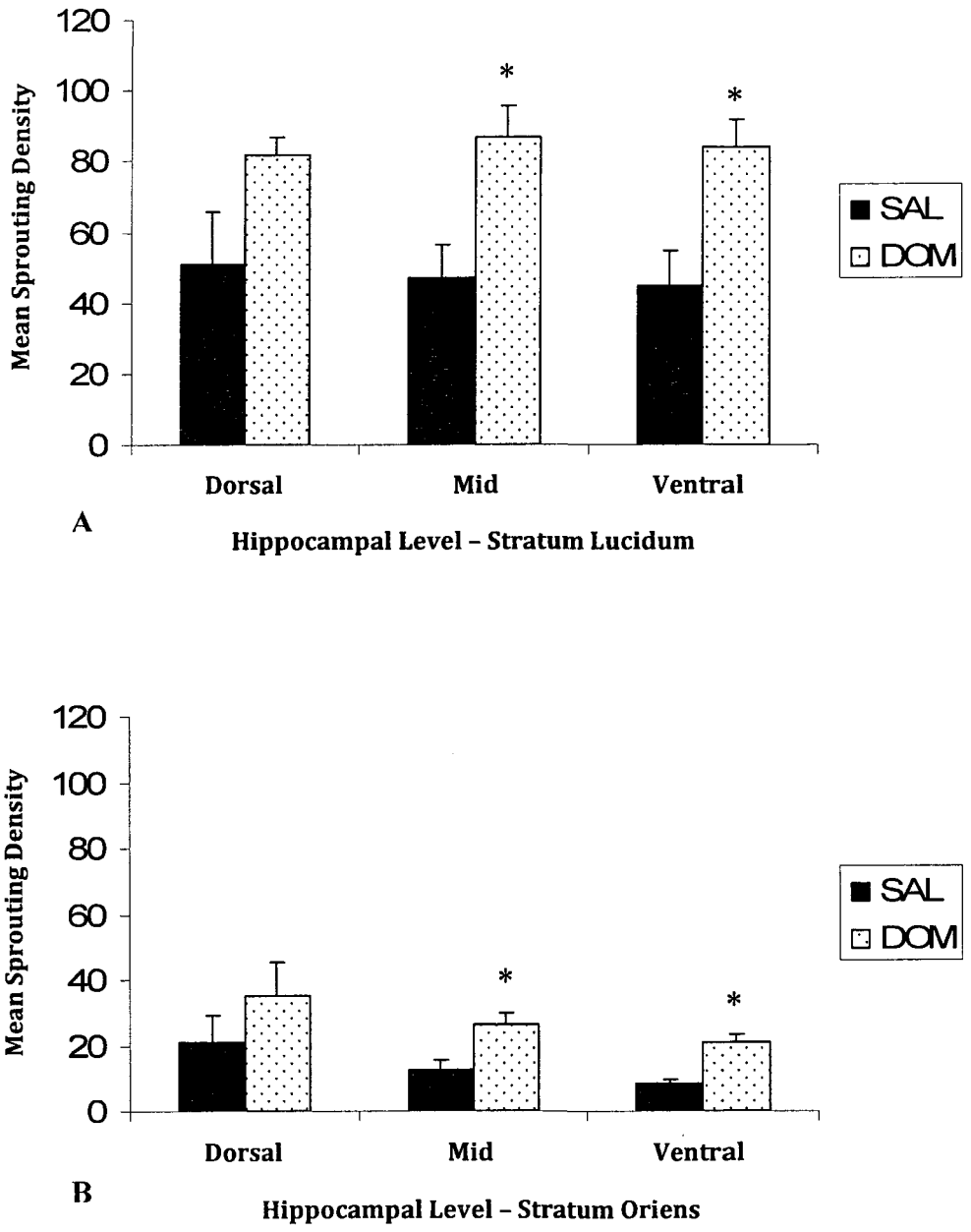

Figure 7.2. Mean mossy fibre sprouting density scores for female-only DOM-treated and control rats in area CA3 at dorsal, mid, and ventral levels. A) Stratum lucidum B) Stratum oriens. Asterisks denote a significant difference from the appropriate control group ($p<0.05$), and error bars indicate SEM.

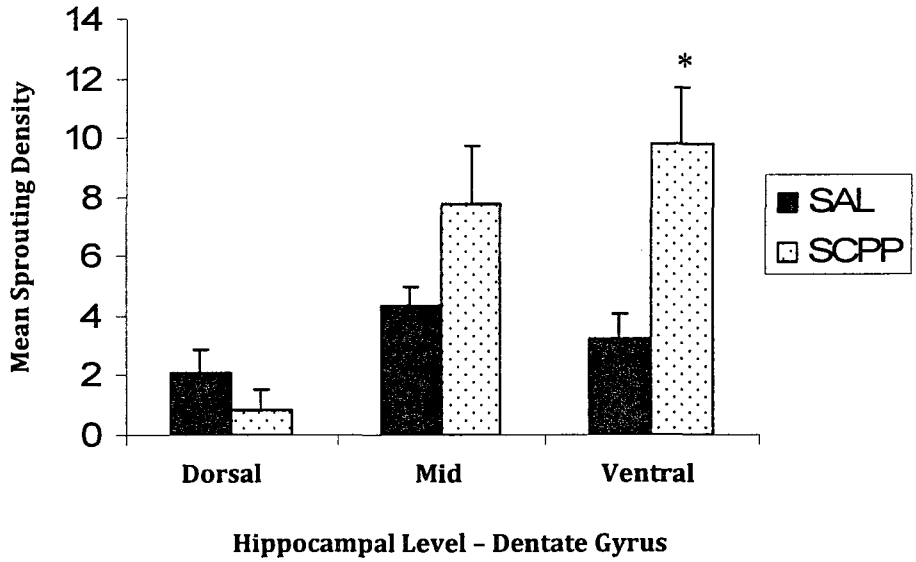

Figure 7.3. Mean mossy fibre sprouting density scores for all CPP-treated and control rats in the inner molecular layer of the dentate gyrus at dorsal, mid, and ventral levels. The asterisk denotes a significant difference from the appropriate control group ($p<0.05$), and error bars indicate SEM.

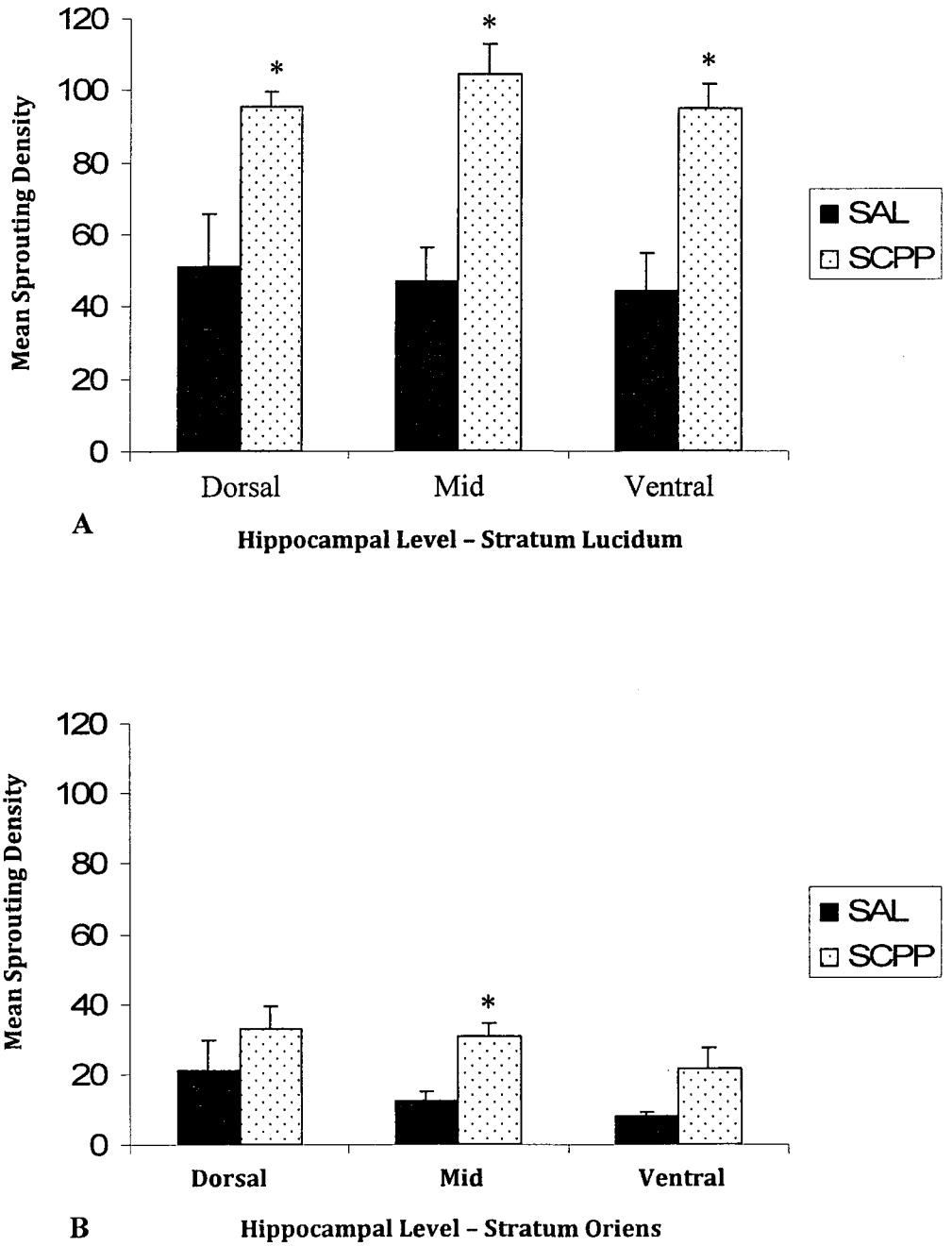

Figure 7.4. Mean mossy fibre sprouting density scores for female-only CPP-treated and control rats in area CA3 at dorsal, mid, and ventral levels. A) Stratum lucidum B) Stratum oriens. Asterisks denote a significant difference from the appropriate control group ($p<0.05$), and error bars indicate SEM.

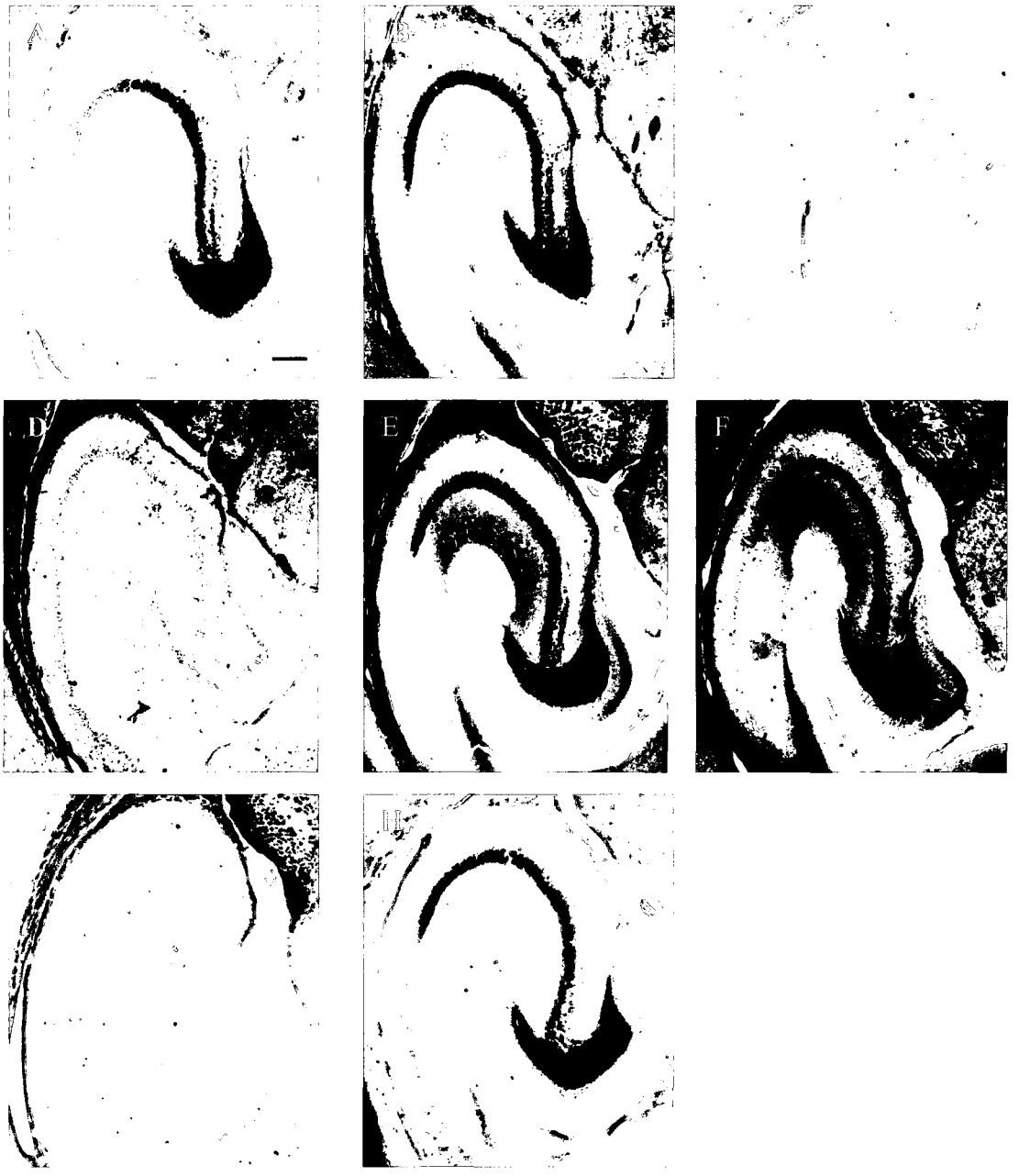

Figure 7.5. Representative images of mossy fibre sprouting for each treatment group in the ventral hippocampus. A) SAL B) DOM C) SNBQX-6 D) DNBQX-6 E) CPP F) DCPP G) SNBQX-1 H) DNBQX-1. (Scale bar = 200μm).

showed only one statistically significant difference in CA3 (mid SL), and interestingly, this was a *decrease* in sprouting for the SCPP group compared to controls [$t_{(8)} = -2.340$, $p = 0.047$]. No differences between the groups were found for males in any other area or level, although male SCPP rats did have consistently less sprouting at every level measured (see Table 7.2, pg 198).

Rats that received concurrent DOM and CPP showed no statistically significant differences from those that received DOM alone or CPP alone in any region or any level with one exception; the dorsal DG. In this region, further investigation into a sex by condition interaction revealed that DCPP males experienced decreased sprouting (similar to males in the SCPP group in area CA3) [$t_{(7)} = -3.326$, $p = 0.013$], while females showed no differences between groups.

The effect of developmental AMPA receptor blockade was investigated in this study through administration of 600μg/kg NBQX plus SAL or 1mg/kg NBQX plus SAL daily between PND8-14 and compared to SAL controls. In addition, DOM-treated rats were evaluated for differences from those receiving both DOM and one of the NBQX treatments.

In the DG, all animals in both NBQX groups displayed decreased Timm staining compared to SAL at the mid level [$F(2,25) = 7.849$, $p = 0.003$] (Tukey's post-hoc: SNBQX-6, $p = 0.005$; SNBQX-1, $p = 0.017$), with a strong tendency toward a decrease for NBQX-6 in the ventral region ($p=0.056$) (Figure 7.6, pg 207). In the HC proper, there was a condition effect in SL seen for males at mid [$F_{(2,12)} = 4.240$, $p = 0.046$]

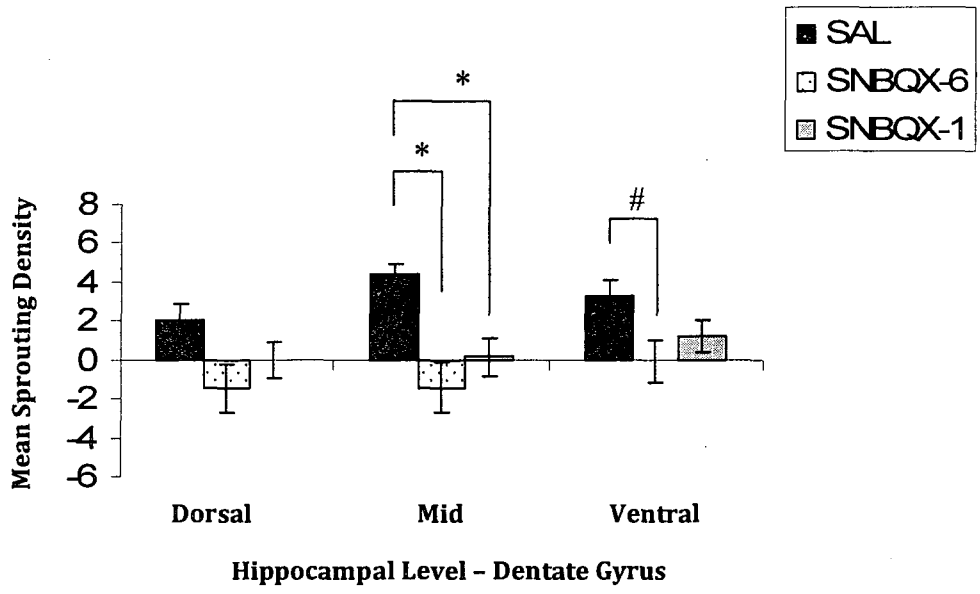

Figure 7.6. Mean mossy fibre sprouting density scores for all SNBQX-treated and control rats in the inner molecular layer of the dentate gyrus at dorsal, mid, and ventral levels. The asterisks denote a significant difference between the indicated groups ($p<0.05$), while the pound sign signifies a tendency ($p=0.056$) toward a decreased score. Error bars indicate SEM.

and ventral [$F_{(2,12)} = 4.821$, $p = 0.034$], with a tendency in the dorsal region ($p=0.054$). Tukey's post-hoc analysis of the noted differences showed a statistical decrease in MFS in the NBQX-1 group compared to SAL controls at the ventral level ($p = 0.029$), but no difference at the mid due to high variability (Figure 7.7A, pg 209). In SO, NBQX-1 again produced a decrease in male MFS compared to controls (Tukey's post-hoc; $p = 0.037$), but only at the dorsal level [$F_{(2,12)}$, = 5.449, $p = 0.025$] (Figure 7.7B, pg 209). It should be noted that, while NBQX-6 often decreased MFS in the female groups (Table 7.2, pg 198), the effect did not reach statistical significance compared to controls for any level or region of CA3.

Compared to DOM only animals, rats treated concurrently with both DOM and the AMPA antagonist NBQX showed a decrease in MFS as assessed through Timm staining. In the DG, both NBQX-6 and NBQX-1 reduced sprouting at the dorsal level [$F_{(2,22)} = 8.839$, $p = 0.002$] (Tukey's post hoc: NBQX-6, $p = 0.04$; NBQX-1, $p = 0.009$), while at the mid level, NBQX-6 was most effective [$F_{(2,23)} = 5.288$, $p = 0.016$] (Tukey's post hoc: NBQX-6, $p = 0.012$; NBQX-1, $p = 0.337$). No effect for treatment was noted in ventral IML due to high variability (Figure 7.8, pg 210). In CA3, DNBQX females showed decreased sprouting in the SL at all levels (dorsal: [$F_{(2,9)} = 4.273$, $p = 0.50$]; mid: [$F_{(2,9)} = 7.036$, $p = 0.014$]; ventral: [$F_{(2,9)} = 5.035$, $p = 0.035$]), as well as for mid [$F_{(2,9)} = 4.919$, $p = 0.036$] and ventral [$F_{(2,9)} = 4.642$, $p = 0.041$] SO. Post-hoc analysis revealed that, in all these cases, NBQX-6 was responsible for the noted sprouting decreases in these animals, while NBQX-1 had an effect only at the mid SL level (Figure 7.9, pg 211). In DOM-treated males, NBQX had no statistically significant effect in the HC proper at any dose, although means in the DNBQX-1 group tended to be less than

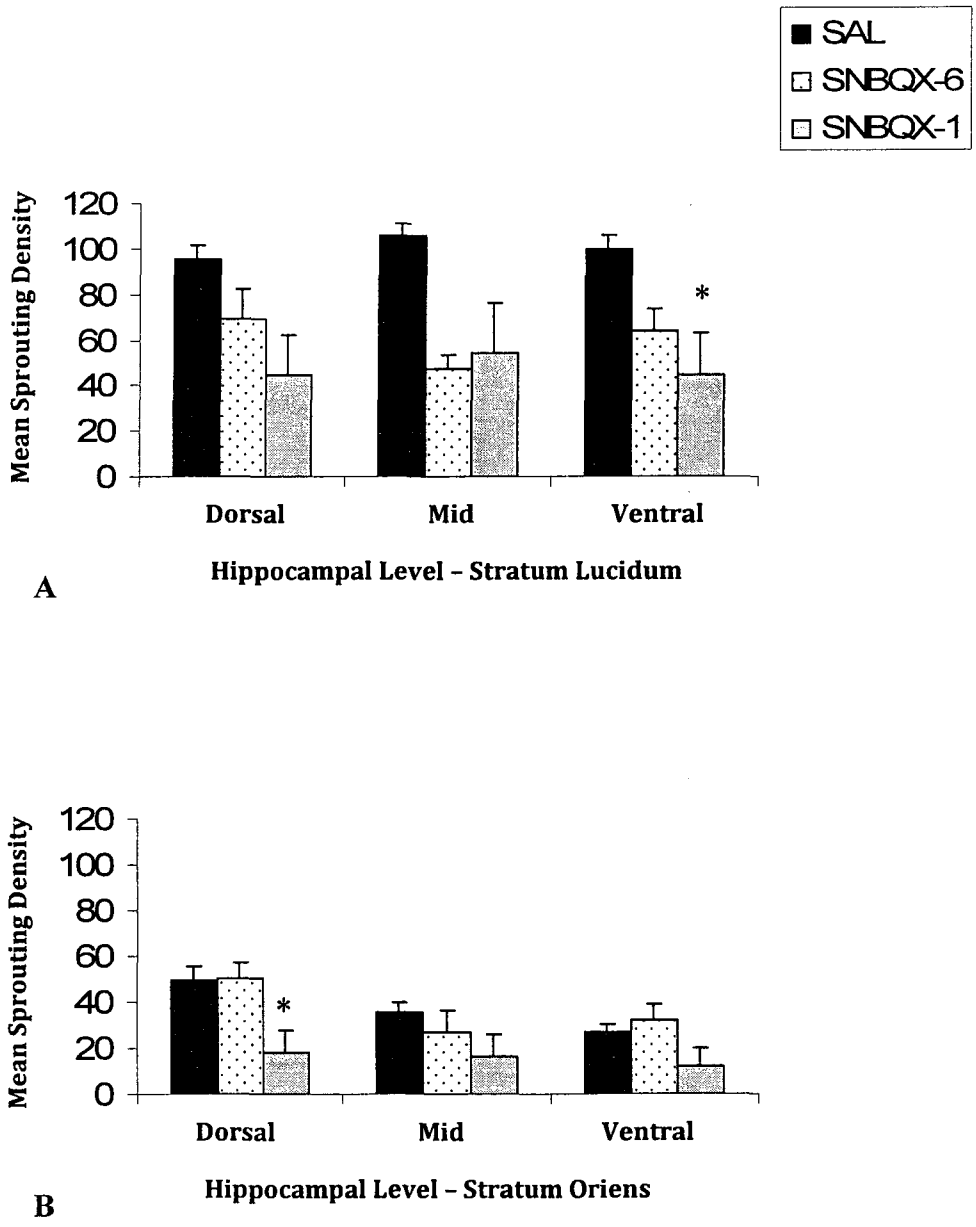

Figure 7.7. Mean mossy fibre sprouting density scores for male-only SNBQX-treated and control rats in area CA3 at dorsal, mid, and ventral levels. A) Stratum lucidum B) Stratum oriens. Asterisks denote a significant difference from the appropriate SAL control group ($p<0.05$), and error bars indicate SEM.

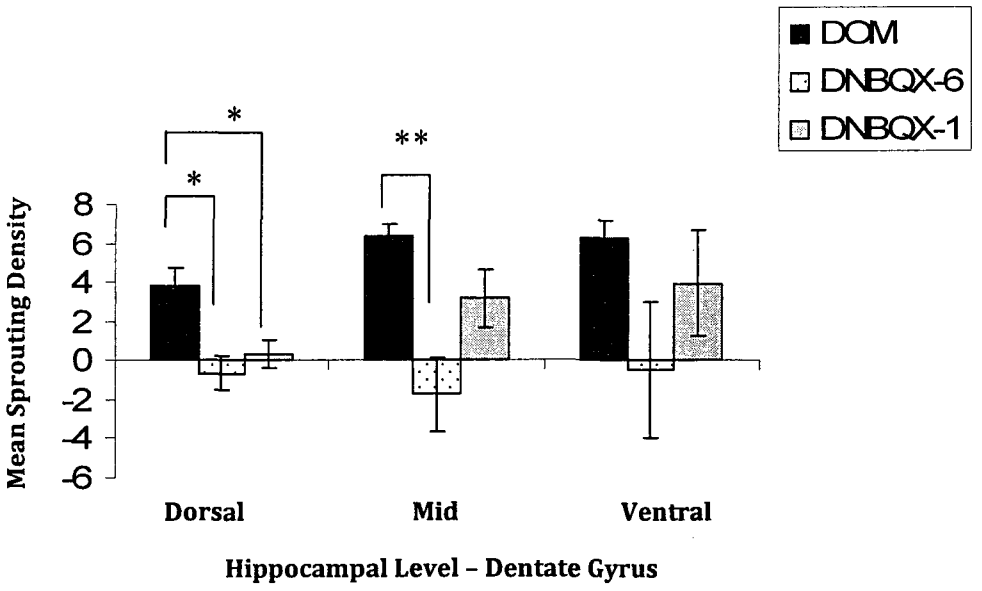

Figure 7.8. Mean mossy fibre sprouting density scores for all DNBQX-treated and DOM control rats in the inner molecular layer of the dentate gyrus at dorsal, mid, and ventral levels. The asterisks denote a significant difference between the indicated groups ($p<0.05$). Error bars show SEM.

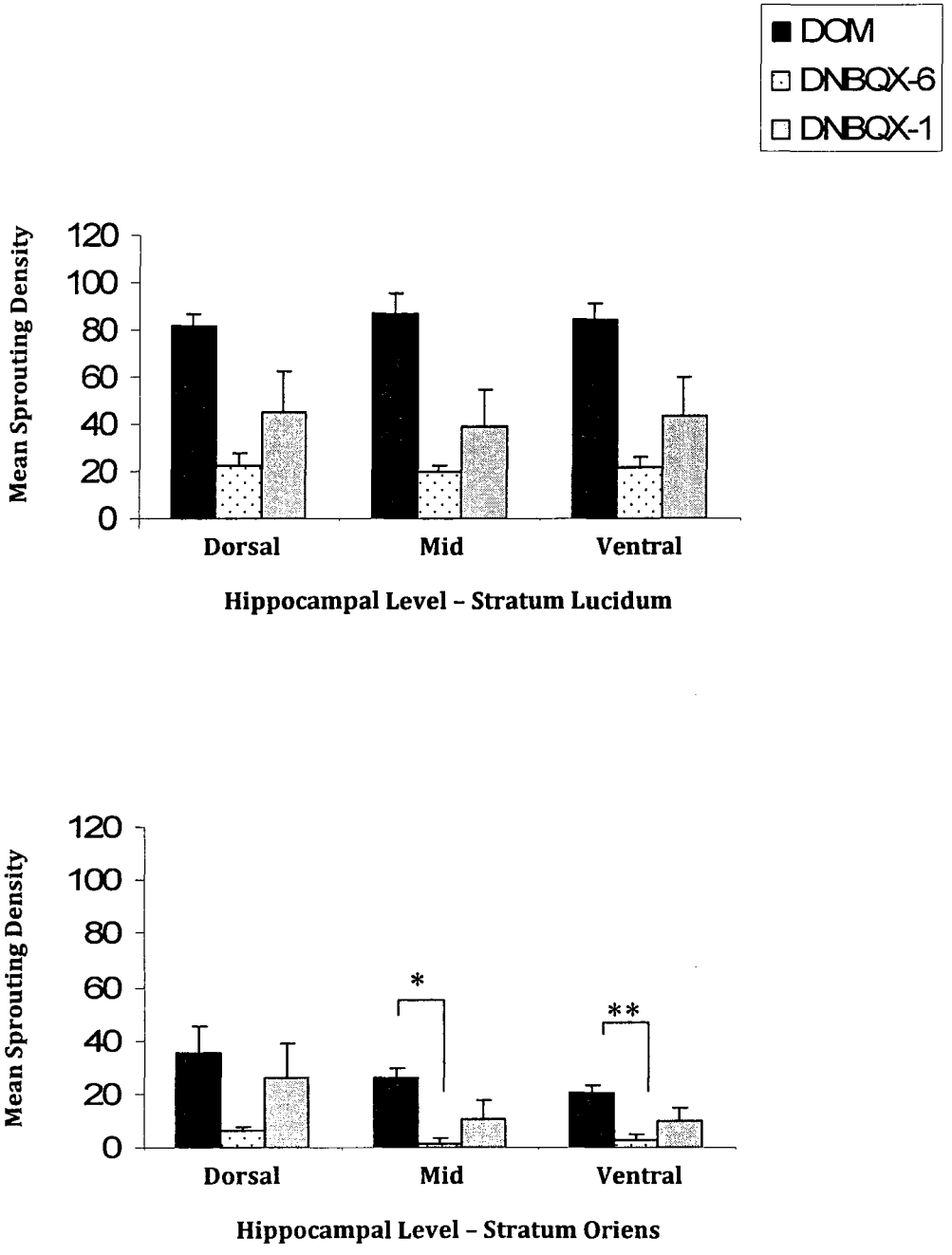

Figure 7.9. Mean mossy fibre sprouting density scores for female-only DNBQX and DOM control rats in area CA3 at dorsal, mid, and ventral levels. A) Stratum lucidum B) Stratum oriens. Asterisks denote a significant difference between the indicated groups ($p<0.05$), and error bars indicate SEM.

DOM alone, while DNBQX-6 means were often equivalent to the DOM only group.

7.4 Discussion

The two major findings of this study are that (1) both NMDA and AMPA receptor antagonism during the second postnatal week of life produce alterations in mossy fibre pathways in adulthood, and (2) the effects of DOM in neonates appear to be mediated through AMPA receptor related mechanisms. In addition, increased MFS was found in DOM-treated rats compared to SAL controls, verifying that DOM administration did have the expected effect.

Interestingly, in the CA3 region, reported alterations were very dependent upon sex. In the SNBQX versus SAL groups, male rats showed sensitivity to AMPAR blockade. Females appeared to be responsive only to the 600μg/kg dose, although this result did not reach statistical significance. When DOM was added into the mix, only female rats showed a decrease in sprouting in response to AMPA antagonism (Figure 7.9, pg 211), while no effect was seen for DOM male groups (further discussion regarding this phenomenon is addressed in subsequent paragraphs). In the DG, on the other hand, both males and females displayed decreased staining in response to AMPAR antagonism regardless of whether they had also received DOM, indicating that both an effect for the antagonist alone (Figure 7.6, pg 207), as well as a blockade of DOM's excitatory effect (Figure 7.8, pg 210) appeared to have occurred. This latter conclusion is further supported by the fact that DOM-induced increases in sprouting had been noted in the DG in the absence of NBQX (Figure 7.1, pg 200), and these increases were subsequently reduced down to levels similar to those found in the SNBQX group when DOM and

NBQX-6 were concurrently administered (see Table 7.2, pg 198). Combined with a similar phenomenon seen in females in the HC proper, it appears possible that the neonatal effects of DOM may be through the same receptor pathway as that of NBQX. However, while NBQX is considered to be an AMPA antagonist, it is also known to affect the closely related KARs as well. Since DOM has a particularly high affinity for KARs (Clarke and Collingridge, 2004; Debonnel *et al.*, 1990; Lomeli *et al.*, 1992; Sommer *et al.*, 1992; Tasker *et al.*, 1996; Verdoorn *et al.*, 1994), effect mediation through these receptors is still a strong possibility. Therefore, whether the changes presented in this study are truly AMPA specific, or whether KAR involvement is also necessary remains to be elucidated.

Antagonism of NMDA receptors using CPP also resulted in sex-dependent alterations in Timm stain intensity in area CA-3, with SCPP female rats showing an increase in staining compared to SAL controls (Figure 7.4, pg 204), while SCPP males displayed either no difference, or (in mid SL) a statistically significant decrease in staining. In the DOM groups in this region, CPP did not appear to have any effect at all on sprouting, as neither DCPP male nor DCPP female rats experienced a change in staining intensity from that seen with DOM alone, suggesting that the NMDA receptor does not participate in the DOM-induced MFS alterations. However, while females in the DCPP group were no different from DOM-only females, there was a decrease in staining noted in the dorsal IML in DCPP males (Table 7.2, pg 202), reminiscent of the similar decrease seen in the male SCPP group in area CA3, although no other differences between DCPP and DOM-only groups was evident at any other IML level. And while SCPP males also tended toward decreased staining in the dorsal IML (not statistically

significant), this tendency was reversed at the mid and ventral levels, with increases in sprouting for all SCPP groups becoming the norm (Figure 7.3, pg 203).

Increases in excitatory activity following chronic NMDAR blockade has been previously demonstrated *in vitro* as measured through the increased frequency of mEPSCs as well as increased synapses and more complex dendritic trees in CA1 (Luthi *et al.*, 2001; Murthy *et al.*, 2001), similar to results seen after a more generalized excitatory blockade using tetrodotoxin (TTX) (Huupponen *et al.*, 2007). This increased activity has been described as a type of homeostatic plasticity, whereby neuronal networks respond to dampened input through heightening their sensitivity to stimuli, an alteration that is believed to occur to ensure adequate stimulation for mechanisms involving learning and memory (Johnston, 1996) and in more extreme scenarios, postulated to be a contributing factor to seizure disorders such as epilepsy (Trasande and Ramirez, 2007). In support of this theory, behavioural and electrographic seizure activity has been reported to result from chronic Na^{++} channel blockade *in vivo* (Galvan *et al.*, 2000). In the current study, statistically significant increases for MFS in the ventral IML of adult rats *in vivo* are reported (Figure 7.3, pg 203) following a daily systemic injection of 150µg/kg CPP during PND8-14, a dose that is substantially less than that utilized in other investigations (e.g. Follett *et al.*, 2000; Jensen *et al.*, 1995; Koh *et al.*, 2004; Rakhade *et al.*, 2008), suggesting that even a subtle amount of interference during critical periods can produce long-term effects that are indicative of heightened network excitability. Additionally, it should be noted that this alteration occurred without chronic antagonism, since the duration of the pharmacological intervention would not be expected to exceed a maximum of 8 hours, even allowing for

a half-life in neonates twice that seen in adult animals (Kristensen *et al.*, 1995). Whether this effect requires the complete one-week dosing regime, or if only one or several more specific days would suffice, was not addressed in the current work.

A substantial increase in MFS in hippocampal area CA-3 occurred in female (Figure 7.4, pg 204), but not in male rats in response to NMDAR antagonism, suggesting that females were more sensitive than males to this treatment. In fact, males tended toward decreased sprouting similar to what occurred with AMPAR blockade (Table 7.2, pg 198). As noted previously, there is a growing body of work describing differences between the sexes in CNS maturation, with males appearing to mature at least one week later than their female counterparts (Galanopoulou, 2008a; Kyrozis *et al.*, 2006; Lemmens *et al.*, 2005; for review, see Galanopoulou, 2008b; McCutcheon and Marinelli, 2009). Subsequently, the timeline for CNS development, determined primarily through studies using male animals, may need to be advanced one week to reflect the true maturational age for females. If this is the case, then females in the current study would actually be in the equivalent of the third postnatal week, a time period where the brain normally undergoes rapid axonal pruning that is believed to be mediated through NMDA channel activity (Johnston, 1996; McDonald and Johnston, 1990). Subsequently, the increased sprouting seen in the female SCPP group later in life may be a result of early interference in this process through NMDAR blockade during a portion of this critical developmental window. The lack of difference seen between DCPP and DOM-only females fits as well, since DOM is known to bind to NMDARs (Hampson and Manalo, 1998; Pulido, 2008), and in competition with CPP, may have simply negated its effects.

Males, in the second postnatal week of development, would be in a predominantly GABA-directed 'switchover' stage where connections are still being formed rather than removed (Khalilov *et al.*, 2005), and thus would not be expected to exhibit a consistently similar phenomenon. The decrease in sprouting seen in the IML of the DCPP males, along with the decrease in CA-3 for the SCPP males appears to substantiate this theory, especially since NMDA also undergoes developmentally-regulated alterations in subunit composition at this time that could presumably produce widely variable effects on function. It is also notable that, while SCPP males showed consistently decreased MFS compared to controls, males receiving both DOM and CPP did not. Thus it appears that for normal male rats in their second week of postnatal development, antagonism of NMDARs (which normally work in concert with the depolarizing effects of GABA until AMPA and KA receptors take over), have an effect similar (albeit less robust) to that of AMPA blockade. This effect appears to be cancelled out when DOM is simultaneously administered and competes with CPP, or (depending on the specific region) is enhanced, making the DCPP males more like the SCPP male group.

It should be noted that the reported increases in Timm staining density in CPP females could also be due to an augmented storage of unbound zinc in the mossy fibre boutons in this region rather than an increase in axonal sprouting. The functional significance of increased $[Zn^{++}]_i$ is currently unknown, although it appears to be involved in modulating excitation through non-competitive inhibition at NMDARs (Christine and Choi, 1990; Legendre and Westbrook, 1990; for review, see Paoletti *et al.*, 2009) and in high concentrations, has been shown to reduce NMDA channel currents, presumably by

binding at the magnesium site within the pore (Legendre and Westbrook, 1990). Previous work examining high-dose NMDA blockade has also shown increases in synapses (Holahan *et al.*, 2007) and dendritic tree complexity (Luthi *et al.*, 2001). However, the protocol utilized in the current study does not provide answers for the functional and anatomical questions surrounding the noted increase in staining. Further investigations to determine if treated rats are less susceptible to seizure activity will help address the functional issues, while a more in-depth histological examination of the axonal network is required to gain a better understanding of any actual architectural changes (e.g. increased synapse formation) that may be occurring.

The differences in area CA-3 seen between males and females following AMPAR blockade are also very intriguing, and similarly to the alterations produced by CPP, may be due to differences in actual maturational age. It has been shown that, at least in males, the second postnatal week is a critical time for AMPAR development, and prior to this period, these receptors do not appear to be fully functional (Khalilov *et al.*, 2005). As mentioned previously, up until this time GABA supplies the necessary membrane-depolarizing activity required to activate existing NMDA channels and drive appropriate synaptogenesis (Ben-Ari *et al.*, 2007). Normally, this period also marks the time (in males) when GABA switches to inhibitory function (Khalilov *et al.*, 2005), and Glu receptors are at a peak (Lujan *et al.*, 2005; McDonald and Johnston, 1990). In light of this knowledge, one explanation for the absence of staining in the HC of SNBQX male rats is that blocking AMPARs at this crucial juncture may have interfered with the assumption of the receptor's adult role as a fast, membrane-depolarizing impetus for NMDA channel activation enough to dampen activity throughout the network for the

lifespan of the animal. This dampening effect could be related to either a decrease in receptor number, possibility thorough alterations in AMPA trafficking (for review, see Greger and Esteban, 2007; Kessels and Malinow, 2009), or through channel composition, particularly in relation to editing of the GluR2 subunit (Kortenbruck *et al.*, 2001; Vollmar *et al.*, 2004). In females, on the other hand, the GABA switch has been demonstrated to occur by at least PND2 (Kyrozis *et al.*, 2006), so presumably, functional (and fewer) AMPARs would already be in place during NBQX administration in this study; therefore their systems should not be affected as drastically as their male counterparts. However, it should be noted that, while not statistically significant in the current analysis, SNBQX-6 (but not SNBQX-1) females did show a dramatic decrease in sprouting in the CA-3 region, indicating that these animals were also not entirely immune to AMPAR blockade. Further investigations looking at the effects of developmental time points for antagonist administration in males and females are needed to clarify these fascinating issues.

Similar to previous suggestions regarding the CPP results, the question of whether the alterations seen in Timm stain in this study reflect changes in actual mossy fibre axonal sprouting or whether they are due to modifications in zinc storage is intriguing. The virtual non-existence of $[Zn^{++}]_i$ in the HC of SNBQX male (and SNBQX-6 female) rats suggest that antagonizing AMPA may have somehow modified zinc handling, but whether this translates to an actual decrease in mossy fibre synapses remains to be seen. Strains of mice with a targeted disruption of the zinc transporter ZnT3 gene (ZnT3 knock out mice) have been shown to completely lack zinc in this area (Cole *et al.*, 1999), so perhaps the alterations seen in rats in the current study reflect a developmental

disruption to this important mechanism. In support of this theory, alterations in AMPAR levels have been reported to correspond to the amount of zinc present in giant mossy fibre terminals, with the ZnT3 transporter playing a key role (Sindreu *et al.*, 2003). Interestingly, those results showed that decreased zinc was an indication of increased AMPAR expression, which raises intriguing questions regarding the functional significance of the changes we report, as well as highlighting the importance of further work to investigate the mechanisms involved.

Again, it is important to consider that the doses of NBQX utilized in this study (600ug/kg and 1mg/kg) were extremely minimal compared to those used in other investigations looking at the efficacy of this compound in developmental rat models of hypoxia-induced epileptogenesis which commonly use a 20mg/kg dose (Follett *et al.*, 2000; Jensen *et al.*, 1995; Koh *et al.*, 2004; Rakhade *et al.*, 2008). While the functional / behavioural impact of the current results have yet to be elucidated, these data nevertheless emphasize how vital consideration of both gender and developmental age are when evaluating possible therapies for clinical application, as well as accentuating the importance of long-term *in vivo* evaluations.

In conclusion, the current study has shown that a subtle blockade of either NMDA or AMPA function during the second postnatal week of life results in long-term alterations in mossy fibre pathways of the adult HC, thus expanding upon the existing literature describing the effects of NMDA and AMPA receptor antagonism. In addition, this work has revealed that the alterations in MFS seen in the NIS-L rat model appear to be mediated through AMPAR pathways, although it is also possible that KARs are

involved as well. While it is not yet clear whether any of these alterations are a result of an actual change in axonal morphology, or represent a modification of zinc handling, or some combination thereof, it is clear that even slight interference with complex developmental processes can have far-reaching implications, warranting further investigation into both the mechanistic and functional aspects of these intriguing findings.

8.0 SUMMARY AND FUTURE DIRECTIONS

Changes in excitatory/inhibitory balance in the brain can have profound and far-reaching consequences. One of the most sensitive periods for alterations in this balance occurs during early postnatal development, when connections in neuronal circuitry are being formed and refined. In this phase, while GABA and Glu are adjusting to and assuming their adult roles for the mediation of appropriate neuronal activity, even subtle insults or injuries have the potential to cause long-term modifications.

The NIS-L rat model, produced through low-dose DOM administration (20μg/kg s.c.) during the second postnatal week of life, demonstrates alterations in adulthood indicative of long-term effects on excitatory/inhibitory circuitry. Previous studies in this model have reported low-grade seizure-like episodes (Doucette *et al.*,2004) as well as cell loss, increased MFS, increases in BDNF mRNA and TrkB receptor expression, and gliosis (Bernard *et al.*, 2007; Doucette *et al.*, 2004; McDonald *et al.*, 2008). In order to further explore the possible consequences of mild interference in glutamatergic/GABAergic development, the aim of the current thesis was to assess the NIS-L model using electrophysiological, behavioural, pharmacological, and histochemical methods in an effort to provide additional information regarding potential alterations in neurological function and underlying mechanistic properties.

An *in vivo* electrophysiological assessment of EEG in NIS-L rats revealed a distinct EEG waveform pattern during NIS-L manifestation and subtle alterations in wave band expression, as well as increased sensitivity to an acute dose of PTZ (Chapter 2). This

increased sensitivity was also seen in response to electrical stimuli during focal seizure threshold testing, but not through increased seizure propagation to the rest of the brain. However, there was a robust increase in NIS-L animals for hippocampal MFS in ventral regions following amygdala kindling (Chapter 3). In addition, alterations in REM sleep patterns, similar to that seen in both human and animal models of TLE, have also been discovered in this model (Chapter 4).

Immunohistochemical analysis of interneuronal subpopulations in the HC and amygdala of NIS-L rats showed decreases in parvalbumin imunoreactivity, particularly in males, as well as a decrease in non-GABAergic cells (e.g. mossy cells) in the hilar region of the DG. However, somatostatin-containing interneuron levels, while consistently lower, were not equivalently affected (Chapter 5). An *in vitro* investigation of DG gating in the NIS-L model using hippocampal slices has shown no alterations in baseline activity levels in the DG or HC proper in response to perforant path stimulation. Application of DOM, on the other hand, produced a concentration-dependent change in inhibitory activity, but whether the effects seen in CA3 were due to DG gating, or to some other mechanism remains unknown. Removing the magnesium block in the NMDA channel through low Mg^{++} perfusion increased activity in both groups, although the tissue from NIS-L rats did show a correspondingly heightened excitatory response once convulsive-like activity was initiated (Chapter 6). And finally, antagonism of NMDA and AMPA receptors during co-administration of DOM revealed that DOM's mechanism of action does not appear to be mediated through NMDAR pathways, but may (at least in part) involve the activation of AMPAR-regulated channels (Chapter 7). The same study has further shown a sex- and receptor-sensitive alteration in MFS patterns in adult rats in

response to a subtle blockade of either AMPA or NMDA receptors during the second postnatal week of development.

Overall, these investigations serve to highlight the variety of permanent alterations that may occur following even subtle insults during a critical period in early excitatory/inhibitory development, and further our understanding of the underlying changes inherent in this process. At the same time, it is clearly evident that much work remains to be done. One of the most important issues that remains unresolved is whether the NIS-L rat experiences spontaneous seizure activity, or whether, like the Mongolian gerbil (Buckmaster, 2006), seizure expression can only be induced through some external manipulation. Through simultaneously monitored EEG and video (see Appendix A.1, pg 228), this question may be readily addressed.

Another important issue relates directly to the developmental nature of the model, and the time frame during which DOM is administered. During the second postnatal week in the rat, two dramatic changes are occurring: 1) the Glu system undergoes a large overshoot in receptor expression as it assumes excitatory control, and 2) GABA switches from a depolarizing to a hyperpolarizing function. Through the activation of Glu receptors, particularly GluK5 subunit-containing KARs (see Chapter 1), DOM has the potential to influence either (or both) excitatory or inhibitory development. Responsible for both inhibitory and modulatory function in the adult brain, the GABA system is especially sensitive to alterations in neuronal balance (Tretter and Moss, 2008), and therefore may be particularly susceptible to DOM's effects. Previous work has indicated that the GABA switchover is dependent upon appropriate changes in chloride transport

proteins (see Chapter 1, section 2.3), and disruptions to this process have been shown to result in altered neuronal function (Kahle *et al.*, 2008). As well, seizure activity can produce similar changes, causing imbalances in intracellular chloride concentrations that predispose the brain to further seizures (Li *et al.*, 2008). Therefore, an assessment of both the expression and the function of these transport mechanisms in the NIS-L rat model, particularly under conditions of heightened activity, may help further our understanding of the changes reported in the current thesis.

Additionally, studies assessing possible sex differences related to the time frame of DOM administration would help determine if the sex-dependent changes seen in the model can be attributed to differences in actual developmental age in male and female rats (Galanopoulou, 2008b), or if some other mechanism should be investigated. If female rats have indeed switched to inhibitory GABA function before PND8 (the time when DOM injections are normally initiated), thus representing several days advanced CNS development compared to males, evaluation of alternative starting dates for DOM administration on long-term consequences in male and female animals should be investigated.

One final intriguing issue is that of the increased (with CPP antagonism) and decreased (with NBQX antagonism) Timm staining noted in control rats as presented in Chapter 7. While excessive MFS is believed to be pathological (Sutula and Dudek, 2007), moderate sprouting is associated with learning (Holahan *et al.*, 2006). The changes in CPP and NBQX treated animals in antagonist study were dramatic, suggesting that equivalent alterations in behaviour should be evident as well. Investigation into the behavioural

consequences of this developmental antagonism is currently underway. In addition, it has been recently reported that the presence of zinc in presynaptic boutons of the rat HC is representative of a low AMPAR content, while NMDAR expression remains constant (Sindreu *et al.*, 2003). Since NMDARs require membrane depolarization to remove the Mg^{++} block in the channel pore (Johnson and Ascher, 1990), these low AMPAR synapses would be expected to have decreased activity due to the decrease in AMPAR-mediated neurotransmission. Alternatively, low zinc content has been correlated with increased AMPAR expression (and unchanged NMDAR levels) (Sindreu *et al.*, 2003), suggesting a higher potential for excitation. Therefore, using an *in vitro* approach, evaluation of the consequences of stimulating granule cells in the HC of CPP and NBQX treated rats should also reveal dramatic and opposite responses.

There are many other possibilities for further exploration arising from the work presented in this thesis, some which have been noted in the individual chapters. Given both the developmental nature of the model, and the enormity of the system with which DOM interacts, the potential for future study is understandably substantial. It should also be noted that, while the focus of this dissertation has been on seizure and epilepsy-related alterations, there are many other neuropathological disorders that may arise from an early-life interference with Glu as well.

Insult or injury to the developing brain can produce changes that are both permanent and extensive. As the most predominant excitatory neurotransmitter in mammalian nervous systems, Glu has the potential to affect multiple systems, and alterations in its connectivity and function may have widespread consequences. This thesis provides a

demonstration of some of the possible changes that may occur in excitatory and inhibitory circuitry in the brain as a result of interference with early developmental processes, and has revealed several underlying mechanisms that may be responsible for these changes. Future studies assessing spontaneity of behavioural expression and evaluating sex-dependent differences in the model, as well as an investigation of the role of GABAergic mechanisms in generating excitatory circuitries are suggested to further evaluate the consequences of interference in the intricate interplay between Glu and GABA systems during critical developmental stages.

APPENDIX A: TELEMETRY STUDY – ADDITIONAL DATA

The following work was conducted at H. Lundbeck A/S in Copenhagen, Denmark in conjunction with the telemetry/EEG study (see Chapter 2).

A.1 Home Cage Analysis

Introduction

Seizure-like activity in the NIS-L rat model can be induced through exposure to novel, stressful environments such as the water maze task (Doucette *et al.*, 2004), but the possibility of spontaneous seizures and/or interictal activity occurring in these animals has not yet been explored. Data collection methods and preliminary results for this on-going investigation are presented herein.

Materials and Methods

Rats were treated postnatally and for cortical electrode placements as described in Chapter 2. At this time, stereotaxic surgery was performed on 3 extra animals (all DOM-treated) to implant both cortical and hippocampal depth electrodes as follows: cortical placements were positioned either side of midline ~2mm anterior to bregma, one bipolar electrode implanted in the right HC (4.8 mm posterior, 5.2 mm lateral, 6.3 mm ventral from bregma), and one EMG lead for a total of 3 bio-potentials (depth electrode surgeries performed by Dr. J. Bastlund, assisted by D. Gill). Following recovery from surgery, transmitters were switched on and EEG/EMG activity was continuously recorded in all rats (n=21) for 24 hours/day over a 14 day period in the home cage. For monitoring, rats were split into two groups: Group 1 (n=9) and Group 2 (n=12). Recordings from these groups were obtained one week apart to ensure that all rats had a minimum of 3 weeks to recover from surgery. In each group, 4 DOM rats were selected for one full week of video monitoring (Monicor TVSP-42 B/W Quad cameras connected to a Panasonic NV-HS870 VCR), to provide visual confirmation for the EEG analysis

and to allow assessment of spontaneous seizure behaviour. All disruptions (e.g. watering, video tape changes, etc) were recorded on a time sheet for further reference.

Results

Preliminary assessment of video/EEG/EMG has not yet revealed any indication of NIS-L behaviour in the home cage. However, several intriguing EEG patterns (see Figures A1.1, pg 230 and A1.2, pg 231) have been noted which appear to warrant more in-depth investigation.

Discussion/Conclusion

Further analysis of the home cage data should be conducted to assess possible non-elicited seizure-like activity, and to characterize interictal EEG patterns in the NIS-L rat model.

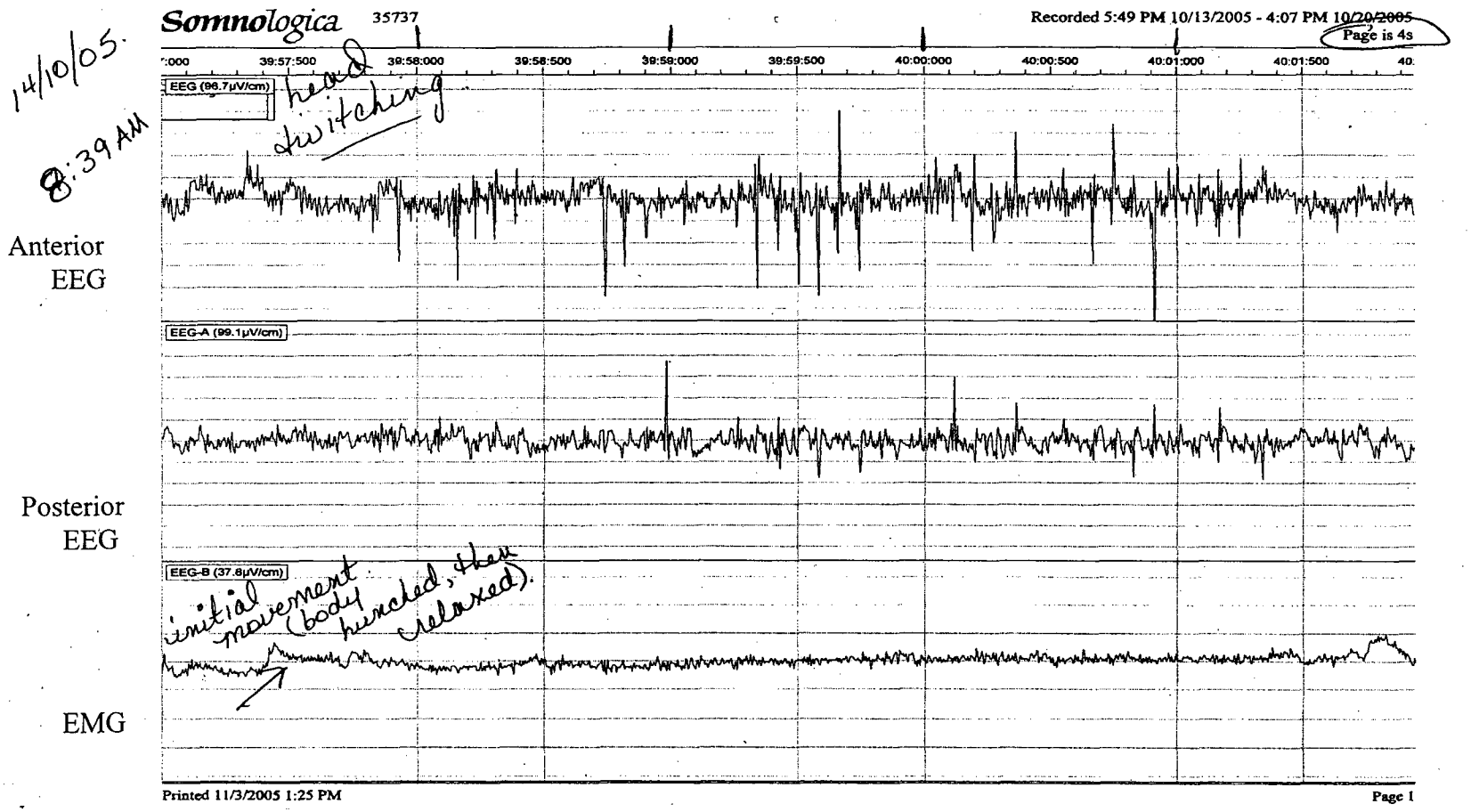

Figure A1.1. An example of EEG patterns from a DOM-treated rat during the first 24 hours of home cage recordings. This tracing shows a 4 second episode of high amplitude, high frequency activity bursts recorded primarily in the anterior lead. EEG amplitude varies between ~96-100µV/cm, while EMG is set at 37.6 µV/cm. Behaviourally, the rat exhibited a quick body contraction, and then head twitching throughout the duration of the episode.

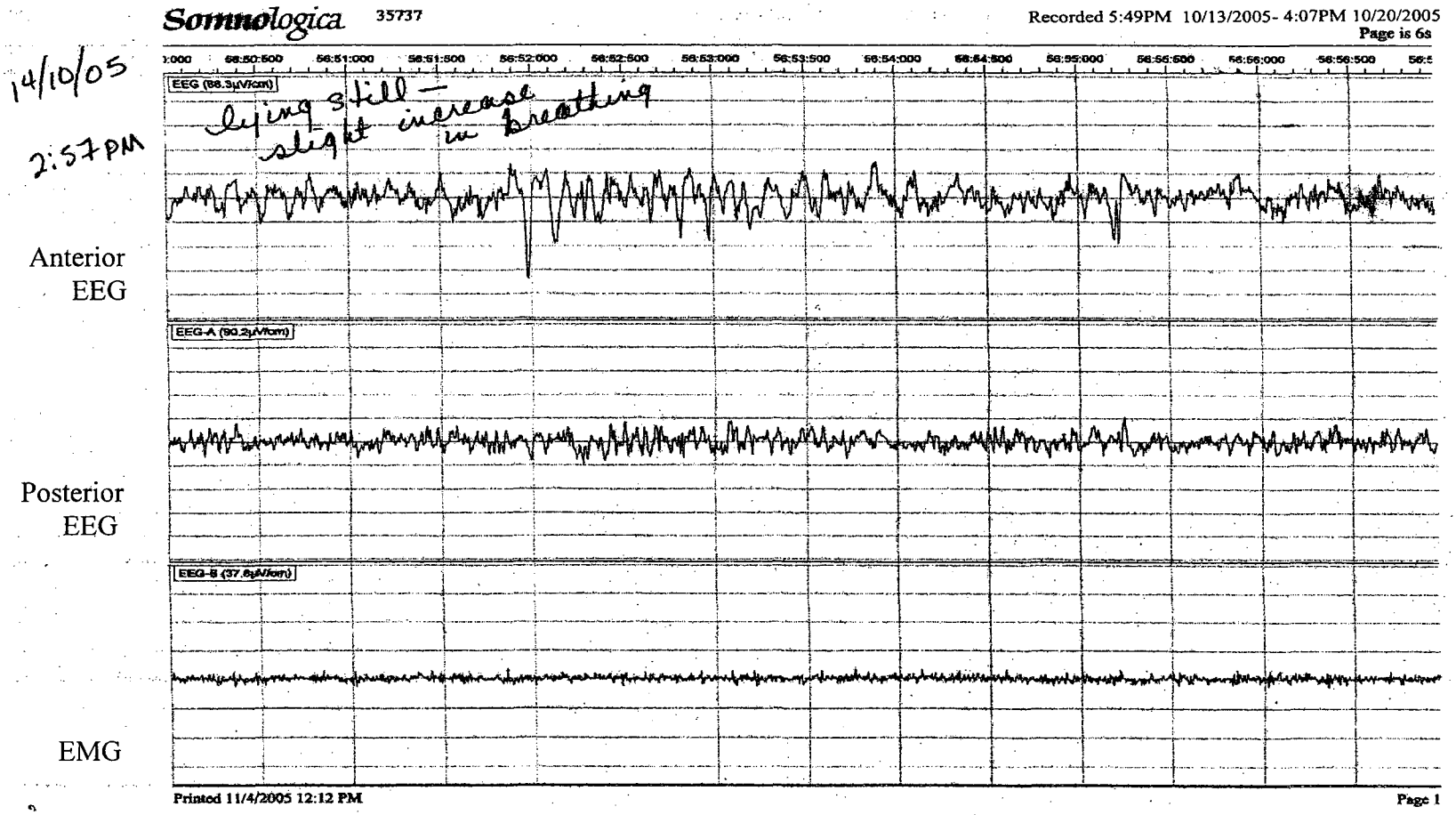

Figure A1.2. An example of EEG patterns from a DOM-treated rat during the first 24 hours of home cage recordings. This tracing shows a 6 second EEG snapshot of the same rat (from Figure A1.1) ~6.5 hours later, again with alterations in the anterior lead. The only visible change in behaviour at this time was a slight increase in breathing rate. EEG amplitude varies between ~88-91μV/cm, while EMG is set at 37.6 μV/cm.

A.2 Morris Water Maze Testing

Introduction

Domoic acid ingestion has been shown to impair learning and memory function in humans (Nakajima and Potvin, 1992; Teitelbaum *et al.*, 1990). As well, studies investigating the effects of repeated seizures show a detrimental effect on cognitive processes (see Carreno *et al.*, 2008 for review). In the NIS-L rat model, however, learning and memory effects appear to be task specific, with animals showing improvements in paradigms such as the radial 8-arm maze, but more variable (and sex-dependent) performances in the Morris water maze (Adams *et al.*, 2009), one of the behavioural tasks that has been shown to elicit seizure-like responses in this model (Doucette *et al.*, 2004) (see Chapter 2). An important consideration, particularly with regard to the low-grade seizure-like episodes elicited in this model in response to initial exposure to the task, is whether the exertion of swimming might play a role in generating these behaviours. The current study was conducted to further assess learning and memory in the NIS-L rat, as well as to provide information regarding overall distance travelled while swimming.

Materials and Methods

The water maze consisted of a black fiberglass pool (1.2m diameter) filled with tepid water (21°C ±1°) to a depth of 27cm. A black escape platform (12x12cm) was submerged ~2cm below the water surface and positioned in the middle of one of the quadrants (north, south, east, west) 22cm from the pool edge. Four screens were located ~60cm from the side of the maze with 2 distinct cues on each. Since the pool is circular and contains no intramaze cues, rats must rely on learning and remembering extramaze

cues for accurate location of the hidden platform. Eight trials, each consisting of a maximum of 60 seconds (s) to locate the platform, 60s on the platform between each trial, and a 20s intertrial interval in a dry cage, were conducted with starting positions from each of the 4 compass points repeated twice (2 blocks of 4 trials each) to provide assessment of learning and memory performance. If a rat did not find the platform within the allocated time, it was guided there by the experimenter. Significantly shorter latencies in the second block of trials indicated that learning had occurred. Overall swim speed, number of entries and time spent in specified pool regions (outer and inner areas – may be used to measure 'emotionality' through thigmotaxic behaviour) and latency to reach the platform was recorded through a monitor (Sony digital w/3.6mm Compunar f/5.6 lens) mounted over the pool, and fed into the Noldus EthoVision (v.2.3 Noldus Information Technology, The Netherlands) tracking program for analysis.

Data Analysis and Results

Nineteen rats (8 SAL, 11 DOM) implanted with cortical and/or cortical-hippocampal electrodes (see Home Cage Analysis) were included in this study. All measures were assessed using independent t-tests or paired t-tests (for between block comparison) (SPSS v.10.0.5 SPSS Inc., Chicago, IL) with $\alpha \leq 0.05$. No difference was found between groups for learning and memory as measured by latency to find the hidden platform during trials, and all rats displayed a statistically significant decrease in latency to platform between blocks, indicating that learning had indeed occurred (Figure A2.1, pg 234). As well, no difference was noted for time spent in outer or inner region, or in swim speed and total distance moved. Table A2.1 (pg 234) provides a summary of these data.

Discussion/Conclusion

Rats in both treatment groups displayed similar cognitive abilities during testing, and there were no differences noted in emotionality or exertion levels that might provide an explanation for the seizure-like behaviours reported in Chapter 2.

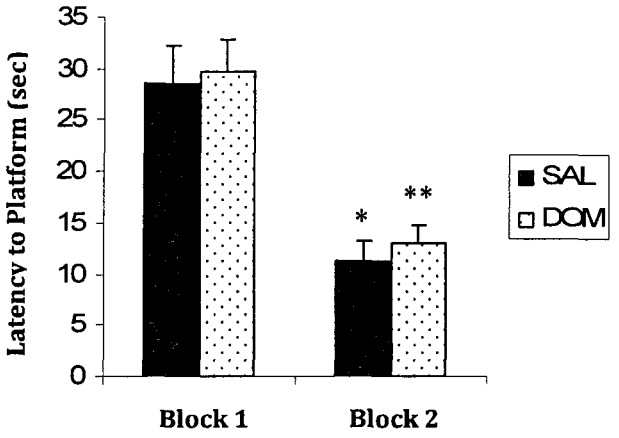

Figure A2.1. Latency to platform between blocks during water maze trials for DOM-treated and saline control rats. Asterisks indicate statistically significant differences from Block 1.

Table A2.1. Comparison of DOM-treated and control rats for mean (±SEM) time spent in the outer pool region, swim velocity, and total distance travelled during water maze exposure.

Measure	**SAL** Mean (±SEM)	**DOM** Mean (±SEM)	p value
Time spent in outer (sec)	18.20 (±5.61)	19.41 (±5.43)	0.403
Swim velocity (cm/sec)	23.73 (±0.58)	21.88 (±0.81)	0.102
Total distance (cm)	473.78 (±50.40)	491.67 (±45.78)	0.798

A.3 PTZ (32mg/kg) Administration

Materials and Methods

Rats were prepared as described in Chapter 2. Two days following acute exposure to low-dose PTZ (25mg/kg), a second, higher dose (32mg/kg) was administered to further assess generalized seizure threshold. Dependent measures were latency to, and number of, absence seizures, latency to, and number of, MCJs, and maximum observed behavioural seizure stage (Racine, 1972a).

Data Analysis and Results

Parametric data were analyzed using independent t-tests, while Chi-square was used for non-parametric comparisons (SPSS v.10.0.5, SPSS Inc., Chicago, IL) with $\alpha \leq 0.05$. As with the 25mg/kg acute PTZ dose, there was no difference found between groups in latency to absence seizure activity. However, there was a difference in the number of absence seizures experienced [$t_{(14)} = -2.951$, $p = 0.011$], with DOM-treated rats showing more absence episodes in the 30 minute observation period than controls. There was also no difference in latency to the first MCJ at this dose level, although controls still exhibited a greater delay to MCJ activity (SAL: 965s ±316.1; DOM: 433s ±200.7), but following this second, higher dose, the number of MCJs were significantly increased in DOM-treated animals [$t(14) = -2.178$, $p = 0.047$]. Most surprising, however, were the Stage 5 seizure results. At this level, 62.5% (5 of 8) of DOM-treated rats experienced Stage 5 (the four rats that had exhibited this behaviour at the lower, acute dose, plus one additional rat), while in the control group (where no rats had displayed this activity at the acute 25mg/kg dose), all rats now reached Stage 5. Although this result did not

reach statistical significance [$X^2 = 3.692$, $p = 0.055$], it is certainly intriguing (see Table A3.1 (below) for a summary of these data compared to the 25mg/kg results).

Table A3.1. Mean number (±SEM) of absence seizures and myoclonic jerk (MCJ) activity exhibited during the 30 minute period following acute (25mg/kg; see Chapter 2) and repeated, higher-dose (35mg/kg) pentylenetetrazol administration.

	SAL-25	SAL-32	DOM-25	DOM-32
Measure:				
Absence (total #)	61.00 (±14.3)	40.75 (±6.1)	34.88 (±9.4)	95.88 (±17.7)*
Absence latency (sec)	42.50 (±201.2)	84.38 (±6.9)	255.00 (±152.4)	93.75 (±26.7)
MCJ (total #)	0.63 (±0.5)	1.38 (±0.7)	14.75 (±7.1) #	9.63 (±3.7)*
MCJ latency (sec)	1560.00 (±176.0)	965.00 (±316.1)	753.75 (±306.4)*	432.50 (±200.7)

tendency toward increased activity
*statistically significant difference from appropriate control group

Discussion/Conclusion

The results from this study demonstrate a continued tendency for DOM-treated rats to experience generalized seizure episodes as evidenced through increased absence seizure and MCJ activity compared to controls following a second, higher systemic dose of PTZ. Combined with the differences in Stage 5 activity, these results appear to confirm that some kind of alteration in generalized excitatory/inhibitory circuitry has indeed occurred in the brains of treated animals. However, in order to examine these alterations further, a more systematic chemical kindling paradigm should be implemented.

A.4 Band Wave Analysis of Hippocampally-implanted DOM Rats

Preamble

Three DOM-treated rats were implanted with hippocampal depth electrodes to allow a more focal assessment of limbic region activity. However, since no SAL controls were similarly implanted, these animals were not included in the main portion of the telemetry study.

Data Analysis and Results

As expected, the 3 depth electrode animals showed an intensified hippocampal EEG response (Table A4.1 below), which translated into differences in band wave activity compared to both control and DOM-treated cortically-recorded rats (One-way ANOVA with Tukey's post-hoc analysis where indicated; $\alpha \leq 0.05$) (SPSS v.10.0.5 SPSS Inc., Chicago, IL).

Table A4.1 Percent activity (±SEM) in depth versus cortical electrode measurements.

	SAL - CORTICAL	DOM – CORTICAL	DOM - DEPTH
Frequency	(% activity ±SEM)	(% activity ±SEM)	(% activity ±SEM)
Delta	10.17 (±1.4)	11.29 (±2.8)	15.33 (±0.7)
Theta	9.50 (±0.9)	9.14 (±0.7)	15.67 (±1.7) *
Alpha	5.00 (±0.3)	5.14 (±0.3)	8.67 (±0.3) *
Sigma	2.17 (±0.2)	2.29 (±0.2)	4.00 (±0.0) *
Beta	11.50 (±0.2)	12.29 (±0.3) #	14.33 (±0.9) *
Gamma	61.83 (±1.9)	60.00 (±3.6)	42.67 (±1.9) *

tendency toward increased activity compared to saline controls (p=0.059)
*significant difference from both cortical groups (Tukey's post-hoc p<0.05)

A.5 Prepulse Inhibition Testing

Introduction

The prepulse inhibition (PPI) test is commonly used in rats and mice to measure their ability to inhibit (or "gate") reflexive startle responses to a loud auditory stimulus (pulse) when it is preceded by a warning tone (prepulse). The startle response is recorded by a pressure plate upon which the animal sits. A normal rat or mouse can learn to inhibit its startle response to the pulse stimulus after just a few trials. However, while prepulse inhibition is a cross-species phenomenon, it is consistently decreased in individuals with schizophrenia. It has also recently been shown to be altered in several other psychiatric disorders (for review, see Geyer, 2008).

Interestingly, while disorders such as schizophrenia have traditionally been linked with changes in dopamine neurotransmission (e.g. Kapur and Mamo, 2003; Seeman, 1987), recent theories have been focusing on the Glu system as a key player in its etiology (Coyle, 2006; Stone *et al.*, 2007). In addition, the co-occurrence of schizophrenia and epilepsy (particularly TLE) has been well documented over the years, and the similarities between these two disorders continue to be investigated (see Cascella *et al.*, 2009 for review). As a putative animal model for TLE produced through systemic injection of a Glu agonist in early development, the NIS-L rat may also be susceptible to schizophrenia pathology. The aim of this pilot study was to determine whether DOM treatment in early postnatal development produces a decreased ability to inhibit startle responses in adulthood.

Materials and Methods

Male rats from the telemetry study (Chapter 2) plus 3 rats implanted with depth electrodes (see Appendix A.1 methods, pg 228 for details) were used for this investigation (n=19; 8 SAL, 11-DOM).

The testing chamber consisted of a metal box (40x52cm) enclosing an inner compartment (17.5cm long x 8cm wide x14cm high) that contained a pressure-sensitive platform. The auditory stimuli were controlled by an autostimulation unit (Med Associates Inc, USA) connected to a Shocker/Startle interface unit (Coulbourn Instruments Inc, USA). Both auditory pulses and background white noise were delivered through four speakers within the outer box. Data from the stimulus protocol (outlined below) was collected through STARWin software (STARWin Industries, USA v.0012).

Stimulation Protocol

Rats were given 5 minutes to habituate to the testing chamber and the background white noise (70dB). The prepulse (30ms duration) was either 4, 8, or 12dB above the background noise level, while the pulse intensity was 120dB, and lasted for 40ms. The time between the prepulse and the pulse (inter-stimulus interval: ISI) was set at 100ms, and the inter-trial interval was 15s. There were 8 blocks of 7 trial types randomly presented during testing: 1) dummy (no pre or pulse) 2) pulse alone 3) pre 4dB + pulse 4) pre 8dB + pulse 5) pre 12dB + pulse 6) pre 12dB alone, and 7) no pulse. In total, each rat received 20 minutes of programmed testing.

Data Analysis and Results

The percentage of startle inhibition to the 120dB pulse in each group was obtained by dividing the startle response at each prepulse level (4dB + pulse, 8dB + pulse, 12dB + pulse) by the startle response to the pulse alone, and was analyzed using an independent t-test (one-tailed) (SPSS v.10.0.5 SPSS Inc., Chicago, IL) $\alpha \leq 0.05$. Results showed no difference between groups for baseline startle (pulse only), or at the 4dB and 8dB prepulse level, but at the 12dB level, the DOM-treated rats exhibited a statistically significant decrease in inhibition of startle response compared to controls [$t_{(17)} = -1.99$, $p = 0.03$] (Figure A5.1).

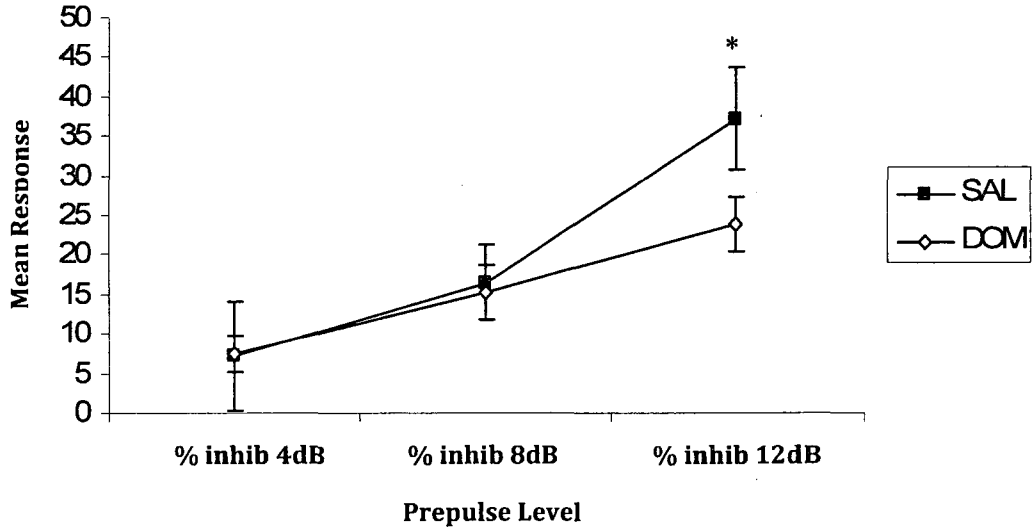

Figure A5.1 Comparison of the ability of DOM-treated and control rats to inhibit response to a 120dB auditory stimulus preceded by various levels of a prepulse warning tone. The asterisk indicates a statistically significant difference from the appropriate control group, and error bars denote SEM.

Discussion/Conclusion

The NIS-L rat model does appear to exhibit PPI alterations similar to those seen in animal models of schizophrenia, as indicated by a reduced ability to inhibit startle responses to an auditory stimuli (pulse) even when it is preceded by a warning (prepulse) tone (Geyer, 2008). These results are in agreement with a recently published report in this model (Adams *et al.,* 2008), showing a similar decrease in inhibition at the 12dB prepulse level in DOM-treated male rats compared to their SAL controls, and strongly indicate that investigation into the NIS-L model should be pursued for both schizophrenia research, as well as to further explore the possible link(s) between epilepsy and schizophrenia pathologies.

A.6 Forced Swim Testing

Introduction

The forced swim test (FST) is a traditional behaviour paradigm used to measure "behavioural despair", as rats are forced to continuously swim in a tank of water for a predesignated period of time (usually 10 or 15 minutes) with no means of escape. It is thus considered to be a model for depression (see West, 1990 for review). Latency to "give up" or cease searching for an escape route is recorded, with three levels of behaviour most commonly assessed: swimming, struggling, and floating. The FST can also be used to elicit high levels of stress and exhaustion.

In a previous section of this thesis (A.2 - Morris water maze), the possibility that the behaviours seen in NIS-L rats following water maze exposure could be due to the physical exertion of swimming rather than a CNS-mediated response was examined through an assessment of swim speed and duration of total time spent in the water maze. In that analysis, no difference was found between the groups for these measures, suggesting that the NIS-L response may indeed be generated by mechanisms unrelated to the experience of physical exhaustion.

However, while the results from the MWM study did suggest that exhaustion was not a mitigating factor for NIS-L behaviours, it did not rule it out entirely. In addition, since stress is one of the most commonly reported triggers for seizure in humans (Frucht *et al.*, 2000; Koutsogiannopoulos *et al.*, 2009; Temkin and Davis, 1984) and since the seizure-like behaviours in the NIS-L rat are most readily elicited by exposure to novel tasks (which inherently involve a stress component) further investigation of the effects of

exhaustion and stress through a task involving high levels of both these elements appeared warranted. To this end, the aim of the current study was to assess both behaviour and EEG responses during a modified forced swim task.

Materials and Methods

Male rats from the telemetry study (Chapter 2) plus 3 rats implanted with depth electrodes (see Appendix A.1 methods, pg 228 for details) were used in this investigation (n=19). However, since the depth-electrode rats could not be blinded for behavioural scoring, their data was not included in the statistical analysis.

In order to provide a means of assessing the NIS-L syndrome during forced swim testing while ensuring a strenuous and equivalent amount of swimming time for each rat, the FST was modified so that all rats experienced 8-one minute swim trials in a large (20x28x50cm) container filled with water to a depth of ~28cm. Each trial was separated by a 1 minute intertrial interval spent in a cage filled with ~2cm of water (to simulate the experience of sitting on the platform in the MWM task). Rats were run 2 at a time (staggered at 30sec intervals). Both EEG (Data Sciences International, USA) and video (Sony digital camera w/3.6mm Compunar f/5.6 lens) were recorded during each intertrial interval. Trials were scored manually for behaviour, and then video reviewed for confirmation.

Data Analysis and Results

The occurrence of NIS-L behaviour was analyzed using Chi-Square (Crosstabs, SPSS v.10.0.5 SPSS Inc., Chicago, IL) with $\alpha \leq 0.05$. However, since all rats were highly

agitated, behavioural scoring was often difficult. Nevertheless, 7 of 8 DOM-treated rats displayed seizure-like behaviours [$X^2 = 4.00$, $p = 0.046$], and, interestingly, so did 2 of the 8 controls (Figure A6.1). Unfortunately, EEG information was not able to be analyzed due to the overwhelming number of artifacts from the exaggerated behavioural responses.

Discussion/Conclusion

While all rats were obviously stressed and exhausted during this task, there was still a statistically significant difference between DOM-treated and control groups for seizure-like behavioural expression (Figure A6.1, pg 245). This result indicates quite conclusively that exhaustion alone does not produce NIS-L expression, since all rats experienced an equivalent amount of activity, yet the DOM-treated group continued to exhibit increased seizure-like behaviour compared to control animals.

Two control rats also displayed the NIS-L syndrome in response to the forced swim experience, suggesting that these behaviours can be induced even without early DOM exposure. This possibility is not surprising, as seizure activity is not solely restricted to specific, susceptible individuals, but rather can occur in any brain through exciting neuronal systems beyond their limits (i.e. seizure threshold). In addition, it could be argued that all the rats in this study were not particularly 'normal' as they had all received telemetry surgery. However, while the high stress of the task was enough to push 2 of the controls beyond their seizure threshold, nearly 100% of the rats in the DOM-treated group were affected, indicating a heightened sensitivity in this group compared to those rats who had not experienced DOM exposure during development.

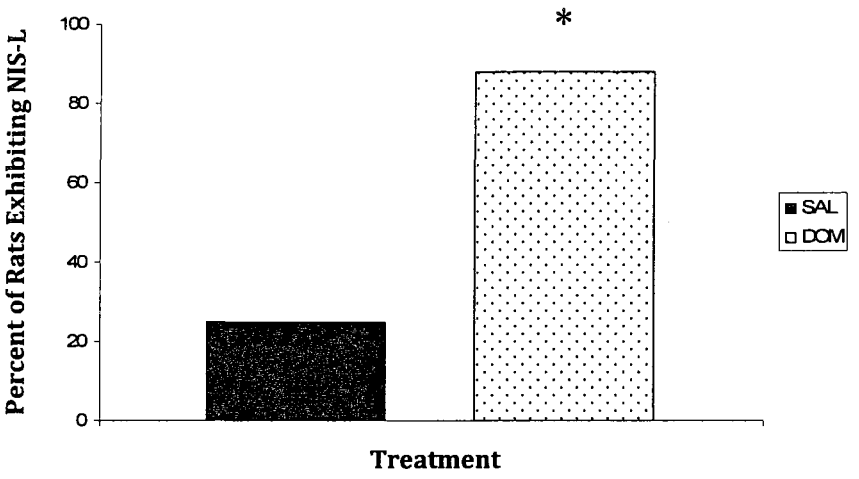

Figure A6.1. Percentage of rats exhibiting NIS-L behaviours during the forced swim test. The asterisk denotes a significant difference from saline controls ($p<0.05$).

APPENDIX B: ADDITIONAL KINDLING STUDY INFORMATION AND DATA

The following information represents supplemental data for the amygdala kindling study outlined in Chapter 3.

B.1 Investigation of tissue damage during electrode verification

During tissue cutting for electrode verification, it was noted that there appeared to be a relatively consistent damage to some of the brains anterior to the electrode position. Further investigation into the matter using H&E stain confirmed that this damage was not related to kindling, and had actually occurred at the time of euthanasia, as viable blood cells were present in the damaged tissue (Figure B1.1 below).

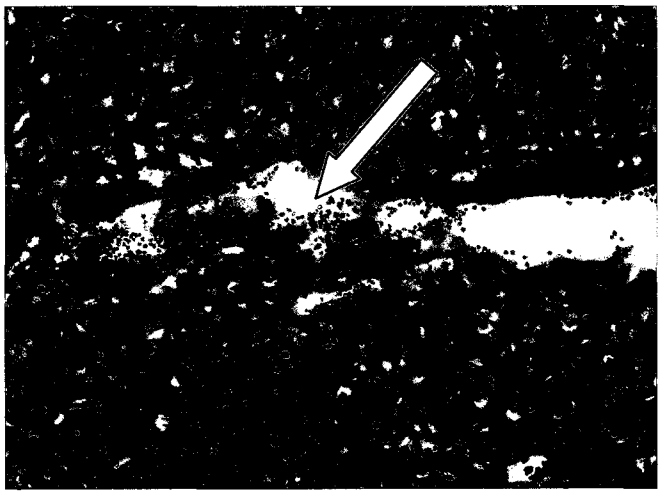

Figure B1.1. H&E stain to assess damage in anterior brain.

B.2 Additional after-discharge data for stress versus no-stress DOM and SAL rats over kindling days

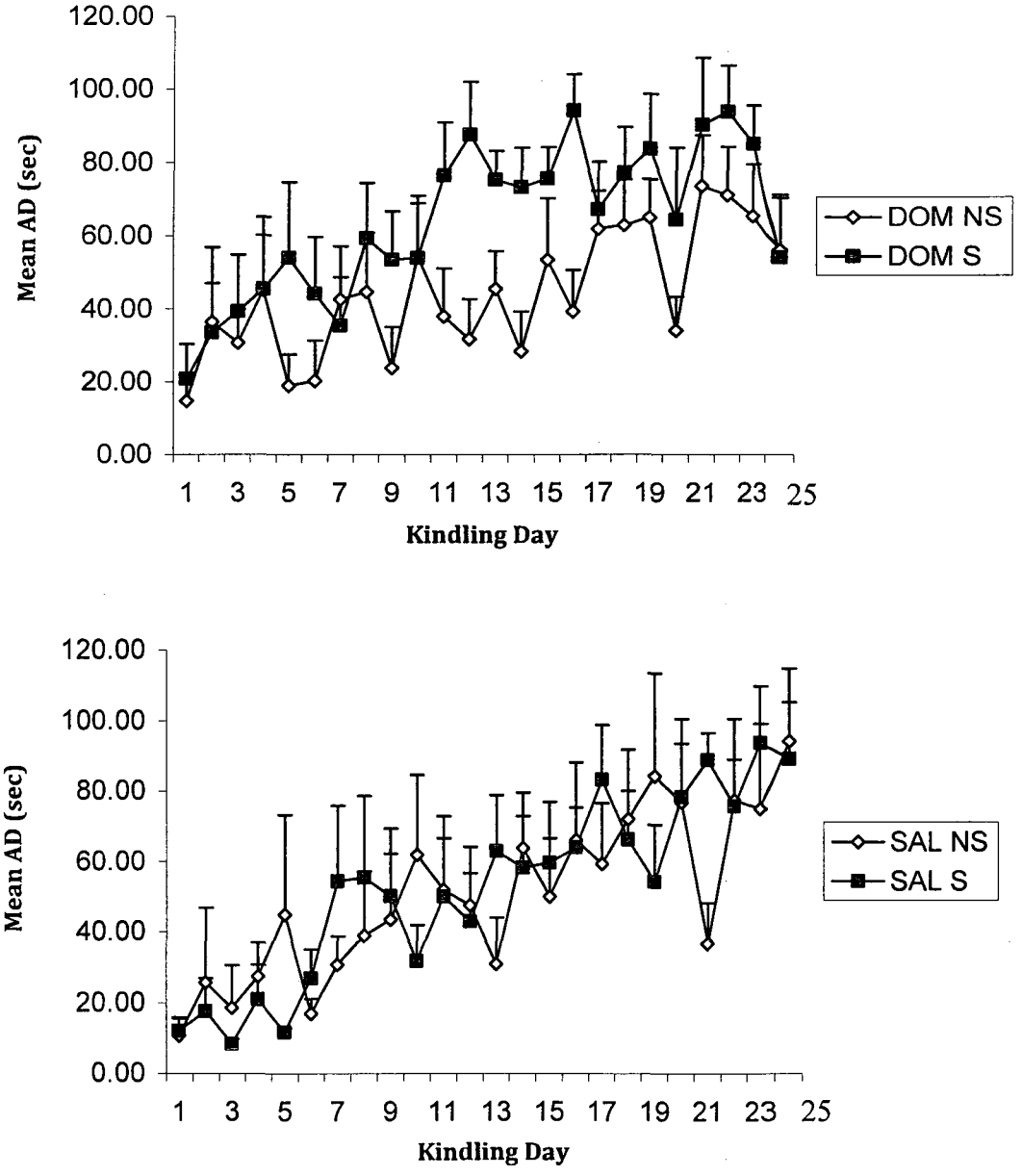

Figure B2.1. Mean after-discharge (AD) duration in seconds during amygdala kindling in DOM-treated and saline stressed and non-stressed rats. A) Duration of AD over kindling days for DOM-treated, acutely stressed (DOM S) compared to DOM-treated, non-stressed (DOM NS) rats. B) Duration of AD over kindling days for acutely stressed (SAL S) compared to non-stressed (SAL NS) control rats.

B.3 Behavioural data for stress and no-stress DOM and SAL rats over kindling days

Table B3.1. Summary of behavioural seizure progression and total behavioural seizures exhibited by acutely-stressed DOM-treated and control rat groups during kindling.

	SAL (mean ±SEM)	**DOM** (mean ±SEM)	p-value
Measure			
Latency to 1st Stage 2 (days)	4.00 (±0.8)	4.29 (±0.9)	0.823
Latency to 1st Stage 5 (days)	10.29 (±2.4)	9.29 (±1.1)	0.712
Total # Stage 5	11.86 (±1.9)	13.14 (±1.2)	0.577

APPENDIX C: ADDITIONAL IMMUNOHISTOCHEMISTRY PROTOCOLS AND QUANTIFICATION METHODS

In addition to the study described in Chapter 5, the following immunohistochemistry and luminescence quantification protocols were developed.

C.1 Somatostatin/Parvalbumin double-label and luminosity measurement

Introduction

In addition to the protocol described in Chapter 5, somatostatin was initially visualized through a double-label fluorescence protocol (SST and PV) to allow for quantification of SST- and PV-containing cells in the hilus. As well, this procedure allowed for a quantitative measure of the presence of SST and PV in both the granule cell layer and CA3 through luminosity (specific background-corrected fluorescent signal) evaluation (Kirkeby and Thomsen, 2005). Since SST is a neuropeptide that has been shown to exhibit anticonvulsant properties, and PV is a calcium-binding protein responsible for calcium level modulation, possible changes in SST or PV availability to the principal cells in these regions can be an important measure for evaluation of neuronal balance.

Experimental animals

All rats were treated as described in Chapter 5.

Materials and Methods

Following HIER, tissue was exposed to a standard blocking solution (3% goat serum, 2% BSA, 0.3% Triton X in TBS (pH 7.4) at RT for 2 hours and rinsed with TBS (2x15 min), then incubated at 4°C for 68 hours with an SST / PV cocktail (SST: rabbit polyclonal antibody 1:2000 Peninsula Labs #T4103; PV: mouse monoclonal antibody 1:2000, Abcam #ab50338, mixed with 1% goat, 0.2% BSA, 0.3% Triton-X and TBS). A green fluorescent secondary marker (Alexa Fluor 488, goat anti-rabbit 1:200, Invitrogen #A-11008) allowed identification of SST, while PV was visualized using

1:200 Alexa Fluor 594 (Invitrogen #A-20004) goat anti-mouse in 2% BSA, 0.3% Triton X and TBS, incubated for 3 hours at RT (see Figure C1.1, pg 253). Following a TBS rinse, slides were cover-slipped with Citifluor (Canemco-Marivac, P.Q.) and sealed with nail polish.

All fluorescent labels were acquired using a Fluroarc exciter lamp with a Zeiss Axioplan2 microscope (10x planar objective), and recorded using an attached AxioCam HR digital camera set manually to ensure image consistency. The luminosity of the granule cell layer and area CA3 was obtained through Adobe Photoshop CS (v.8.0) using macros designed to run in a 2-step process. The first step (pre-processing) provided contrast adjustment and low-pass filtering, allowing for subsequent selection of the appropriate region of interest (ROI). The second step was quantification of the mean luminosity for the ROI through histogram analysis (see Kirkeby and Thomsen (2005) for details). Statistical analysis of the resulting data was performed using a multivariate analysis of variance (SEX x COND) (v.10.0.5 SPSS Inc., Chicago IL), with t-tests for independent means utilized to evaluate any interactions if present. The criterion for statistical significance was set at $p \leq 0.05$.

Results

Although DOM treated rats generally exhibited less immunoreactivity than controls, quantification of SST-containing cells in the hilus revealed no statistically significant differences, similar to the results using the DAB protocol as presented in Chapter 5 (Figure C1.2, pg 253). In addition, there were no statistically significant differences noted in luminosity in any region measured (data not shown), although there was a SEX

x COND interaction in the dorsal DG for SST, with further investigation revealing a tendency for DOM-treated females to show less fluorescent signal [$t_{(7)} = 2.096$, $p = 0.074$] in the granule cell layer at that level.

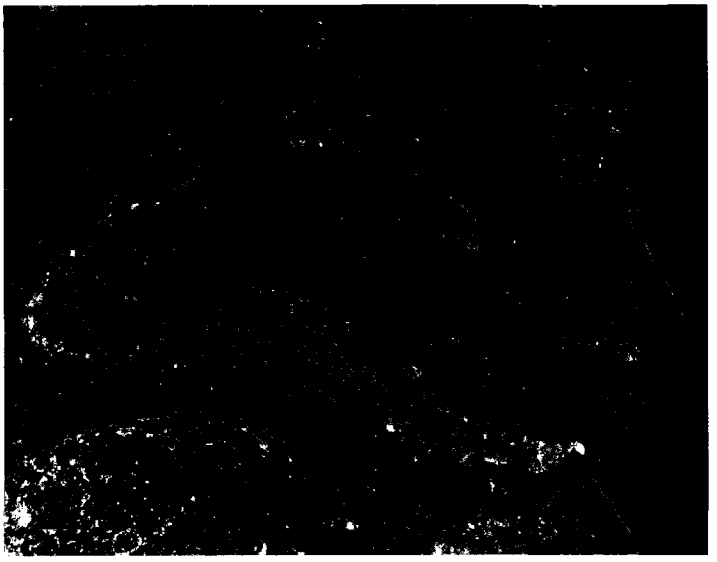

Figure C1.1. Representative somatostatin (green) and parvalbumin (red) double-labeled slice from the dorsal hippocampus.

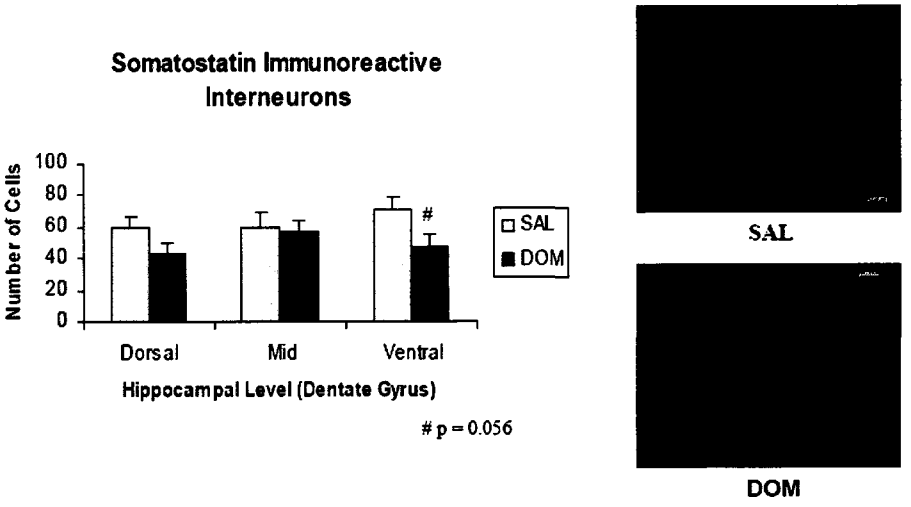

Figure C1.2. Mean somatostatin cell counts in the dentate gyrus of DOM-treated versus control rats. Error bars indicate SEM. Micrographs show representative images of the fluorescent labeling in ventral hippocampus for each group.

C.2 Mossy cell Protocol Development

Mossy cells, the principal neurons in the hilar region of the DG, are known to be very susceptible to seizure activity, and an antibody against calcitonin gene-related peptide (CGRP) is often used as a marker for these excitatory cells. Subsequently, a protocol for CGRP was developed, but the antibody did not appear to be specific enough to use for this purpose, even when counterstained with cresyl violet. Similarly, a run using GAD with a DAB secondary and counterstained with cresyl violet (to allow GAD to be subtracted from the total cell count through cresyl staining) was also unreliable (see Figure C2.1 below for representative images). Finally, NeuN, a neuron-specific marker, was used, with the intention of subtracting the GAD counts from the total neuronal population, a method that is also very commonly utilized in seizure studies. Unfortunately, although initial test runs seemed fine, the study tissue results were unreliable, with some slides exhibiting appropriate immunoreactivity, and others showing poor to almost nonexistent binding, rendering the NeuN counts unusable.

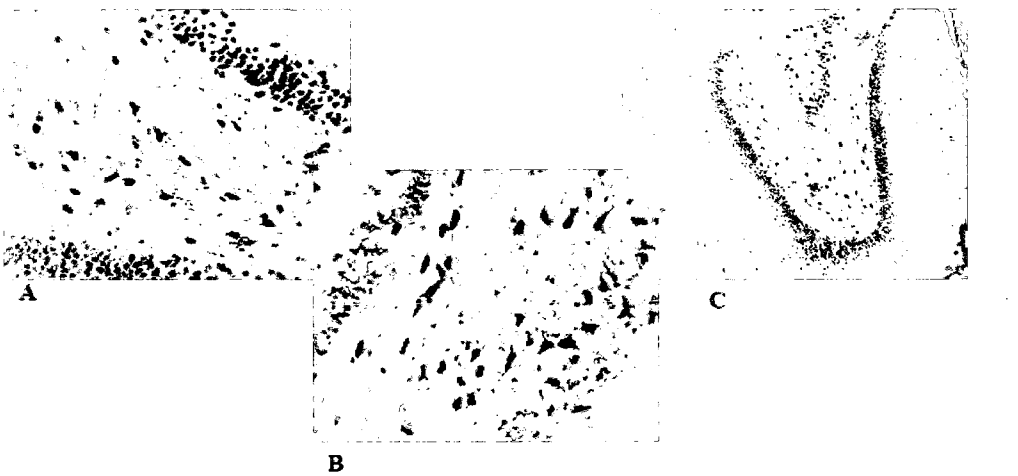

Figure C2.1. Micrographs of hippocampal tissue during protocol development for mossy cell visualization. A) DAB (nickel) labeled CGRP, but note the reactivity in the granule cells. B) GAD antibody with DAB and cresyl violet counterstain. C) CGRP with DAB and cresyl violet counterstain.

References

Acsady, L., Kamondi, A., Sik, A., Freund, T. & Buzsaki, G. (1998) GABAergic cells are the major postsynaptic targets of mossy fibers in the rat hippocampus. J. Neurosci., **18**, 3386-3403.

Adams, A. L., Doucette, T.A., James, R. & Ryan, C.L. (2009) Persistent changes in learning and memory in rats following neonatal treatment with domoic acid. Physiol. Behav., **96**, 505-512.

Adams, A. L., Doucette, T.A. & Ryan, C.L. (2008) Altered pre-pulse inhibition in adult rats treated neonatally with domoic acid. Amino Acids, **35**, 157-160.

Adams, B., Lee, M., Fahnestock, M. & Racine, R.J. (1997) Long-term potentiation trains induce mossy fiber sprouting. Brain Research, **775**, 193-197.

Aftanas, L. I., Reva, N.V., Savotina, L.N. & Makhnev, V.P. (2006) Neurophysiological correlates of induced discrete emotions in humans: An individually oriented analysis. Neurosci. Behav. Physiol., **36**, 119-130.

Ahern, T. H., Javors, M.A., Eagles, D.A., Martillotti, J., Mitchell, H.A., Liles, L.C. & Weinshenker, D. (2006) The effects of chronic norepinephrine transporter inactivation on seizure susceptibility in mice. Neuropsychopharmacology, **31**, 730-738.

Alsaadi, T. M., Thieman, C., Shatzel, A. & Farias, S. (2004) Video-EEG telemetry can be a crucial tool for neurologists experienced in epilepsy when diagnosing seizure disorders. Seizure, **13**, 32-34.

Amaral, D. G., Scharfman, H.E. & Lavenex, P. (2007) The dentate gyrus: Fundamental neuroanatomical organization (dentate gyrus for dummies). Prog. Brain Res., **163**, 3-22.

Amaral, D. G. & Witter, M.P. (1989) The three-dimensional organization of the hippocampal formation: A review of anatomical data. Neuroscience, **31**, 571-591.

Anch, A. M. & Laposky, A.D. (2000) Rat sleep and eye movement density as biological markers of demyelinating disease. Physiol. Behav., **71**, 269-275.

Andrade, R., Malenka, R.C. & Nicoll, R.A. (1986) A G protein couples serotonin and GABAB receptors to the same channels in hippocampus. Science, **234**, 1261-1265.

Andre, V., Pineau, N., Motte, J.E., Marescaux, C. & Nehlig, A. (1998) Mapping of neuronal networks underlying generalized seizures induced by increasing doses of pentylenetetrazol in the immature and adult rat: A c-fos immunohistochemical study. Eur. J. Neurosci., **10**, 2094-2106.

Ang, C. W., Carlson, G.C. & Coulter, D.A. (2006) Massive and specific dysregulation of direct cortical input to the hippocampus in temporal lobe epilepsy. J. Neurosci., **26**, 11850-11856.

Anwyl, R. (1991) Modulation of vertebrate neuronal calcium channels by transmitters. Brain Res. Brain Res. Rev., **16**, 265-281.

Arellano, J. I., Munoz, A., Ballesteros-Yanez, I., Sola, R.G. & DeFelipe, J. (2004) Histopathology and reorganization of chandelier cells in the human epileptic sclerotic hippocampus. Brain, **127**, 45-64.

Aroniadou-Anderjaska, V., Qashu, F. & Braga, M.F. (2007) Mechanisms regulating GABAergic inhibitory transmission in the basolateral amygdala: Implications for epilepsy and anxiety disorders. Amino Acids, **32**, 305-315.

Arrieta, O., Palencia, G., Garc¡a-Arenas, G., Morales-Espinosa, D., Hern ndez-Pedro, N. & Sotelo, J. (2005) Prolonged exposure to lead lowers the threshold of pentylenetetrazole-induced seizures in rats. Epilepsia, **46**, 1599-1602.

Avanzini, G. & Franceschetti, S. (2003) Cellular biology of epileptogenesis. The Lancet Neurology, **2**, 33-42.

Babb, T. L. (1991) Bilateral pathological damage in temporal lobe epilepsy. Can. J. Neurol. Sci., **18**, 645-648.

Bacci, A., Huguenard, J.R. & Prince, D.A. (2005) Modulation of neocortical interneurons: Extrinsic influences and exercises in self-control. Trends Neurosci., **28**, 602-610.

Banke, T. G. & McBain, C.J. (2006) GABAergic input onto CA3 hippocampal interneurons remains shunting throughout development. J. Neurosci., **26**, 11720-11725.

Barnard, E. A., Skolnick, P., Olsen, R.W., Mohler, H., Sieghart, W., Biggio, G., Braestrup, C., Bateson, A.N. & Langer, S.Z. (1998) International union of pharmacology. XV. subtypes of gamma-aminobutyric acidA receptors: Classification on the basis of subunit structure and receptor function. Pharmacol. Rev., **50**, 291-313.

Bartesaghi, R., Gessi, T. & Migliore, M. (1995) Input-output relations in the entorhinal-hippocampal-entorhinal loop: Entorhinal cortex and dentate gyrus. Hippocampus, **5**, 440-451.

Bassetti, C. L. & Aldrich, M.S. (2001) Sleep electroencephalogram changes in acute hemispheric stroke. Sleep Med., **2**, 185-194.

Bastlund, J. F., Jennum, P., Mohapel, P., Penschuck, S. & Watson, W.P. (2005) Spontaneous epileptic rats show changes in sleep architecture and hypothalamic pathology. Epilepsia, **46**, 934-938.

Bastlund, J. F., Jennum, P., Mohapel, P., Vogel, V. & Watson, W.P. (2004) Measurement of cortical and hippocampal epileptiform activity in freely moving rats by means of implantable radiotelemetry. J. Neurosci. Methods, **138**, 65-72.

Bazil, C. W. (2007) Sleep and epilepsy; FAQ. **2007.** http://www.epilepsy.com/articles.ar. Accessed August 2009.

Bazil, C. W. (2000) Sleep and epilepsy. Curr. Opin. Neurol., **13**, 171-175.

Behr, J., Lyson, K.J. & Mody, I. (1998) Enhanced propagation of epileptiform activity through the kindled dentate gyrus. J. Neurophysiol., **79**, 1726-1732.

Behr, J., Gloveli, T., Gutierrez, R. & Heinemann, U. (1996) Spread of low Mg2+ induced epileptiform activity from the rat entorhinal cortex to the hippocampus after kindling studied in vitro. Neurosci. Lett., **216**, 41-44.

Ben-Ari, Y., Gaiarsa, J.L., Tyzio, R. & Khazipov, R. (2007) GABA: A pioneer transmitter that excites immature neurons and generates primitive oscillations. Physiol. Rev., **87**, 1215-1284.

Ben-Ari, Y. (2006a) Basic developmental rules and their implications for epilepsy in the immature brain. Epileptic Disord., **8**, 91-102.

Ben-Ari, Y. (2006b) Seizures beget seizures: The quest for GABA as a key player. Crit. Rev. Neurobiol., **18**, 135-144.

Ben-Ari, Y., Khalilov, I., Represa, A. & Gozlan, H. (2004) Interneurons set the tune of developing networks. Trends Neurosci., **27**, 422-427.

Ben-Ari, Y. (2002) Excitatory actions of GABA during development: The nature of the nurture. Nature Reviews, **3**, 728-739.

Ben-Ari, Y. & Cossart, R. (2000) Kainate, a double agent that generates seizures: Two decades of progress. Trends in Neuroscience, **23**, 580-587.

Ben-Ari, Y., Cherubini, E., Corradetti, R. & Gaiarsa, J.L. (1989) Giant synaptic potentials in immature rat CA3 hippocampal neurones. J. Physiol., **416**, 303-325.

Bender, R. A. & Baram, T.Z. (2007) Epileptogenesis in the developing brain: What can we learn from animal models? Epilepsia, **48 Suppl 5**, 2-6.

Bengzon, J., Kokaia, Z., Elmer, E., Nanobashvili, A., Kokaia, M. & Lindvall, O. (1997) Apoptosis and proliferation of dentate gyrus neurons after single and intermittent limbic seizures. Proc. Natl. Acad. Sci. U. S. A., **94**, 10432-10437.

Benveniste, M. & Mayer, M.L. (1991) Kinetic analysis of antagonist action at N-methyl-D-aspartic acid receptors. two binding sites each for glutamate and glycine. Biophys. J., **59**, 560-573.

Bernard, C. (2006) Hippocampal slices: Designing and interpreting studies in epilepsy research. In Pitkanen, A., Schwartzkroin, P. A. & Moshe, S. L. (eds), Elsevier Inc., USA, pp. 59.

Bernard, A., Ferhat, L., Dessi, F., Charton, G., Represa, A., Ben-Ari, Y. & Khrestchatisky, M. (1999) Q/R editing of the rat GluR5 and GluR6 kainate receptors in vivo and in vitro: Evidence for independent developmental, pathological and cellular regulation. Eur. J. Neurosci., **11**, 604-616.

Bernard, C., Marsden, D.P. & Wheal, H.V. (2001) Changes in neuronal excitability and synaptic function in a chronic model of temporal lobe epilepsy. Neuroscience, **103**, 17-26.

Bernard, P. B., Macdonald, D.S., Gill, D.A., Ryan, C.L. & Tasker, R.A. (2007) Hippocampal mossy fiber sprouting and elevated trkB receptor expression following systemic administration of low dose domoic acid during neonatal development. Hippocampus, **17**, 1121-1133.

Berretta, S. (2005) Cortico-amygdala circuits: Role in the conditioned stress response. Stress, **8**, 221-232.

Bertram, E. H. (2009) Temporal lobe epilepsy: Where do the seizures really begin? Epilepsy Behav., **14 Suppl 1**, 32-37.

Bertram, E. H. (2006) Monitoring for seizures in rodents. In Pitkanen, A., Schwartzkroin, P. A. & Moshe, S. L. (eds), *Models of Seizure and Epilepsy.* Elsevier Inc., USA, pp. 569-600.

Bertram, E. H., Mangan, P.S., Zhang, D., Scott, C.A. & Williamson, J.M. (2001) The midline thalamus: Alterations and a potential role in limbic epilepsy. Epilepsia, **42**, 967-978.

Bertram, E. H., Zhang, D.X., Mangan, P., Fountain, N. & Rempe, D. (1998) Functional anatomy of limbic epilepsy: A proposal for central synchronization of a diffusely hyperexcitable network. Epilepsy Res., **32**, 194-205.

Bettler, B., Kaupmann, K., Mosbacher, J. & Gassmann, M. (2004) Molecular structure and physiological functions of $GABA_B$ receptors. Physiol. Rev., **84**, 835-867.

Bianchi, M. T., Haas, K.F. & Macdonald, R.L. (2001) Structural determinants of fast desensitization and desensitization-deactivation coupling in GABAa receptors. J. Neurosci., **21**, 1127-1136.

Bibbig, A., Middleton, S., Racca, C., Gillies, M.J., Garner, H., Lebeau, F.E., Davies, C.H. & Whittington, M.A. (2007) Beta rhythms (15-20 hz) generated by nonreciprocal communication in hippocampus. J. Neurophysiol., **97**, 2812-2823.

Binaschi, A., Bregola, G. & Simonato, M. (2003) On the role of somatostatin in seizure control: Clues from the hippocampus. Rev. Neurosci., **14**, 285-301.

Bischoff, S., Leonhard, S., Reymann, N., Schuler, V., Shigemoto, R., Kaupmann, K. & Bettler, B. (1999) Spatial distribution of GABA(B)R1 receptor mRNA and binding sites in the rat brain. J. Comp. Neurol., **412**, 1-16.

Bleakman, D., Gates, M.R., Ogden, A.M. & Mackowiak, M. (2002) Kainate receptor agonists, antagonists and allosteric modulators. Curr. Pharm. Des., **8**, 873-885.

Blume, W. T. (2006) The progression of epilepsy. Epilepsia, **47 Suppl 1**, 71-78.

Bonan, C. D., Amaral, O.B., Rockenback, I.C., Walz, R., Battastini, A.M.O., Izquierdo, I. & Sarkis, J.J.F. (2000) Altered ATP hydrolysis induced by pentylenetetrazol kindling in rat brain synaptosomes. Neurochem. Res., **25**, 775-779.

Bordey, A. & Sontheimer, H. (1998) Properties of human glial cells associated with epileptic seizure foci. Epilepsy Res., **32**, 286-303.

Boulton, C. L., von Haebler, D. & Heinemann, U. (1992) Tracing of axonal connections by rhodamine-dextran-amine in the rat hippocampal-entorhinal cortex slice preparation. Hippocampus, **2**, 99-106.

Braga, M. F. M., Aroniadou-Anderjaska, V. & Li, H. (2004) The physiological role of kainate receptors in the amygdala. Mol. Neurobiol., **30**, 127-141.

Braga, M. F. M., Aroniadou-Anderjaska, V., Xie, J. & Li, H. (2003) Bidirectional modulation of GABA release by presynaptic glutamate receptor 5 kainate receptors in the basolateral amygdala. The Journal of Neuroscience, **23**, 442-452.

Bragin, A., Wilson, C.L. & Engel, J.,Jr (2002) Increased afterdischarge threshold during kindling in epileptic rats. Exp. Brain Res., **144**, 30-37.

Braun, H., Schulz, S., Becker, A., Schroder, H. & Hollt, V. (1998) Protective effects of cortistatin (CST-14) against kainate-induced neurotoxicity in rat brain. Brain Res., **803**, 54-60.

Brauner-Osborne, H., Wellendorph, P. & Jensen, A.A. (2007) Structure, pharmacology and therapeutic prospects of family C G-protein coupled receptors. Curr. Drug Targets, **8**, 169-184.

Breustedt, J. & Schmitz, D. (2004) Assessing the role of GluK5 and GluK6 at hippocampal mossy fiber synapses. The Journal of Neuroscience, **24**, 10093-10098.

Brooks-Kayal, A. R. (2005) Rearranging receptors. Epilepsia, **46 Suppl 7**, 29-38.

Buckmaster, P. S. (2006) Inherited epilepsy in mongolian gerbils. In Pitkanen, A., Schwartzkroin, P. A. & Moshe, S. L. (eds), *Models of Seizure and Epilepsy.* Elsevier Inc, USA, pp. 273-294.

Buckmaster, P. S. (2004) Laboratory animal models of temporal lobe epilepsy. Comp. Med., **54**, 473-485.

Buckmaster, P. S. & Dudek, F.E. (1997a) Network properties of the dentate gyrus in epileptic rats with hilar neuron loss and granule cell axon reorganization. J. Neurophysiol., **77**, 2685-2696.

Buckmaster, P. S. & Dudek, F.E. (1997b) Neuron loss, granule cell axon reorganization, and functional changes in the dentate gyrus of epileptic kainate-treated rats. J. Comp. Neurol., **385**, 385-404.

Buckmaster, P. S. & Schwartzkroin, P.A. (1994) Hippocampal mossy cell function: A speculative view. Hippocampus, **4**, 393-402.

Burgard, E. C. & Hablitz, J.J. (1993) Developmental changes in NMDA and non-NMDA receptor-mediated synaptic potentials in rat neocortex. J. Neurophysiol., **69**, 230-239.

Burt, M. A., Ryan, C.L. & Doucette, T.A. (2008a) Low dose domoic acid in neonatal rats abolishes nicotine induced conditioned place preference during late adolescence. Amino Acids, **35**, 247-249.

Burt, M. A., Ryan, C.L. & Doucette, T.A. (2008b) Altered responses to novelty and drug reinforcement in adult rats treated neonatally with domoic acid. Physiol. Behav., **93**, 327-336.

Buzsaki, G. (2002) Theta oscillations in the hippocampus. Neuron, **33**, 1-20.

Carreno, M., Donaire, A. & Sanchez-Carpintero, R. (2008) Cognitive disorders associated with epilepsy: Diagnosis and treatment. Neurologist, **14**, S26-34.

Cascella, N. G., Schretlen, D.J. & Sawa, A. (2009) Schizophrenia and epilepsy: Is there a shared susceptibility? Neurosci. Res., **63**, 227-235.

Castillo, P. E., Malenka, R.C. & Nicoll, R.A. (1997) Kainate receptors mediate a slow postsynaptic current in hippocampal CA3 neurons. Nature, **388**, 182-186.

Cavazos, J. E., Golarai, G. & Sutula, T.P. (1991) Mossy fiber synaptic reorganization induced by kindling: Time course of development, progression, and permanence. The Journal of Neuroscience, **11**, 2795-2803.

Cendes, F., Andermann, F., Carpenter, S., Zatorre, R.J. & Cashman, N.R. (1995) Temporal lobe epilepsy caused by domoic acid intoxication: Evidence for glutamate receptor-mediated excitotoxicity in humans. Ann. Neurol., **37**, 123-126.

Chadderton, P., Margrie, T.W. & Hausser, M. (2004) Integration of quanta in cerebellar granule cells during sensory processing. Nature, **428**, 856-860.

Chang, H. R. & Kuo, C.C. (2008) The activation gate and gating mechanism of the NMDA receptor. J. Neurosci., **28**, 1546-1556.

Chittajallu, R., Vignes, M., Dev, K.K., Barnes, J.M., Collingridge, G.L. & Henley, J.M. (1996) Regulation of glutamate release by presynaptic kainate receptors in the hippocampus. Nature, **379**, 78-81.

Choi, D. W. & Rothman, S.M. (1990) The role of glutamate neurotoxicity in hypoxic-ischemic neuronal death. Annu. Rev. Neurosci., **13**, 171-182.

Choi, D. W. (1988) Glutamate neurotoxicity and diseases of the nervous system. Neuron, **1**, 623-634.

Christine, C. W. & Choi, D.W. (1990) Effect of zinc on NMDA receptor-mediated channel currents in cortical neurons. J. Neurosci., **10**, 108-116.

Chudotvorova, I., Ivanov, A., Rama, S., Hubner, C.A., Pellegrino, C., Ben-Ari, Y. & Medina, I. (2005a) Early expression of KCC2 in rat hippocampal cultures augments expression of functional GABA synapses. J. Physiol., **566**, 671-679.

Clancy, B., Darlington, R.B. & Finlay, B.L. (2001) Translating developmental time across mammalian species. Neuroscience, **105**, 7-17.

Clarke, V. R. & Collingridge, G.L. (2004) Characterisation of the effects of ATPA, a GLU(K5) kainate receptor agonist, on GABAergic synaptic transmission in the CA1 region of rat hippocampal slices. Neuropharmacology, **47**, 363-372.

Clements, J. D. & Westbrook, G.L. (1991) Activation kinetics reveal the number of glutamate and glycine binding sites on the N-methyl-D-aspartate receptor. Neuron, **7**, 605-613.

Cole, T. B., Wenzel, H.J., Kafer, K.E., Schwartzkroin, P.A. & Palmiter, R.D. (1999) Elimination of zinc from synaptic vesicles in the intact mouse brain by disruption of the ZnT3 gene. Proc. Natl. Acad. Sci. U. S. A., **96**, 1716-1721.

Commission on Classification and Terminology of the International League Against Epilepsy (1981) Proposal for revised clinical and electroencephalographic classification of epileptic seizures. Epilepsia, **22**, 489-501.

Conn, P. J. & Pin, J.P. (1997) Pharmacology and functions of metabotropic glutamate receptors. Annu. Rev. Pharmacol. Toxicol., **37**, 205-237.

Cortez, M. A. & Snead, O. C. (2006) Pharmacologic models of generalized absence seizures in rodents. In Pitkanen, A., Schwartzkroin, P. A. & Moshe, S. L. (eds), Elsevier Inc., USA, pp. 111.

Cossart, R., Tyzio, R., Dinocourt, C., Esclapez, M., Hirsch, J.C., Ben-Ari, Y. & Bernard, C. (2001) Presynaptic kainate receptors that enhance the release of GABA on CA1 hippocampal interneurons. Neuron, **29**, 497-508.

Coussen, F. (2009) Molecular determinants of kainate receptor trafficking. Neuroscience, **158**, 25-35.

Coyle, J. T. (2006) Glutamate and schizophrenia: Beyond the dopamine hypothesis. Cell. Mol. Neurobiol., **26**, 365-384.

Csaba, Z., Richichi, C., Bernard, V., Epelbaum, J., Vezzani, A. & Dournaud, P. (2004) Plasticity of somatostatin and somatostatin sst2A receptors in the rat dentate gyrus during kindling epileptogenesis. Eur. J. Neurosci., **19**, 2531-2538.

Cunha, R. A., Constantino, M.D. & Ribeiro, J.A. (1997) Inhibition of [3H] gamma-aminobutyric acid release by kainate receptor activation in rat hippocampal synaptosomes. Eur. J. Pharmacol., **323**, 167-172.

Dakshinamurti, K., Sharma, S.K., Sundaram, M. & Watanabe, T. (1993) Hippocampal changes in developing postnatal mice following intrauterine exposure to domoic acid. J. Neurosci., **13**, 4486-4495.

D'Ambrosio, R., Maris, D.O., Grady, M.S., Winn, H.R. & Janigro, D. (1999) Impaired K(+) homeostasis and altered electrophysiological properties of post-traumatic hippocampal glia. J. Neurosci., **19**, 8152-8162.

Davies, S. N., Alford, S.T., Coan, E.J., Lester, R.A. & Collingridge, G.L. (1988) Ketamine blocks an NMDA receptor-mediated component of synaptic transmission in rat hippocampus in a voltage-dependent manner. Neurosci. Lett., **92**, 213-217.

Davis, M. & Whalen, P.J. (2001) The amygdala: Vigilance and emotion. Mol. Psychiatry, **6**, 13-34.

de Lanerolle, N. C., Kim, J.H., Robbins, R.J. & Spencer, D.D. (1989) Hippocampal interneuron loss and plasticity in human temporal lobe epilepsy. Brain Res., **495**, 387-395.

Debonnel, G., Weiss, M. & de Montigny, C. (1990) Neurotoxic effect of domoic acid: Mediation by kainate receptor electrophysiological studies in the rat. Can. Dis. Wkly. Rep., **16 Suppl 1E**, 59-68.

Deco, G. & Thiele, A. (2009) Attention - oscillations and neuropharmacology. Eur. J. Neurosci., .

Deller, T., Adelmann, G., Nitsch, R. & Frotscher, M. (1996) The alvear pathway of the rat hippocampus. Cell Tissue Res., **286**, 293-303.

Delpire, E. (2000) Cation-chloride cotransporters in neuronal communication. News Physiol. Sci., **15**, 309-312.

DeReuter, J. (2004) GABAminergic neurotransmission: Introduction. www.*auburn.edu* /~deruija/*GABA*_Intro2002.pdf . Accessed June 2009.

Dingledine, R., Borges, K., Bowie, D. & Traynelis, S.F. (1999) The glutamate receptor ion channels. Pharmacol. Rev. **51**, 7-61.

Dingledine, R., Kleckner, N.W. & McBain, C.J. (1990) The glycine coagonist site of the NMDA receptor. Adv. Exp. Med. Biol., **268**, 17-26.

Dingledine, R., Boland, L.M., Chamberlin, N.L., Kawasaki, K., Kleckner, N.W., Traynelis, S.F. & Verdoorn, T.A. (1988) Amino acid receptors and uptake systems in the mammalian central nervous system. Crit. Rev. Neurobiol., **4**, 1-96.

Dobbing, J. & Sands, J. (1979) Comparative aspects of the brain growth spurt. Early Hum. Dev., **3**, 79-83.

Dobbing, J. & Smart, J.L. (1974) Vulnerability of developing brain and behaviour. Br. Med. Bull., **30**, 164-168.

Doucette, T. A., Ryan, C.L. & Tasker, R.A. (2007) Gender-based changes in cognition and emotionality in a new rat model of epilepsy. Amino Acids, **32**, 317-322.

Doucette, T. A., Bernard, P.B., Husum, H., Perry, M.A., Ryan, C.L. & Tasker, R.A. (2004) Low doses of domoic acid during postnatal development produce permanent changes in rat behaviour and hippocampal morphology. Neurotoxicity Research, **6**, 555-563.

Doucette, T. A., Bernard, P.B., Yuill, P.C., Tasker, R.A. & Ryan, C.L. (2003) Low doses of non-NMDA glutamate receptor agonists alter neurobehavioural development in the rat. Neurotoxicol. Teratol., **25**, 473-479.

Doucette, T. A., Strain, S.M., Allen, G.V., Ryan, C.L. & Tasker, R.A.R. (2000) Comparative behavioural toxicity of domoic acid and kainic acid in neonatal rats. Neurotoxicol. Teratol., **22**, 863-869.

Dragunow, M. & Robertson, H.A. (1988) Brain injury induces c-fos protein(s) in nerve and glial-like cells in adult mammalian brain. Brain Res., **455**, 295-299.

Duchowny, M. S. & Burchfiel, J.L. (1981) Facilitation and antagonism of kindled seizure development in the limbic system of the rat. Electroencephalogr. Clin. Neurophysiol., **51**, 403-416.

Dudek, F. E. & Sutula, T.P. (2007) Epileptogenesis in the dentate gyrus: A critical perspective. Prog. Brain Res., **163**, 755-773.

Dugich-Djordjevic, M. M., Tocco, G., Willoughby, D.A., Najm, I., Pasinetti, G., Thompson, R.F., Baudry, M., Lapchak, P.A. & Hefti, F. (1992) BDNF mRNA expression in the developing rat brain following kainic acid-induced seizure activity. Neuron, **8**, 1127-1138.

Durand, G. M., Kovalchuk, Y. & Konnerth, A. (1996) Long-term potentiation and functional synapse induction in developing hippocampus. Nature, **381**, 71-75.

Durand, G. M., Bennett, M.V. & Zukin, R.S. (1993) Splice variants of the N-methyl-D-aspartate receptor NR1 identify domains involved in regulation by polyamines and protein kinase C. Proc. Natl. Acad. Sci. U. S. A., **90**, 6731-6735.

Durkin, M. M., Gunwaldsen, C.A., Borowsky, B., Jones, K.A. & Branchek, T.A. (1999) An in situ hybridization study of the distribution of the GABA(B2) protein mRNA in the rat CNS. Brain Res. Mol. Brain Res., **71**, 185-200.

Ehrlich, I., Humeau, Y., Grenier, F., Ciocchi, S., Herry, C. & Luthi, A. (2009) Amygdala inhibitory circuits and the control of fear memory. Neuron, **62**, 757-771.

El-Hassar, L., Esclapez, M. & Bernard, C. (2007) Hyperexcitability of the CA1 hippocampal region during epileptogenesis. Epilepsia, **48 Suppl 5**, 131-139.

Engel, D., Pahner, I., Schulze, K., Frahm, C., Jarry, H., Ahnert-Hilger, G. & Draguhn, A. (2001) Plasticity of rat central inhibitory synapses through GABA metabolism. J. Physiol., **535**, 473-482.

Engel, J.Jr & Schwartzkroin, P. A. (2006) What good are animal models? In Pitkanen, A., Schwartzkroin, P. A. & Moshe, S. L. (eds), *Models of Seizure and Epilepsy.* Elsevier Inc., Massachusettes, USA, pp. 659.

Epilepsy Foundation of America (a) Epilepsy treatment. **2009**. http://www.epilepsyfoundation.org/about/treatment/ Accessed July 2009.

Epilepsy Foundation of America (b) Diagnosing epilepsy: The EEG test. **2009**.http://www.epilepsyfoundation.org/about/diagnosis/eeg.cfm. Accessed August 2009.

Epilepsy Foundation of America (c) The human brain: Seizure mechanisms and threshold. **2009**. http://www.epilepsyfoundation.org/answerplace/Medical/seizures/science/mechanisms.cfm. Accessed July 2009.

Essrich, C., Lorez, M., Benson, J.A., Fritschy, J.M. & Luscher, B. (1998) Postsynaptic clustering of major GABAA receptor subtypes requires the gamma 2 subunit and gephyrin. Nat. Neurosci., **1**, 563-571.

Eugene, E., Depienne, C., Baulac, S., Baulac, M., Fritschy, J.M., Le Guern, E., Miles, R. & Poncer, J.C. (2007) GABAA receptor {gamma}2 subunit mutations linked to human epileptic syndromes differentially affect phasic and tonic inhibition. J. Neurosci., **27**, 14108-14116.

Evans, R. H., Francis, A.A., Jones, A.W., Smith, D.A. & Watkins, J.C. (1982) The effects of a series of omega-phosphonic alpha-carboxylic amino acids on electrically evoked and excitant amino acid-induced responses in isolated spinal cord preparations. Br. J. Pharmacol., **75**, 65-75.

Faber, E. S., Callister, R.J. & Sah, P. (2001) Morphological and electrophysiological properties of principal neurons in the rat lateral amygdala in vitro. J. Neurophysiol., **85**, 714-723.

Farb, C. R., Aoki, C. & Ledoux, J.E. (1995) Differential localization of NMDA and AMPA receptor subunits in the lateral and basal nuclei of the amygdala: A light and electron microscopic study. J. Comp. Neurol., **362**, 86-108.

Farrant, M. & Nusser, Z. (2005) Variations on an inhibitory theme: Phasic and tonic activation of GABA(A) receptors. Nat. Rev. Neurosci., **6**, 215-229.

Farrar, S. J., Whiting, P.J., Bonnert, T.P. & McKernan, R.M. (1999) Stoichiometry of a ligand-gated ion channel determined by fluorescence energy transfer. J. Biol. Chem., **274**, 10100-10104.

Fisahn, A., Contractor, A., Traub, R.D., Buhl, E.H., Heinemann, S.F. & McBain, C.J. (2004) Distinct roles for the kainate receptor subunits GluR5 and GluR6 in kainate-induced hippocampal gamma oscillations. J. Neurosci., **24**, 9658-9668.

Fisher, R. S. (1989) Animal models of the epilepsies. Brain Res. Rev., **14**, 245-278.

Fleck, M. W., Cornell, E. & Mah, S.J. (2003) Amino-acid residues involved in glutamate receptor 6 kainate receptor gating and desensitization. J. Neurosci., **23**, 1219-1227.

Flynn, C. & Teskey, G.C. (2007) Reduction of seizure thresholds following electrical stimulation of sensorimotor cortex is dependent on stimulation intensity and is not related to synaptic potentiation. Neuroscience, **149**, 263-272.

Follett, P. L., Rosenberg, P.A., Volpe, J.J. & Jensen, F.E. (2000) NBQX attenuates excitotoxic injury in developing white matter. J. Neurosci., **20**, 9235-9241.

Franceschetti, S., Guatteo, E., Panzica, F., Sancini, G., Wanke, E. & Avanzini, G. (1995) Ionic mechanisms underlying burst firing in pyramidal neurons: Intracellular study in rat sensorimotor cortex. Brain Res., **696**, 127-139.

Frerking, M., Petersen, C.C. & Nicoll, R.A. (1999) Mechanisms underlying kainate receptor-mediated disinhibition in the hippocampus. Proc. Natl. Acad. Sci. U. S. A., **96**, 12917-12922.

Frerking, M., Malenka, R.C. & Nicoll, R.A. (1998) Synaptic activation of kainate receptors on hippocampal interneurons. Nat. Neurosci., **1**, 479-486.

Freund, T. F. & Buzsaki, G. (1996) Interneurons of the hippocampus. Hippocampus, **6**, 347-470.

Frotscher, M., Jonas, P. & Sloviter, R.S. (2006) Synapses formed by normal and abnormal hippocampal mossy fibers. Cell Tissue Res., **326**, 361-367.

Frucht, M. M., Quigg, M., Schwaner, C. & Fountain, N.B. (2000) Distribution of seizure precipitants among epilepsy syndromes. Epilepsia, **41**, 1534-1539.

Furukawa, H., Singh, S.K., Mancusso, R. & Gouaux, E. (2005) Subunit arrangement and function in NMDA receptors. Nature, **438**, 185-192.

Gaitatzis, A., Trimble, M.R. & Sander, J.W. (2004) The psychiatric comorbidity of epilepsy. Acta Neurol. Scand., **110**, 207-220.

Galanopoulou, A. S. (2008a) Dissociated gender-specific effects of recurrent seizures on GABA signaling in CA1 pyramidal neurons: Role of GABA(A) receptors. J. Neurosci., **28**, 1557-1567.

Galanopoulou, A. S. (2008b) Sexually dimorphic expression of KCC2 and GABA function. Epilepsy Res., **80**, 99-113.

Galvan, C. D., Hrachovy, R.A., Smith, K.L. & Swann, J.W. (2000) Blockade of neuronal activity during hippocampal development produces a chronic focal epilepsy in the rat. The Journal of Neuroscience, **20**, 2904-2916.

Garcia-Rill, E., Charlesworth, A., Heister, D., Ye, M. & Hayar, A. (2008) The developmental decrease in REM sleep: The role of transmitters and electrical coupling. Sleep, **31**, 673-690.

Gerber, U. & Gahwiler, B.H. (1994) GABAB and adenosine receptors mediate enhancement of the K+ current, IAHP, by reducing adenylyl cyclase activity in rat CA3 hippocampal neurons. J. Neurophysiol., **72**, 2360-2367.

Geyer, M. A. (2008) Developing translational animal models for symptoms of schizophrenia or bipolar mania. Neurotox Res., **14**, 71-78.

Gigli, G. L. & Gotman, J. (1992) Effects of seizures, kindling, and carbamazepine on sleep organization in cats. Epilepsia, **33**, 14-22.

Gloveli, T., Schmitz, D. & Heinemann, U. (1998) Interaction between superficial layers of the entorhinal cortex and the hippocampus in normal and epileptic temporal lobe. Epilepsy Res., **32**, 183-193.

Glykys, J. & Mody, I. (2007) Activation of GABAA receptors: Views from outside the synaptic cleft. Neuron, **56**, 763-770.

Goddard, G. V. (1967) Development of epileptic seizures through brain stimulation at low intensity. Nature, **214**, 1020-1021.

Goddard, G. V., McIntyre, D.C. & Leech, C.K. (1969) A permanent change in brain function resulting from daily electrical stimulation. Exp. Neurol., **25**, 295-330.

Goldstein, L. E., Rasmusson, A.M., Bunney, B.S. & Roth, R.H. (1996) Role of the amygdala in the coordination of behavioral, neuroendocrine, and prefrontal cortical monoamine responses to psychological stress in the rat. The Journal of Neuroscience, **16**, 4787-4798.

Gouaux, E. (2004) Structure and function of AMPA receptors. J. Physiol., **554**, 249-253.

Greger, I. H. & Esteban, J.A. (2007) AMPA receptor biogenesis and trafficking. Curr. Opin. Neurobiol., **17**, 289-297.

Grimmelt, B., Nijjar, M.S., Brown, J., Macnair, N., Wagner, S., Johnson, G.R. & Amend, J.F. (1990) Relationship between domoic acid levels in the blue mussel (mytilus edulis) and toxicity in mice. Toxicon, **28**, 501-508.

Gubellini, P., Ben-Ari, Y. & Gaïarsa, J. (2001) Activity- and age-dependent GABAergic synaptic plasticity in the developing rat hippocampus. Eur. J. Neurosci., **14**, 1937-1946.

Gulyas, A. I., Megias, M., Emri, Z. & Freund, T.F. (1999) Total number and ratio of excitatory and inhibitory synapses converging onto single interneurons of different types in the CA1 area of the rat hippocampus. J. Neurosci., **19**, 10082-10097.

Haas, K. F. & Macdonald, R.L. (1999) GABAA receptor subunit gamma2 and delta subtypes confer unique kinetic properties on recombinant GABAA receptor currents in mouse fibroblasts. J. Physiol., **514 (Pt 1)**, 27-45.

Haas, K. Z., Sperber, E.F., Moshe, S.L. & Stanton, P.K. (1996) Kainic acid-induced seizures enhance dentate gyrus inhibition by downregulation of GABA(B) receptors. J. Neurosci., **16**, 4250-4260.

Haas, K. Z., Sperber, E.F. & Moshe, S.L. (1992) Kindling in developing animals: Interactions between ipsilateral foci. Brain Res. Dev. Brain Res., **68**, 140-143.

Haas, K. Z., Sperber, E.F. & Moshe, S.L. (1990) Kindling in developing animals: Expression of severe seizures and enhanced development of bilateral foci. Brain Res. Dev. Brain Res., **56**, 275-280.

Hamann, M., Rossi, D.J. & Attwell, D. (2002) Tonic and spillover inhibition of granule cells control information flow through cerebellar cortex. Neuron, **33**, 625-633.

Hampson, D. R. & Manalo, J.L. (1998) The activation of glutamate receptors by kainic acid and domoic acid. Nat. Toxins, **6**, 153-158.

Hanchar, H. J., Dodson, P.D., Olsen, R.W., Otis, T.S. & Wallner, M. (2005) Alcohol-induced motor impairment caused by increased extrasynaptic GABA(A) receptor activity. Nat. Neurosci., **8**, 339-345.

Hardison, J. L., Okazaki, M.M. & Nadler, J.V. (2000) Modest increase in extracellular potassium unmasks effect of recurrent mossy fiber growth. J. Neurophysiol., **84**, 2380-2389.

Hassan, H., Pohle, W., Rüthrich, H., Brödemann, R. & Krug, M. (2000) Repeated long-term potentiation induces mossy fibre sprouting and changes the sensibility of hippocampal granule cells to subconvulsive doses of pentylenetetrazol. Eur. J. Neurosci., **12**, 1509-1515.

Hausser, M. & Clark, B.A. (1997) Tonic synaptic inhibition modulates neuronal output pattern and spatiotemporal synaptic integration. Neuron, **19**, 665-678.

Hayes, D. M., Braud, S., Hurtado, D.E., McCallum, J., Standley, S., Isaac, J.T. & Roche, K.W. (2003) Trafficking and surface expression of the glutamate receptor subunit, KA2. Biochem. Biophys. Res. Commun., **310**, 8-13.

Heinemann, U., Kann, O. & Schuchmann, S. (2006) An overview of *in vitro* seizure models in acute and organotypic slices. In Pitkanen, A., Schwartzkroin, P. A. & Moshe, S. L. (eds), Elsevier Inc., USA, pp. 35.

Henley, J. M. (2003) Proteins interactions implicated in AMPA receptor trafficking: A clear destination and an improving route map. Neurosci. Res., **45**, 243-254.

Herin, G. A. & Aizenman, E. (2004) Amino terminal domain regulation of NMDA receptor function. Eur. J. Pharmacol., **500**, 101-111.

Hermans, E. & Challiss, R.A. (2001) Structural, signalling and regulatory properties of the group I metabotropic glutamate receptors: Prototypic family C G-protein-coupled receptors. Biochem. J., **359**, 465-484.

Hevers, W. & Luddens, H. (2002) Pharmacological heterogeneity of gamma-aminobutyric acid receptors during development suggests distinct classes of rat cerebellar granule cells in situ. Neuropharmacology, **42**, 34-47.

Hewapathirane, D. S. & Burnham, W.M. (2005) Propagation of amygdala-kindled seizures to the hippocampus in the rat: Electroencephalographic features and behavioural correlates. Neurosci. Res., **53**, 369-375.

Hinterkeuser, S., Schroder, W., Hager, G., Seifert, G., Blumcke, I., Elger, C.E., Schramm, J. & Steinhauser, C. (2000) Astrocytes in the hippocampus of patients with temporal lobe epilepsy display changes in potassium conductances. Eur. J. Neurosci., **12**, 2087-2096.

Hiyoshi, T., Mori, N. & Wada, J.A. (1989) Feline amygdaloid kindling and sleep. Electroencephalogr. Clin. Neurophysiol., **73**, 254-259.

Hlinak, Z. & Krejci, I. (1994) Effects of excitatory amino acid antagonists on social recognition of male rats. Behav. Pharmacol., **5**, 239-244.

Holahan, M. R., Honegger, K.S. & Routtenberg, A. (2007) Expansion and retraction of hippocampal mossy fibers during postweaning development: Strain-specific effects of NMDA receptor blockade. Hippocampus, **17**, 58-67.

Holahan, M. R., Rekart, J.L., Sandoval, J. & Routtenberg, A. (2006) Spatial learning induces presynaptic structural remodeling in the hippocampal mossy fiber system of two rat strains. Hippocampus, **16**, 560-570.

Hollmann, M., Boulter, J., Maron, C., Beasley, L., Sullivan, J., Pecht, G. & Heinemann, S. (1993) Zinc potentiates agonist-induced currents at certain splice variants of the NMDA receptor. Neuron, **10**, 943-954.

Hougaard, K. A., Andersen, M.B., Kjær, S.L., Hansen, A.M., Werge, T. & Lund, S.P. (2005) Prenatal stress may increase vulnerability to life events: Comparison with the effects of prenatal dexamethasone. Dev. Brain Res., **159**, 55-63.

Houser, C. R. (1990) Granule cell dispersion in the dentate gyrus of humans with temporal lobe epilepsy. Brain Res., **535**, 195-204.

Hsu, D. (2007) The dentate gyrus as a filter or gate: A look back and a look ahead. Prog. Brain Res., **163**, 601-613.

Huettner, J. E. (2003) Kainate receptors and synaptic transmission. Prog. Neurobiol., **70**, 387-407.

Hughes, J. R. (2009) Absence seizures: A review of recent reports with new concepts. Epilepsy Behav., .

Hume, R. I., Dingledine, R. & Heinemann, S.F. (1991) Identification of a site in glutamate receptor subunits that controls calcium permeability. Science, **253**, 1028-1031.

Huupponen, J., Molchanova, S.M., Taira, T. & Lauri, S.E. (2007) Susceptibility for homeostatic plasticity is down-regulated in parallel with maturation of the rat hippocampal synaptic circuitry. J. Physiol., **581**, 505-514.

Isaacson, J. S., Solis, J.M. & Nicoll, R.A. (1993) Local and diffuse synaptic actions of GABA in the hippocampus. Neuron, **10**, 165-175.

Ishizuka, N. (2001) Laminar organization of the pyramidal cell layer of the subiculum in the rat. J. Comp. Neurol., **435**, 89-110.

Iverson, F., Truelove, J., Nera, E., Tryphonas, L., Campbell, J. & Lok, E. (1989) Domoic acid poisoning and mussel-associated intoxication: Preliminary investigations into the response of mice and rats to toxic mussel extract. Food and Chemical Toxicology, **27**, 377-384.

Jarolimek, W., Lewen, A. & Misgeld, U. (1999) A furosemide-sensitive K+-cl-cotransporter counteracts intracellular Cl^- accumulation and depletion in cultured rat midbrain neurons. J. Neurosci., **19**, 4695-4704.

Jaseja, H. (2004) Purpose of REM sleep: Endogenous anti-epileptogenesis in man -- a hypothesis. Med. Hypotheses, **62**, 546-548.

Jeffery, B., Barlow, T., Moizer, K., Paul, S. & Boyle, C. (2004) Amnesic shellfish poison. Food and Chemical Toxicology, **42**, 545-557.

Jefferys, J. G. R. (2003) Models and mechanisms of experimental epilepsies. Epilepsia, **44**, 44-50.

Jensen, F. E., Blume, H., Alvarado, S., Firkusny, I. & Geary, C. (1995) NBQX blocks acute and late epileptogenic effects of perinatal hypoxia. Epilepsia, **36**, 966-972.

Jensen, O., Kaiser, J. & Lachaux, J. (2007) Human gamma-frequency oscillations associated with attention and memory. Trends Neurosci., **30**, 317-324.

Jiang, L., Xu, J., Nedergaard, M. & Kang, J. (2001) A kainate receptor increases the efficacy of GABAergic synapses. Neuron, **30**, 503-513.

Jobe, P. C. (2003) Common pathogenic mechanisms between depression and epilepsy: An experimental perspective. Epilepsy Behav., **4 Suppl 3**, S14-24.

Johnson, J. W. & Ascher, P. (1990) Voltage-dependent block by intracellular Mg2+ of N-methyl-D-aspartate-activated channels. Biophys. J., **57**, 1085-1090.

Johnson, J. W. & Ascher, P. (1987) Glycine potentiates the NMDA response in cultured mouse brain neurons. Nature, **325**, 529-531.

Johnston, M. V. (1996) Developmental aspects of epileptogenesis. Epilepsia, **37 Suppl 1**, S2-9.

Kahle, K. T., Staley, K.J., Nahed, B.V., Gamba, G., Hebert, S.C., Lifton, R.P. & Mount, D.B. (2008) Roles of the cation-chloride cotransporters in neurological disease. Nat. Clin. Pract. Neurol., **4**, 490-503.

Kaila, K. (1994) Ionic basis of GABAA receptor channel function in the nervous system. Prog. Neurobiol., **42**, 489-537.

Kakegawa, W., Kohda, K. & Yuzaki, M. (2007) The delta2 'ionotropic' glutamate receptor functions as a non-ionotropic receptor to control cerebellar synaptic plasticity. J. Physiol., **584**, 89-96.

Kapur, S. & Mamo, D. (2003) Half a century of antipsychotics and still a central role for dopamine D2 receptors. Prog. Neuro-Psychopharmacol. Biol. Psychiatry, **27**, 1081-1090.

Kashiwabuchi, N., Ikeda, K., Araki, K., Hirano, T., Shibuki, K., Takayama, C., Inoue, Y., Kutsuwada, T., Yagi, T. & Kang, Y. (1995) Impairment of motor coordination, purkinje cell synapse formation, and cerebellar long-term depression in GluR delta 2 mutant mice. Cell, **81**, 245-252.

Kaupmann, K., Malitschek, B., Schuler, V., Heid, J., Froestl, W., Beck, P., Mosbacher, J., Bischoff, S., Kulik, A., Shigemoto, R., Karschin, A. & Bettler, B. (1998) GABA(B)-receptor subtypes assemble into functional heteromeric complexes. Nature, **396**, 683-687.

Kemppainen, S. & Pitkanen, A. (2000) Distribution of parvalbumin, calretinin, and calbindin-D(28k) immunoreactivity in the rat amygdaloid complex and colocalization with gamma-aminobutyric acid. J. Comp. Neurol., **426**, 441-467.

Kerr, D. S., Razak, A. & Crawford, N. (2002) Age-related changes in tolerance to the marine algal excitotoxin domoic acid. Neuropharmacology, **43**, 357-366.

Kessels, H. W. & Malinow, R. (2009) Synaptic AMPA receptor plasticity and behavior. Neuron, **61**, 340-350.

Kew, J.N. & Kemp, J.A. (2005) Ionotropic and metabotropic glutamate receptor structure and pharmacology. Phsychopharmacholgy, **179**, 4-29.

Khalilov, I., Le Van Quyen, M., Gozlan, H. & Ben-Ari, Y. (2005) Epileptogenic actions of GABA and fast oscillations in the developing hippocampus. Neuron, **48**, 787-796.

Khazipov, R., Khalilov, I., Tyzio, R., Morozova, E., Ben-Ari, Y. & Holmes, G.L. (2004) Developmental changes in GABAergic actions and seizure susceptibility in the rat hippocampus. Eur. J. Neurosci., **19**, 590-600.

Khera, K. S., Whalen, C., Angers, G. & Arnold, D.L. (1994) Domoic acid: A teratology and homeostatic study in rats. Bull. Environ. Contam. Toxicol., **53**, 18-24.

Kim, E. & Sheng, M. (2004) PDZ domain proteins of synapses. Nat. Rev. Neurosci., **5**, 771-781.

Kim, J. J., Song, E.Y. & Kosten, T.A. (2006) Stress effects in the hippocampus: Synaptic plasticity and memory. Stress, **9**, 1-11.

Kirkby, R. D., Gilbert, T.H., Westcott, M.C. & Corcoran, M.E. (1995) Further characterization of kindling antagonism. Epilepsy Res., **21**, 115-124.

Kirkby, R. D., Gilbert, T.H. & Corcoran, M.E. (1993) Kindling antagonism: Mapping of susceptible sites. Brain Res., **616**, 17-24.

Kirkeby, S. & Thomsen, C.E. (2005) Quantitative immunohistochemistry of fluorescence labelled probes using low-cost software. J. Immunol. Methods., 301, 102-13.

Klass, D. W. (1975) Electroencephalographic manifestations of complex partial seizures. Adv. Neurol., **11**, 113-140.

Klausberger, T., Marton, L.F., Baude, A., Roberts, J.D., Magill, P.J. & Somogyi, P. (2004) Spike timing of dendrite-targeting bistratified cells during hippocampal network oscillations in vivo. Nat. Neurosci., **7**, 41-47.

Kleckner, N. W. & Dingledine, R. (1988) Requirement for glycine in activation of NMDA-receptors expressed in xenopus oocytes. Science, **241**, 835-837.

Kobayashi, M. & Buckmaster, P.S. (2003) Reduced inhibition of dentate granule cells in a model of temporal lobe epilepsy. J. Neurosci., **23**, 2440-2452.

Kofuji, P. & Newman, E.A. (2004) Potassium buffering in the central nervous system. Neuroscience, **129**, 1045-1056.

Koh, S., Tibayan, F.D., Simpson, J.N. & Jensen, F.E. (2004) NBQX or topiramate treatment after perinatal hypoxia-induced seizures prevents later increases in seizure-induced neuronal injury. Epilepsia, **45**, 569-575.

Kohler, M., Burnashev, N., Sakmann, B. & Seeburg, P.H. (1993) Determinants of Ca2+ permeability in both TM1 and TM2 of high affinity kainate receptor channels: Diversity by RNA editing. Neuron, **10**, 491-500.

Kortenbruck, G., Berger, E., Speckmann, E.J. & Musshoff, U. (2001) RNA editing at the Q/R site for the glutamate receptor subunits GLUR2, GLUR5, and GLUR6 in hippocampus and temporal cortex from epileptic patients. Neurobiol. Dis., **8**, 459-468.

Kotagal, P. & Yardi, N. (2008) The relationship between sleep and epilepsy. Seminars in Pediatric Neurology, **15**, 42-49.

Kotti, T., Riekkinen PJ, S. & Miettinen, R. (1997) Characterization of target cells for aberrant mossy fiber collaterals in the dentate gyrus of epileptic rat. Exp. Neurol., **146**, 323-330.

Koutsogiannopoulos, S., Adelson, F., Lee, V. & Andermann, F. (2009) Stressors at the onset of adult epilepsy: Implications for practice. Epileptic Disord., **11**, 42-47.

Kristensen, J. D., Hartvig, P., Karlsten, R., Gordh, T. & Halldin, M. (1995) CSF and plasma pharmacokinetics of the NMDA receptor antagonist CPP after intrathecal, extradural and i.v. administration in anaesthetized pigs. Br. J. Anaesth., **74**, 193-200.

Kumar, G., Couper, A., O'Brien, T.J., Salzberg, M.R., Jones, N.C., Rees, S.M. & Morris, M.J. (2007) The acceleration of amygdala kindling epileptogenesis by chronic low-dose corticosterone involves both mineralocorticoid and glucocorticoid receptors. Psychoneuroendocrinology, **32**, 834-842.

Kumar, P. & Raju, T.R. (2001) Seizure susceptibility decreases with enhancement of rapid eye movement sleep. Brain Res., **922**, 299-304.

Kuner, R., Kohr, G., Grunewald, S., Eisenhardt, G., Bach, A. & Kornau, H.C. (1999) Role of heteromer formation in GABAB receptor function. Science, **283**, 74-77.

Kyrozis, A., Chudomel, O., Moshe, S.L. & Galanopoulou, A.S. (2006) Sex-dependent maturation of GABAA receptor-mediated synaptic events in rat substantia nigra reticulata. Neurosci. Lett., **398**, 1-5.

Lambert, J. D. & Jones, R.S. (1990) A reevaluation of excitatory amino acid-mediated synaptic transmission in rat dentate gyrus. J. Neurophysiol., **64**, 119-132.

Larkum, M. E., Kaiser, K.M. & Sakmann, B. (1999) Calcium electrogenesis in distal apical dendrites of layer 5 pyramidal cells at a critical frequency of back-propagating action potentials. Proc. Natl. Acad. Sci. U. S. A., **96**, 14600-14604.

LeDoux, J.E. (2009) Scholarpedia 3, http://www.scholarpedia.org/article/Amygdala

Lee, H., Chen, C.X., Liu, Y., Aizenman, E. & Kandler, K. (2005) KCC2 expression in immature rat cortical neurons is sufficient to switch the polarity of GABA responses. Eur. J. Neurosci., **21**, 2593-2599.

Lefebvre, K. A. & Robertson, A. (2009) Domoic acid and human exposure risks: A review. Toxicon, .

Legendre, P. & Westbrook, G.L. (1990) The inhibition of single N-methyl-D-aspartate-activated channels by zinc ions on cultured rat neurones. J. Physiol., **429**, 429-449.

Lemmens, E. M., Lubbers, T., Schijns, O.E., Beuls, E.A. & Hoogland, G. (2005) Gender differences in febrile seizure-induced proliferation and survival in the rat dentate gyrus. Epilepsia, **46**, 1603-1612.

Lerma, J. (2006) Kainate receptor physiology. Curr. Opin. Pharmacol., **6**, 89-97.

Lerma, J., Paternain, A.V., Rodriguez-Moreno, A. & Løpez-Garcia, J.C. (2001) Molecular physiology of kainate receptors. Physiol. Rev., **81**, 971-998.

Lester, R. A., Clements, J.D., Westbrook, G.L. & Jahr, C.E. (1990) Channel kinetics determine the time course of NMDA receptor-mediated synaptic currents. Nature, **346**, 565-567.

Levin, E. D., Pizarro, K., Pang, W.G., Harrison, J. & Ramsdell, J.S. (2005) Persisting behavioral consequences of prenatal domoic acid exposure in rats. Neurotoxicol. Teratol., **27**, 719-725.

Levitt, P. (2005) Disruption of interneuron development. Epilepsia, **46**, 22-28.

Li, X., Zhou, J., Chen, Z., Chen, S., Zhu, F. & Zhou, L. (2008) Long-term expressional changes of Na^+ -K^+ -Cl^- co-transporter 1 (NKCC1) and K^+ -Cl^- co-transporter 2 (KCC2) in CA1 region of hippocampus following lithium-pilocarpine induced status epilepticus (PISE). Brain Res., **1221**, 141-146.

Li, X. G., Somogyi, P., Ylinen, A. & Buzsaki, G. (1994) The hippocampal CA3 network: An in vivo intracellular labeling study. J. Comp. Neurol., **339**, 181-208.

Liao, D. & Malinow, R. (1996) Deficiency in induction but not expression of LTP in hippocampal slices from young rats. Learn. Mem., **3**, 138-149.

Lojkova, D., Zivanovic, D. & Mares, P. (2006) Different effects of nonNMDA and NMDA receptor antagonists (NBQX and dizocilpine) on cortical epileptic afterdischarges in rats. Brain Res., **1124**, 167-175.

Lomeli, H., Mosbacher, J., Melcher, T., Hoger, T., Geiger, J.R., Kuner, T., Monyer, H., Higuchi, M., Bach, A. & Seeburg, P.H. (1994) Control of kinetic properties of AMPA receptor channels by nuclear RNA editing. Science, **266**, 1709-1713.

Lomeli, H., Sprengel, R., Laurie, D.J., Kohr, G., Herb, A., Seeburg, P.H. & Wisden, W. (1993) The rat delta-1 and delta-2 subunits extend the excitatory amino acid receptor family. FEBS Lett., **315**, 318-322.

Lomeli, H., Wisden, W., Kohler, M., Keinanen, K., Sommer, B. & Seeburg, P.H. (1992) High-affinity kainate and domoate receptors in rat brain. FEBS Lett., **307**, 139-143.

London, E. D. & Coyle, J.T. (1979) Specific binding of [3H]kainic acid to receptor sites in rat brain. Mol. Pharmacol., **15**, 492-505.

Loscher, W. (2002) Animal models of epilepsy for the development of antiepileptogenic and disease-modifying drugs. A comparison of the pharmacology of kindling and post-status epilepticus models of temporal lobe epilepsy. Epilepsy Res., **50**, 105-123.

Lujan, R., Shigemoto, R. & Lopez-Bendito, G. (2005) Glutamate and GABA receptor signalling in the developing brain. Neuroscience, **130**, 567-580.

Luthi, A., Schwyzer, L., Mateos, J.M., Gahwiler, B.H. & McKinney, R.A. (2001) NMDA receptor activation limits the number of synaptic connections during hippocampal development. Nat. Neurosci., **4**, 1102-1107.

Lynch, M. & Sutula, T. (2000) Recurrent excitatory connectivity in the dentate gyrus of kindled and kainic acid-treated rats. J. Neurophysiol., **83**, 693-704.

MacDermott, A. B., Mayer, M.L., Westbrook, G.L., Smith, S.J. & Barker, J.L. (1986) NMDA-receptor activation increases cytoplasmic calcium concentration in cultured spinal cord neurones. Nature, **321**, 519-522.

MacDonald, D.S., Bernard, P.B., Ramsay, L.A., Gill, D.A. & Tasker, R. (2008) Progressive changes in hippocampal cytoarchitecture in a non-convulsive developmental model of TLE. 38th Annual Society for Neuroscience Conference, Washington abstract #449.8.

Macdonald, R. L. & Olsen, R.W. (1994) GABAA receptor channels. Annu. Rev. Neurosci., **17**, 569-602.

MacLean, P. D. (1952) Some psychiatric implications of physiological studies on frontotemporal portion of limbic system (visceral brain). Electroencephalogr. Clin. Neurophysiol., **4**, 407-418.

Magloczky, Z. & Freund, T.F. (2005) Impaired and repaired inhibitory circuits in the epileptic human hippocampus. Trends Neurosci., **28**, 334-340.

Mah, S. J., Cornell, E., Mitchell, N.A. & Fleck, M.W. (2005) Glutamate receptor trafficking: Endoplasmic reticulum quality control involves ligand binding and receptor function. J. Neurosci., **25**, 2215-2225.

Malow, B. A. (2007) The interaction between sleep and epilepsy. Epilepsia, **48 Suppl 9**, 36-38.

Mandema, J. W. & Danhof, M. (1992) Electroencephalogram effect measures and relationships between pharmacokinetics and pharmacodynamics of centrally acting drugs. Clin. Pharmacokinet., **23**, 191-215.

Manni, R., Terzaghi, M. & Zambrelli, E. (2006) REM sleep behavior disorder and epileptic phenomena: Clinical aspects of the comorbidity. Epilepsia, **47 Suppl 5**, 78-81.

Martin, D. L. & Rimvall, K. (1993) Regulation of gamma-aminobutyric acid synthesis in the brain. J. Neurochem., **60**, 395-407.

Masukawa, L. M., Benardo, L.S. & Prince, D.A. (1982) Variations in electrophysiological properties of hippocampal neurons in different subfields. Brain Res., **242**, 341-344.

Maucher, J. M. & Ramsdell, J.S. (2007) Maternal-fetal transfer of domoic acid in rats at two gestational time points. Environ. Health Perspect., **115**, 1743-1746.

Mayer, A. M. (2000) The marine toxin domoic acid may affect the developing brain by activation of neonatal brain microglia and subsequent neurotoxic mediator generation. Med. Hypotheses, **54**, 837-841.

Mayer, M. L. (2005) Glutamate receptor ion channels. Curr. Opin. Neurobiol., **15**, 282-288.

Mayer, M. L. & Armstrong, N. (2004) Structure and function of glutamate receptor ion channels. Annu. Rev. Physiol., **66**, 161-181.

Mayer, M. L. & Westbrook, G.L. (1987) The physiology of excitatory amino acids in the vertebrate central nervous system. Prog. Neurobiol., **28**, 197-276.

Mayer, M. L., Westbrook, G.L. & Guthrie, P.B. (1984) Voltage-dependent block by Mg2+ of NMDA responses in spinal cord neurones. Nature, **309**, 261-263.

McBain, C. J. & Mayer, M.L. (1994) N-methyl-D-aspartic acid receptor structure and function. Physiol. Rev., **74**, 723-760.

McCormick, D. A. & Contreras, D. (2001) On the cellular and network bases of epileptic seizures. Annu. Rev. Physiol., **63**, 815-846.

McCutcheon, J. E. & Marinelli, M. (2009) Age matters. Eur. J. Neurosci., **29**, 997-1014.

McDonald, A. J. & Mascagni, F. (2001) Colocalization of calcium-binding proteins and GABA in neurons of the rat basolateral amygdala. Neuroscience, **105**, 681-693.

McDonald, A. J. (1998) Cortical pathways to the mammalian amygdala. Prog. Neurobiol., **55**, 257-332.

McDonald, J. W. & Johnston, M.V. (1990) Physiological and pathophysiological roles of excitatory amino acids during central nervous system development. Brain Res. Rev., **15**, 41-70.

McEwen, B. S. (2002) Sex, stress and the hippocampus: Allostasis, allostatic load and the aging process. Neurobiol. Aging, **23**, 921-939.

McGaugh, J. L. (2002) Memory consolidation and the amygdala: A systems perspective. Trends Neurosci., **25**, 456.

McIntyre, D. C. (2006) The kindling phenomenon. In Pitkanen, A., Schwartzkroin, P. A. & Moshe, S. L. (eds), *Models of Seizure and Epilepsy.* Elsevier Academic Press, Burlington, MA, pp. 351-363.

McLeod, V. M. (2007) Electrophysiological characterization of a developmental rat model of temporal lobe epilepsy in area CA1 or the hippocampus.

McNamara, J. O., Huang, Y.Z. & Leonard, A.S. (2006) Molecular signaling mechanisms underlying epileptogenesis. Sci. STKE, **2006**, re12.

McNaughton, B. L., Barnes, C.A. & Andersen, P. (1981) Synaptic efficacy and EPSP summation in granule cells of rat fascia dentata studied in vitro. J. Neurophysiol., **46**, 952-966.

Meldrum, B. & Chapman, A. (1999) Epileptic seizure and epilepsy. In Siegel, G. J. (ed), *Basic Neurochemistry: Molecular, Cellular and Medical Aspects.* Lippincott-Raven Publishers, Philadelphia,USA, pp. 755-768.

Meldrum, B. & Garthwaite, J. (1990) Excitatory amino acid neurotoxicity and neurodegenerative disease. Trends Pharmacol. Sci., **11**, 379-387.

Miles, R. & Wong, R.K. (1983) Single neurones can initiate synchronized population discharge in the hippocampus. Nature, **306**, 371-373.

Miller, J. W., Turner, G.M. & Gray, B.C. (1994) Anticonvulsant effects of the experimental induction of hippocampal theta activity. Epilepsy Research, **18**, 195-204.

Misgeld, U., Bijak, M. & Jarolimek, W. (1995) A physiological role for GABAB receptors and the effects of baclofen in the mammalian central nervous system. Prog. Neurobiol., **46**, 423-462.

Mohler, H. (2006) GABA(A) receptor diversity and pharmacology. Cell Tissue Res., **326**, 505-516.

Moldrich, R. X., Chapman, A.G., De Sarro, G. & Meldrum, B.S. (2003) Glutamate metabotropic receptors as targets for drug therapy in epilepsy. Eur. J. Pharmacol., **476**, 3-16.

Molnar, E., Pickard, L. & Duckworth, J.K. (2002) Developmental changes in ionotropic glutamate receptors: Lessons from hippocampal synapses. Neuroscientist, **8**, 143-153.

Monaghan, D. T., Bridges, R.J. & Cotman, C.W. (1989) The excitatory amino acid receptors: Their classes, pharmacology, and distinct properties in the function of the central nervous system. Annu. Rev. Pharmacol. Toxicol., **29**, 365-402.

Monnet, F. P., Debonnel, G. & de Montigny, C. (1992) In vivo electrophysiological evidence for a selective modulation of N-methyl-D-aspartate-induced neuronal activation in rat CA3 dorsal hippocampus by sigma ligands. J. Pharmacol. Exp. Ther., **261**, 123-130.

Monti, J. M. & Monti, D. (2005) Sleep disturbance in schizophrenia. Int. Rev. Psychiatry., **17**, 247-253.

Morgan, J. I., Cohen, D.R., Hempstead, J.L. & Curran, T. (1987) Mapping patterns of c-fos expression in the central nervous system after seizure. Science, **237**, 192-197.

Morgane, P. J., Galler, J.R. & Mokler, D.J. (2005) A review of systems and networks of the limbic forebrain/limbic midbrain. Prog. Neurobiol., **75**, 143-160.

Morimoto, K., Fahnestock, M. & Racine, R.J. (2004) Kindling and status epilepticus models of epilepsy: Rewiring the brain. Prog. Neurobiol., **73**, 1-60.

Mortensen, M. & Smart, T.G. (2006) Extrasynaptic alphabeta subunit GABAA receptors on rat hippocampal pyramidal neurons. J. Physiol., **577**, 841-856.

Mosbacher, J., Schoepfer, R., Monyer, H., Burnashev, N., Seeburg, P.H. & Ruppersberg, J.P. (1994) A molecular determinant for submillisecond desensitization in glutamate receptors. Science, **266**, 1059-1062.

Moshe, S. L. & Albala, B.J. (1983) Maturational changes in postictal refractoriness and seizure susceptibility in developing rats. Ann. Neurol., **13**, 552-557.

Murthy, V. N., Schikorski, T., Stevens, C.F. & Zhu, Y. (2001) Inactivity produces increases in neurotransmitter release and synapse size. Neuron, **32**, 673-682.

Nadler, J. V. (2003) The recurrent mossy fiber pathway of the epileptic brain. Neurochem. Res., **28**, 1649-1658.

Nakajima, S. & Potvin, J.L. (1992) Neural and behavioural effects of domoic acid, an amnesic shellfish toxin, in the rat. Can. J. Psychol., **46**, 569-581.

National Institutes of Health (2009) http://www.niaaa.nih.gov/.../gaba_receptor.htm. Accessed July 2009.

Nishi, M., Hinds, H., Lu, H.P., Kawata, M. & Hayashi, Y. (2001) Motoneuron-specific expression of NR3B, a novel NMDA-type glutamate receptor subunit that works in a dominant-negative manner. J. Neurosci., **21**, RC185.

Nitsch, R., Bergmann, I., Kuppers, K., Mueller, G. & Frotscher, M. (1990) Late appearance of parvalbumin-immunoreactivity in the development of GABAergic neurons in the rat hippocampus. Neurosci. Lett., **118**, 147-150.

Nouws, J. F. M. (1992) Pharmacokinetics in immature animals: A review. J. Anim. Sci., **70**, 3627-3634.

Novelli, A., Fernandez-Sanchez, M. T., Doucette, T. A. & Tasker, R. A. R. (2000) Chemical and biological detection methods. In Botana, L. M. (ed), *Seafood and Freshwater Toxins.* Marcel Dekker, Inc, New York, NY, pp. 383-399.

Nusser, Z. & Mody, I. (2002) Selective modulation of tonic and phasic inhibitions in dentate gyrus granule cells. J. Neurophysiol., **87**, 2624-2628.

Okazaki, M. M., Evenson, D.A. & Nadler, J.V. (1995) Hippocampal mossy fiber sprouting and synapse formation after status epilepticus in rats: Visualization after retrograde transport of biocytin. J. Comp. Neurol., **352**, 515-534.

O'Keefe, J. & Recce, M.L. (1993) Phase relationship between hippocampal place units and the EEG theta rhythm. Hippocampus, **3**, 317-330.

Olney, J. W., Rhee, V. & Ho, O.L. (1974) Kainic acid: A powerful neurotoxic analogue of glutamate. Brain Res., **77**, 507-512.

O'Mara, S. M., Commins, S., Anderson, M. & Gigg, J. (2001) The subiculum: A review of form, physiology and function. Prog. Neurobiol., **64**, 129-155.

Ono, J., Vieth, R.F. & Walson, P.D. (1990) Electrocorticographical observation of seizures induced by pentylenetetrazol (PTZ) injection in rats. Funct. Neurol., **5**, 345-352.

Orchinik, M., Carroll, S.S., Li, Y.H., McEwen, B.S. & Weiland, N.G. (2001) Heterogeneity of hippocampal GABA(A) receptors: Regulation by corticosterone. J. Neurosci., **21**, 330-339.

Paoletti, P., Vergnano, A.M., Barbour, B. & Casado, M. (2009) Zinc at glutamatergic synapses. Neuroscience, **158**, 126-136.

Paoletti, P. & Neyton, J. (2007) NMDA receptor subunits: Function and pharmacology. Curr. Opin. Pharmacol., **7**, 39-47.

Parent, J. M., Janumpalli, S., McNamara, J.O. & Lowenstein, D.H. (1998) Increased dentate granule cell neurogenesis following amygdala kindling in the adult rat. Neurosci. Lett., **247**, 9-12.

Parent, J. M., Yu, T.W., Leibowitz, R.T., Geschwind, D.H., Sloviter, R.S. & Lowenstein, D.H. (1997) Dentate granule cell neurogenesis is increased by seizures and contributes to aberrant network reorganization in the adult rat hippocampus. J. Neurosci., **17**, 3727-3738.

Parton, M. & Cockerell, O.C. (2003) Epilepsy-the aetiology and patholgenesis. Royal Pharmaceutical Society, **10(7)**, 288-295.

Pathak, H. R., Weissinger, F., Terunuma, M., Carlson, G.C., Hsu, F.C., Moss, S.J. & Coulter, D.A. (2007a) Disrupted dentate granule cell chloride regulation enhances synaptic excitability during development of temporal lobe epilepsy. J. Neurosci., **27**, 14012-14022.

Patrylo, P. R. & Dudek, F.E. (1998) Physiological unmasking of new glutamatergic pathways in the dentate gyrus of hippocampal slices from kainate-induced epileptic rats. J. Neurophysiol., **79**, 418-429.

Paulsen, O. & Moser, E.I. (1998) A model of hippocampal memory encoding and retrieval: GABAergic control of synaptic plasticity. Trends Neurosci., **21**, 273-278.

Paxinos, G. & Watson, C. (2007) *The Rat Brain in Stereotaxic Coordinates.* Elsevier Inc., USA.

Payne, J. A., Rivera, C., Voipio, J. & Kaila, K. (2003) Cation–chloride co-transporters in neuronal communication, development and trauma. Trends Neurosci., **26**, 199-206.

Pellegrini-Giampietro, D. E., Gorter, J.A., Bennett, M.V. & Zukin, R.S. (1997) The GluR2 (GluR-B) hypothesis: Ca(2+)-permeable AMPA receptors in neurological disorders. Trends Neurosci., **20**, 464-470.

Perez-Otano, I. & Ehlers, M.D. (2005) Homeostatic plasticity and NMDA receptor trafficking. Trends Neurosci., **28**, 229-238.

Perl, T. M., Bedard, L., Kosatsky, T., Hockin, J.C., Todd, E.C. & Remis, R.S. (1990) An outbreak of toxic encephalopathy caused by eating mussels contaminated with domoic acid. N. Engl. J. Med., **322**, 1775-1780.

Perry, M. A., Ryan, C.L. & Tasker, R.A. (2009) Effects of low dose neonatal domoic acid administration on behavioural and physiological response to mild stress in adult rats. Physiol. Behav. **98**, 53-59.

Pilc, A., Chaki, S., Nowak, G. & Witkin, J.M. (2008) Mood disorders: Regulation by metabotropic glutamate receptors. Biochem. Pharmacol., **75**, 997-1006.

Pinel, J. P., Skelton, R. & Mucha, R.F. (1976) Kindling-related changes in afterdischarge "thresholds". Epilepsia, **17**, 197-206.

Pinikahana, J. & Dono, J. (2009) Initial symptoms, precipitant factors, and techniques to control epileptic seizures: The carer's perspective. Epilepsy & Beh., doi:10.1016/j.yebeh.2009.07.045.

Pitkanen, A., Schwartzkroin, P. A. & Moshe, S. L. (2006) *Models of Seizures and Epilepsy.* In Anonymous Elsevier Inc, USA, .

Pitkanen, A., Tuunanen, J., Kalviainen, R., Partanen, K. & Salmenpera, T. (1998) Amygdala damage in experimental and human temporal lobe epilepsy. Epilepsy Res., **32**, 233-253.

Porter, B. E. (2008) Neurogenesis and epilepsy in the developing brain. Epilepsia, **49 Suppl 5**, 50-54.

Porter, R. J. (1988) Therapy of epilepsy. Current Opinions in Neurology and Neurosurgery, **1**, 206-211.

Priel, A., Selak, S., Lerma, J. & Stern-Bach, Y. (2006) Block of kainate receptor desensitization uncovers a key trafficking checkpoint. Neuron, **52**, 1037-1046.

Pulido, O. M. (2008) Domoic acid toxicologic pathology: A review. Mar. Drugs, **6**, 180-219.

Qiu, S., Jebelli, A.K., Ashe, J.H. & Curras-Collazo, M.C. (2009) Domoic acid induces a long-lasting enhancement of CA1 field responses and impairs tetanus-induced long-term potentiation in rat hippocampal slices. Toxicol. Sci., **111**, 140-150.

Racine, R. J. (1972a) Modification of seizure activity by electrical stimulation: II. motor seizure. Electroencephlography and Clinical Neurophysiology, **32**, 281-294.

Racine, R. J. (1972b) Modification of seizure activity by electrical stimulation. I. after-discharge threshold. Electroencephalogr. Clin. Neurophysiol., **32**, 269-279.

Raedt, R., Van Dycke, A., Van Melkebeke, D., Smedt, T.D., Claeys, P., Wyckhuys, T., Vonck, K., Wadman, W. & Boon, P. (2009) Seizures in the intrahippocampal kainic acid epilepsy model: Characterization using long-term video-EEG monitoring in the rat. Acta Neurol. Scand., **119**, 293-303.

Rakhade, S. N., Zhou, C., Aujla, P.K., Fishman, R., Sucher, N.J. & Jensen, F.E. (2008) Early alterations of AMPA receptors mediate synaptic potentiation induced by neonatal seizures. J. Neurosci., **28**, 7979-7990.

Ramirez-Amaya, V., Escobar, M.L., Chao, V. & Bermudez-Rattoni, F. (1999) Synaptogenesis of mossy fibers induced by spatial water maze overtraining. Hippocampus, **9**, 631-636.

Ramirez-Amaya, V., Balderas, I., Sandoval, J., Escobar, M.L. & Bermudez-Rattoni, F. (2001) Spatial long-term memory is related to mossy fiber synaptogenesis. J. Neurosci., **21**, 7340-7348.

Ramsdell, J. S. & Zabka, T.S. (2008) *In utero* domoic acid toxicity: A fetal basis to adult disease in the california sea lion (zalophus californianus). Marine Drugs, **6(2)**, 262-290.

Ransom, R. W. & Deschenes, N.L. (1988) NMDA-induced hippocampal [3H]norepinephrine release is modulated by glycine. Eur. J. Pharmacol., **156**, 149-155.

Raol, Y. H. & Meti, B.L. (1998) Sleep-wakefulness alterations in amygdala-kindled rats. Epilepsia, **39**, 1133-1137.

Ratzliff, A. H., Santhakumar, V., Howard, A. & Soltesz, I. (2002) Mossy cells in epilepsy: Rigor mortis or vigor mortis? Trends Neurosci., **25**, 140-144.

Ren, Z., Riley, N.J., Garcia, E.P., Sanders, J.M., Swanson, G.T. & Marshall, J. (2003) Multiple trafficking signals regulate kainate receptor KA2 subunit surface expression. J. Neurosci., **23**, 6608-6616.

Represa, A. & Ben-Ari, Y. (1992) Kindling is associated with the formation of novel mossy fibre synapses in the CA3 region. Exp. Brain Res., **92**, 69-78.

Rivera, C., Li, H., Thomas-Crusells, J., Lahtinen, H., Viitanen, T., Nanobashvili, A., Kokaia, Z., Airaksinen, M.S., Voipio, J., Kaila, K. & Saarma, M. (2002) BDNF-induced TrkB activation down-regulates the K+-cl- cotransporter KCC2 and impairs neuronal cl- extrusion. J. Cell Biol., **159**, 747-752.

Robertson, H., Renton, K., Kohn, J. & White, T. (1992) Patterns of fos expression suggest similar mechanisms of action for the excitotoxins domoic and kainic acid. Ann. N. Y. Acad. Sci., **648**, 330-334.

Rodriguez, A. J. & Kuzniecky, R.I. (2008) The interactions between sleep and epilepsy. Rev. Neurol. Dis., **5**, 1-7.

Rogawski, M. A. (2006) Diverse mechanisms of antiepileptic drugs in the development pipeline. Epilepsy Res., **69**, 273-294.

Rogawski, M. A., Gryder, D., Castaneda, D., Yonekawa, W., Banks, M.K. & Li, H. (2003) GluR5 kainate receptors, seizures, and the amygdala. Annuals of the New York Academy of Science, **985**, 150-162.

Rogawski, M. A. & Donevan, S.D. (1999) AMPA receptors in epilepsy and as targets for antiepileptic drugs. Adv. Neurol., **79**, 947-963.

Rossi, D. J. & Hamann, M. (1998) Spillover-mediated transmission at inhibitory synapses promoted by high affinity alpha6 subunit GABA(A) receptors and glomerular geometry. Neuron, **20**, 783-795.

Rothman, S. M. & Olney, J.W. (1986) Glutamate and the pathophysiology of hypoxic--ischemic brain damage. Ann. Neurol., **19**, 105-111.

Sachs, G., Anderer, P., Dantendorfer, K. & Saletu, B. (2004) EEG mapping in patients with social phobia. Psychiatry Res., **131**, 237-247.

Sah, P., Faber, E.S., Lopez De Armentia, M. & Power, J. (2003) The amygdaloid complex: Anatomy and physiology. Physiol. Rev., **83**, 803-834.

Sammaritano, M., Gigli, G.L. & Gotman, J. (1991) Interictal spiking during wakefulness and sleep and the localization of foci in temporal lobe epilepsy. Neurology, **41**, 290-297.

Santos, N. F., Correia, M.L., Sinigaglia-Coimbra, R., Calderazzo, L., Sanabria, E.R.G. & Cavalheiro, E.A. (2000) Multiple pilocarpine-induced status epilepticus in developing rats; A long-term behavioral and electrophysiological study. Epilepsia, **41**, S57-S63.

Sapolsky, R. M. (2003) Stress and plasticity in the limbic system. Neurochem. Res., **28**, 1735-1742.

Sapolsky, R. M. (1990) Glucocorticoids, hippocampal damage and the glutamatergic synapse. Prog. Brain Res., **86**, 13-23.

Sapolsky, R. M., Krey, L.C. & McEwen, B.S. (1985) Prolonged glucocorticoid exposure reduces hippocampal neuron number: Implications for aging. J. Neurosci., **5**, 1222-1227.

Sari, P. & Kerr, D.S. (2001) Domoic acid-induced hippocampal CA1 hyperexcitability independent of region CA3 activity. Epilepsy Res., **47**, 65-76.

Sarkisan, M. R. (2001) Overview of the current animal models for human seizure and epileptic disorders. Epilepsy and Behavior, **2**, 201-216.

Scallet, A. C., Kowalke, P.K., Rountree, R.L., Thorn, B.T. & Binienda, Z.K. (2004) Electroencephalographic, behavioral, and c-fos responses to acute domoic acid exposure. Neurotoxicol. Teratol., **26**, 331-342.

Scharfman, H. E. (2007) The CA3 "backprojection" to the dentate gyrus. Prog. Brain Res., **163**, 627-637.

Scharfman, H. E. (2002) Epilepsy as an example of neural plasticity. Neuroscientist, **8**, 154-173.

Scharfman, H. E. (2000) Epileptogenesis in the parahippocampal region. parallels with the dentate gyrus. Ann. N. Y. Acad. Sci., **911**, 305-327.

Scharfman, H. E., Goodman, J.H. & Sollas, A.L. (2000) Granule-like neurons at the hilar/CA3 border after status epilepticus and their synchrony with area CA3 pyramidal cells: Functional implications of seizure-induced neurogenesis. J. Neurosci., **20**, 6144-6158.

Scharfman, H. E. (1993) Activation of dentate hilar neurons by stimulation of the fimbria in rat hippocampal slices. Neurosci. Lett., **156**, 61-66.

Schilling, M., Wetzel, W., Grecksch, G. & Becker, A. (2006) Pentylenetetrazole kindling affects sleep in rats. Epilepsia, **47**, 2075-2082.

Schmoll, H., Badan, I., Grecksch, G., Walker, L., Kessler, C. & Popa-Wagner, A. (2003) Kindling status in sprague-dawley rats induced by pentylenetetrazole. Am. J. Pathol., **162**, 1027-1034.

Schneiderman, J.H., Cairns, A. & Sterling, C.A. (1992) Low concentrations of penicillin partially suppress CA3 hippocampal IPSPs in vitro. Brain Res. **592**, 298-304.

Schoepp, D. D. (2001) Unveiling the functions of presynaptic metabotropic glutamate receptors in the central nervous system. J. Pharmacol. Exp. Ther., **299**, 12-20.

Schreiber, S. S., Tocco, G., Najm, I., Finch, C.E., Johnson, S.A. & Baudry, M. (1992) Absence of c-fos induction in neonatal rat brain after seizures. Neurosci. Lett., **136**, 31-35.

Schwarzer, C., Sperk, G., Samanin, R., Rizzi, M., Gariboldi, M. & Vezzani, A. (1996) Neuropeptides-immunoreactivity and their mRNA expression in kindling: Functional implications for limbic epileptogenesis. Brain Res. Brain Res. Rev., **22**, 27-50.

Scott, B. W., Wojtowicz, J.M. & Burnham, W.M. (2000) Neurogenesis in the dentate gyrus of the rat following electroconvulsive shock seizures. Exp. Neurol., **165**, 231-236.

Scotti, A. L., Bollag, O., Kalt, G. & Nitsch, C. (1997) Loss of perikaryal parvalbumin immunoreactivity from surviving GABAergic neurons in the CA1 field of epileptic gerbils. Hippocampus, **7**, 524-535.

Seeburg, P. H. (1993) The TINS/TiPS lecture. the molecular biology of mammalian glutamate receptor channels. Trends Neurosci., **16**, 359-365.

Seeman, P. (1987) Dopamine receptors and the dopamine hypothesis of schizophrenia. Synapse, **1**, 133-152.

Shekhar, A., Truitt, W., Rainnie, D. & Sajdyk, T. (2005) Role of stress, corticotrophin releasing factor (CRF) and amygdala plasticity in chronic anxiety. Stress, **8**, 209-219.

Shouse, M. N., Farber, P.R. & Staba, R.J. (2000) Physiological basis: How NREM sleep components can promote and REM sleep components can suppress seizure discharge propagation. Clin. Neurophysiol., **111 Suppl 2**, S9-S18.

Shouse, M. N. & Sterman, M.B. (1981a) Sleep and kindling: I. effects of initial afterdischarge threshold determination. Experimental Neurology, **71**, 550-562.

Shouse, M. N. & Sterman, M.B. (1981b) Sleep and kindling: II. effects of generalized seizure induction. Exp. Neurol., **71**, 563-580.

Sieghart, W. & Sperk, G. (2002) Subunit composition, distribution and function of GABA(A) receptor subtypes. Curr. Top. Med. Chem., **2**, 795-816.

Sieghart, W., Fuchs, K., Tretter, V., Ebert, V., Jechlinger, M. & Hoger, H. (1999) Structure and subunit composition of GABA-A receptors. Neurochem. Int., **34**, 379-385.

Simeone, T. A., Sanchez, R.M. & Rho, J.M. (2004) Molecular biology and ontogeny of glutamate receptors in the mammalian central nervous system. J. Child Neurol., **19**, 343-60; discussion 361.

Simonds, W. F. (1999) G protein regulation of adenylate cyclase. Trends Pharmacol. Sci., **20**, 66-73.

Sindreu, C. B., Varoqui, H., Erickson, J.D. & Perez-Clausell, J. (2003) Boutons containing vesicular zinc define a subpopulation of synapses with low AMPAR content in rat hippocampus. Cereb. Cortex, **13**, 823-829.

Sipila, S. T., Huttu, K., Soltesz, I., Voipio, J. & Kaila, K. (2005) Depolarizing GABA actis on intrinsically bursting pyramidal neurons to drive giant depolarizing potentials in the immature hippocampus. The Journal of Neuroscience, **25**, 5280-5289.

Skaggs, W. E., McNaughton, B.L., Wilson, M.A. & Barnes, C.A. (1996) Theta phase precession in hippocampal neuronal populations and the compression of temporal sequences. Hippocampus, **6**, 149-172.

Slomianka, L. (1992a) Neurons of origin of zinc-containing pathways and the distribution of zinc-containing boutons in the hippocampal region of the rat. Neuroscience, **48**, 325-352.

Sloviter, R. S. (2005) The neurobiology of temporal lobe epilepsy: Too much information, not enough knowledge. C. R. Biol., **328**, 143-153.

Sloviter, R. S., Sollas, A.L., Barbaro, N.M. & Laxer, K.D. (1991) Calcium-binding protein (calbindin-D28K) and parvalbumin immunocytochemistry in the normal and epileptic human hippocampus. J. Comp. Neurol., **308**, 381-396.

Sloviter, R. S. (1989) Calcium-binding protein (calbindin-D28k) and parvalbumin immunocytochemistry: Localization in the rat hippocampus with specific reference to the selective vulnerability of hippocampal neurons to seizure activity. J. Comp. Neurol., **280**, 183-196.

Solbach, S. & Celio, M.R. (1991) Ontogeny of the calcium binding protein parvalbumin in the rat nervous system. Anat. Embryol. (Berl), **184**, 103-124.

Sommer, B., Burnashev, N., Verdoorn, T.A., Kein,,nen, K., Sakmann, B. & Seeburg, P.H. (1992) A glutamate receptor channel with high affinity for domoate and kainate. EMBO J., **11**, 1651-1656.

Sommer, B., Kohler, M., Sprengel, R. & Seeburg, P.H. (1991) RNA editing in brain controls a determinant of ion flow in glutamate-gated channels. Cell, **67**, 11-19.

Sommer, B., Keinanen, K., Verdoorn, T.A., Wisden, W., Burnashev, N., Herb, A., Kohler, M., Takagi, T., Sakmann, B. & Seeburg, P.H. (1990) Flip and flop: A cell-specific functional switch in glutamate-operated channels of the CNS. Science, **249**, 1580-1585.

Song, I. & Huganir, R.L. (2002) Regulation of AMPA receptors during synaptic plasticity. Trends Neurosci., **25**, 578-588.

Sperber, E. F., Haas, K.Z., Stanton, P.K. & Moshe, S.L. (1991) Resistance of the immature hippocampus to seizure-induced synaptic reorganization. Brain Res. Dev. Brain Res., **60**, 88-93.

Sperk, G., Marksteiner, J., Gruber, B., Bellmann, R., Mahata, M. & Ortler, M. (1992) Functional changes in neuropeptide Y- and somatostatin-containing neurons induced by limbic seizures in the rat. Neuroscience, **50**, 831-846.

Sprengel, R., Higuchi, M., Monyer, H. & Seeburg, P.H. (1999) Glutamate receptor channels: A possible link between RNA editing in the brain and epilepsy. Adv. Neurol., **79**, 525-534.

Spruston, N. & McBain, C. (2007) Structural and functional properties of hippocampal neurons. In Anderson, P., Morris, R., Amaral, D., Bliss, T. & O'Keefe, J. (eds), Oxford University Press, New York, pp. 133-201.

Stafstrom, C. E. & Sutula, T.P. (2005) Models of epilepsy in the developing and adult brain: Implications for neuroprotection. Epilepsy Behav., **7 Suppl 3**, S18-24.

Stern, J. M. (2009) Overview of evaluation and treatment guidelines for epilepsy. Curr. Treat. Options Neurol., **11**, 273-284.

Stone, J. M., Morrison, P.D. & Pilowsky, L.S. (2007) Glutamate and dopamine dysregulation in schizophrenia--a synthesis and selective review. J. Psychopharmacol., **21**, 440-452.

Stone, W. S. & Gold, P.E. (1988) Amygdala kindling effects on sleep and memory in rats. Brain Research, **449**, 135-140.

Stoop, R. & Pralong, E. (2000) Functional connections and epileptic spread between hippocampus, entorhinal cortex and amygdala in a modified horizontal slice preparation of the rat brain. Eur. J. Neurosci., **12**, 3651-3663.

Stripling, J. S. & Russell, R.D. (1989) Twenty-four-hour post-seizure inhibition during limbic kindling requires seizure generalization. Neurosci. Lett., **99**, 208-213.

Sutula, T. (2002) Seizure-induced axonal sprouting: Assessing connections between injury, local circuits, and epileptogenesis. Epilepsy Curr., **2**, 86-91.

Sutula, T., Cascino, G., Cavazos, J., Parada, I. & Ramirez, L. (1989) Mossy fiber synaptic reorganization in the epileptic human temporal lobe. Ann. Neurol., **26**, 321-330.

Sutula, T., He, X.X., Cavazos, J. & Scott, G. (1988) Synaptic reorganization in the hippocampus induced by abnormal functional activity. Science, **239**, 1147-1150.

Sutula, T. P. & Dudek, F.E. (2007) Unmasking recurrent excitation generated by mossy fiber sprouting in the epileptic dentate gyrus: An emergent property of a complex system. Prog. Brain Res., **163**, 541-563.

Swanson, T. H., Sperling, M.R. & O'Connor, M.J. (1998) Strong paired pulse depression of dentate granule cells in slices from patients with temporal lobe epilepsy. J. Neural Transm., **105**, 613-625.

Szot, P., Weinshenker, D., White, S.S., Robbins, C.A., Rust, N.C., Schwartzkroin, P.A. & Palmiter, R.D. (1999) Norepinephrine-deficient mice have increased susceptibility to seizure-inducing stimuli. J. Neurosci., **19**, 10985-10992.

Tallent, M. K. (2007) Somatostatin in the dentate gyrus. Prog. Brain Res., **163**, 265-284.

Tasker, R. A., Perry, M.A., Doucette, T.A. & Ryan, C.L. (2005) NMDA receptor involvement in the effects of low dose domoic acid in neonatal rats. Amino Acids, **28**, 193-196.

Tasker, R. A., Strain, S.M. & Drejer, J. (1996) Selective reduction in domoic acid toxicity in vivo by a novel non-N-methyl-D-aspartate receptor antagonist. Can. J. Physiol. Pharmacol., **74**, 1047-1054.

Tasker, R. A., Connell, B.J. & Strain, S.M. (1991) Pharmacology of systemically administered domoic acid in mice. Can. J. Physiol. Pharmacol., **69**, 378-382.

Tauck, D. L. & Nadler, J.V. (1985) Evidence of functional mossy fiber sprouting in hippocampal formation of kainic acid-treated rats. J. Neurosci., **5**, 1016-1022.

Teitelbaum, J. S., Zatorre, R.J., Carpenter, S., Gendron, D., Evans, A.C., Gjedde, A. & Cashman, N.R. (1990) Neurologic sequelae of domoic acid intoxication due to the ingestion of contaminated mussels. N. Engl. J. Med., **322**, 1781-1787.

Temkin, N. R. & Davis, G.R. (1984) Stress as a risk factor for seizures among adults with epilepsy. Epilepsia, **25**, 450-456.

Teyler, T. J. & Alger, B.E. (1976) Monosynaptic habituation in the vertebrate forebrain: The dentate gyrus examined in vitro. Brain Res., **115**, 413-425.

Thurber, S. J., Mikati, M.A., Stafstrom, C.E., Jensen, F.E. & Holmes, G.L. (1994) Quisqualic acid-induced seizures during development: A behavioral and EEG study. Epilepsia, **35**, 868-875.

Tiedeken, J. A. & Ramsdell, J.S. (2007) Embryonic exposure to domoic acid increases the susceptibility of zebrafish larvae to the chemical convulsant pentylenetetrazole. Environ. Health Perspect., **115**, 1547-1552.

Touchon, J., Baldy-Moulinier, M., Billiard, M., Besset, A. & Cadilhac, J. (1991) Sleep organization and epilepsy. Epilepsy Res. Suppl., **2**, 73-81.

Trasande, C. A. & Ramirez, J.M. (2007) Activity deprivation leads to seizures in hippocampal slice cultures: Is epilepsy the consequence of homeostatic plasticity? J. Clin. Neurophysiol., **24**, 154-164.

Traynelis, S. F., Burgess, M.F., Zheng, F., Lyuboslavsky, P. & Powers, J.L. (1998) Control of voltage-independent zinc inhibition of NMDA receptors by the NR1 subunit. J. Neurosci., **18**, 6163-6175.

Tretter, V. & Moss, S.J. (2008) GABA(A) receptor dynamics and constructing GABAergic synapses. Front. Mol. Neurosci., **1**, 7.

Tretter, V., Ehya, N., Fuchs, K. & Sieghart, W. (1997) Stoichiometry and assembly of a recombinant GABAA receptor subtype. J. Neurosci., **17**, 2728-2737.

Trevelyan, A.J. (2009) The direct relationship between inhibitory currents and local field potentials. J. Neurosci. **29**, 15299-15307.

Tryphonas, L., Truelove, J. & Iverson, F. (1990a) Acute parenteral neurotoxicity of domoic acid in cynomolgus monkeys (M. fascicularis). Toxicol. Pathol., **18**, 297-303.

Tryphonas, L., Truelove, J., Nera, E. & Iverson, F. (1990b) Acute neurotoxicity of domoic acid in the rat. Toxicol. Pathol., **18**, 1-9.

Turner, D. A., Buhl, E.H., Hailer, N.P. & Nitsch, R. (1998) Morphological features of the entorhinal-hippocampal connection. Prog. Neurobiol., **55**, 537-562.

Tuunanen, J., Halonen, T. & Pitkanen, A. (1997) Decrease in somatostatin-immunoreactive neurons in the rat amygdaloid complex in a kindling model of temporal lobe epilepsy. Epilepsy Res., **26**, 315-327.

Tyzio, R., Holmes, G.L., Ben-Ari, Y. & Khazipov, R. (2007) Timing of the developmental switch in GABA(A) mediated signaling from excitation to inhibition in CA3 rat hippocampus using gramicidin perforated patch and extracellular recordings. Epilepsia, **48 Suppl 5**, 96-105.

Tyzio, R., Represa, A., Jorquera, I., Ben-Ari, Y., Gozlan, H. & Aniksztejn, L. (1999) The establishment of GABAergic and glutamatergic synapses on CA1 pyramidal neurons is sequential and correlates with the development of the apical dendrite. The Journal of Neuroscience, **19**, 10372-10382.

Unnerstall, J. R. & Wamsley, J.K. (1983) Autoradiographic localization of high-affinity [3H]kainic acid binding sites in the rat forebrain. Eur. J. Pharmacol., **86**, 361-371.

Ure, J. A. & Perassolo, M. (2000) Update on the patholphysiology of the epilepsies. J. Neurol. Sci., **177**, 1-17.

Uva, L., Avoli, M. & deCurtis, M. (2009) Synchronous GABA-receptor-dependent potentials in limbic areas of the in-vitro isolated adult guinea pig brain. Eur. J. Neurosci. **29**, 911-920.

Valluru, L., Xu, J., Zhu, Y., Yan, S., Contractor, A. & Swanson, G.T. (2005) Ligand binding is a critical requirement for plasma membrane expression of heteromeric kainate receptors. J. Biol. Chem., **280**, 6085-6093.

van den Pol, A. N., Obrietan, K. & Chen, G. (1996) Excitatory actions of GABA after neuronal trauma. J. Neurosci., **16**, 4283-4292.

van Lier, H., Drinkenburg, W.H.I.M., van Eeten, Y.J.W. & Coenen, A.M.L. (2004) Effects of diazepan and zolpidem on EEG beta frequencies are behavior-specific in rats. Neuropharmacology, **47**, 163-174.

Velíšek, L. (2006) Models of chemically-induced acute seizures. In Pitkanen, A., Schwartzkroin, P. A. & Moshe, S. L. (eds), *Models of Seizures and Epilepsy.* Elsevier Inc, U.S.A., pp. 127-152.

Verdoorn, T. A., Johansen, T.H., Drejer, J. & Nielsen, E.O. (1994) Selective block of recombinant glur6 receptors by NS-102, a novel non-NMDA receptor antagonist. Eur. J. Pharmacol., **269**, 43-49.

Visser, S. A. G., Wolters, F.L.C., Gubbens-Stibbe, J.M., Tukker, E., van der Graaf, P.H., Peletier, L.A. & Danhof, M. (2003a) Mechanism-based pharmacokinetic/pharmacodynamic modelling of the electroencephalogram effects of

GABA-A receptor modulators: In vitro-in vivo correlations. J. Pharmacol. Exp. Ther., **304**, 88-101.

Visser, S. A. G., Wolters, F.L.C., van der Graaf, P.H., Peletier, L.A. & Danhof, M. (2003b) Dose-dependent EEG effects of zolpidem provide evidence for GABA-A receptor subtype selectivity in vivo. J. Pharmacol. Exp. Ther., **304**, 1251-1257.

Vollmar, W., Gloger, J., Berger, E., Kortenbruck, G., Kohling, R., Speckmann, E.J. & Musshoff, U. (2004) RNA editing (R/G site) and flip-flop splicing of the AMPA receptor subunit GluR2 in nervous tissue of epilepsy patients. Neurobiol. Dis., **15**, 371-379.

Wagner, S., Castel, M., Gainer, H. & Yarom, Y. (1997) GABA in the mammalian suprachiasmatic nucleus and its role in diurnal rhythmicity. Nature, **387**, 598-603.

Walker, D. L. & Davis, M. (2002) The role of amygdala glutamate receptors in fear learning, fear-potentiated startle, and extinction. Pharmacol. Biochem. Behav., **71**, 379-392.

Walther, H., Lambert, J.D., Jones, R.S., Heinemann, U. & Hamon, B. (1986) Epileptiform activity in combined slices of the hippocampus, subiculum and entorhinal cortex during perfusion with low magnesium medium. Neurosci. Lett., **69**, 156-161.

Wei, W., Zhang, N., Peng, Z., Houser, C.R. & Mody, I. (2003) Perisynaptic localization of delta subunit-containing GABA(A) receptors and their activation by GABA spillover in the mouse dentate gyrus. J. Neurosci., **23**, 10650-10661.

Weiss, S. R., Eidsath, A., Li, X.L., Heynen, T. & Post, R.M. (1998) Quenching revisited: Low level direct current inhibits amygdala-kindled seizures. Exp. Neurol., **154**, 185-192.

Wenthold, R. J., Sans, N., Standley, S., Prybylowski, K. & Petralia, R.S. (2003) Early events in the trafficking of N-methyl-D-aspartate (NMDA) receptors. Biochem. Soc. Trans., **31**, 885-888.

Wenzel, H. J., Woolley, C.S., Robbins, C.A. & Schwartzkroin, P.A. (2000) Kainic acid-induced mossy fiber sprouting and synapse formation in the dentate gyrus of rats. Hippocampus, **10**, 244-260.

West, A.P. (1990) Neurobehavioral studies of forced swimming: the role of learning and memory in the forced swim test. Prog. Neuropsychopharmacol. Biol. Psychiatry, 14, 863-877.

Williams, P., White, A., Ferraro, D., Clark, S., Staley, K. & Dudek, F.E. (2006) The use of radiotelemetry to evaluate electrographic seizures in rats with kainate-induced epilepsy. J. Neurosci. Methods, **155**, 39-48.

Willoughby, J. O. & Mackenzie, L. (1992) Nonconvulsive electrocotricographic paroxysms (absence epilepsy) in rat strains. Lab. Anim. Sci., **42**, 551-554.

Wisden, W. & Seeburg, P.H. (1993) A complex mosaic of high-affmity kainate receptors in rat brain. J. Neurosci., **13**, 3582-3598.

Witter, M. P. (2007) The perforant path: Projections from the entorhinal cortex to the dentate gyrus. Prog. Brain Res., **163**, 43-61.

Wittner, L., Eross, L., Czirjak, S., Halasz, P., Freund, T.F. & Magloczky, Z. (2005) Surviving CA1 pyramidal cells receive intact perisomatic inhibitory input in the human epileptic hippocampus. Brain, **128**, 138-152.

Wohlfarth, K. M., Bianchi, M.T. & Macdonald, R.L. (2002) Enhanced neurosteroid potentiation of ternary GABA(A) receptors containing the delta subunit. J. Neurosci., **22**, 1541-1549.

Wollmuth, L. P. & Sobolevsky, A.I. (2004) Structure and gating of the glutamate receptor ion channel. Trends Neurosci., **27**, 321-328.

Wong, E. H., Kemp, J.A., Priestley, T., Knight, A.R., Woodruff, G.N. & Iversen, L.L. (1986) The anticonvulsant MK-801 is a potent N-methyl-D-aspartate antagonist. Proc. Natl. Acad. Sci. U. S. A., **83**, 7104-7108.

Wong, M. (2005) Advances in the pathophysiology of developmental epilepsies. Semin. Pediatr. Neurol., **12**, 72-87.

World Health Organization (2009) Epilepsy. **2009.** http://www.who.int/mediacentre/factsheets/fs999/en/index.html

Wu, H., Jin, Y., Buddhala, C., Osterhaus, G., Cohen, E., Jin, H., Wei, J., Davis, K., Obata, K. & Wu, J.Y. (2007) Role of glutamate decarboxylase (GAD) isoform, GAD65, in GABA synthesis and transport into synaptic vesicles-evidence from GAD65-knockout mice studies. Brain Res., **1154**, 80-83.

Xi, D., Peng, Y.G. & Ramsdell, J.S. (1997) Domoic acid is a potent neurotoxin to neonatal rats. Nat. Toxins, **5**, 74-79.

Xi, D. & Ramsdell, J.S. (1996) Glutamate receptors and calcium entry mechanisms for domoic acid in hippocampal neurons. Neuroreport, **7**, 1115-1120.

Yan, Y., Dempsey, R.J. & Sun, D. (2001) Na+-K+-cl- cotransporter in rat focal cerebral ischemia. J. Cereb. Blood Flow Metab., **21**, 711-721.

Yang, J. W., Hanganu-Opatz, I.L., Sun, J.J. & Luhmann, H.J. (2009) Three patterns of oscillatory activity differentially synchronize developing neocortical networks in vivo. J. Neurosci., **29**, 9011-9025.

Zhang, C. L., Gloveli, T. & Heinemann, U. (1994) Effects of NMDA- and AMPA-receptor antagonists on different forms of epileptiform activity in rat temporal cortex slices. Epilepsia, **35 Suppl 5**, S68-73.

Zhang, D., Pan, Z.H., Awobuluyi, M. & Lipton, S.A. (2001) Structure and function of GABA(C) receptors: A comparison of native versus recombinant receptors. Trends Pharmacol. Sci., **22**, 121-132.

Zhang, G., Raol, Y.S., Hsu, F.C. & Brooks-Kayal, A.R. (2004) Long-term alterations in glutamate receptor and transporter expression following early-life seizures are associated with increased seizure susceptibility. J. Neurochem., **88**, 91-101.

Zhang, N. & Houser, C.R. (1999) Ultrastructural localization of dynorphin in the dentate gyrus in human temporal lobe epilepsy: A study of reorganized mossy fiber synapses. J. Comp. Neurol., **405**, 472-490.

Zhu, Z. Q., Armstrong, D.L., Hamilton, W.J. & Grossman, R.G. (1997) Disproportionate loss of CA4 parvalbumin-immunoreactive interneurons in patients with ammon's horn sclerosis. J. Neuropathol. Exp. Neurol., **56**, 988-998.

Zuo, J., De Jager, P.L., Takahashi, K.A., Jiang, W., Linden, D.J. & Heintz, N. (1997) Neurodegeneration in lurcher mice caused by mutation in delta2 glutamate receptor gene. Nature, **388**, 769-773.